The Design and Synthesis of Novel HIV-1 Protease Inhibitors

THESIS

Submitted in fulfilment of the requirement of the degree of

Master of Science

of

Rhodes University

by

Matshawandile Tukulula
B.Sc.Hons (Rhodes)

January, 2009

ABSTRACT

This study has focused on the synthesis of truncated analogues of the hydroxyethylene dipeptide isosteres, such as Ritonavir®, currently in clinical use as HIV-1 protease inhibitors. The reactions of pyridine-2- and quinoline-2-carbaldehydes with methyl acrylate, in the presence of 1,4-diazabicyclo[2.2.2]octane (DABCO) or 3-hydroxyquinuclidine (3-HQ) as nucleophilic catalysts, have afforded a series of Baylis-Hillman adducts, acetylation and cyclisation of which have provided access to a series of indolizine-2-carboxylate esters. The carboxylic acids, obtained by base-catalyzed hydrolysis of these esters, have been coupled with various protected (and unprotected) amino compounds using the peptide coupling agent, 1,1'-carbonyldiimidazole (CDI), to afford a series of indolizine-2-carboxamides as indolizine-based truncated Ritonavir® analogues in quantitative yield. Aza-Michael reactions of pyridine-3-carbaldehyde-derived Baylis-Hillman adducts with various amino compounds have provided access to a range of pyridine-based products as mixtures of diastereomeric aza-Michael products. The assignment of the relative stereochemistry of the aza-Michael products has been established using 1-D and 2-NOESY experiments and computer modelling techniques.

Computer modelling studies have also been conducted on selected aza-Michael products using ACCELRYS Cerius^2 software, followed by interactive docking into the HIV-1 protease receptor site, using AUTODOCK 4.0. The docking studies have revealed hydrogen-bonding interactions between the enzyme and the synthetic ligands. Saturation Transfer Difference (STD) NMR experiments have also indicated binding of some of the aza-Michael products to the HIV-1 protease subtype C enzyme, thus indicating their binding and possible inhibitory potential.

Acknowledgements

I would like to thank the Heavenly Father Almighty, for giving me the strength and the opportunity to embark on this project from the start until the completion stage.

To my supervisor, Prof P.T. Kaye, thank you so much for the support, guidance and motivation you provided throughout the duration of this project and being part of your research group was an honour for me. The freedom you gave to all of us to think outside the box was most appreciated. Dr R. Klein, my co-supervisor, thank you for always being there, willing to listen and discuss matters within and outside chemistry and for all the help you provided during this project. I also wish to thank Dr K. Lobb, without your assistance an important part of this project would not have seen a light of day-thank you!

I would also like to thank the National Research foundation (NRF) for their generous financial assistance.

To the members of the Chemistry Department, thank you all for your valuable inputs, support and technical assistance, especially Mr. A. Soper with NMR, Mr. A. Sonemann for collecting LRMS data, MS units at North-West and Stellenbosch Universities for collecting HRMS data, Dr Yasien Sayed from the HIV/AIDS Research Unit -School of Molecular and Cell Biology, University of Witwatersrand for providing the HIV-1 sub-type C protease enzyme, Mrs. B. Tarr and Ms B. An-Yui for their willingness to help, Mathew Adendorff for providing much needed assistance with computer modelling and the whole Organic Synthesis group in Lab F22 (past members: Dr D. Molefe, Dr. B. Gxoyiya, Dr. S. Salisu, Mlu (Thank you for making me work on Christmas and new year's day!), Nathan, Nceba, Tanya and Jason; current: Marius, Lulama, Dubekile, Mrs. Idahosa (thank you for proof-reading early chapters), Annalene, Anne, Lilly, Threneshin and a special thank you to Mr. Idris Olusapo).

To my family: Mama, SisKabongiwe, Makazi, Tata kaKhazi, Phumza kunye nabanye endingababizanga ngamagama ndiyabulela, andiyonto ngaphandle kwenu, thank you to

Dr. K, Mrs. and Mbasa Ngcoza, Mr Maselwa and my friends (Gee, Proph, Tibha, Diba, X-Jozi and Prozine) for your continuous support, prayers and encouragement during the duration of this project. Lastly, to my girlfriend, Nokubonga “Sma” Ngcamu, thank you for always being there for me.

LIST OF ABREVIATIONS

Asp	Aspartile
Ala	Alanine
Ile	Isolucine
Thr	Threonine
Gly	Glycine
Pd/C	Palladium on carbon
Me_2S	Dimethylsulphide
MeOH	Methanol
EtOAc	Ethyl acetate
CH_2Cl_2	Dichloromethane
THF	Tetrahydrofuran
Me_3N	Trimethylamine
LAH	Lithium aluminium hydride
DMF	Dimethyl formamide
CDI	1,1'-Carbonyldiimidazole
EDC	N-ethyl-N'-(dimethyaminopropyl)carbodiimide
HOBt	1-hydroxybenzotriazole
CCl_4	Carbon tetrachloride
COSY	Correlation spectroscopy (^1H-^1H)
HSQC	Heteronuclear single quantum coherence (^1H-^{13}C)
HMBC	Heteronuclear multiple bond coherence (^1H-^{13}C)
NOESY	Nuclear overhauser effect spectroscopy

CONTENTS

1. INTRODUCTION

1.1. HIV/AIDS

The Acquired Immunodeficiency Syndrome (AIDS) pandemic dates as far back as 1959 to a human blood sample collected in West-Central Africa.[1] By 1971 AIDS had spread to several regions of the world, killing its first reported victim in 1979.[2] AIDS presents a severe immune deficiency that involves the destruction of helper T-cells and is usually accompanied by multiple opportunistic infections which may later be dominated by *Kaposi's sarcoma*, a rare skin disease.[1-3] An aggressive and deadly variant of *Kaposi's sarcoma* was isolated by Friedman-Kien and his colleagues in 1981 from homosexual men who exhibited low levels of the helper T-cell CD4 count.[4] Gallo and co-workers showed in 1984, from "serological and viral isolation studies", that AIDS arises from infection with a human retrovirus similar to those of the family of Human T-cell Lymphotropic virus types I and II (HTLV-I and -II).[5] In 1983, the collaboration of Montagnier in France and Gallo in America resulted in the isolation of human immunodeficiency virus (HIV) from cultured human cells for the first time and, in 1985, showed it to be the causative agent of AIDS.[6-7]

HIV belongs to a family of rapidly mutating viruses called lentiviruses.[7] This family includes retroviruses like Simian Immunodeficiency Virus (SIV), visna virus and Equine Infection Anaemia Virus (EIAV).[7] HIV is divided into two strains, HIV-1 and HIV-2, the former being the deadly, dominant form that accounts for nearly 90% of global HIV/AIDS deaths. HIV-2 was discovered in 1986 and is less transmissible and pathogenic, with lower levels of viral load and slower progression to AIDS.[8] Both forms of the virus are believed to have originated through cross-species infection from chimpanzees to humans. The primate reservoir of HIV-2 has been identified from sooty mangabey (*cervocebus atys*) chimpanzee species from Western Africa, the region where HIV-2 is known to be endemic, while HIV-1 originated from Pan troglodytes troglodytes (*P.t. troglodyte*), a common chimpanzee species in Central Africa.[9-10] HIV-1 is further

divided into three sub-strains, M (Major), N (New) and O (Outlier), with M being the main strain responsible for the global AIDS epidemic.[1] Furthermore, sub-strain M is divided into nine subtypes, *viz*., A-D, F-H, J and K.[11] Subtype C is the most abundant, accounting for 47% of new HIV-1 infections, especially in Sub-Saharan Africa and Asia.[12-14] Subtype A is the second most abundant source of infection, making up 30%, while subtype B, which is dominant in North America and Eastern Europe, makes up 12%; the rest is due to "inter-subtype recombination".[12, 15]

Since the discovery of HIV/AIDS in 1981, the disease is estimated to have killed some 25 million people world-wide with 68% of the reported deaths in Sub-Saharan Africa. Currently it is estimated that there are nearly 40 million people living with the virus, including 2.5 million children, and 5 million new infections every year.[16-17]Although the death-toll has reached millions, AIDS has become a manageable chronic disease provided appropriate treatment programmes are implemented. However a vaccine still remains a necessity, especially for third-world countries like those in Africa and Asia where the highest number of new infections and deaths are reported annually.

1.1.2. HIV-1 viral structure and life cycle

The gut lining-lymphoid tissue, which is rich in CD4 T-cells, has been recognized as the primary site for HIV-1 replication.[6] HIV-1 has developed unique shielding mechanisms that prevent it from being recognized by the host's antibodies; these include the interaction of its cellular receptors with those of the host's cell and a dense carbohydrate sheet that surrounds its otherwise exposed antigen thus avoiding neutralization by antibodies.[18] It is also very important to note that the HIV-1 genome does not have the necessary genes for the production of this dense carbohydrate sheet but relies entirely on the host's cellular material for this feature.[6, 18-20]

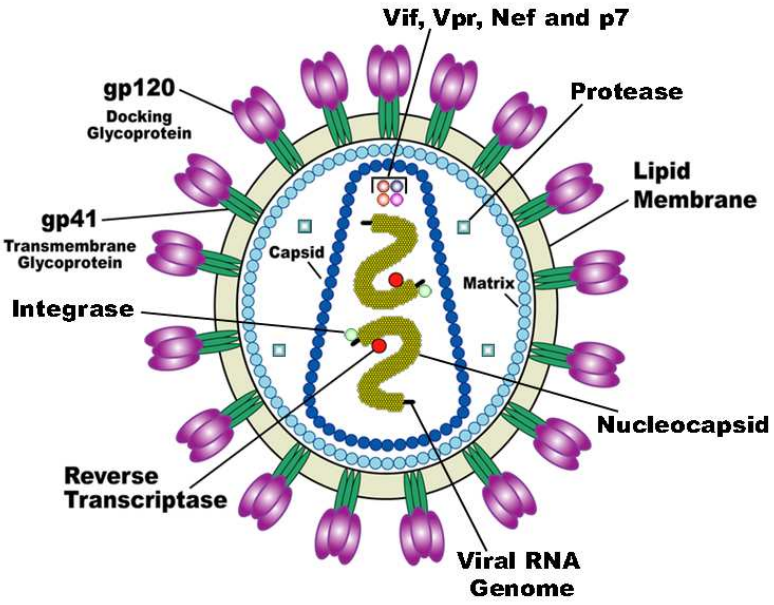

Figure 1. Mature HIV-1 virion structure. (Reproduced with permission from the publisher.) [21]

Other features which lie on the surface of the HIV-1 particles (Figure 1) are: -

(i) the viral lipid membrane lined with spike-like structures consisting of glycoprotein 120 (gp 120), a sub-unit that mediates viral attachment to the host's receptors and co-receptors unnoticed by the antibodies; and

(ii) glycoprotein 41 (gp 41), the transmembrane sub-unit that initiates fusion of the virus with the host's cell membrane.[19, 22]

In the HIV-1 core, there are two regulatory genes, *tat* and *rev*, and four accessory genes, *viz*., *vif*, *vpr*, *vpu* and *nef*, that contain the genetic material necessary for the production of proteins that enable the virus to infect other cells, and a nucleocapsid protein called p7.[22]

The HIV-1 viral particles exhibit very specific binding in that they only bind to cells bearing CD4, a protein that functions in immune recognition.[7] The first step in the HIV-1 life-cycle (Figure 2) involves recognition of the target cell by the virion. The gp 120 binds to CD4 molecules and anchors the virion to the cell surface; this process leads to fusion, and uncoating (which is not well understood) then occurs.[23-25]

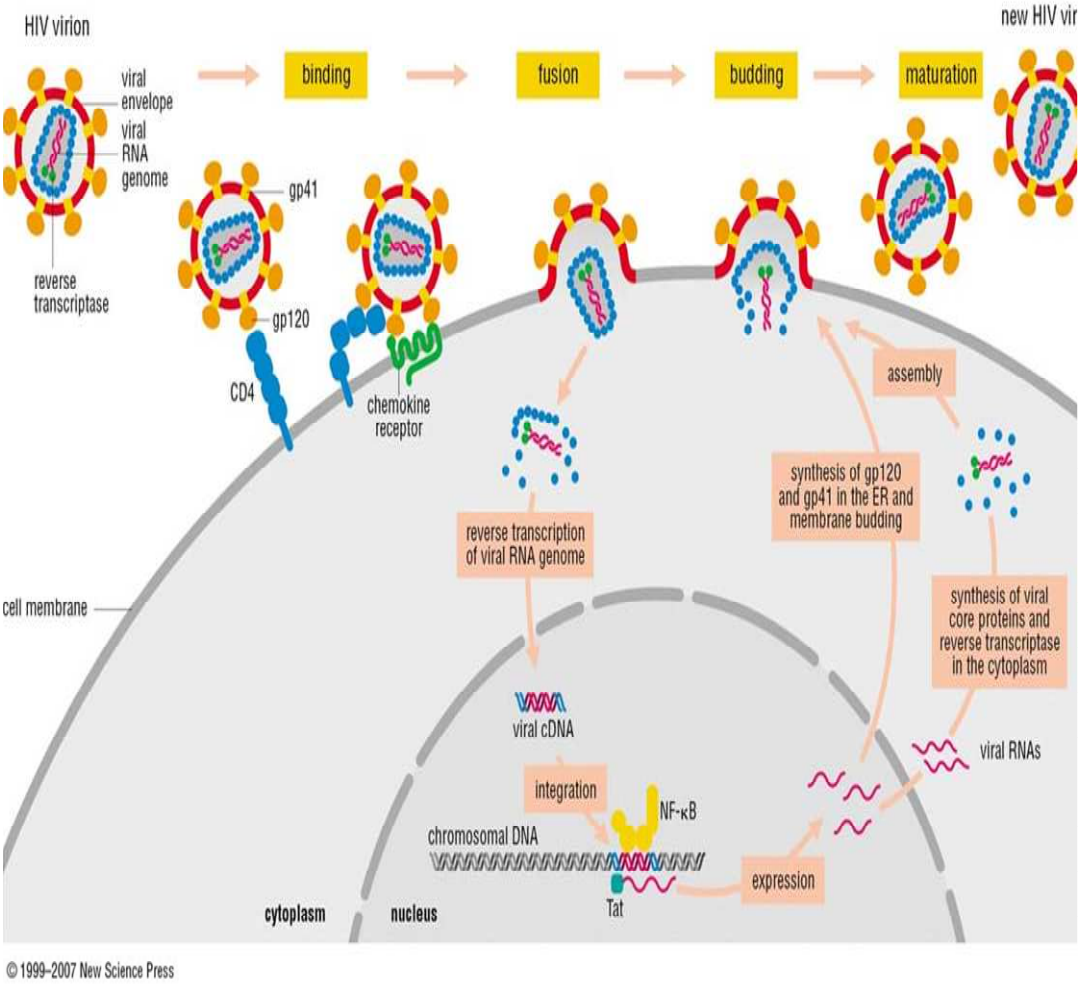

Figure 2. HIV-1 life-cycle. (Reproduced with permission from the publisher.) [26]

Following fusion with the host's cell membrane and uncoating of the viral particle, a single-stranded viral RNA is transcribed into double-stranded DNA by the first virally encoded enzyme, reverse transcriptase (HIV-RT). The transcribed viral DNA is then transported to the cell's nucleus where it is integrated with the host's genetic material by another viral enzyme, integrase (HIV-IN). Activation of the cell follows and this results in transcription of the viral DNA into messenger RNA (mRNA). [22] This mRNA is then translated into viral polyproteins which are cleaved into individual proteins by the protease enzyme (HIV-PR). HIV-PR functions as a "pair of molecular scissors" by hydrolyzing the *gag-pol* precursor proteins.[19] The individual proteins and two molecules

of viral RNA then assemble within the envelope protein to form a mature virion which buds out of the cell, leaving the infected cell to die. The new virions then infect other healthy host cells, repeating the cycle.[25] By examining the life cycle of HIV-1 several target sites for viable therapeutic agents can be identified; one of these sites is the fusion stage. Inhibiting the fusion process would prevent the viral particles from entering the host's cell thus stopping the life cycle before it even begins. One way of achieving this would be to alter the CD4 receptors and co-receptors on the cell's surface because HIV viral particles bind specifically to this protein molecule.[25, 27-28] One of the mechanisms for disguise, which the virus uses, is its dense carbohydrate sheet and interference with this sheet could make the virus vulnerable to neutralization by antibodies.[20]

There are three other obvious sites that could be targeted in the HIV-1 life-cycle, *viz*., reverse transcriptase (HIV-RT), [4] integrase (HIV-IN) [7] and protease (HIV-PR).[28] The transcription stage of the viral RNA to DNA would be severely compromised by inhibiting the HIV-RT enzyme. The critical problem with the HIV-RT enzyme lies in its inability to proof-read amino acid sequences; its 'error prone' habit increases the risk of drug resistance and the emergence of new multi-resistant strains.[7, 29] Inhibiting the HIV-IN enzyme would stop the integration of the viral DNA into that of the host. The third enzyme, HIV-PR, has shown tremendous potential for drug discovery because of its cleavage of polyproteins into mature virions;[22] inhibition would lead to the production of immature virions lacking the ability to infect other cells, thus lowering the viral load in HIV positive patients. The critical importance of these enzymes in the viral life-cycle makes them promising targets for drug discovery.

Unless the viral life-cycle is interrupted, virus infection spreads rapidly throughout the body, resulting in a weakened and compromised immune system, thus leading to the inability of the body to protect itself against opportunistic infections like pneumonia, diarrhoea and tuberculosis (TB).

1.1.3. The HIV-1 protease enzyme and its function

HIV-1 protease (HIV-PR) belongs to a family of aspartyl protease enzymes, which includes enzymes like renin and pepsin, all of which have a hydrophobic core cavity.[29-31] HIV-PR is a homodimer made up of a pair of identical 99 amino acid residue protein chains, and has a C_2 axis of symmetry. The active site of HIV-PR is located at the "bottom" of the enzyme's cavity near the dimeric interface (Figure 3), and is lined with a pair of catalytic triads, comprising the residues: Asp 25 (or 25') - Thr 26 (or 26') - Gly 27 (or 27').[22, 31] The cavity of the active site is covered by two flexible flaps, one from each monomer, and these play a critical role during substrate binding. The flaps are situated at the "top" of the catalytic site and have extended β-sheet regions.[31] The dimeric interface is largely made up of and stabilized by four anti-parallel β-sheets formed by N and C terminal strands.[22, 31-32] Among the catalytic triad residues, Asp 25 and 25' have been identified as the critical components involved in the catalytic action of the enzyme.[7] X-ray crystallographic analysis of HIV-PR reveals a structural water molecule located just above the catalytic residues; this structural water is essential for the hydrolysis of peptide bonds.[22, 29-31]

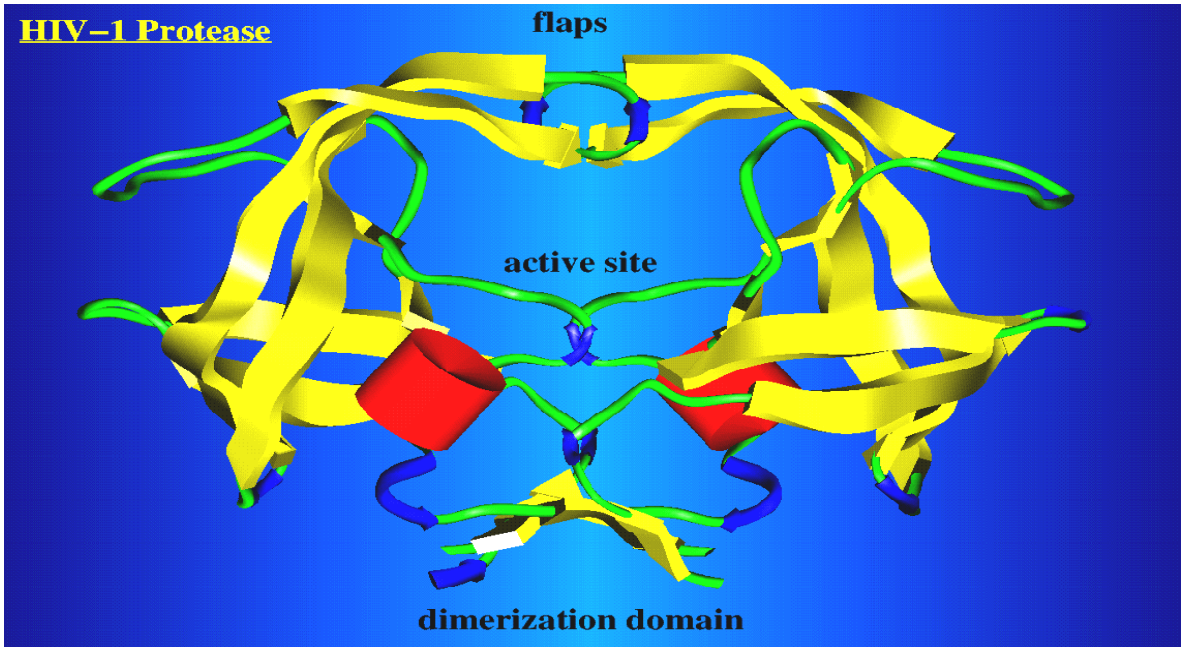

Figure 3. Ribbon representation of the structure of HIV-1 protease enzyme. (Reproduced with permission from the publisher.) [33-35]

The standard nomenclature commonly employed for the HIV-PR-inhibitor (or substrate) complex was developed by Berger *et al*., [22, 36] and is shown in Figure 4, where $S_1 \ldots S_n$ are the binding pockets in the enzyme's active site and are referred to as subsites, while $P_1 \ldots P_n$ denote the corresponding amino acid residues of the peptide inhibitor or substrate.[37] The amide C-N bond at which cleavage occurs is termed the scissile bond.

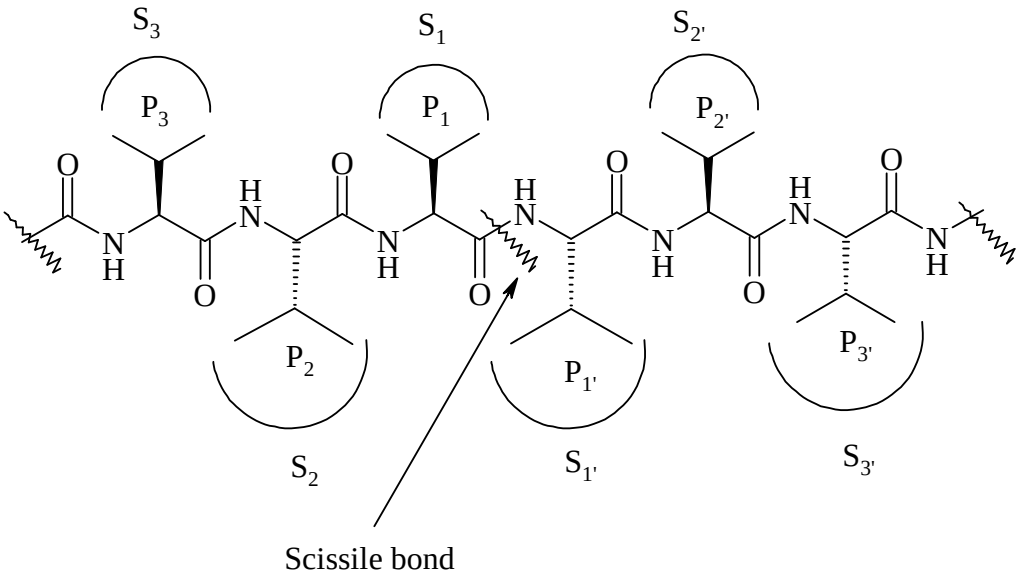

Figure 4. Standard nomenclature for HIV-PR-peptidic substrate complexes. (Adapted from References 22, 36 and 37).

As indicated earlier, HIV-PR functions by hydrolyzing the viral *gag-pol* precursor proteins into mature structural proteins.[19, 36] The proposed catalytic mechanism of HIV-PR uses the structural water molecule in hydrolyzing the scissile amide carbonyl bond of the substrate (Figure 5).[36-37] This structural water molecule is activated by the two catalytic aspartyl residues, Asp 25 and 25', found in the active site.[22]

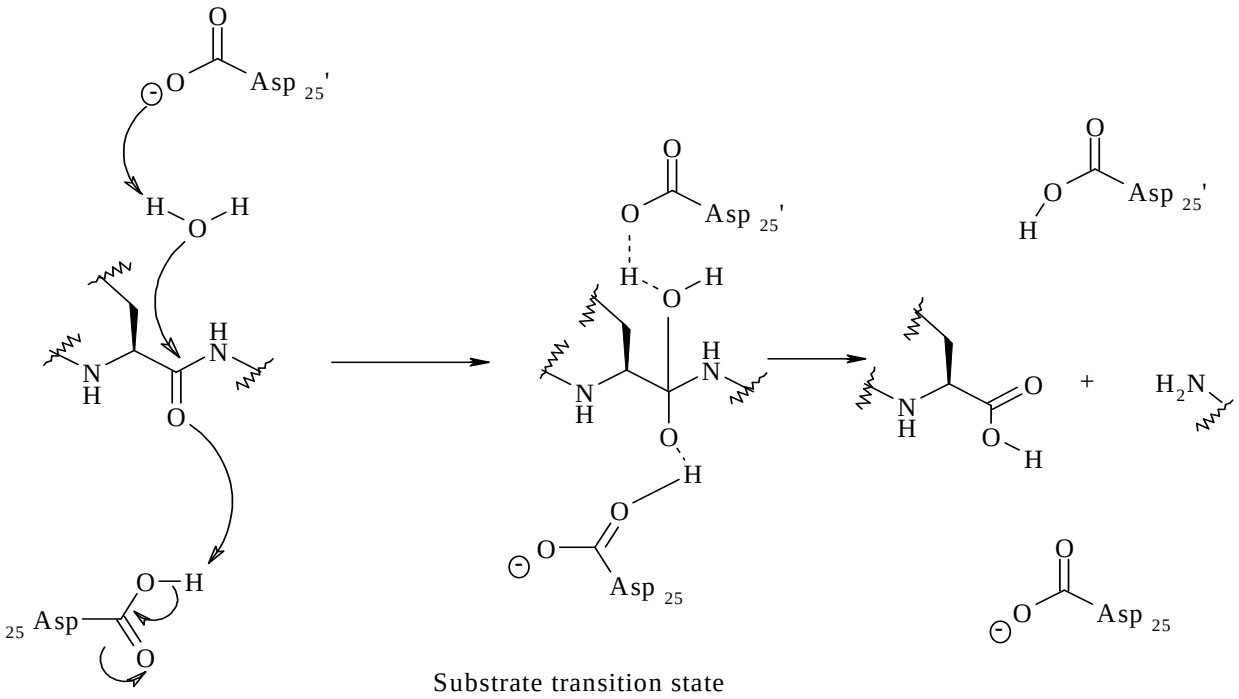

Figure 5. Catalytic action of HIV-PR enzyme. (Adapted from reference 37.)

Therefore, for the protease inhibitor to be effective and viable it must be non-hydrolysable (*i.e.* non-cleavable) around the $P_1/P_{1'}$ region. HIV-PR inhibitors can either be peptide or non-peptide based systems.[22, 36-37] Since 1995, the U.S Food and Drug Administration (FDA) has approved for clinical use the ten HIV-PR inhibitors illustrated in Figure 6. These are the eight peptide based inhibitors: Invirase (Hoffmann-La Roche, 1995), Ritonavir (Abbott Laboratories, 1996), Indinavir (Merck, 1996), Viracept (Agouron Pharmaceuticals, 1997), Amprenavir (GlaxoSmithKline, 1999), Kaletra (Abbott Laboratories, 2000), Reyataz (Bristol-Myers Squibb, 2003), Lexiva (GlaxoSmithKline, 2003); and the two non-peptide based: Tipranavir (Boehringer Ingelheim, 2005) and Darunavir (Tibotec Inc, 2006).[22, 38]

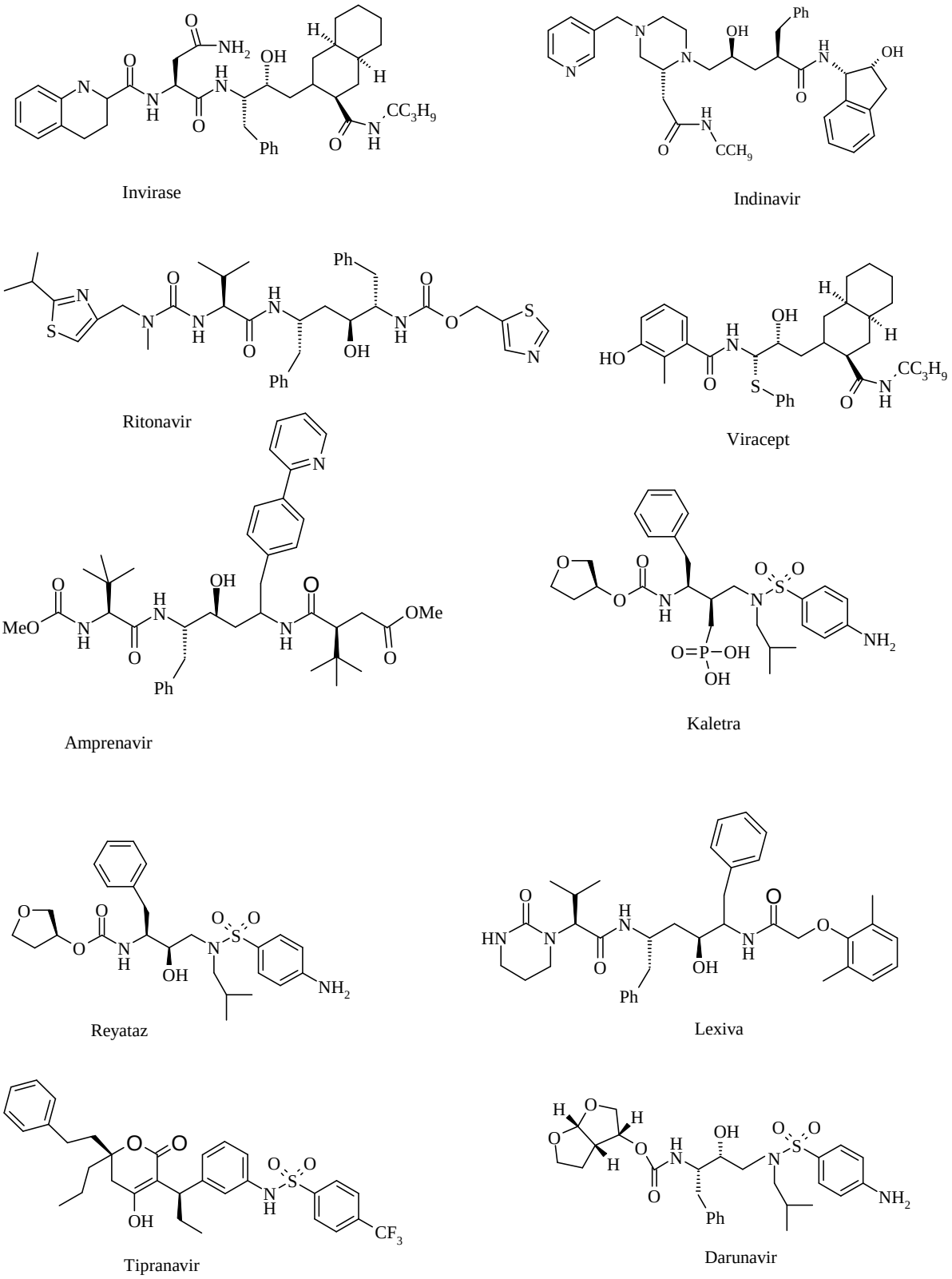

Figure 6. FDA approved HIV-PR inhibitors.

Since the introduction of these anti-HIV-1 drugs some thirteen years ago, millions of people's lives have improved significantly, resulting in an apparent decline in the number of HIV/AIDS-related deaths, especially following the introduction in 1996 of Highly Active Antiretroviral Therapy (HAART), which involves the combination of HIV-PR and HIV-RT.[39]Although these drugs have improved people's lives, their effectiveness decreases over time due mainly to drug toxicity and resistance. Moreover, their use is inhibited by high costs and patient compliance is influenced by unpleasant side-effects. There is thus a pressing need for new and improved drugs that can overcome these obstacles.[30, 40-41] The present study has focused on the HIV-1 protease (HIV-PR) enzyme as an attractive target since its structure and function are well established. Particular use has been made of Baylis-Hillman methodology in providing access to a series of pyridine- and indolizine-based potential inhibitors.

1.2. Properties and synthesis of indolizines

Indolizine **1**, also known as pyrrolo[1,2-*a*]pyridine, consists of a 10π conjugated electronic structure.[42] Indolizines are important structural motifs frequently found in nature and have been used as key scaffolds in the pharmaceutical industry due to their broad spectrum of biological activity. The indolizine skeleton is also found in naturally occurring erythrina alkaloids such as 3-dimethoxyerythratidinone **2** and β-erythrolidine **3**, alkaloids possessing potent central nervous system (CNS) activity.[43] Indolizines were first discovered in 1890, and prepared in 1912 by Scholtz from α-picoline and acetic anyhydride.[44] They are weak bases, and when reacted with a strong acid they form salts. The generally accepted numbering of the indolizine is shown in the parent system **1**.

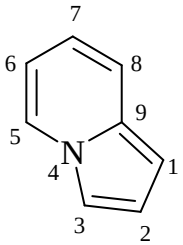

1

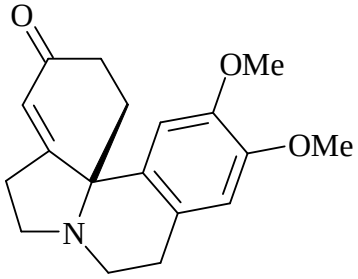

2

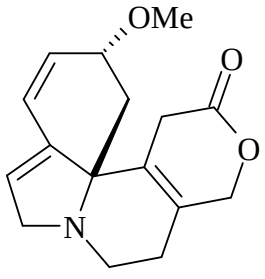

3

1.2.1. Biological Importance of indolizines

Indolizines are structurally similar to indoles and isoindoles, which are important "molecular templates" for many naturally occurring therapeutics.[45-47] Indolizine derivatives have been reported to exhibit valuable biological activity against diseases, such as cancer and HIV.[48-49] Indolizine derivatives have also been shown to be antagonistic against neurokinin B (NKB), which is believed to be a major factor in chronic diseases, such as asthma, in psychiatric disorders and in certain inflammatory diseases.[47, 50-51] Furthermore, Rise *et al.* [52] have shown that some indolizine derivatives, especially indolizines with an oxygen atom at C-1 position, *i.e*. *O*-protected indolizine esters, ethers and sulfonates, exhibit activity against lipid peroxidation. Gundersen *et al.* [53] have reported that indolizine derivatives, oxygenated at C-1, are potent anti-oxidants which inhibit 15-lipoxygenase, an enzyme involved in the oxidation of "low density lipoproteins", thus leading to the development of atherosclerosis, prostate cancer and spontaneous abortion in animals. Indolizine derivatives have also been reported to inhibit tyrosine phosphatases (TPP) which are responsible for the virulence of various pathogenic bacteria, *viz.*, *salmonella typhiminium*, (the typhus pathogen) and *yersinia pestis*, (the plague pathogen).[48]

Recently, indolizine derivatives have been reported as potential calcium entry blockers, [49] cardiovascular agents, [49, 54] anti-5-hydroxytryptamine, [55-56] anti-histamine, [55-56] anti-acetylcholine, [55-56] anti-tumor, [46-47, 57] anti-*mycobacterium tuberculosis* (TB) [58] and anticancer agents.[47, 49] They also appear to have potential in the treatment of angina pectoris and as central nervous system depressants.[49, 54-56]

Different methods for the synthesis of indolizine derivatives, which are summarized in the review by Uchida and Matsumoto, [44] include: - condensation reactions (*i.e.* the Scholtz [44, 59] and Chichibabin reactions [55, 60]), 1,3-dipolar cycloaddition [45, 48-50, 61-62] and 1,5-dipolar cycloaddition.[44, 63-64] Another particularly useful method for the synthesis of indolizine derivatives involves the use of the Baylis-Hillman methodology.[65-70]

1.2.2. Condensation reactions: the Scholtz and Chichibabin reactions

The Scholtz reaction involves heating a mixture of 2-methylpyridine **4** and acetic anhydride **5** at 200-220°C to give "picolide" or 1,3-diacetylindolizine **6** which, on hydrolysis, affords indolizine **1** (Scheme 1).[44] This method was applied in the preparation of 1-acetyl-5-methylindolizines and 1-benzylideneamino-3-phenylindolizines by Boekelheide in 1959 and by Kröhnke and co-workers in 1971, respectively.[44, 71]

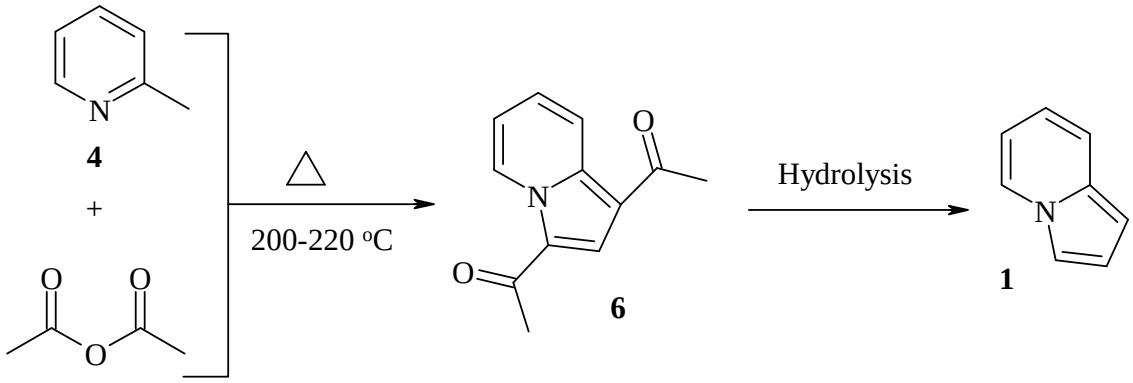

Scheme 1

In 1927, Chichibabin reported a useful modification of the Scholtz reaction for the synthesis of 2-alkyl- and 2-arylindolizines, which subsequently became known as the Chichibabin reaction.[44] This modification involves base-mediated cyclisation of quaternary pyridinium salts; [44, 60] thus, treatment of the picoline derivative **7** with an α-haloketone **8** gives the pyridinium salt **9** which, on treatment with the base, affords an akyl- or arylindolizine **10** (Scheme 2).[60]

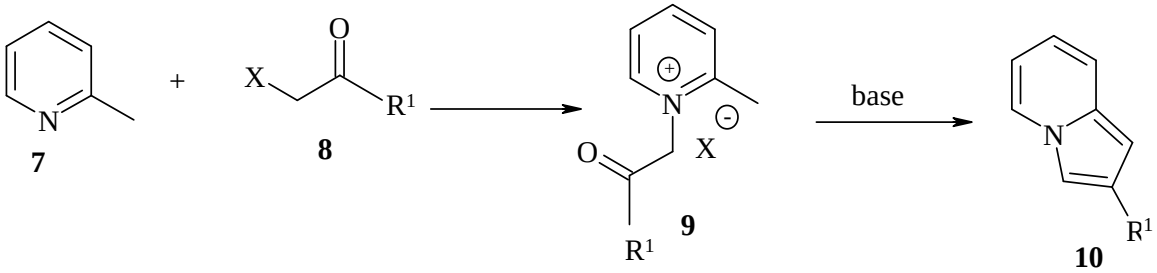

Scheme 2

The Chichibabin reaction is deficient in that it is only useful for the synthesis of indolizines bearing substituents on the five membered ring, and is thus not suitable for the synthesis of unsubstituted indolizines.[55, 60] However, modification of the Chichibabin reactions has broadened the scope of this methodology.

1.2.3. Synthesis of indolizines *via* 1,3-dipolar cycloaddition

Intermolecular 1,3-dipolar cycloaddition provides a very powerful approach to the synthesis of five-membered heterocyclic systems.[44, 48-50, 61] This reaction involves addition of a heteroaromatic *N*-ylide **11** to an electron-deficient acetylene **12** or alkene under dehydrogenating conditions to give indolizine derivatives **13** (Scheme 3).[45, 48-49, 61-64] However, the dehydrogenation was later shown to be unnecessary, and higher yields were obtained under mild conditions (*e.g.* the use of solid support).

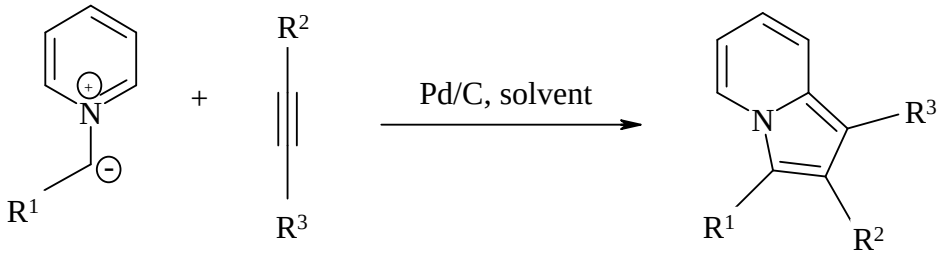

11 **12** **13**

Scheme 3

The intermolecular 1,3-dipolar cycloaddition reaction is particularly valuable in indolizine synthesis, being a simple two-step process.[44] However, the reaction suffers from low yields and regioselectivity problems when unsymmetrical, highly functionalized or sterically hindered acetylenes are used as substrates.[49] Another drawback is the fact that the pyridinium salt intermediates are highly hygroscopic, and are usually unstable.[45, 61]

1.2.4. Synthesis of indolizines *via* 1,5-dipolar cycloaddition

Uchida and Matsumoto have described 1,5-dipolar cycloaddition (sometimes referred to as intramolecular 1,5-dipolar cycloaddition) as the most powerful method for the synthesis of heterocyclic compounds.[44] The indolizine derivatives synthesized by this method were first reported in 1962 by Zecher and Kröhnke.[71] This synthesis involves treatment of a pyridine derivative **7** with an allyl halide **14** under mild conditions to afford the corresponding *N*-allylpyridinium halide **15** in reasonable yield. The *N*-allylpyridinium halide is then treated with a mild base (*i.e.* potassium carbonate) to give a stable dihydroindolizine **16**, which can generally be isolated; rapid oxidation then affords the indolizine **17** (Scheme 4).[72-73]

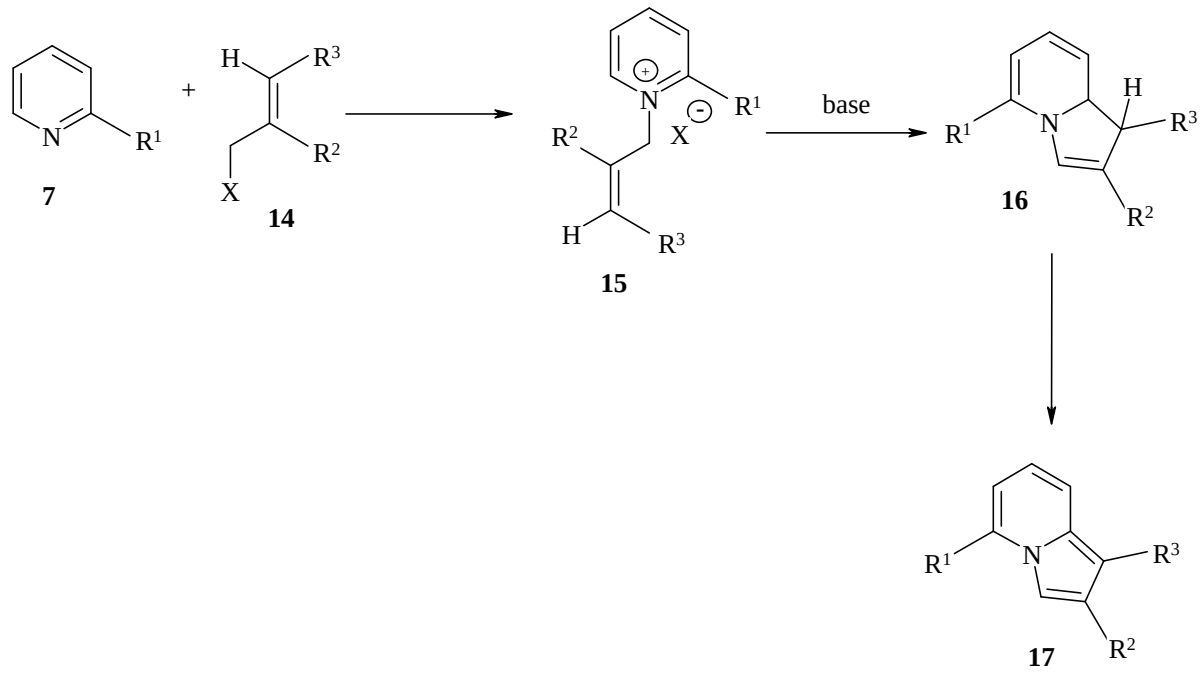

Scheme 4

1.3. The Baylis-Hillman reaction

In 1968, Morita *et al.*[74] reported for the first time, the reaction of an aldehyde with various acrylic compounds in the presence of a phosphine catalyst, tricyclohexylphosphine. Four years later, in 1972, Baylis and Hillman from the Celanese Corporation of New York were granted a patent for similar reactions, obtaining higher yields using a cyclic tertiary amine catalyst, 1,4-diazabicyclo[2.2.2]octane (DABCO) **18**.[75] Following their success, a wide range of other cyclic and non-cyclic amine catalysts, such as quinuclidine **19**, 3-hydroxyquinuclidine (3-HQ) **20** and 1,8-diazabicyclo[5.4.0]undec-7-ene (DBU) **21** emerged for this transformation, which was later referred to as the Baylis-Hillman (B-H) or Morita-Baylis-Hillman reaction.[76] This reaction permits the formation of a carbon-carbon bond at the α-carbon of the vinylic moiety, giving rise to α,β-unsaturated adducts from readily available starting materials.[77-78] These α,β-unsaturated Baylis-Hillman adducts are particularly useful as synthetic precursors in organic and medicinal chemistry.[78]

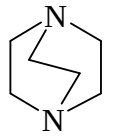

18

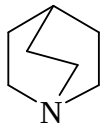

19

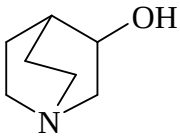

20

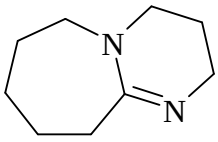

21

The Baylis-Hillman reaction thus involves the coupling of aldehydes **22** and activated alkenes **23**, in the presence of a tertiary amine or phosphine catalyst to afford allylic alcohols with a new stereogenic centre (designated with an asterisk) **24** (Scheme 5). Various aldehydes are used with activated alkenes, such as alkyl vinyl ketones, acrylonitrile, vinyl sulfones, acrylamides, allenic esters, vinyl sulfonates, vinyl sulfoxides, vinyl phosphonates and acrylate esters.[76, 79-81]

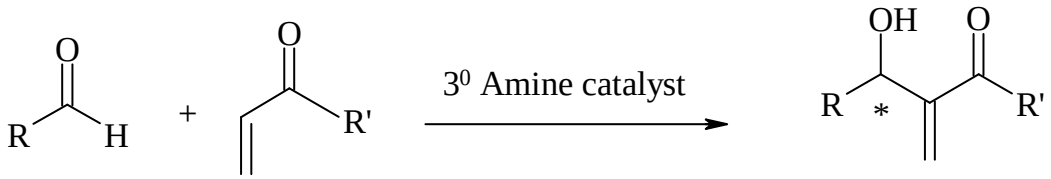

22 **23** **24**

Scheme 5

Baylis-Hillman methodology may be sub-divided into three types of reactions: (i) asymmetric, (ii) intramolecular and (iii) non-assymmetric and non-intramolecular.[82] In 1986, Brown and co-workers were the first group to show the versatility of Baylis-Hillman products in asymmetric synthesis.[83] The goal of the asymmetric Baylis-Hillman reaction is to selectively control the stereochemistry of the resulting products, and in so doing, produce an enantiomerically pure adduct in high enantiomeric (ee) or diastereomeric excess (de) (>98%).[84-86] This selectivity has been achieved in various ways as illustrated in the following three examples.

(a) Using a chiral Michael acceptor, such as acrylate derivatives **25** (Scheme 6).[87]

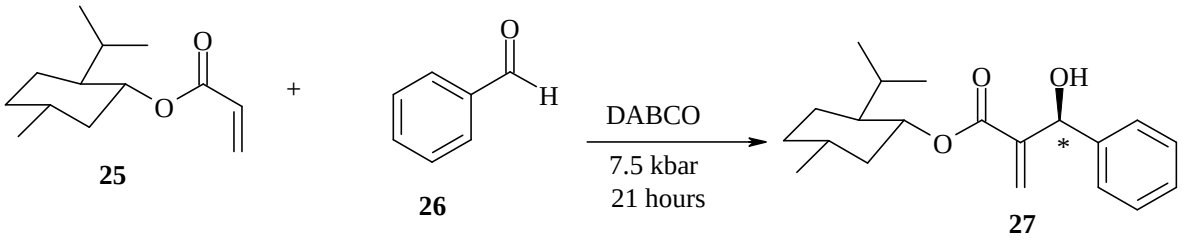

25 **26** **27**

100% de

Scheme 6

(b) Using chirally modified electrophiles, such as the phenylmethyl oxoacetate **28** (Scheme 7).[87]

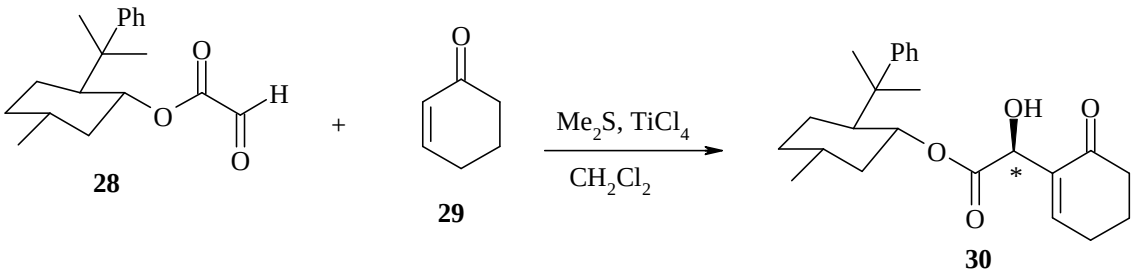

> 95% de

Scheme 7

(c) Using chiral catalysts (*e.g*. the chiral DABCO derivative **33**; Scheme 8).[82, 87-88] Ideally, chiral reagents and/or catalyst(s) used in asymmetric Baylis-Hillman reactions need to be easily removed at the end of the reaction and readily available.[89]

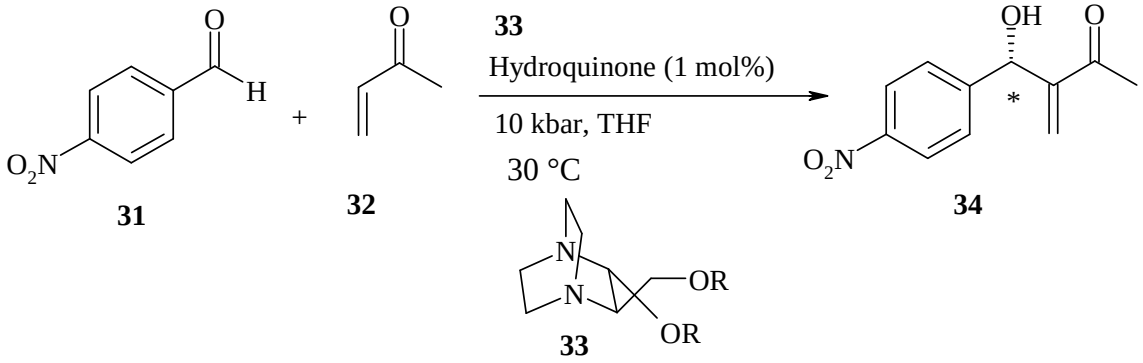

Scheme 8

Frater *et al*.,[90] in 1992, were the first to describe an intramolecular Baylis-Hillman reaction, followed by Murphy in 1993.[91-92] Intramolecular Baylis-Hillman reactions occur when both the aldehyde and the activated alkene moieties are present in the same compound **35**, and are in sufficient proximity for the reaction to occur (Scheme 9). The

intramolecular Baylis-Hillman reaction provides convenient access to cyclic ketones that contain an α-hydroxy group, but relatively few substrates are readily available to undergo this reaction.[93]

35 **36**

Scheme 9

Over the last two decades, the Baylis-Hillman reaction has gained popularity due to its atom economy and the mild reaction conditions typically required.[93-95] However, in many cases there are limitations, such as very long reaction times, low to moderate yields and the lack of "a universal solvent system" suitable for all substrates.[96-98] A number of physical and chemical methods have been developed which address these shortcomings. These methods may not only accelerate the reaction, but also activate "previously unreactive" substrates.[99-102] Chemical methods have been shown to be more convenient than physical methods because they do not require any specialized equipment.[100] Among the chemical methods employed in accelerating the Baylis-Hillman reaction are the use of aqueous solutions or hydrogen donor solvents,[99, 102] ionic liquids,[103] highly basic amines [104] and Lewis acid or basic catalysts.[94, 105] Microwave irradiation, high pressure, sonication or ultrasound and temperature variation are among the most widely used physical methods.[98, 100, 106]

1.3.1. Mechanism of the Baylis-Hillman reaction

The generally accepted mechanism (Scheme 10) for the Baylis-Hillman reaction is based on data obtained from both kinetic and computational studies.[65, 107] The first step involves conjugate addition of a tertiary amine catalyst to the activated alkene (or Michael acceptor) **23**, affording a zwitterionic enolate intermediate **37**.[65] This zwitterionic

intermediate then attacks the aldehyde **22** to give an aldol type zwitterionic intermediate **38**- a step previously thought to be the rate determining step (RDS).[97, 104] However, the results of theoretical studies suggest that proton transfer to give another zwitterionic enolate intermediate **39** is the rate determining step. Subsequent $E1_{CB}$ elimination of the catalyst then gives the desired product **24**. It is important to note that, to date, none of the zwitterionic intermediates have been isolated experimentally.

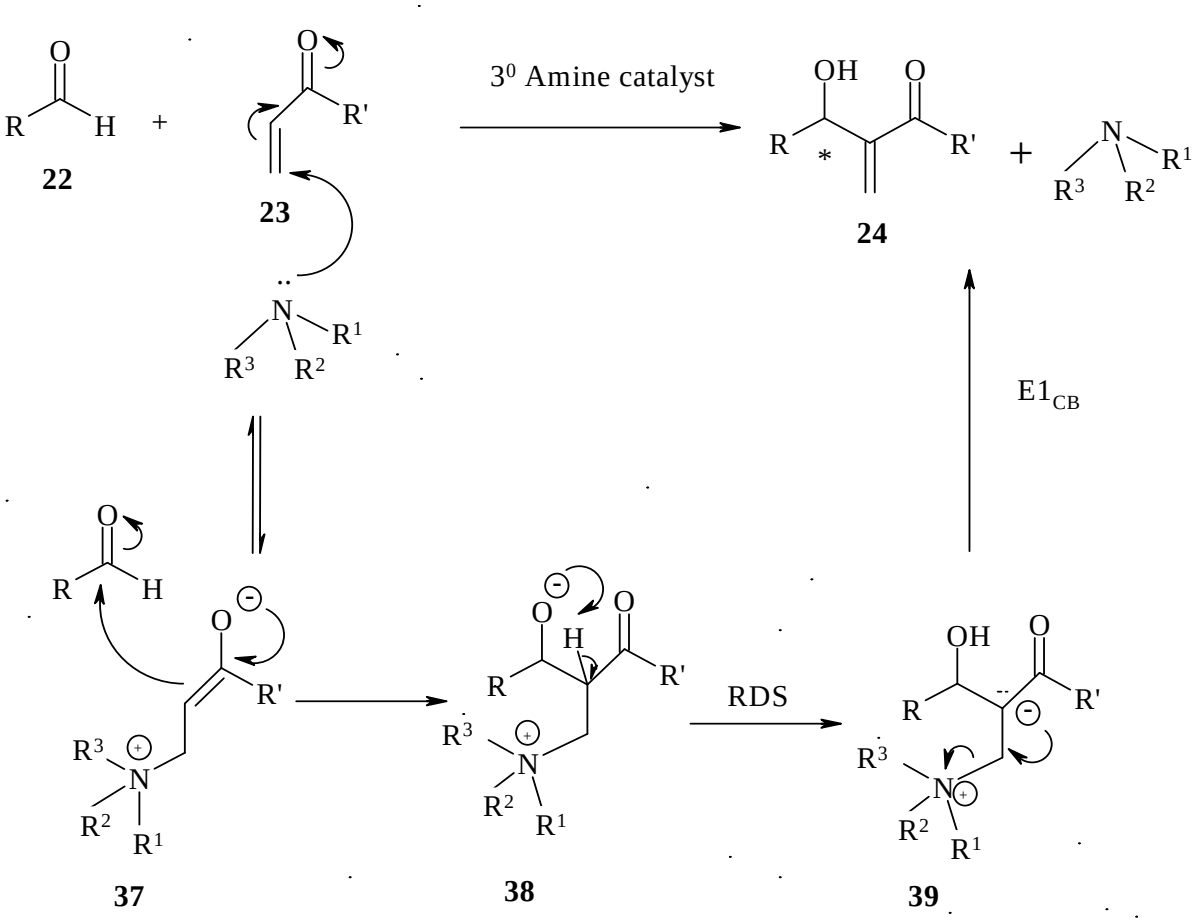

Scheme 10

1.3.2. Applications of the Baylis-Hillman reaction

Careful examination of the Baylis-Hillman reaction mechanism suggests that this transformation may be defined as a one-pot combination of successive Michael, [108] Aldol [109, 110] and Elimination reactions. Diels-Alder,[111] Friedel-Crafts,[112] Mannich [113] and ring-closing metathesis [114] are among the many organic transformations which have been carried out on Baylis-Hillman adducts in the synthesis of various natural and unnatural biologically important products, such as peptides,[115] azetidines,[116] carbamates,[117] acrylamides,[118] methylene-β-hydroxylactones,[92] β-lactams [119] and acaterin,[120] an inhibitor of cholesterol acyltranferase.

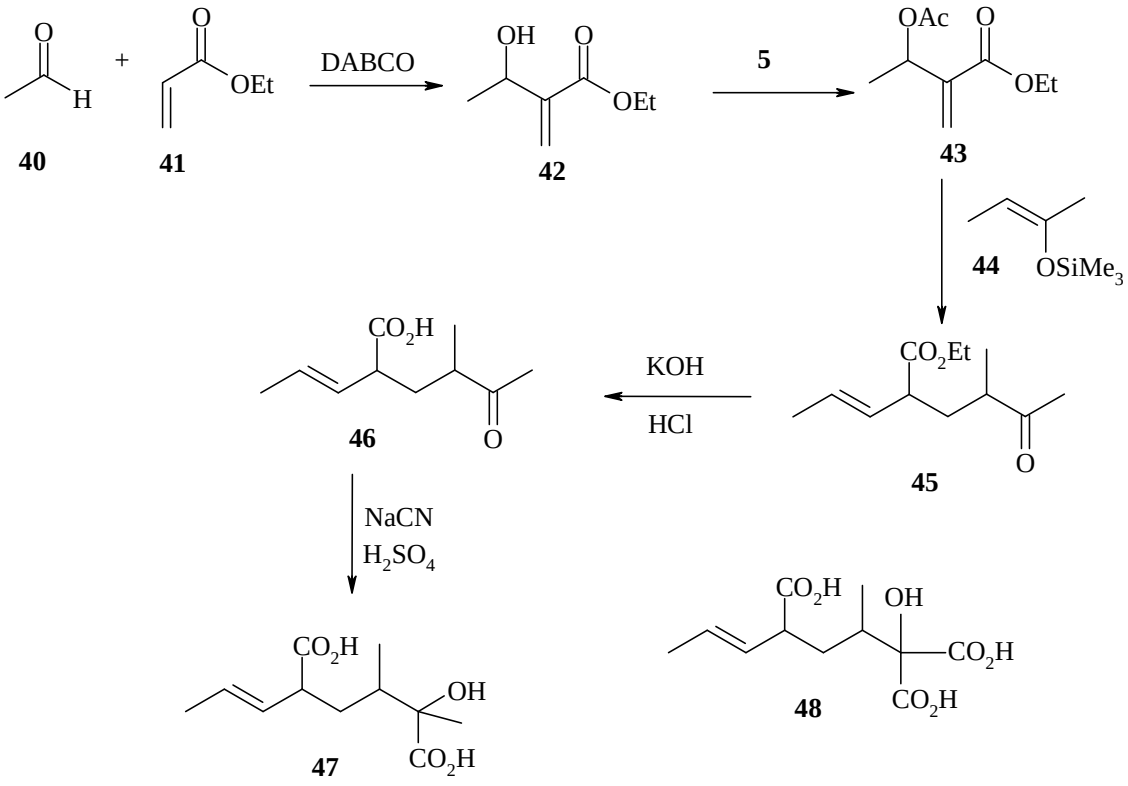

Scheme 11

In 1982, Drewes *et al.* [121] were the first to exploit the versatility of the Baylis-Hillman reaction when they synthesized integerrinecic acid **47** (Scheme 11) and retronecic acid **48**, two commonly occurring necic acids, which are C_{10} compounds found in many senecio alkaloids.[122-123] The synthesis involved reaction of acetaldehyde **40** with ethyl

acrylate **41** in the presence of DABCO, to yield Baylis-Hillman adduct **42**, which was subsequently acetylated. The acetylated Baylis-Hillman adduct **43** was then reacted with 2-trimethylsilyloxybut-2-ene **44** to obtain the ester product **45**; hydrolysis to the carboxylic acid **46**, followed by a cyanohydrin reaction and further hydrolysis yielded integerrinecic acid **47**.[121, 124] In 1983, Hoffman and Rabe also utilized the Baylis-Hillman reaction in conjunction with the Diels-Alder reaction in synthesizing mikanecic acid as a racemic mixture.[125] Mikanecic acid is a terpene dicarboxylic acid, a product of alkaline hydrolysis of the alkaloid mikanoidine obtained from *Senecio mikanioides otto*.[126]

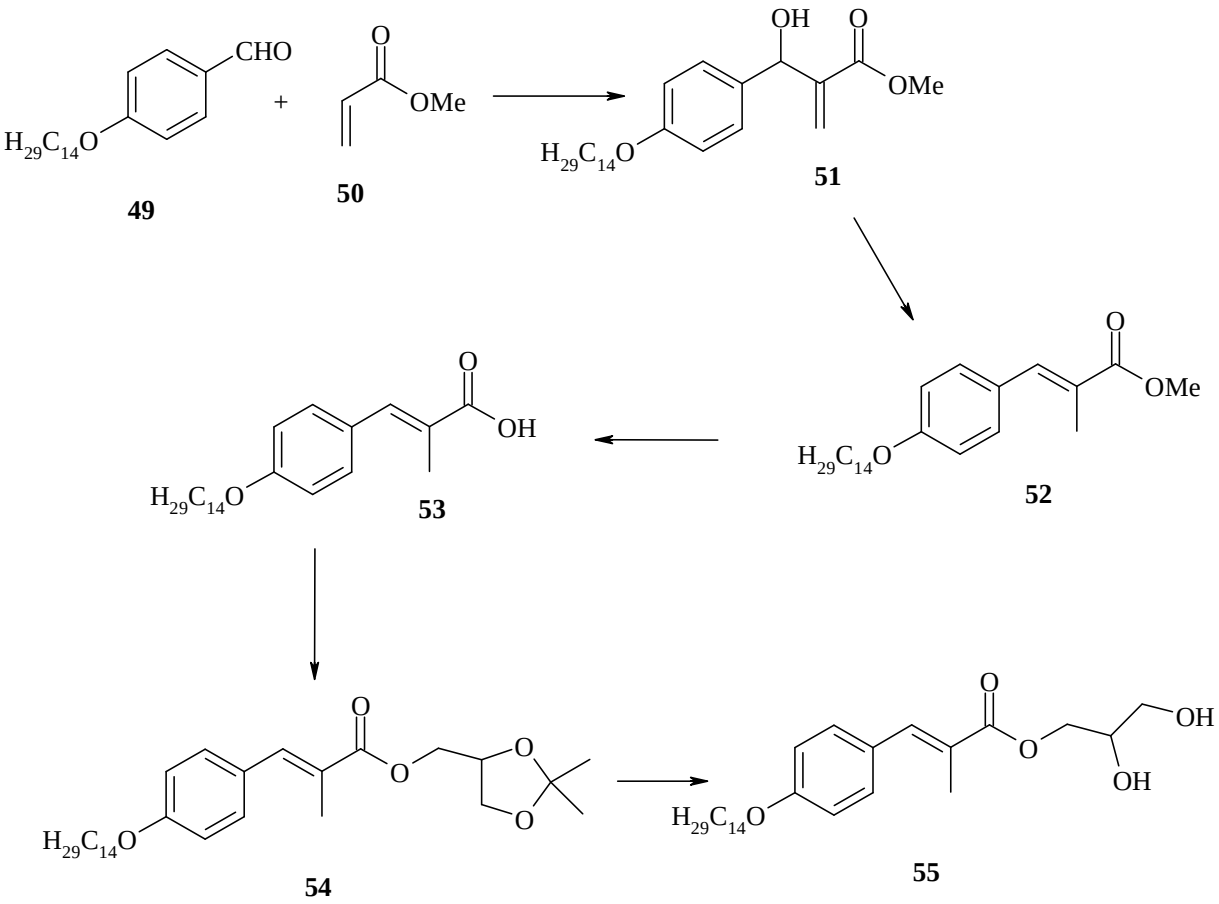

Scheme 12

Das *et al*., [127] have also demonstrated the application of Baylis-Hillman methodology in the synthesis of the active hypocholesterolemic agent, LK-903 **55**, which contains the (*E*)-α-methylcinnamic acid moiety as the key structural unit. The preparation of

compound **55** involves reaction of 4-(myristyloxy)benzaldehyde **49** with methyl acrylate **50a** in the presence of DABCO as a catalyst, to afford Baylis-Hillman adduct **51**, which is then reduced to the ester **52**, hydrolysis of which gives the cinnamic acid derivative **53**. Esterification of the cinnamic acid **53** affords the protected compound **54**. Deprotection by removal of the acetonide group finally affords LK-903 **55** (Scheme 12).

Another critically important application of the Baylis-Hillman reaction has been in the synthesis of heterocyclic systems including indolizines.

1.3.2.1. Application of Baylis-Hillman reaction in the synthesis of indolizine derivatives

In 1990, our research group at Rhodes University was the first to apply the Baylis-Hillman methodology in the synthesis of indolizine derivatives (see section 1.4.1).[67] In 2003, Basavaiah *et* a*l*. [69] reported an efficient one-pot synthesis of indolizine derivatives employing the Baylis-Hillman reaction. In this method, pyridine-2-carbaldehyde **56** is reacted with various conjugated alkenes **23**, in acetonitrile, under the inluence of triflouromethanesulfonate (TMSOTf) and basic conditions, to afford indolizine derivatives **57** (Scheme 13).

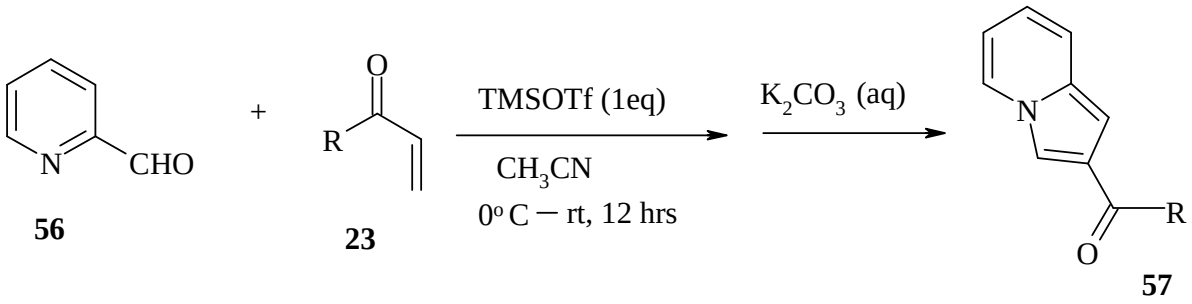

Scheme 13

Within the same year, Basavaiah and Rao also reported the synthesis of indolizine-fused-chromone derivatives using Baylis-Hillman methodology.[143] Chromones **58** were shown

to react with pyridine-2-carbaldehyde **56** in methanol, in the presence of trimethylamine, to afford the corresponding Baylis-Hillman adducts **59**. When the adducts **59** were refluxed in acetic anhydride **5** the indolizine-fused-chromone derivatives **60** were obtained in good yields (Scheme 14).

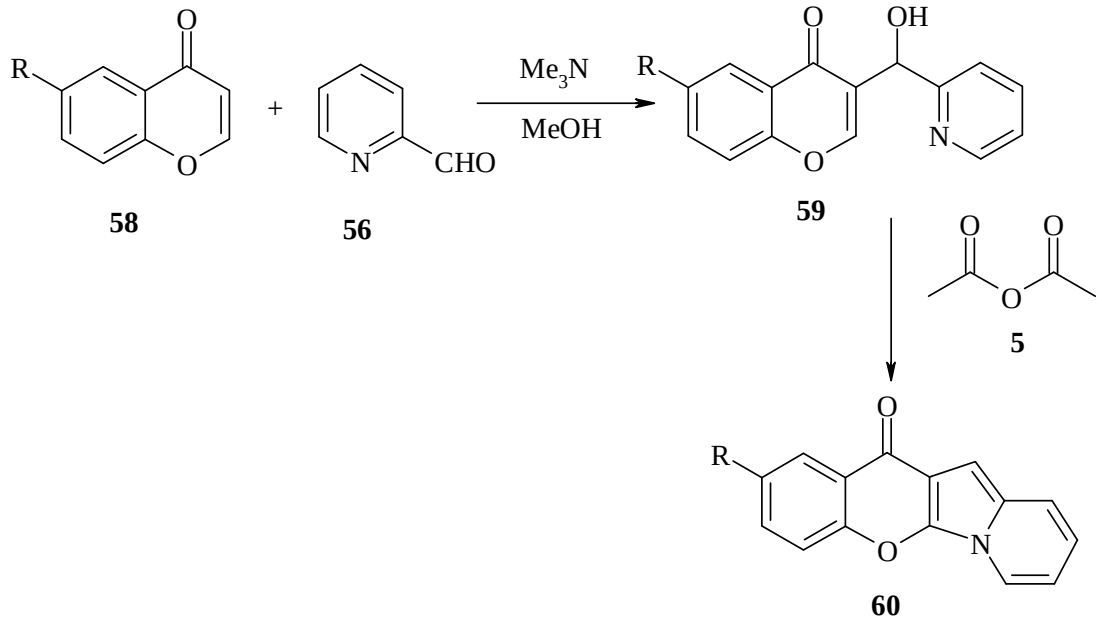

Scheme 14

1.4. Previous work done in our research group at Rhodes

1.4.1. Synthesis of various heterocyclic derivatives

As mentioned earlier in the previous section, the application of the Baylis-Hillman methodology in the synthesis of indolizine derivatives was first reported by Kaye and Bode in 1990.[67] This approach involved the treatment of various aldehydes **56a-c** with methyl acrylate **50a**, methyl vinyl ketone **50d**, ethyl vinyl ketone **50e** or acrylonitrile **50f** in chloroform, in the presence of DABCO at room temperature, to give the corresponding Baylis-Hillman adducts **61a-f** in good yields after 3 days. Distillation of the Baylis-Hillman adducts **61a-f** afforded the indolizine derivatives **63a-f** in low yields (Scheme 15, route I).[67]

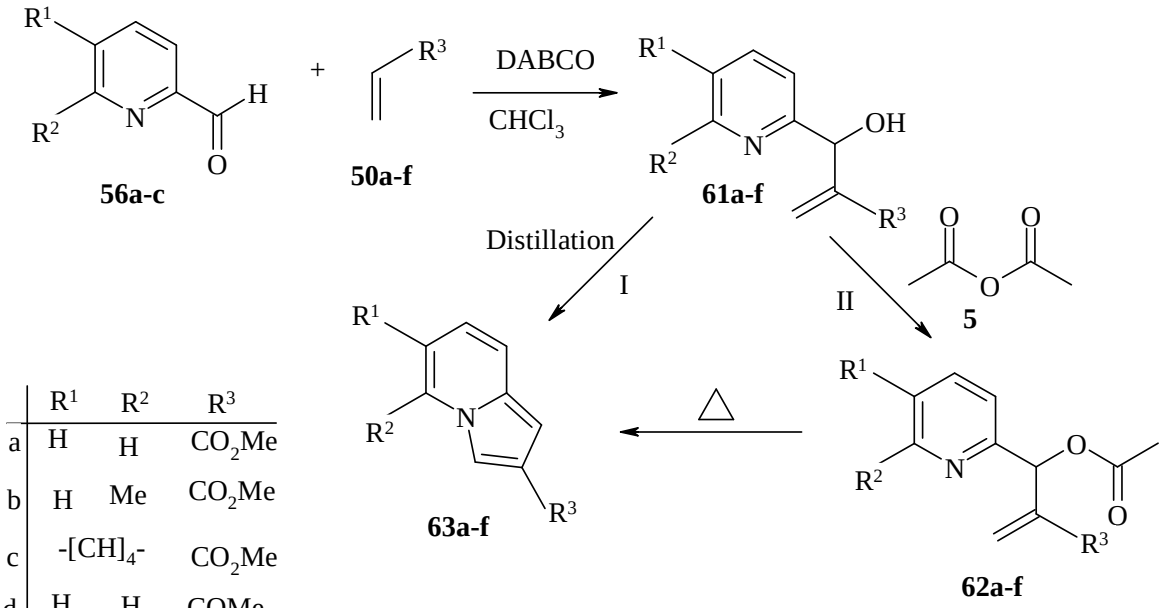

	R1	R2	R3
a	H	H	CO_2Me
b	H	Me	CO_2Me
c	-[CH]$_4$-		CO_2Me
d	H	H	COMe
e	H	H	COEt
f	H	H	CN

Scheme 15

The method was then modified to improve the yields by refluxing Baylis-Hillman adducts **61a-f** in acetic anhydride **5** to obtain the acetylated Baylis-Hillman derivatives **62a-f**.[67, 70] Thereafter, thermal cyclisation of the acetylated Baylis-Hillman derivatives **62a-f** afforded the indolizine derivatives **63a-f** in good yields (Scheme 15, route II).[70]

Attention was also given to -: (i) the synthesis of indolizine-2-carboxamides from the reaction of indolizine-2-carboxylic acid with various amines in the presence of the coupling agent, 1,1'-carbonyldiimidazole (CDI);[68] (ii) exploring physical organic properties of these indolizine-2-carboxamides, in particular Dynamic NMR studies of rotational isomerism;[68] and (iii) kinetic and mechanistic studies on the formation of indolizine derivatives *via* thermal cyclisation of the acetylated Baylis-Hillman adduct.[70]

Success in the synthesis of indolizine derivatives using Baylis-Hillman methodology prompted further investigations into the preparation of other heterocyclic systems. These studies led to the chemoselective synthesis of chromene derivatives **66** (Scheme 16, path I) and coumarin derivatives **67** (Scheme 16, path II) from various salicyldehydes **64** and activated alkenes **50a,** or **50d**.[129-133] Also, the synthesis of quinoline and quinolone derivatives from the reactions of 2-nitrobenzaldehyde **68** and methyl acrylate **50a** or ethyl acrylate **50b** in the presence of DABCO, afforded the Baylis-Hillman adduct **69**, which was then subjected to catalytic hydrogenation to afford a mixture of quinoline **70** and 2-quinolone **71** derivatives (Scheme 17).[134-141] The applicability of the Baylis-Hillman methodology was also shown in the synthesis of heterocyclic systems containing sulfur heteroatom(s), namely the thiochromenes,[65, 144] where 2-mercaptobenzoic acid **72** was reduced to mercaptobenzyl alcohol **73**, followed by spontaneous formation of the disulphide **74**. The disulphide was then subjected to the Baylis-Hillman reaction conditions to afford the desired thiochromene derivative **75** (Scheme 18).

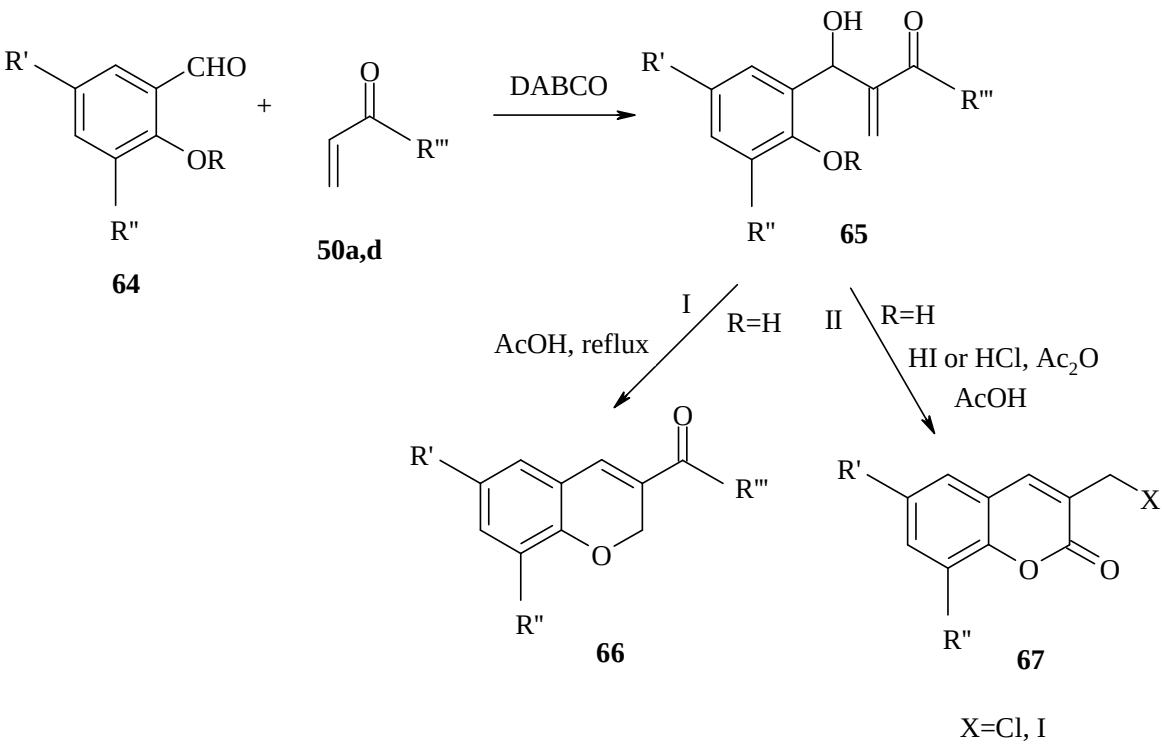

Scheme 16

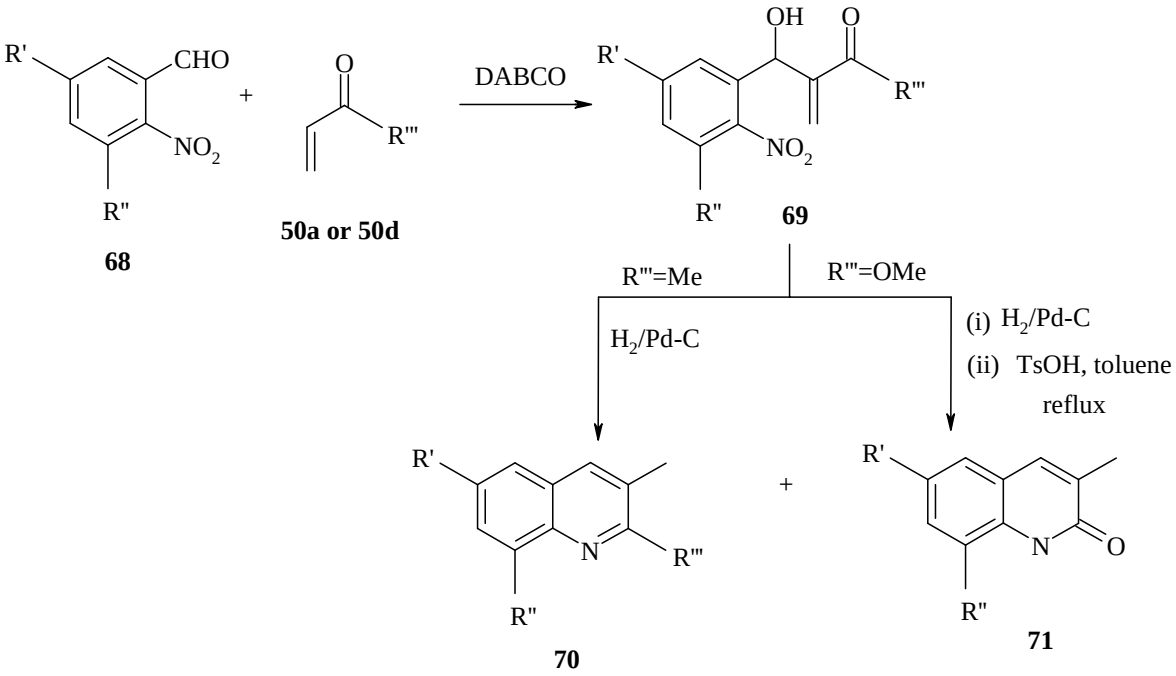

Scheme 17

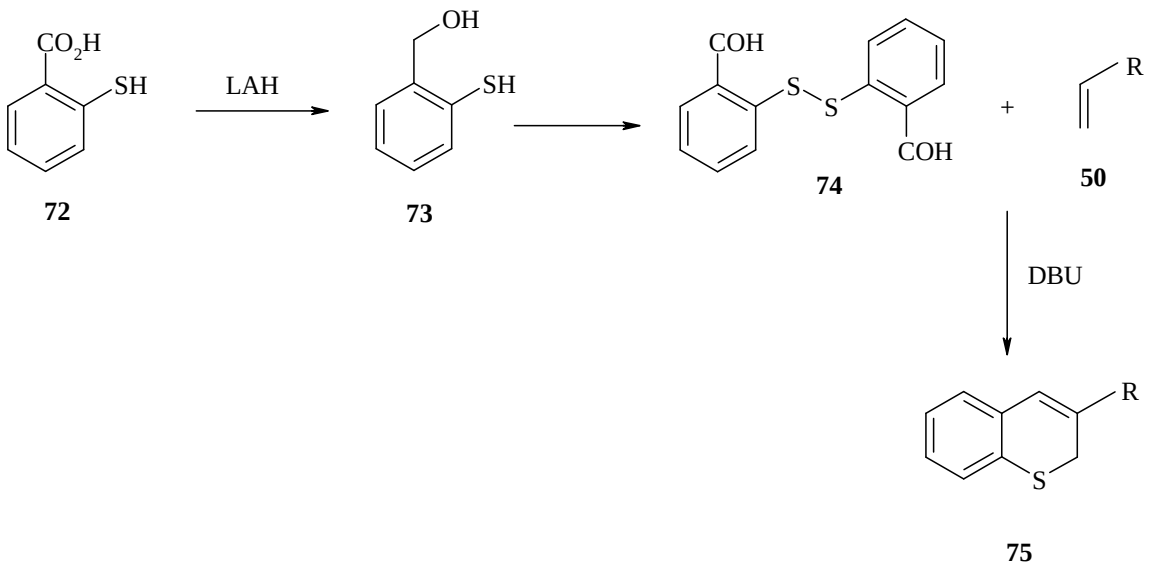

Scheme 18

1.4.2. Previous work on HIV-1 protease inhibitors

Attention within the group has also been given to the preparation of Baylis-Hillman derived heterocyclic systems as analogues of Ritonavir, [22, 38] an HIV-1 protease inhibitor (Figure 7). The heterocyclic systems employed for this study were chromene, coumarin and thiochromene derivatives.[145] The approach involved the attachment of the amino termini of the hydroxyethylene dipeptide isostere **76** (Scheme 19) to the synthesized heterocyclic systems *via* a coupling reaction.

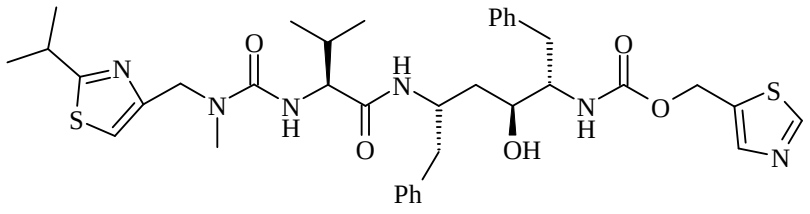

Ritonavir

Figure 7. Ritonavir structure.

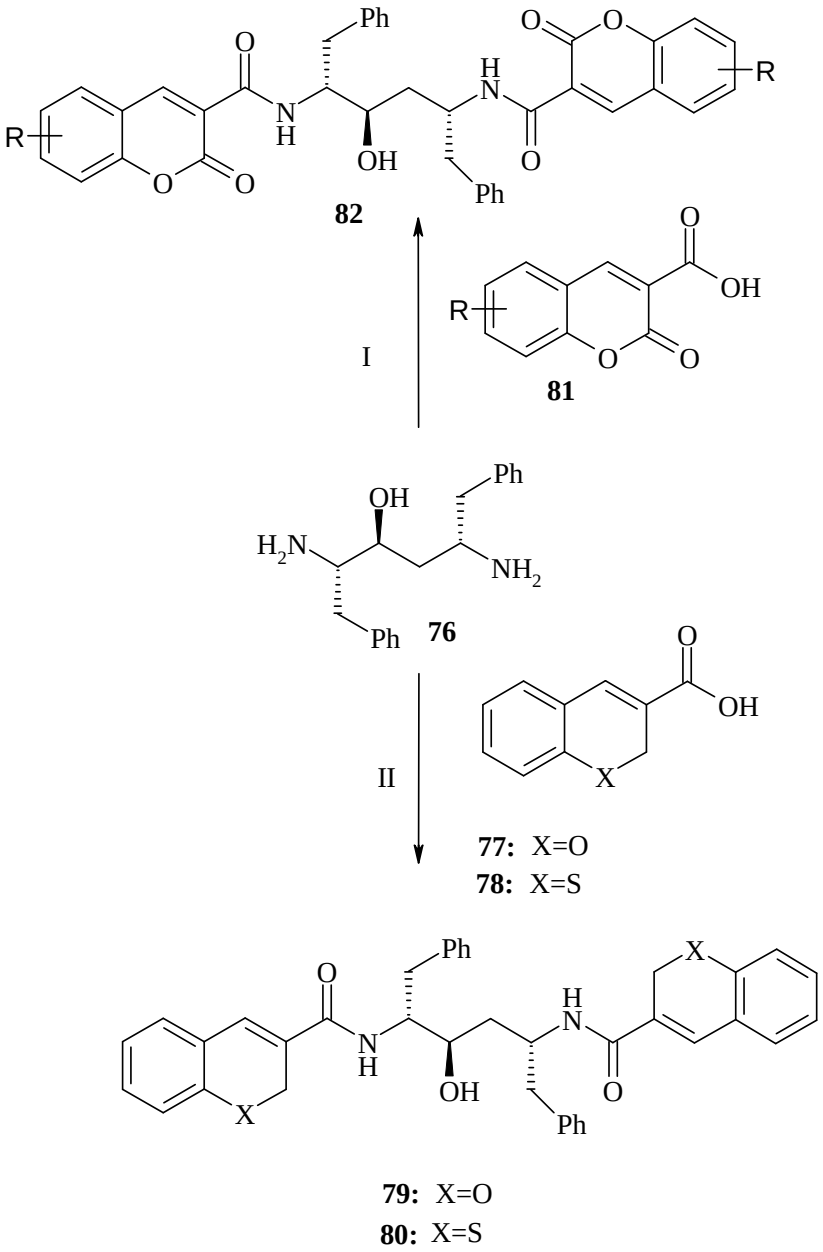

Scheme 19
Reagents: EDC, HOBt, Et_3N, DMF

The first step in the synthetic sequence involved the preparation of the hydroxyethylene dipeptide isostere moiety **76** following a literature method. A series of coumarin-2-carboxylic acids **81** were then coupled to the free terminal amino groups of the non-hydrolysable dipeptide isostere **76**, in the presence of the coupling agent, *N*-ethyl-*N*'-(dimethylaminopropyl)carbodiimide hydrochloride (EDC), and 1-hydroxybenzotriazole

(HOBt), to afford *bis*-coumarin Ritonavir® analogues **82** (Scheme 19, path I). The same synthetic procedure was applied to the chromone- **77** and thiochromene-2-carboxylic acids **78** to afford the corresponding *bis*-chromene and *bis*-thiochromene Ritonavir® analogues (Scheme 19, path II).[65, 145] In computer modelling studies, the ligands **79-82** showed negative Van der Waals protein-ligand interaction energies, indicating their potential to bind to the HIV-1 protease receptor cavity.[145] Furthermore, *in vitro* enzyme-inhibition assays indicated that some of these analogues have the potential to act as HIV-1 protease inhibitors.[145]

1.5. Aims of the present study

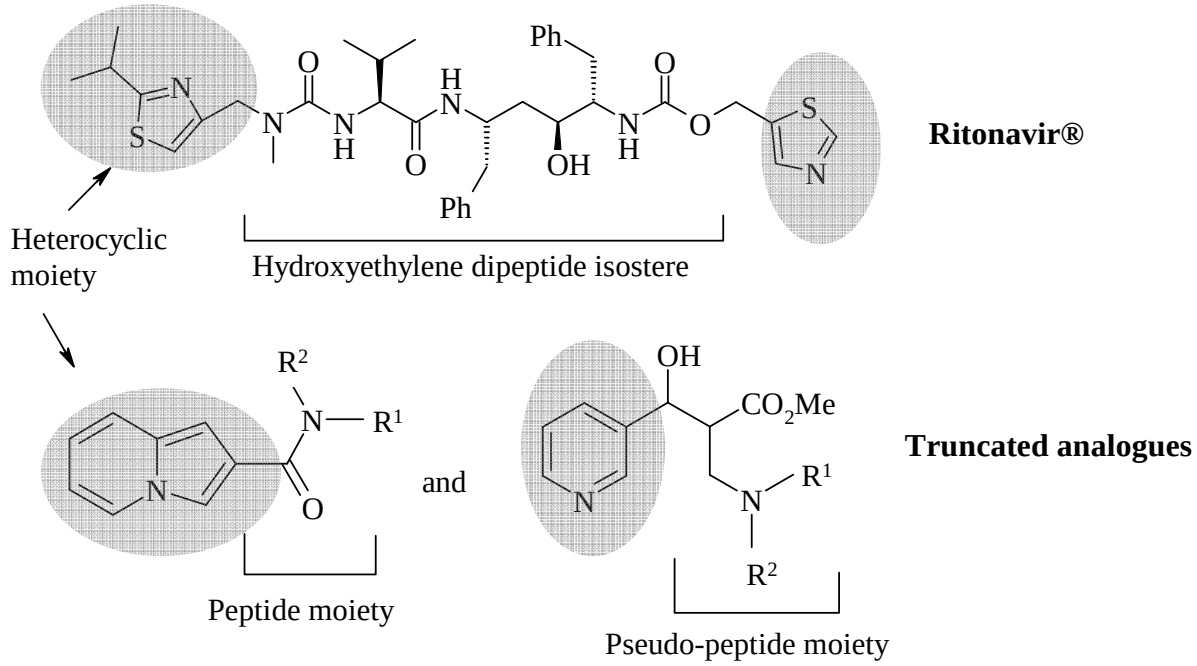

Figure 8.

In light of the previous work done in our research group, the aims of the present study have been to synthesize pseudo-peptide based truncated Ritonavir® analogues bearing an indolizine or pyridine heterocyclic moiety as potential inhibitors of HIV-1 protease (Figure 8). More specifically, this project has involved the following objectives.

(i) The preparation of a range of *N*-substituted indolizine-2- and pyrrolo[1,2-*a*]quinoline-2-carboxamides and pyridine-based aza-Michael adducts using Baylis-Hillman methodology.

(ii) The application of 1-D and 2-D NMR spectroscopy and computer modelling techniques in assigning the relative stereochemistry of the aza-Michael products.

(iii) The application of AUTODOCK 4.0 software to explore *in silico* docking of the synthetic ligands in the HIV-1 protease enzyme receptor cavity.

(iv) Saturation transfer difference (STD) protein NMR analysis of the binding potential of various ligand systems.

2. DISCUSSION

In line with the identified aims, attention in this discussion will be given to: - the preparation of Baylis-Hillman adducts (Section 2.1); thermal cyclisation of the Baylis-Hillman adducts to afford indolizine derivatives (Section 2.2); one-pot synthesis of indolizine derivatives (2.2.1); synthesis of indolizine-2-carboxamide and pyrrolo[1,2-*a*]quinoline-2-carboxamide derivatives (Section 2.3); synthesis of aza-Michael products (Section 2.4); and, finally, computer modelling, molecular docking and protein NMR studies of selected compounds (Section 2.5).

2.1. Preparation of Baylis-Hillman adducts

In this study, Baylis-Hillman methodology was used to prepare pyridine- and quinoline-based Baylis-Hillman adducts. The approach developed in our research group by Bode, [66-67] involved the reaction of aldehydes **56a-c, g** and **h** with methyl acrylate **50a** in chloroform, using DABCO or 3-hydroxyquinuclidine (3-HQ) as the nucleophilic catalyst (Scheme 20). The reactions proceeded as anticipated; the crude products were purified by flash chromatography to afford the desired adducts **61a-c, g** and **h** in yields ranging from good to excellent as shown in the Table 1. In each case, the progress of the Baylis-Hillman reaction was monitored by thin layer chromatography (TLC) and it was observed that all of the aldehydes were completely consumed in the presence of DABCO except quinoline-2-carbaldehyde **56c**, which had undergone little conversion after 7 days.

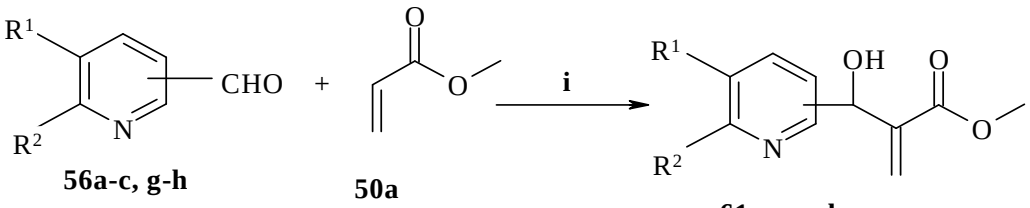

	R^1	R^2
a	H	H
b	H	Me
c	$-C_4H_4-$	
g	H	H
h	H	H

Scheme 20

Reagents: (i) DABCO or 3-HQ, $CHCl_3$

This problem was solved by using 3-HQ as the catalyst; again the reaction was monitored by TLC and, after 4 days, conversion to the desired Baylis-Hillman adduct **61c** was found to be almost complete. The adducts **61a-c, g** and **h** were fully characterized by spectroscopic (IR, 1- and 2-dimensional NMR) analysis.

Table 1. Reaction times and yields of the Baylis-Hillman adducts **61a-c, g** and **h**. (scheme 20)

61	Compound name	Time (hrs)	Yield (%)
a	Methyl 2-[hydroxy(pyridin-2-yl)methyl]acrylate	72	93
b	Methyl 2-[hydroxy(6-methylpyridin-2-yl)methyl]acrylate	48	87
c	Methyl 2-[hydroxy(quinolin-2-yl)methyl]acrylate	96	96
g	Methyl 2-[hydroxy(pyridin-3-yl)methyl]acrylate	72	100
h	Methyl 2-[hydroxy(pyridin-4-yl)methyl]acrylate	72	79

Figure 9 illustrates the assignment of significant proton signals in the ^{1}H NMR spectrum of compound **61c**. The spectrum reveals a singlet at 3.67 ppm corresponding to the methoxy group (OMe), a broad singlet at 5.68 ppm due to the hydroxyl proton (OH) and three signals, characteristic of Baylis-Hillman products, at 5.87, 5.97 and 6.36 ppm corresponding to the methine proton on the stereogenic centre C-3 and the diastereotopic vinylic methylene protons, respectively. The quinoline ring protons resonate, as expected, in the aromatic region, with the two doublets at 7.42 and 7.82 ppm due to the 3'- and 4'-methine protons, respectively. The two triplets at 7.52 and 7.70 ppm are due to the 7'- and 8'-methine protons, while the doublets at 8.08 and 8.11 ppm are due to the 6'- and 9'-protons. The corresponding ^{13}C NMR spectrum (Figure 10) of product **61c** exhibits 14 carbon signals as expected. The methoxy carbon resonates at 51.6 ppm, the stereogenic centre C-3 resonates at 71.7 ppm, the methylene carbon at 127.1 ppm, the aromatic and vinylic (C-2) carbons in the range of 118-160 ppm and the carbonyl carbon at 166.3 ppm. Infra-red spectroscopy revealed the hydroxyl (OH) and carbonyl (C=O) stretching bands

at 3260 and 1735 cm^{-1}, respectively, while the base peak in the low-resolution mass spectrum at *m*/*z* 244 corresponds to the protonated molecular ion.

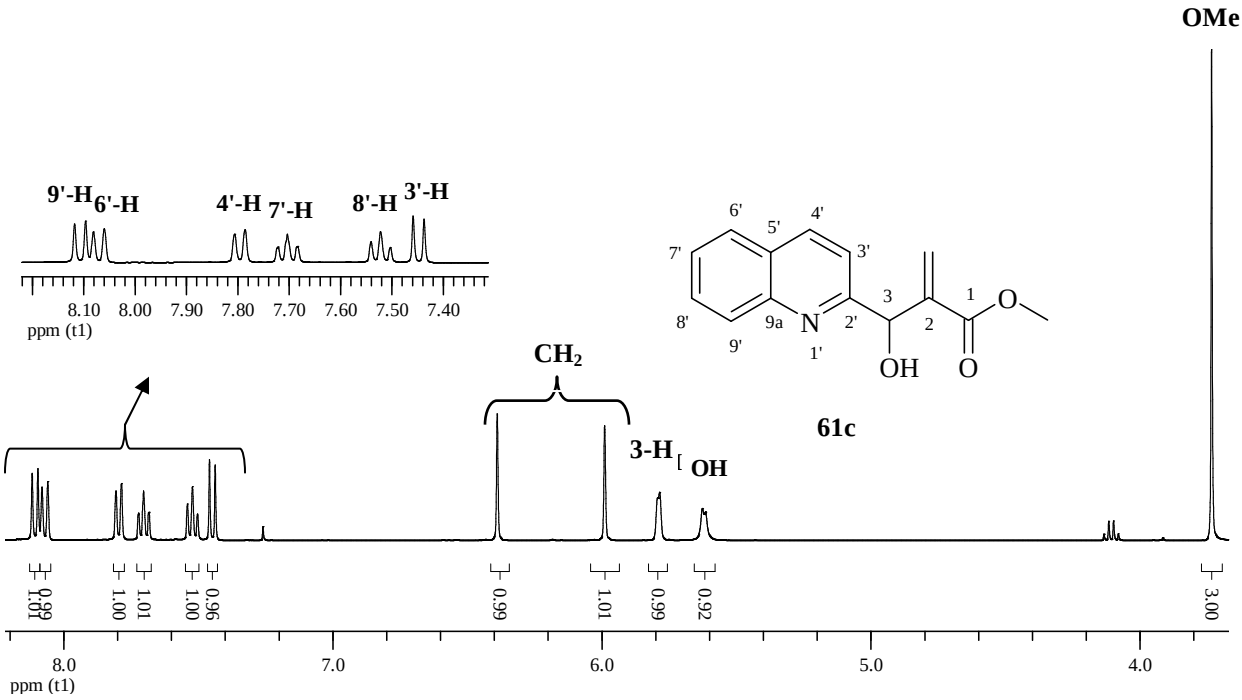

Figure 9. 400 MHz ^{1}H NMR spectrum of the Baylis-Hillman adduct **61c** in $CDCl_3$.

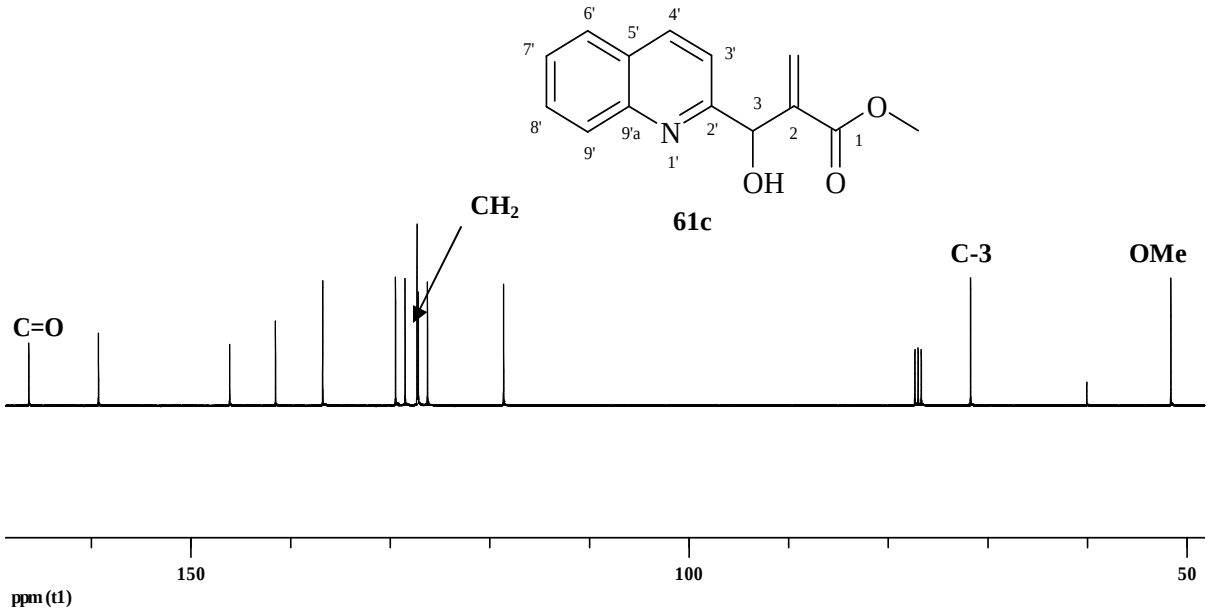

Figure 10. 100 MHz ^{13}C NMR spectrum of the Baylis-Hillman adduct **61c** in $CDCl_3$.

With the multi-functional Baylis-Hillman adducts in hand, a number of transformations could be achieved. Examples of these transformations included oxidation of the hydroxyl group (Dess-Martin) [95] (path **A**), cyclisation (path **B**), conjugate addition (path **C**) [65, 117] and nucleophilic substitution with allylic rearrangement (S_N') (path **D**) (Scheme 21).

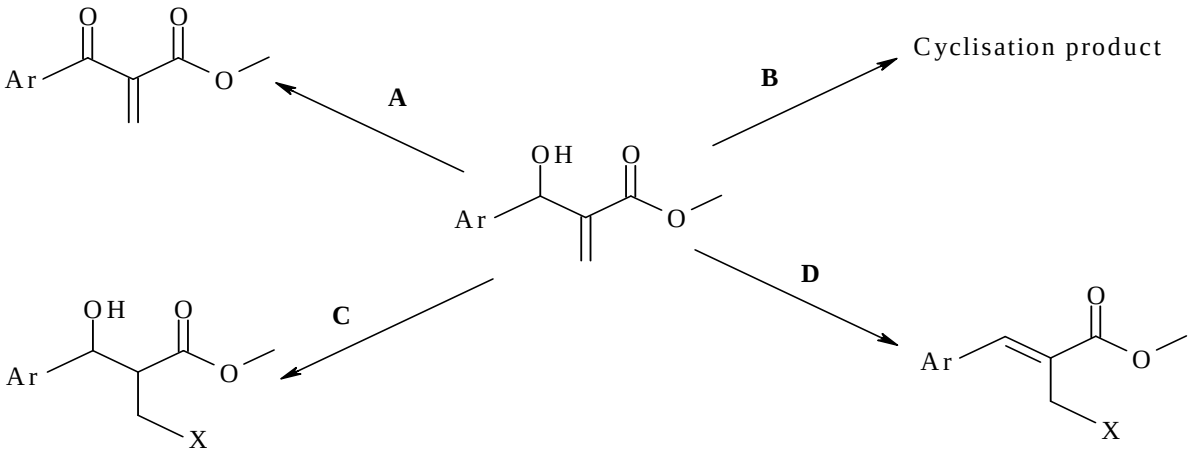

Scheme 21

2.2. Thermal cyclisation of the Baylis-Hillman adducts into indolizine derivatives

2.2.1. Step-wise synthesis of indolizine derivatives

Only those Baylis-Hillman adducts containing a nucleophilic centre at position 2 of the attached heterocyclic system are able to undergo intramolecular cyclisation. The first step in the cyclisation method involved refluxing the Baylis-Hillman adducts **61a-c** with acetic anhydride **5** to give the acetylated Baylis-Hillman adducts **62a-c.** In the event, the acetylated derivatives were isolated together with the corresponding indolizine derivatives **63a-c** (Scheme 22). Moreover, during the acetylation of adduct **61c**, an acetylated indolizine derivative **83** was formed and isolated as a minor product (5.8%). Thermal cyclisation to indolizine derivatives can be achieved directly without acetylating the Baylis-Hillman adducts **61a-c**, but Bode [66-67] had discovered that this leads to lower indolizine yields. Changing the hydroxyl group of the Baylis-Hillman adducts into an

acetoxy group affords a better leaving group. The structures of all the products (**62a-c** and **63a-c**) obtained were confirmed by ^{1}H and ^{13}C NMR analysis.

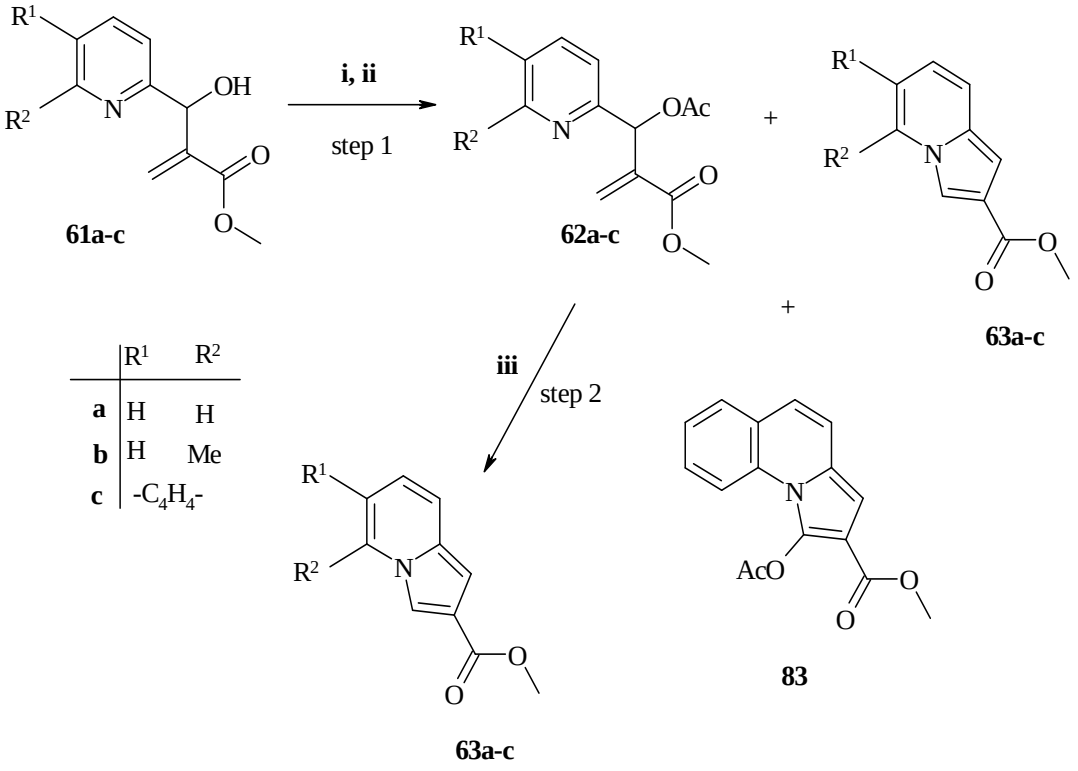

Scheme 22
Reagents: (i) Acetic anhydride, reflux, 30 minutes; (ii) $NaHCO_3$-ice; (iii) 120 °C.

The only significant differences between the ^{1}H NMR spectrum of the acetylated derivative **62c** (Figure 11) and that of the precursor **61c** (Figure 9) are the disappearance of the hydroxyl proton signal at 5.68 ppm and the appearance of the new methyl signal of the acetoxy group at 2.17 ppm, thus confirming acetylation of the hydroxyl group. Similarly, the differences between the ^{13}C NMR spectrum (Figure 10) of compound **61c** and that of compound **62c** (Figure 12) are the appearance in the latter of the signals at 20.9 and 169.5 ppm due to the acetyl methyl and carbonyl carbons, respectively.

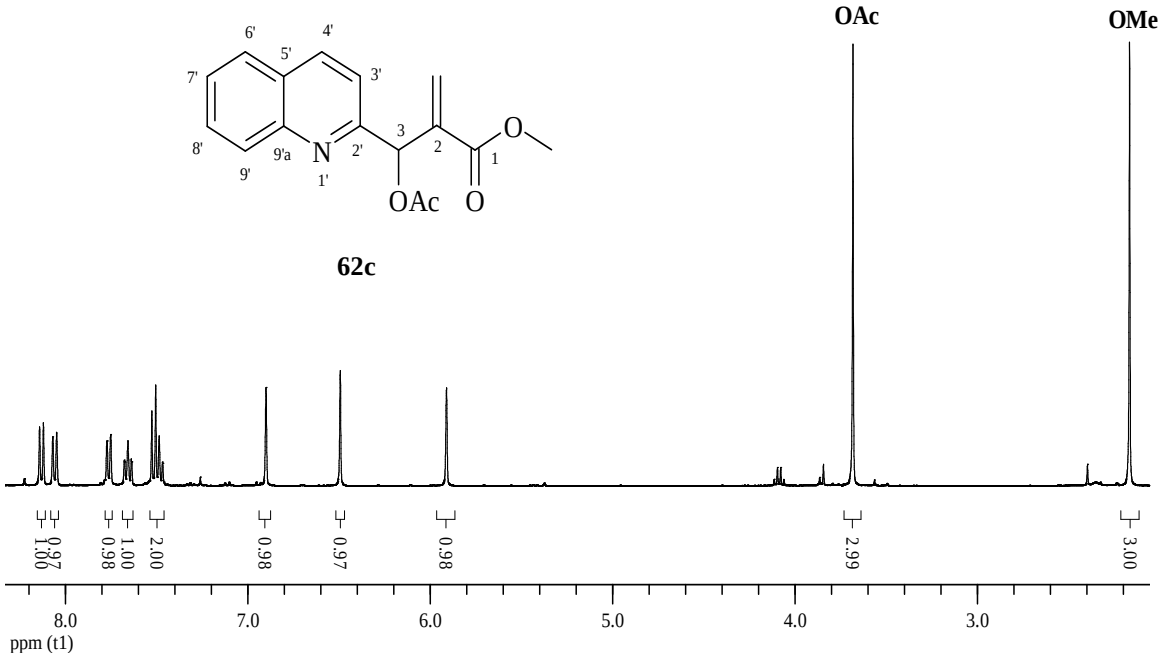

Figure 11. 400 MHz ^{1}H NMR spectrum of the Baylis-Hillman adduct **62c** in $CDCl_3$.

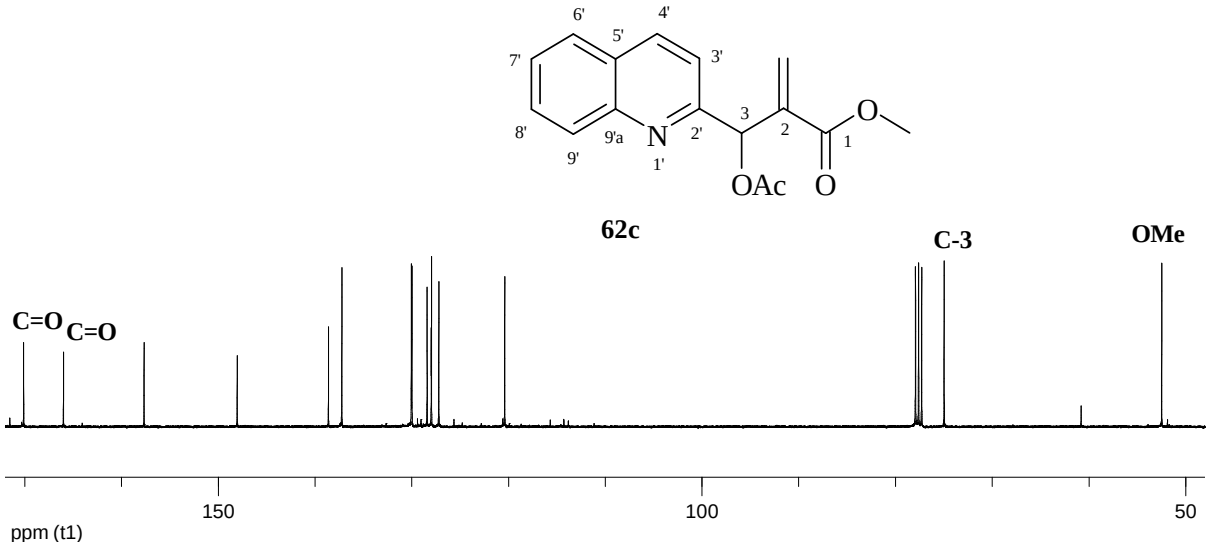

Figure 12. 100 MHz ^{13}C NMR spectrum of the Baylis-Hillman adduct **62c** in $CDCl_3$.

The structure of compound **83** is supported by the 1-D and 2-D NMR, IR, high-resolution mass spectroscopy (HRMS) data and the fragmentation pattern in the low-resolution mass spectrum. The isolation of compound **83** was surprising due to the fact that the acetoxy functional group, a good leaving group, was still attached and it was located at C-1 (not C-3) of the indolizine system. The proposed mechanism (Scheme 23) for the

formation of compound **83** involves conjugate addition of the acetate ion *via* an S_N' allylic rearrangement pathway [to the Baylis-Hillman adduct **61c** (R=H) or its acetylated derivative **62c** (R=Ac)] to afford the acetylated compound **84a**. Subsequent loss of a proton to another acetate ion then yields a resonance-stabilised anion **84b**. Intramolecular cyclisation *via* the "aza-Nazarov" cyclisation [146] affords compound **85**, which is further stabilized by the loss of a second proton to give the acetylated indolizine derivative **83**.

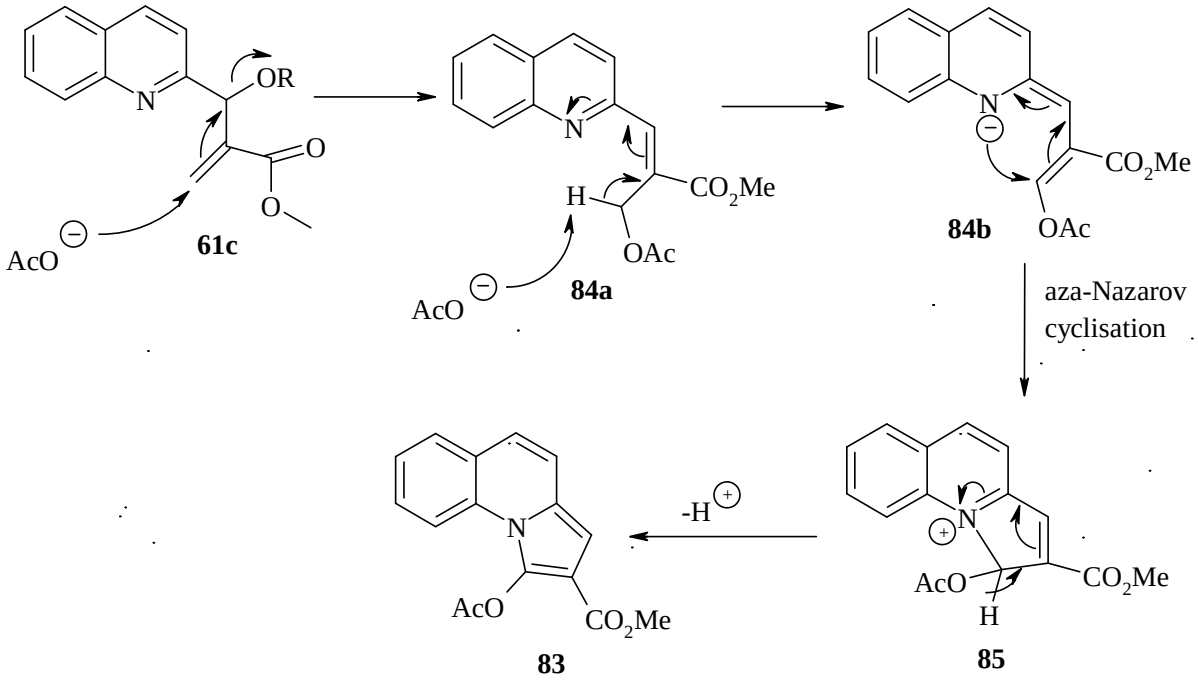

Scheme 23

The ^{1}H NMR spectrum (Figure 13) of compound **83** reveals clearly the disappearance of the characteristic Baylis-Hillman vinylic protons, usually found in the region 5.5-6.5 ppm, while a number of new signals are present in the aromatic region. The upfield singlets at 2.42 and 3.86 ppm are due to the acetoxy and methoxy protons, respectively. The data from the HSQC spectrum (Figure 14) was used to assign the aromatic signals and confirm other signal assignments. The carbon signals resonating at 113.8 and 114.3 ppm correlate with 3- and 9-methine protons at 8.26 and 7.88 ppm, while the carbon signals at 111.0, 122.7 and 124.7 are assigned to the quaternary carbons, C-1, C-2 and C-3a, respectively, because of the lack of correlation to any proton signals. Similarly, the signals beyond 129.3 ppm correspond to the other quartenary carbons, C-5a and C-9a and

the carbonyl carbons, as evidenced by the lack of correlation with any proton signals in the HSQC spectrum (Figure 14). Infra-red spectroscopy revealed the two carbonyl stretching bands at 1701 and 1752 cm^{-1}, while the base peak in the low-resolution mass spectrum at *m/z* 209 corresponds to the loss of $C_3H_6O_2$ from the molecular ion involving, we suggest, the loss of methyl acetate *via* the fragmentation detailed in Scheme 24.

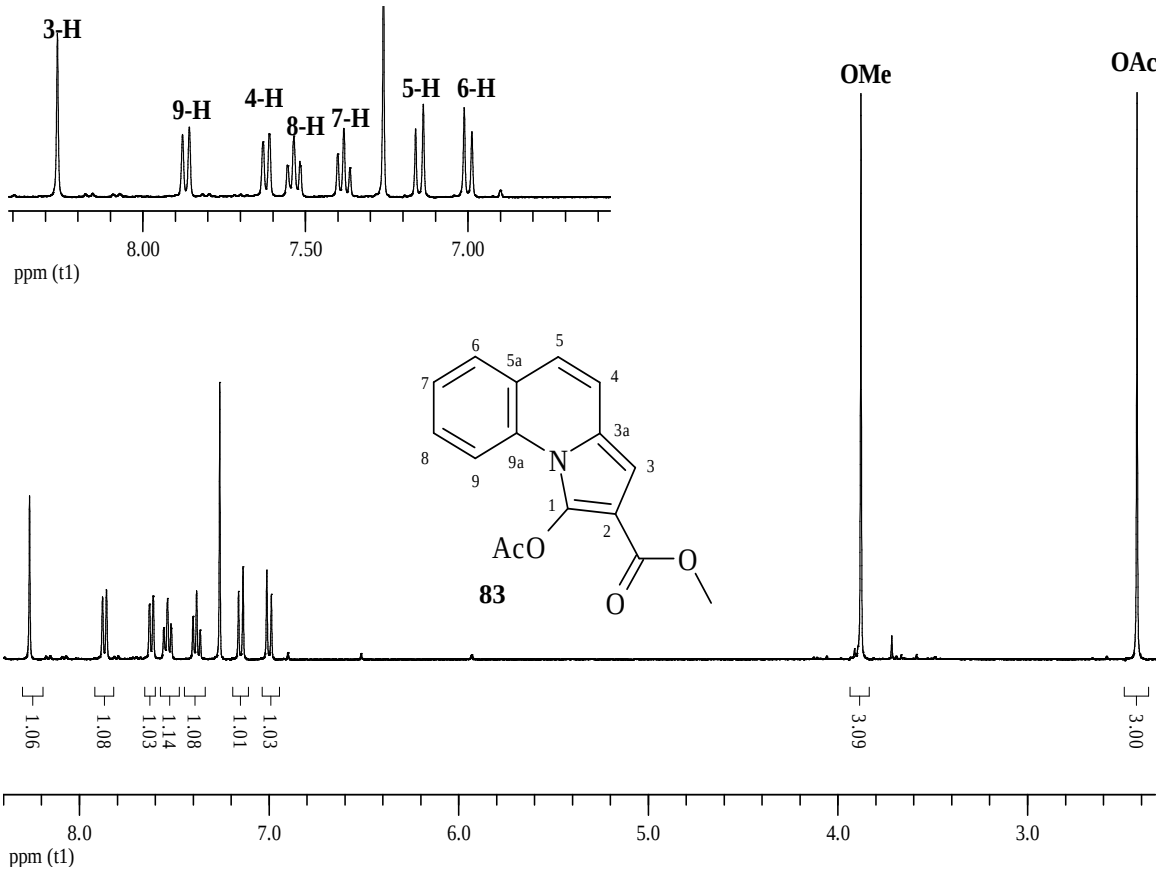

Figure 13. 400 MHz ^{1}H NMR spectrum of compound **83** in $CDCl_3$.

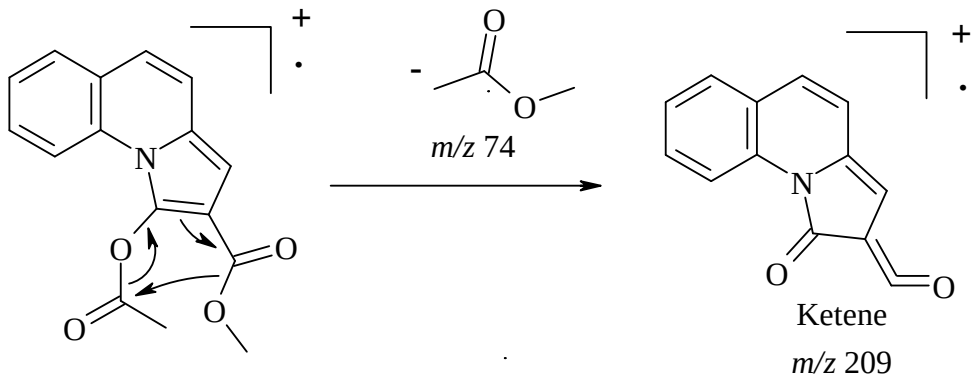

Scheme 24

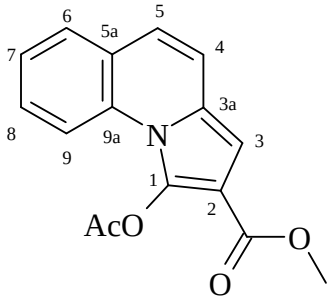

83

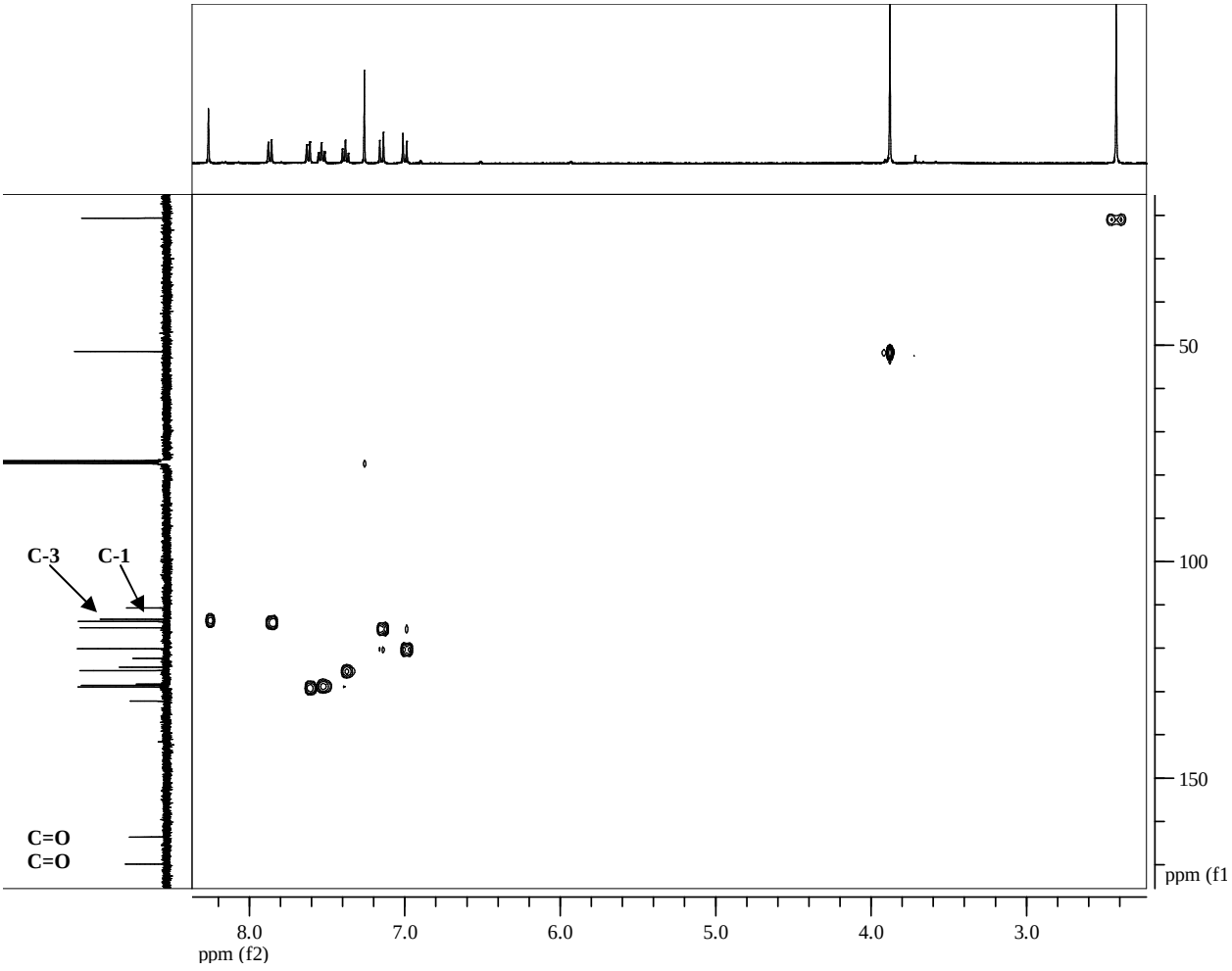

Figure 14. HSQC NMR spectrum of compound **83** in $CDCl_3$.

The second step in the cyclisation sequence involved heating the acetylated adducts **62a-c** at 120 °C for 1hr to obtain the indolizine derivatives **63a-c** in 70-77% yield (Scheme 22). The mechanism proposed by Bode *et al*. [66-67] for the observed cyclisation involves the addition-elimination sequence as outlined in Scheme 25. The first step (contrary to the proposed mechanism for compound **83**) is the intramolecular cyclisation, which is followed by allylic rearrangement and loss of the leaving group, designated OR (II) and, lastly, loss of a proton to give rise to the fully conjugated indolizine derivative (III).

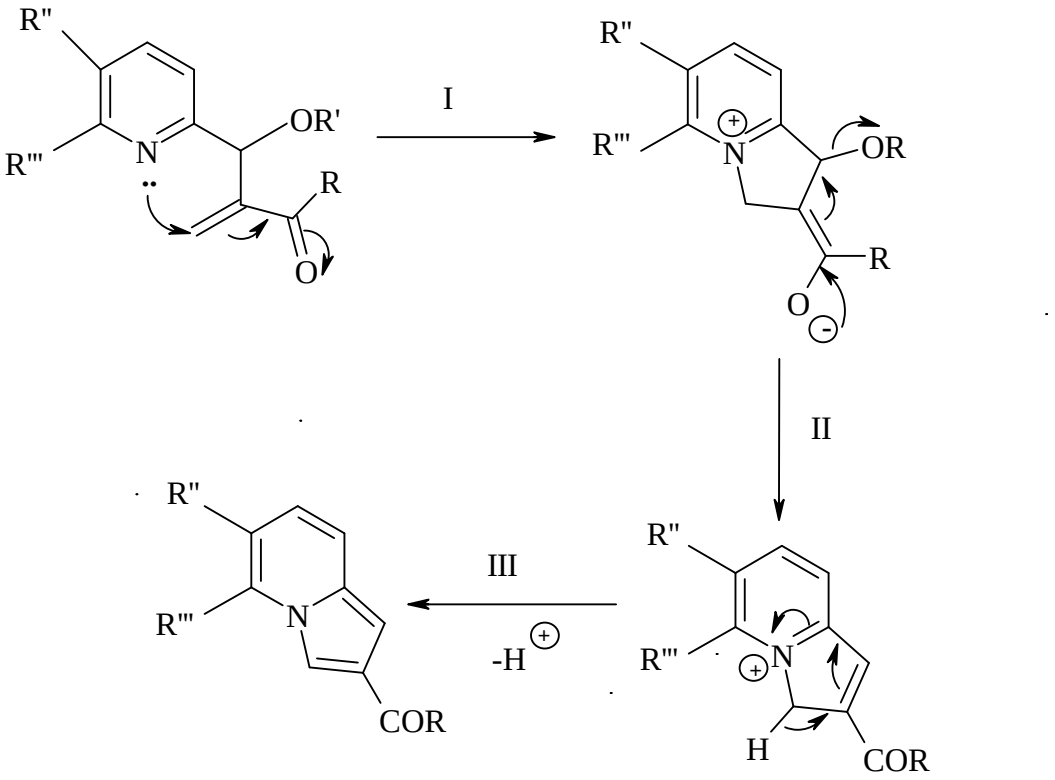

Scheme 25

Figure 15 illustrates the assignment of the proton signals in the ^{1}H NMR spectrum of compound **63b**. The spectrum, like that of compound **83**, reveals that the characteristic Baylis-Hillman vinylic proton signals have disappeared, while a number of new signals are present in the aromatic region; the singlets at 2.50 and 3.90 ppm correspond to the 5-methyl (C-10) and the methoxy protons, respectively. The doublets at 6.43 and 7.32 ppm are due to the 8- and 6-methine protons, and the singlets at 6.91 and 7.72 ppm are due to the 1- and 3-methine protons, respectively. The ^{13}C NMR spectrum (Figure 16) shows the

expected 11 carbon signals, with the 10-methyl carbon resonating at 18.5 ppm, the methoxy carbon at 51.4 ppm and the carbonyl carbon at 165.8 ppm.

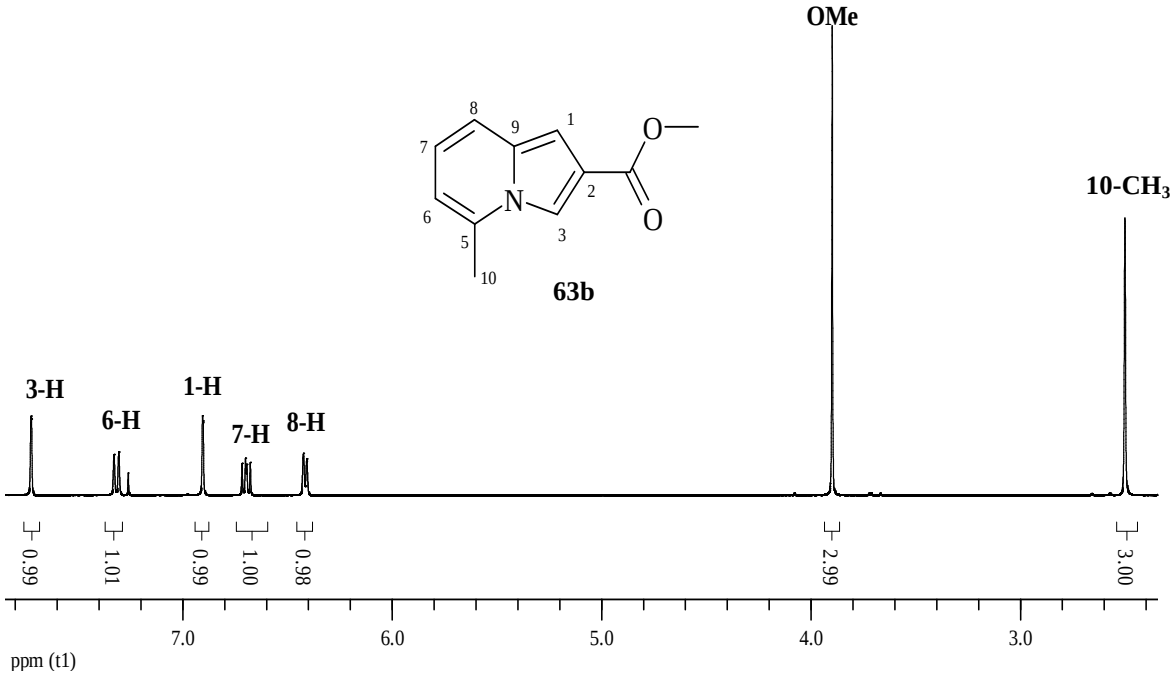

Figure 15. 400 MHz ^{1}H NMR spectrum of compound **63b** in $CDCl_3$.

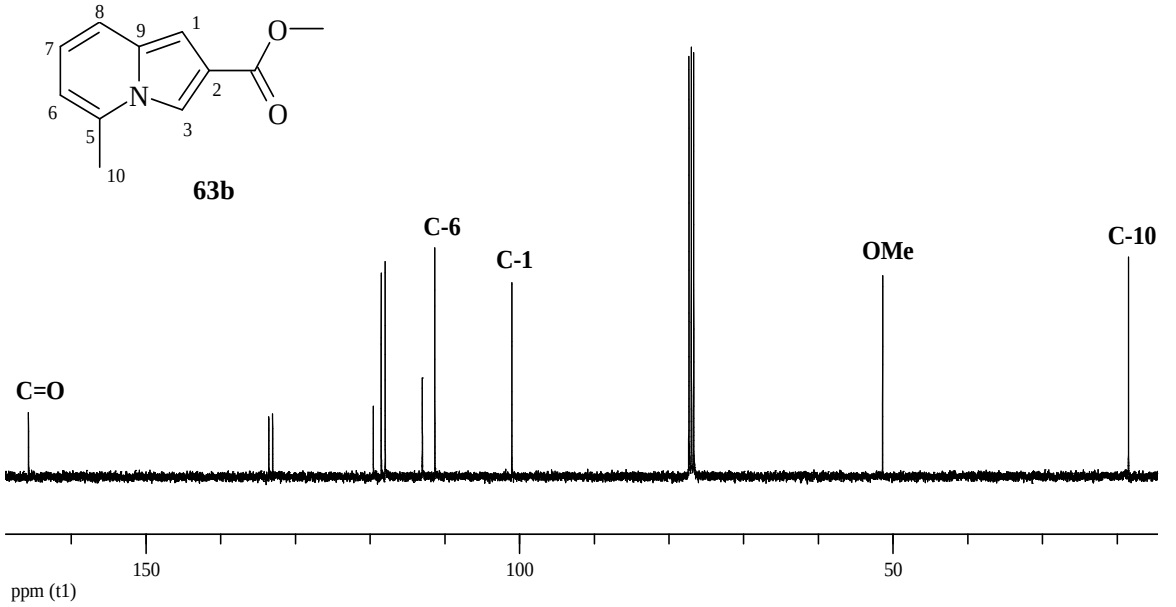

Figure 16. 100 MHz ^{13}C NMR spectrum of compound **63b** in $CDCl_3$.

2.2.2. One-pot synthesis of indolizine derivatives

Following the one-pot procedure described by Basavaiah *et al*., [69] 2-acetylindolizine **63d**, 2-propanoylindolizine **63e** and indolizine-2-carbonitrile **63f** were synthesized successfully in 91, 39 and 66% yield, respectively (Scheme 26), from the reaction of pyridine-2-carbaldehyde **56** with methyl vinyl ketone **50d**, ethyl vinyl ketone **50e** and acrylonitrile **50f** in the presence of trimethylsilyl chloride (TMSCl), instead of the triflouromethanesulfonate (TMSOTf) used in the original publication. These compounds have been synthesized previously in our group, using DABCO as the catalyst.[66-67] However, attempts to generalize the application of this method [69] failed to yield the desired products when the activated alkenes, methyl acrylate **50a**, phenyl vinyl sulfone **50g** and phenyl vinyl sulfonate **50h**, were used.

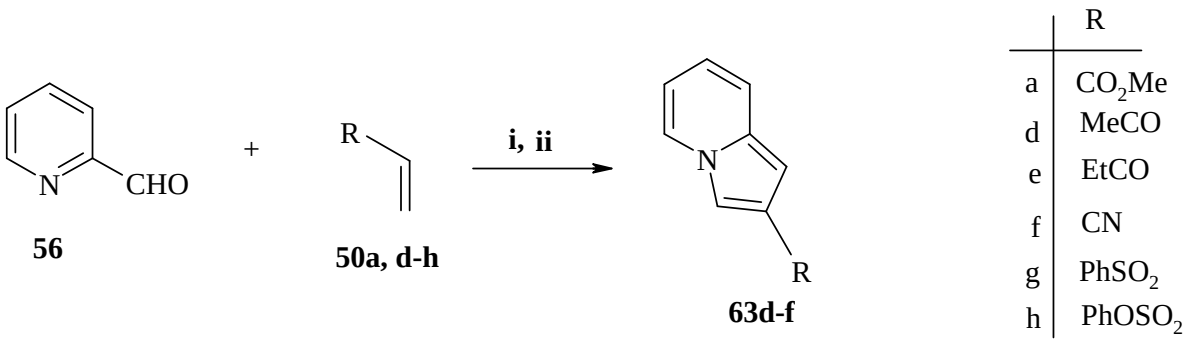

Scheme 26
Reagents: (i) TMSCl (1 eq), CH_3CN, 0 °C to rt, 12 h.; (ii) K_2CO_3 (aq)

The assignment of signals in the ^1H NMR spectrum of compound **63f** are shown in Figure 17. The ^{13}C NMR spectrum (Figure 18) shows the expected 9 carbon signals, with the nitrile carbon resonating at 116.4 ppm. Infra-red spectroscopy confirmed the presence of the nitrile stretching band at 2355 cm^{-1}, while the base peak in the low-resolution mass spectrum at *m/z* 142 corresponds to the molecular ion.

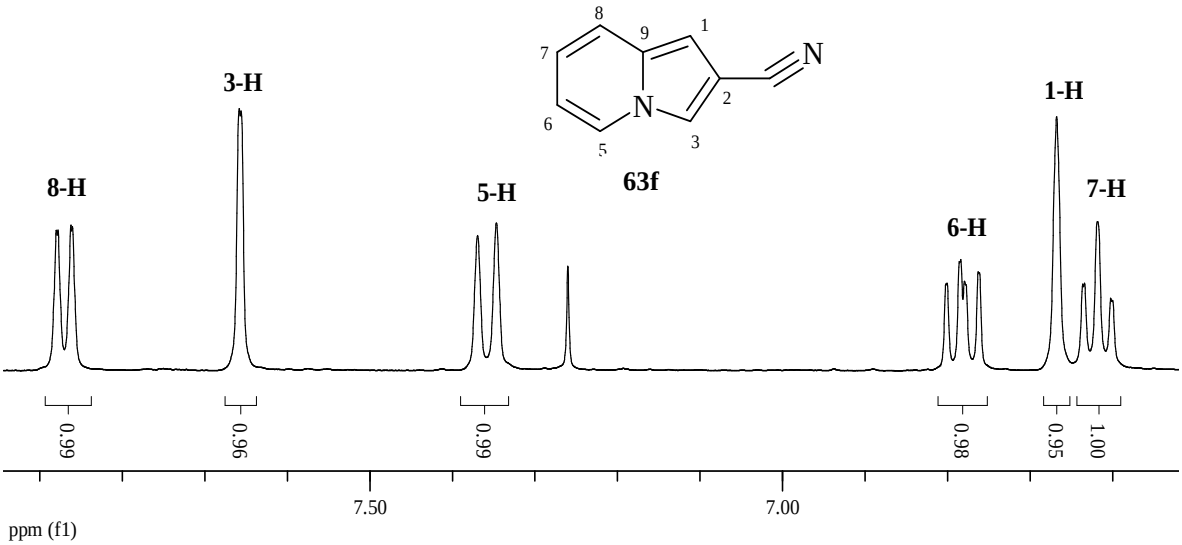

Figure 17. 400 MHz ^{1}H NMR spectrum of compound **63f** in $CDCl_3$.

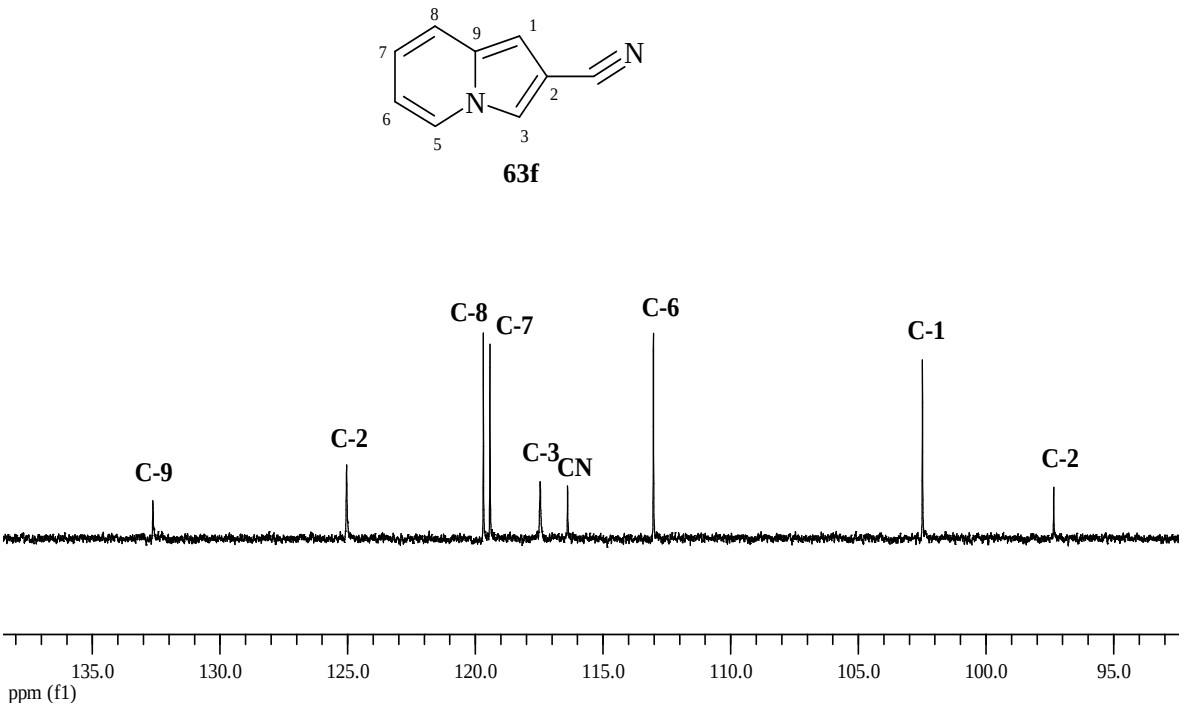

Figure 18. 100 MHz ^{13}C NMR spectrum of compound **63f** in $CDCl_3$.

2.3. Synthesis of indolizine-2- and pyrrolo[1,2-*a*]quinoline-2-carboxamides

The procedure followed for the preparation of indolizine-2-carboxamides **89**-**101**, first reported by Bode [66-68] in 1994, involves a two step process. Hydrolysis of the indolizine-2-carboxylate esters to afford indolizine-2-carboxylic acids was effected by refluxing the esters in ethanolic potassium hydroxide for 16 hrs; the neutralized acids were then reacted with amines using 1,1'-carbonyldiimidazole (CDI) as the coupling agent. In the present study, the indolizine-2-carboxylic acids **87a-c** were obtained in quantitative yields using this approach, and their formation was confirmed by NMR, IR and low-resolution MS analysis. The carboxylic acids were then reacted with various amino compounds, *viz*., 1-methyl-5-(diethylamino)butylamine **88**, *S*-benzylcysteamine **90**, glycine ethyl ester **92**, L-serine ethyl ester **94**, glycine methyl ester **96**, L-proline methyl ester **98**, and the dipeptide, *N*-acetyl-glycine-lysine methyl ester **100**, in the presence of (CDI), to afford the corresponding indolizine-2-carboxamides **89**-**101** (Scheme 27, Table 2). Amines available as hydrochloride salts were neutralized by the addition of a base and the novel indolizine-2-carboxamides **89**-**101** were all fully characterized by spectroscopic (IR, 1- and 2-dimensional NMR) and elemental (HRMS) analysis.

2.3.1. Coupling with *S*-benzylcysteamine hydrochloride

The indolizine-2-carboxylic acids **87a-c** and CDI were each dissolved in dry DMF and the mixtures heated at 40°C for 5 minutes. Thereafter, the mixtures were allowed to cool to room temperature and then treated with *S*-benzylcysteamine hydrochloride **90** and pyridine, an organic base, to neutralize the hydrochloride salt and release the nucleophilic amine (Scheme 27). Purification of the crude products using preparative layer chromatography afforded the corresponding indolizine-2-carboxamide derivatives **91a-c** in 64-97% (see Table 2).

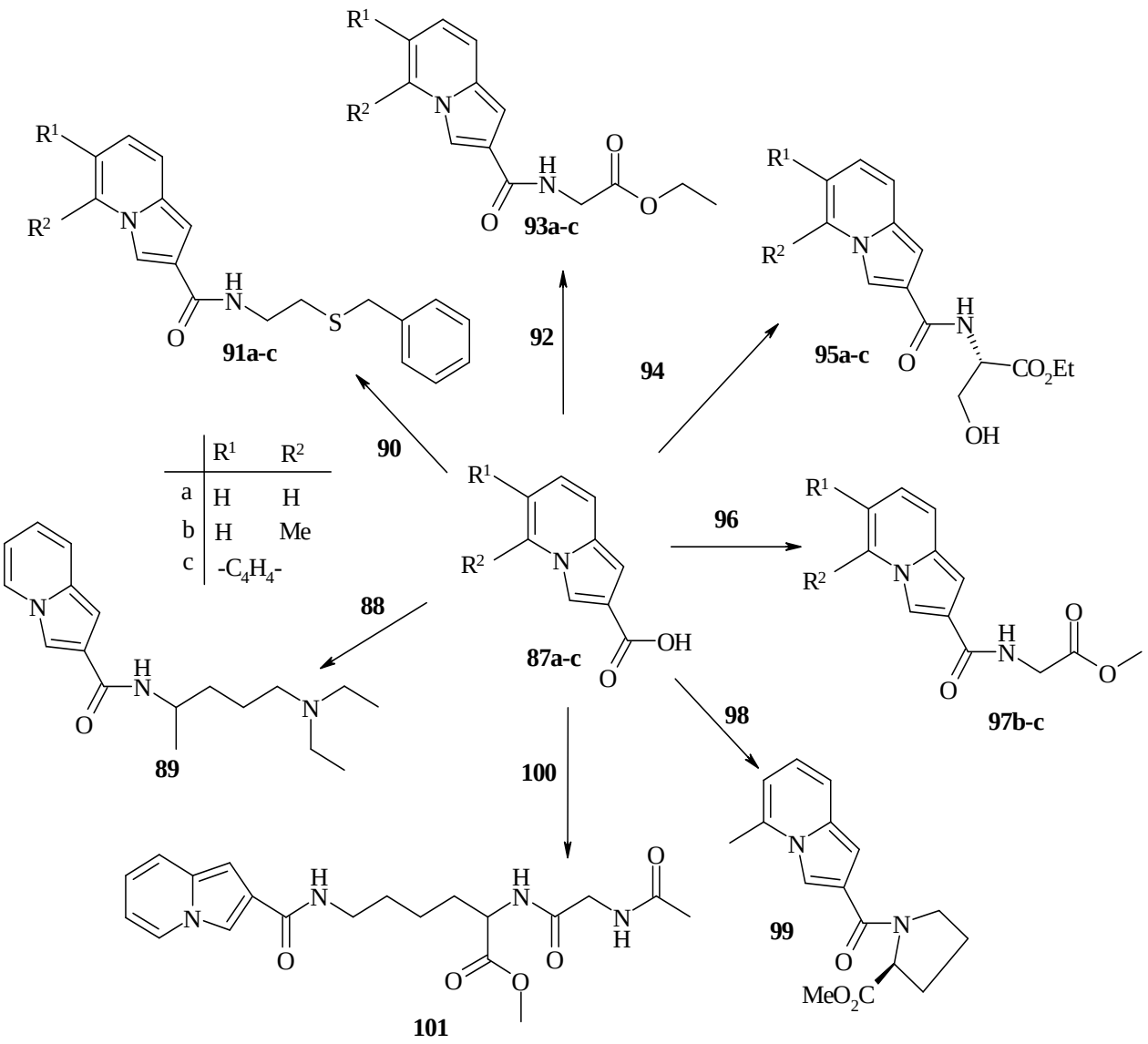

Scheme 27. Reactions of indolizines **87a-c** with amino compounds R^3NH_2 (see Table 2) using the coupling agent CDI in DMF.

Table 2. Reaction yields of indolizine-2-carboxamides **89-101**, with the general structure:-

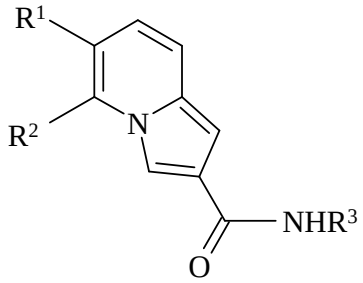

Compound	R^1	R^2	R^3	Yield (%)
89	H	H	$-CH(CH_3)(CH_2)_3N(CH_2CH_3)_2$	69
91a	H	H	$-(CH_2)_2SCH_2Ph$	64
91b	H	Me	$-(CH_2)_2SCH_2Ph$	79
91c	$-C_4H_4-$		$-(CH_2)_2SCH_2Ph$	97
93a	H	H	$-CH_2CO_2Et$	66
93b	H	Me	$-CH_2CO_2Et$	40
93c	$-C_4H_4-$		$-CH_2CO_2Et$	58
95a	H	H	$-CH(CH_2OH)CO_2Et$	47
95b	H	Me	$-CH(CH_2OH)CO_2Et$	44
95c	$-C_4H_4-$		$-CH(CH_2OH)CO_2Et$	34
97b	H	Me	$-CH_2CO_2Me$	82
97c	$-C_4H_4-$		$-CH_2CO_2Me$	70
99	H	Me	$-[(CH_2)_3C(H)CO_2Me]$	50
101	H	H	$-(CH_2)_4CH(CO_2Me)N_2H_7C_4O_2$	60

The ^{1}H NMR spectrum (Figure 19) of the indolizine-2-carboxamide **91b** reveals a singlet at 2.46 ppm corresponding to the 5-methyl protons, a triplet at 2.69 ppm corresponding to the 11-methylene protons, a multiplet at 3.61 ppm corresponding to the 10-methylene protons and the singlet at 3.74 ppm corresponding to the 12-methylene protons. It is important to note that the 10-methylene protons do not appear as a triplet because they also couple to the NH amide proton. The multiplet at 7.27 ppm is due to the phenyl protons (14-H, 15-H and 16-H). The remaining signals in the aromatic region correspond to the indolizine protons, while the NH amide proton resonates at 6.68 ppm. The ^{13}C NMR spectrum (Figure 20) shows the 17 expected carbon signals, with the 5-methyl carbon resonating at 18.5 ppm and the three *S*-benzylcysteamine methylene carbons (C-10, C-11 and C-12) resonating at 35.7, 31.1 and 38.0 ppm, respectively. The aromatic carbon signals lie downfield with the amide carbonyl carbon, being the most deshielded, resonating at 165.0 ppm. The DEPT 135 spectrum (Figure 21) confirms the presence of only three methylene carbons, while the COSY spectrum (Figure 22) reveals vicinal couplings (**A**) between the NH proton and 10-methylene protons and (**B**) between the 10- and 11-methylene protons.

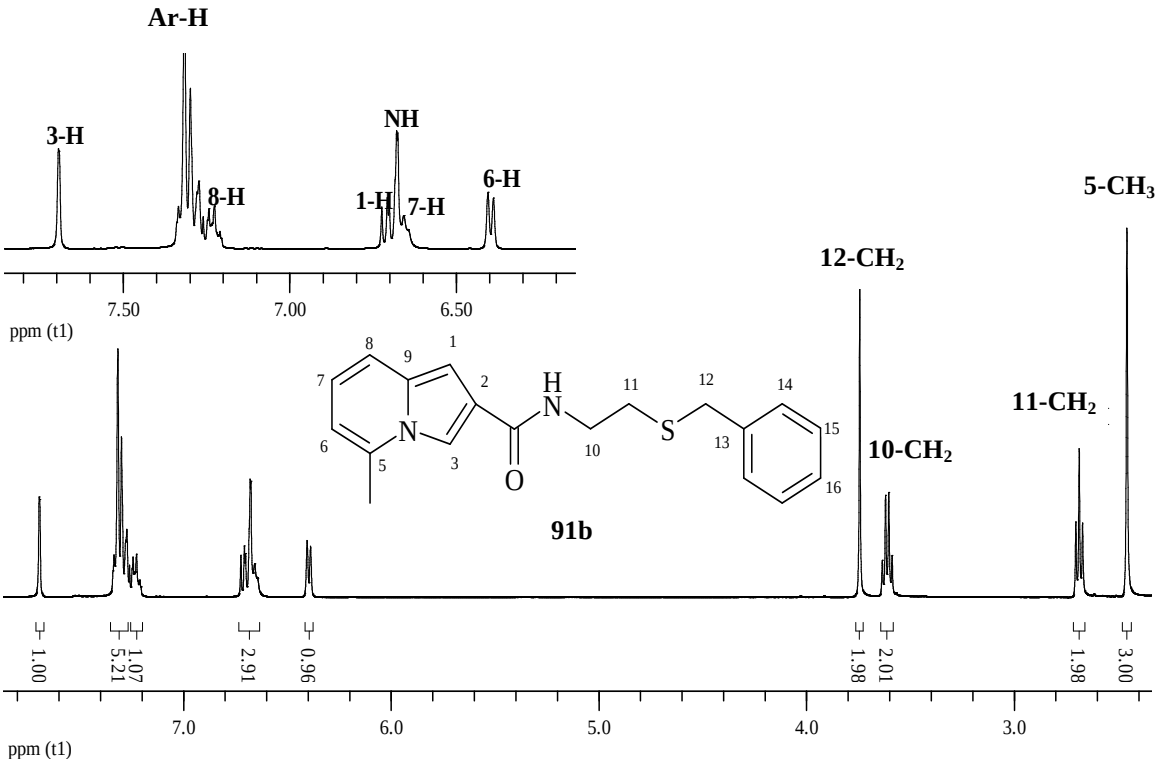

Figure 19. 400 MHz ^{1}H NMR spectrum of compound **91b** in $CDCl_3$.

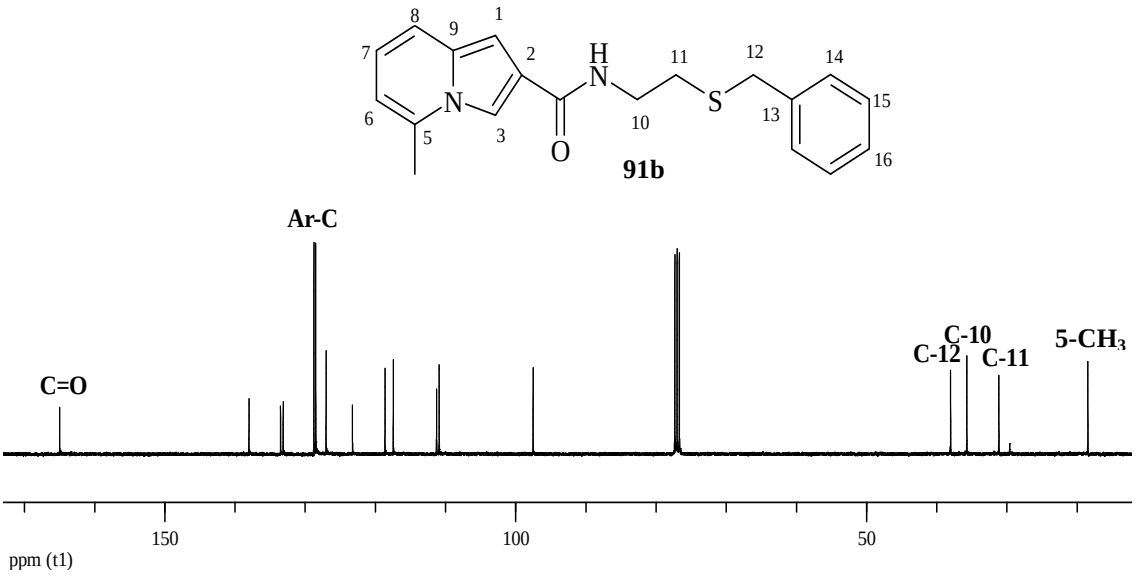

Figure 20. 100 MHz ^{13}C NMR spectrum of compound **91b** in $CDCl_3$.

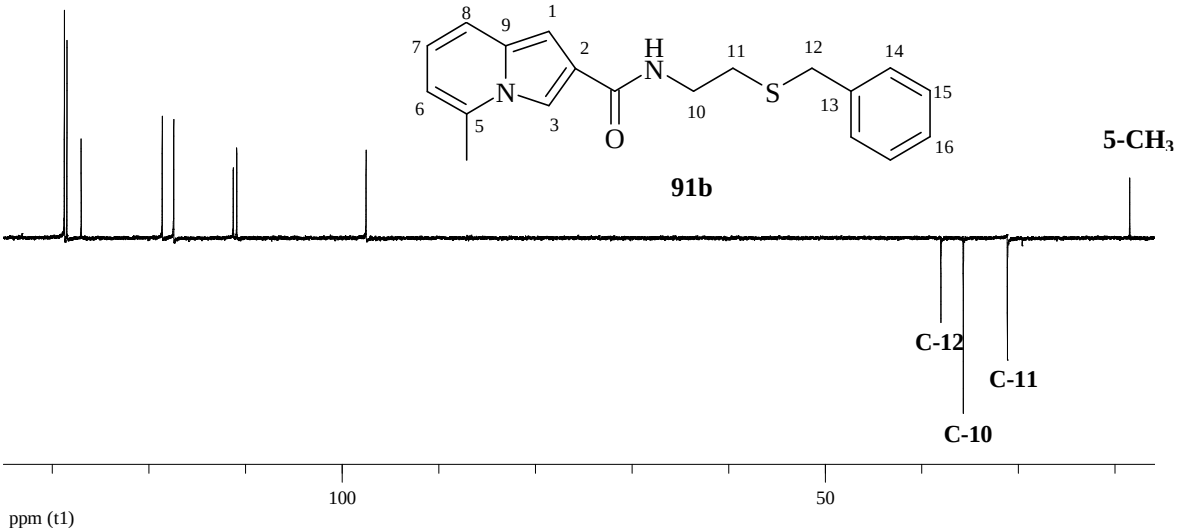

Figure 21. DEPT 135 NMR spectrum of compound **91b** in $CDCl_3$.

The data from HSQC spectrum (Figure 23) was used to confirm other signal assignments in compound **91b**, with the 5-methyl protons at 2.46 ppm correlating to the carbon resonating at 18.5 ppm and the 10-, 11- and 12-methylene protons correlating to carbon signals at 31.1, 35.7 and 38.0 ppm, respectively. The assignments of the quartenary carbons lying downfield is also confirmed because they have no correlation with any protons.

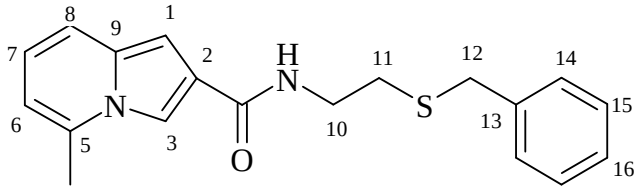

91b

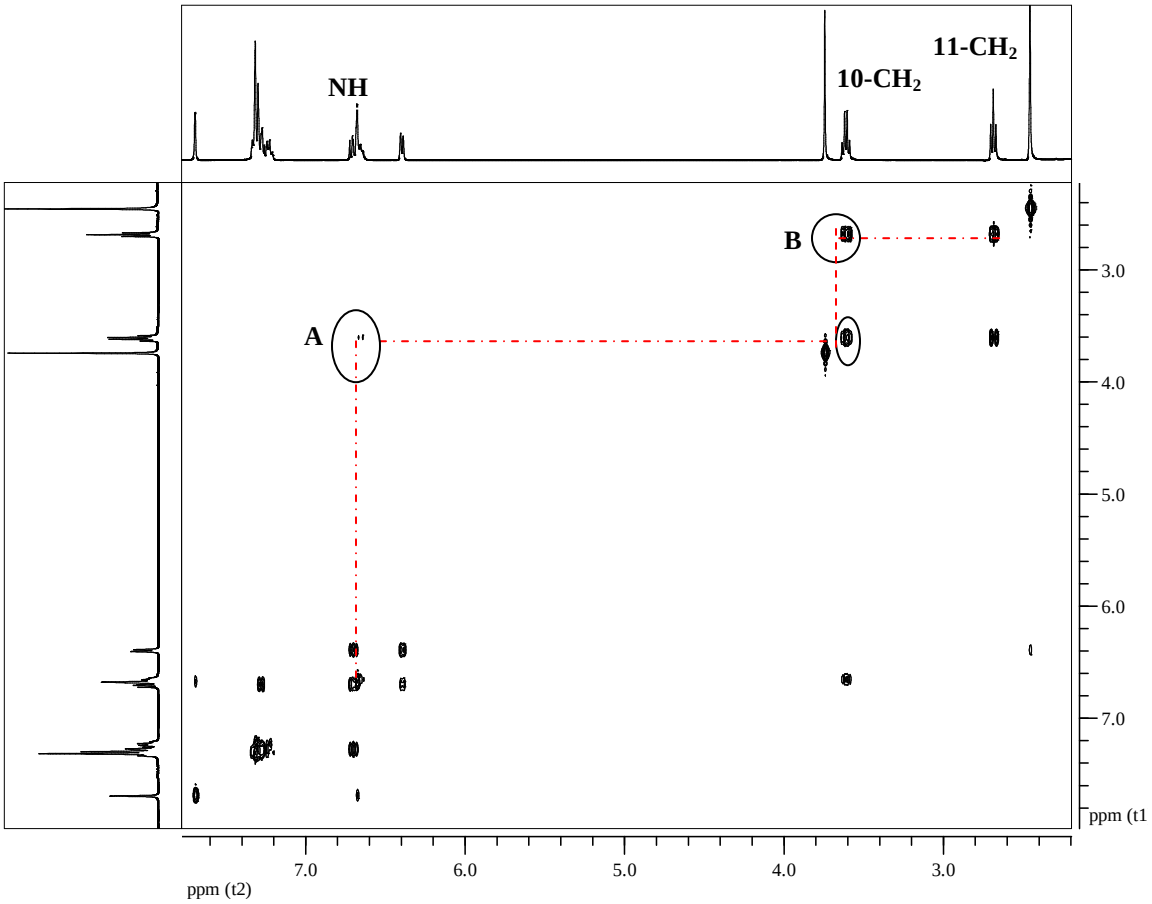

Figure 22. 400 MHz COSY NMR spectrum of compound **91b** in $CDCl_3$.

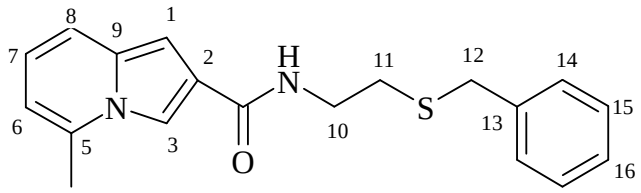

91b

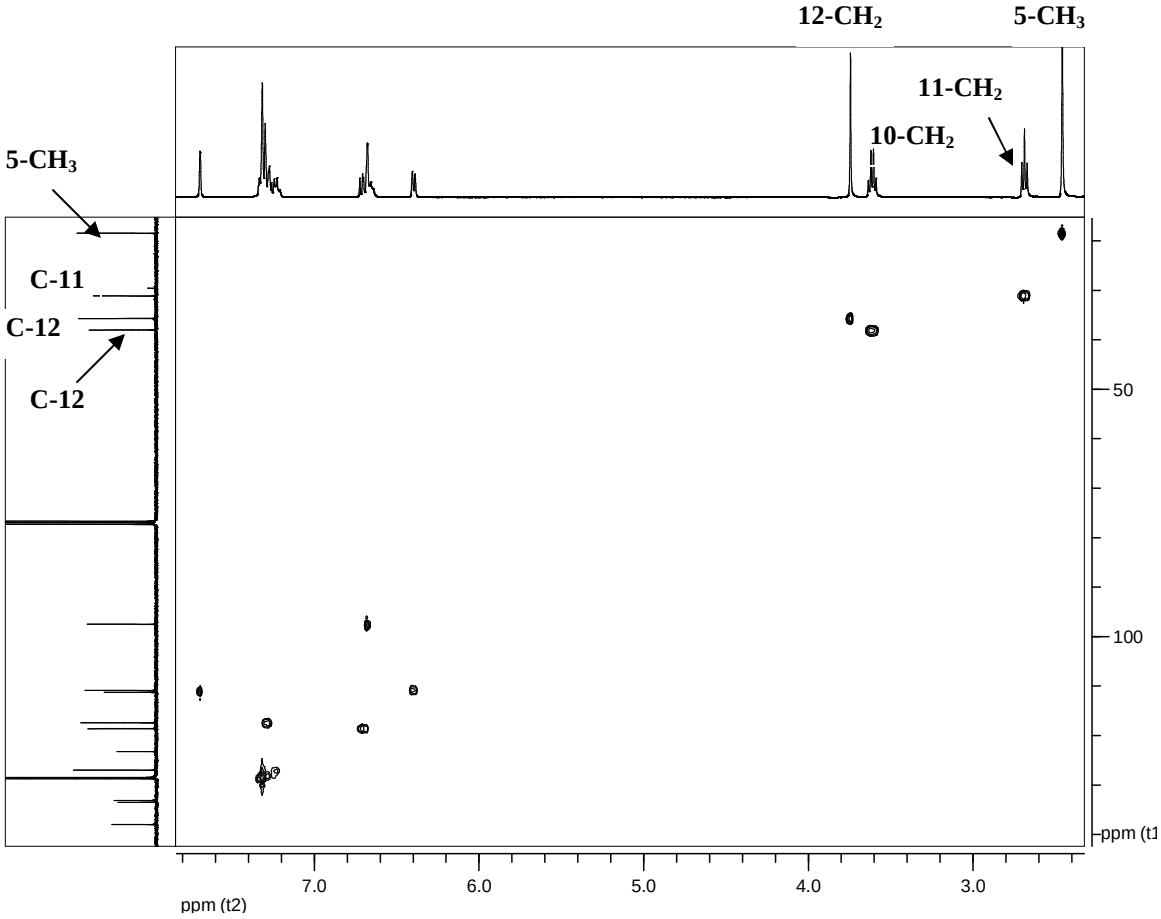

Figure 23. HSQC NMR spectrum of compound **91b** in $CDCl_3$.

2.3.2. Coupling with glycine ethyl ester hydrochloride

The indolizine-2-carboxylic acids **87a-c** were also reacted with glycine ethyl ester hydrochloride **92**, following the procedure used for the carboxamides **91a-c**, to give indolizine-2-carboxamides **93a-c** (Scheme 27, Table 2). Figure 24 illustrates the assignment of signals in the ^{1}H NMR spectrum of the indolizine-2-carboxamide **93b**. The triplet at 1.29 ppm corresponds to the 12-methyl protons, singlets at 2.24 and 4.21 ppm to the 5-methyl and 10-methylene protons, respectively, and the quartet at 4.24 ppm to the 11-methylene protons. In the aromatic region six signals are observed, five corresponding to the indolizine protons and the broad multiplet at 6.80 ppm to the NH proton. The ^{13}C NMR spectrum (Figure 25) shows the 14 expected carbon signals, with the 12- and 5-methyl carbons resonating at 14.1 and 18.6 ppm, 10- and 11-methylene carbons resonating at 41.5 and 61.5 ppm, respectively, and the two carbonyl carbons at 165.1 and 170.4 ppm. The DEPT 135 spectrum (Figure 26) confirms the presence of the two methylene carbons, C-10 and C-11.

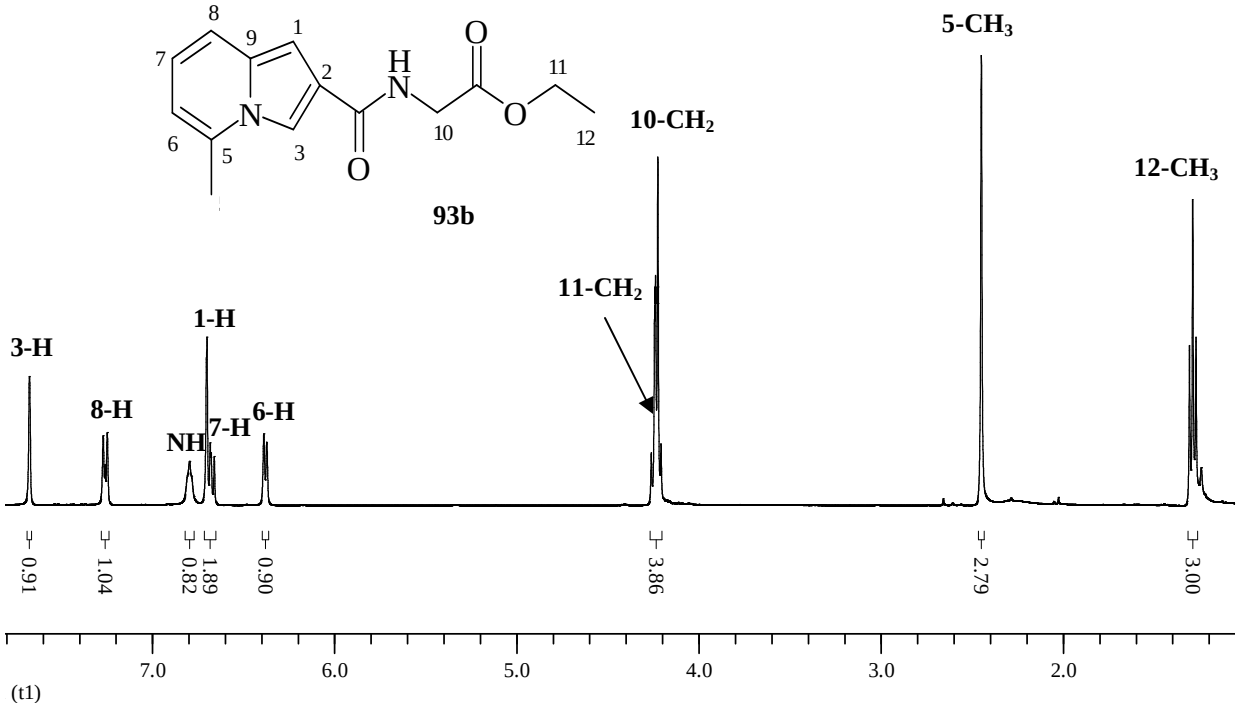

Figure 24. 400 MHz ^{1}H NMR spectrum of compound **93b** in $CDCl_3$.

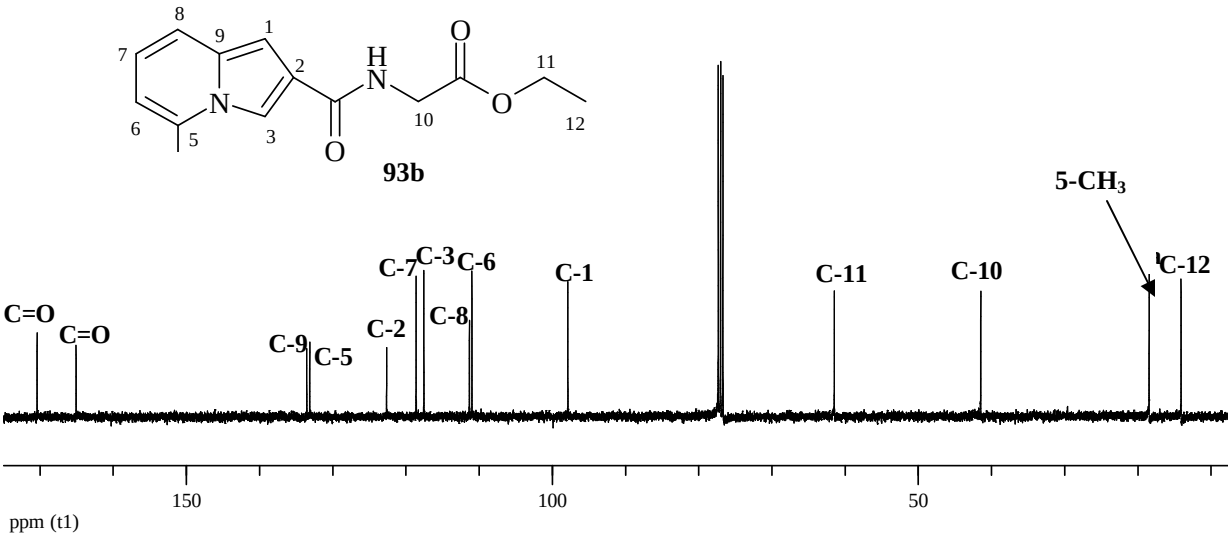

Figure 25. 100 MHz ^{13}C NMR spectrum of compound **93b** in $CDCl_3$.

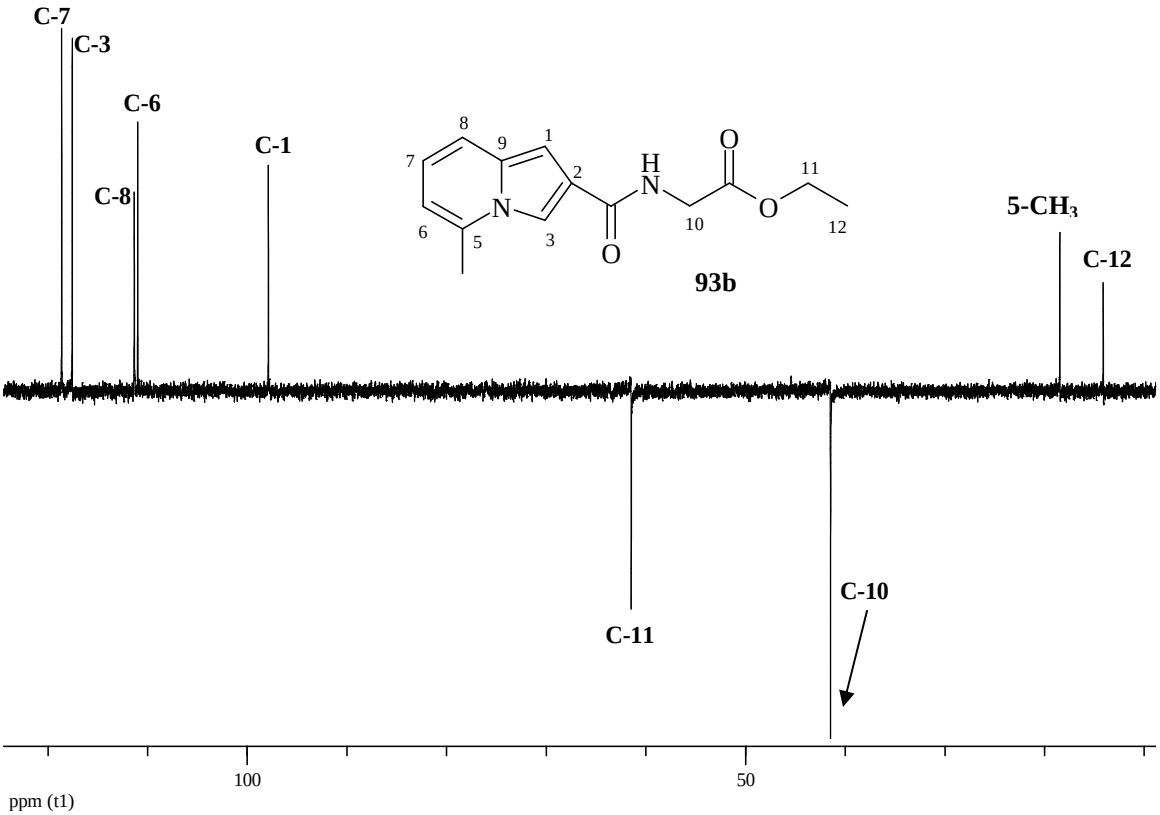

Figure 26. DEPT 135 NMR spectrum of compound **93b** in $CDCl_3$.

2.3.3. Coupling with L-serine ethyl ester hydrochloride

The indolizine-2-carboxylic acids **87a-c** were also reacted with L-serine ethyl ester hydrochloride **94**, following the procedure described for the synthesis of carboxamides **91a-c**, to afford the chiral indolizine-2-carboxamides **95a-c** in reasonable yields (Scheme 27, Table 2). The ^{1}H NMR spectrum (Figure 27) of the indolizine-2-carboxamide **95a** reveals a triplet at 1.27 ppm (which overlaps with the hydroxyl signal) corresponding to the 5-methyl protons, the doublet at 4.03 ppm to the diastereotopic 3-methylene protons, the quartet at 4.24 ppm to the 4-methylene protons and the multiplet at 4.83 ppm to the 2-methine proton. The DEPT 135 spectrum (Figure 28) confirms the presence of two methylene carbons.

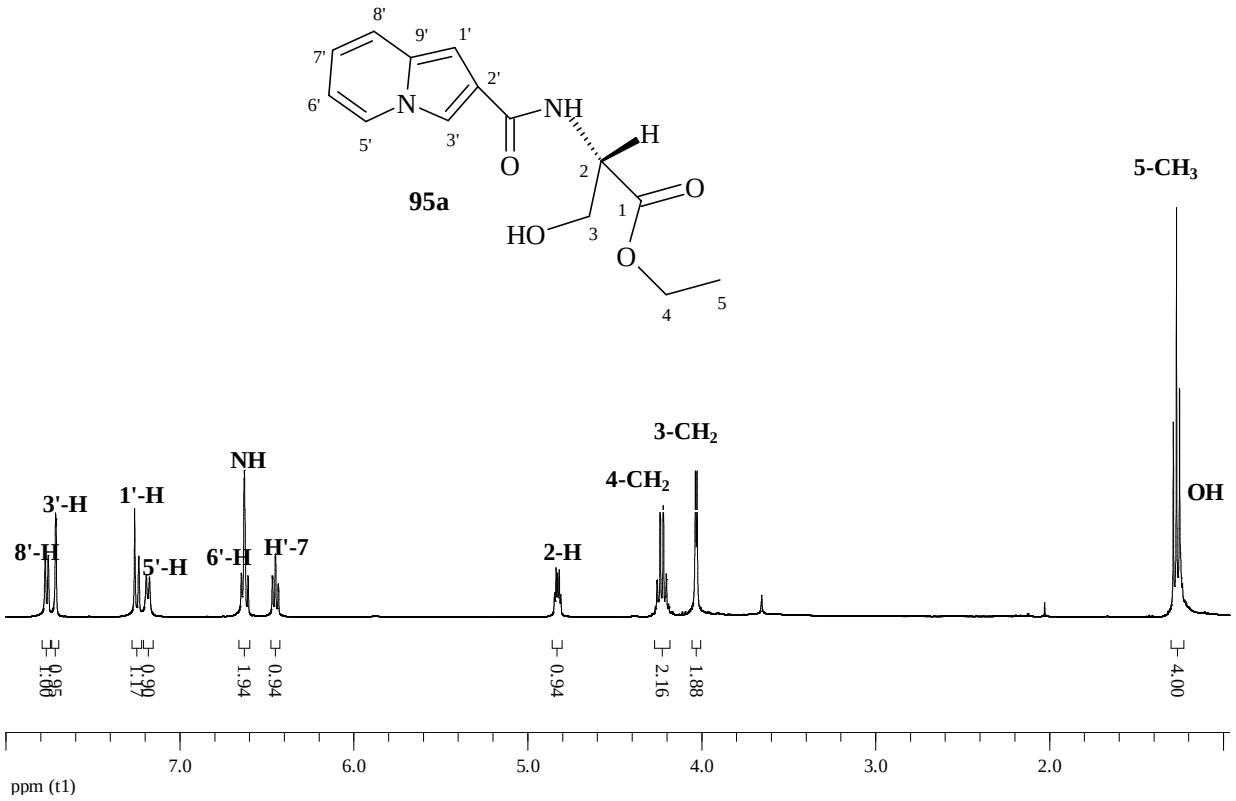

Figure 27. 400 MHz ^{1}H NMR spectrum of compound **95a** in $CDCl_3$.

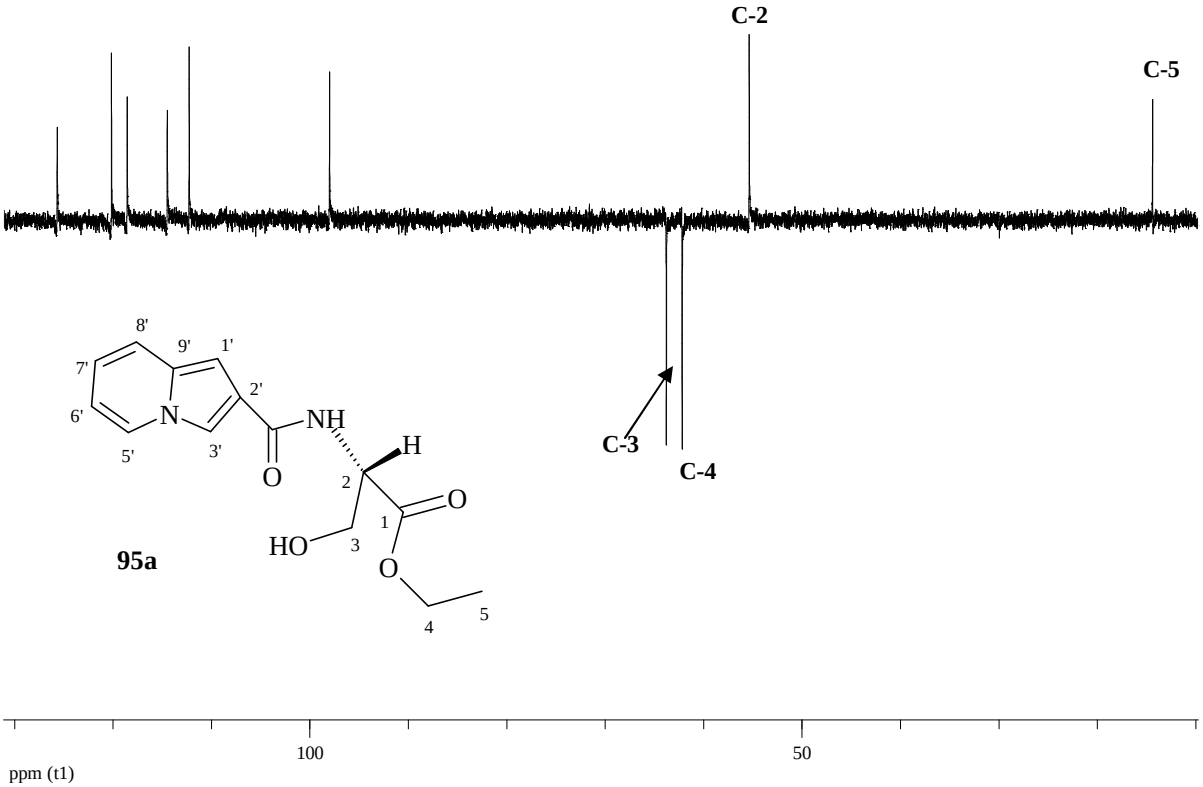

Figure 28. DEPT 135 NMR spectrum of compound **95a** in $CDCl_3$

2.3.4. Coupling with glycine methyl ester hydrochloride

The indolizine-2-carboxylic acids **87b-c** were also reacted with glycine methyl ester hydrochloride **96**, following the procedure described for the synthesis of carboxamides **91a-c**, to afford indolizine-2-carboxamides **97b-c** (Scheme 27 and Table 2). Figure 29 illustrates the assignment of signals in the ^{1}H NMR spectrum of the indolizine-2-carboxamide **97c**. The singlet at 3.80 ppm corresponds to the methoxy protons and the doublet at 4.27 ppm to the 10-methylene protons. In the aromatic region nine signals are observed, eight corresponding to the indolizine aromatic protons and the broad multiplet at 6.75 ppm to the NH proton.

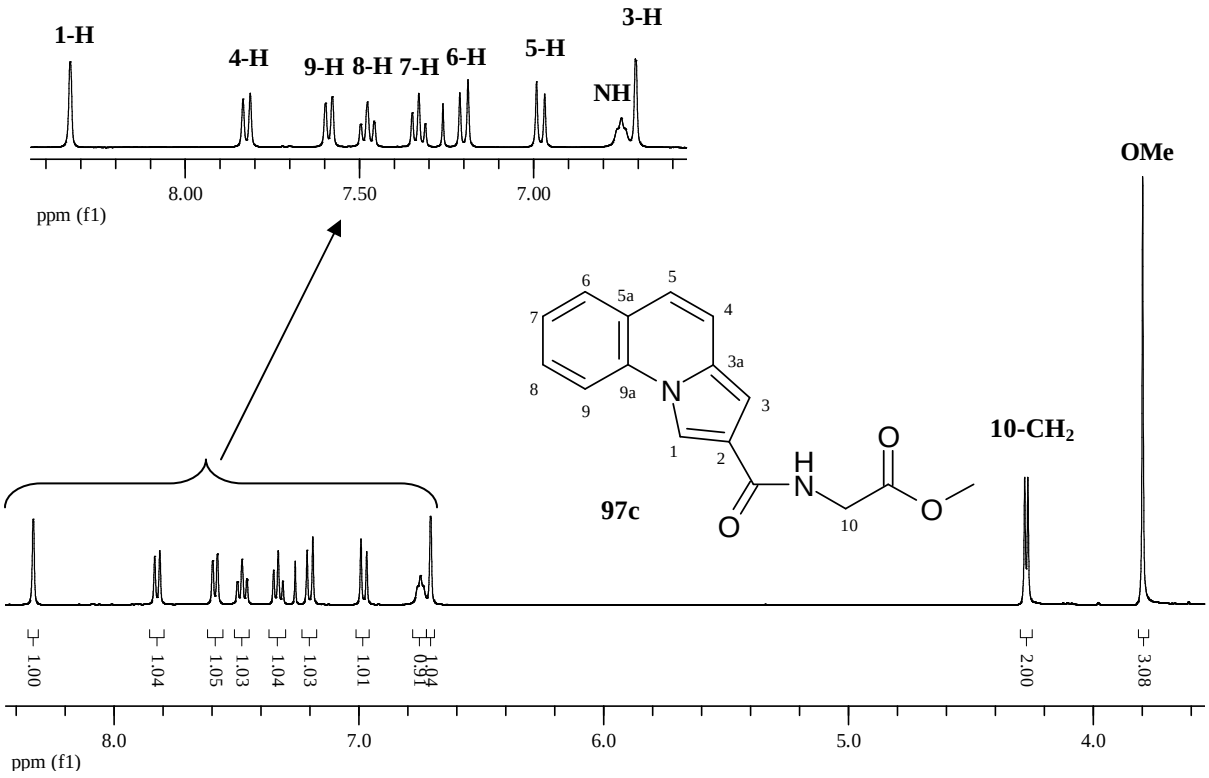

Figure 29. 400 MHz ^{1}H NMR spectrum of compound **97c** in $CDCl_3$.

2.3.5. Coupling with L-proline methyl ester hydrochloride

Indolizine-2-carboxylic acid **87b** was reacted with L-proline methyl ester hydrochloride **98**, following the procedure described for the synthesis of carboxamides **91a-c**, to afford indolizine-2-carboxamide **99** (Scheme 27 and Table 2). The ^{1}H NMR spectrum (Figure 30) of the indolizine-2-carboxamide **99** reveals a multiplet at 2.00 ppm corresponding to the 3-methylene protons, the splitting of the 4-methylene proton signals with one proton resonating as a multiplet at 2.13 ppm (4-Ha) and the other at 2.30 ppm (4-Hb), singlets at 2.48 and 3.75 ppm corresponding to the 5'-methyl protons and the methoxy group, respectively. The multiplet at 3.96 ppm corresponds to the 5-methylene protons, the quartet at 4.69 ppm to the 2-methine proton and the signals in the aromatic region to the indolizine protons.

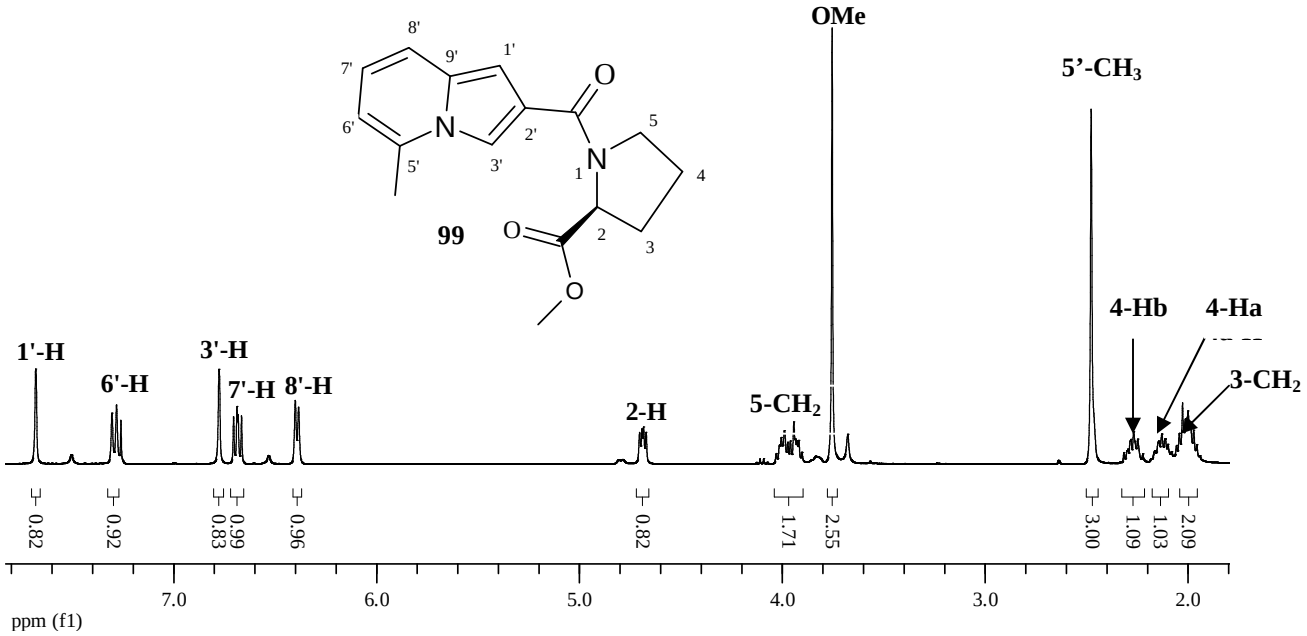

Figure 30. 400 MHz ^{1}H NMR spectrum of compound **99** in $CDCl_3$.

2.3.6. Coupling with the unprotected amine 88 and the dipeptide 100

1-Methyl-5-(diethylamino)butylamine **88** and *N*-acetyl-glycine-lysine methyl ester **100** were the only two unprotected amino compounds employed successfully in the synthesis of indolizine-2-carboxamides, *viz*., compounds **89** and **101**, respectively (Scheme 27, Table 2). Figure 31 shows the ^{1}H NMR spectrum of the indolizine-2-carboxamide **89**, the triplet at 1.00 ppm corresponding to the 15- and 15'-methyl protons, the doublet at 1.23 ppm to the 10-methyl protons, the multiplet at 1.55 ppm to the diastereotopic 11- and 12-methylene protons. The multiplet at 2.44 ppm is due to the 13-methylene protons, the quartet at 2.52 ppm to the 14- and 14'-methylene protons, the multiplet at 4.21 ppm to the methine proton of the stereogenic C-10. The remaining signals are due to the indolizine aromatic protons and the NH proton.

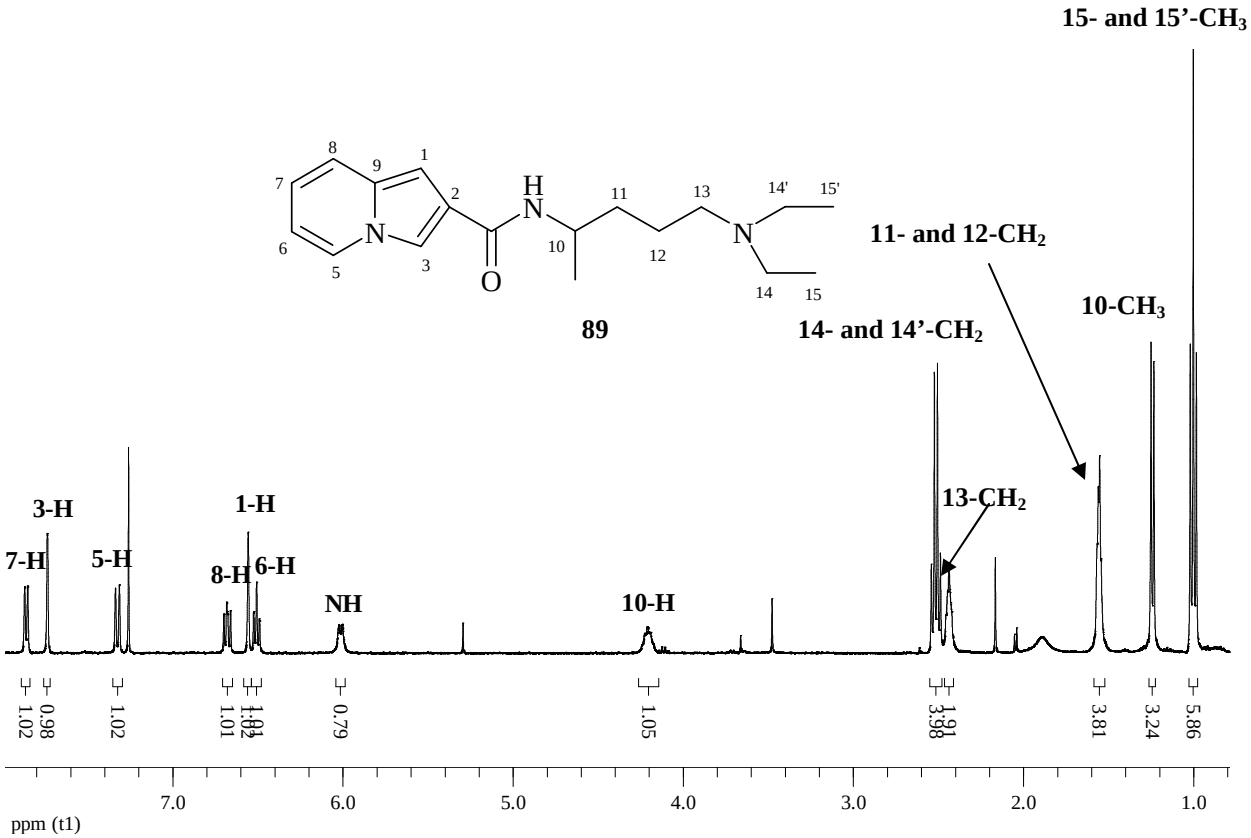

Figure 31. 400MHz ^{1}H NMR spectrum of compound **89** in $CDCl_3$.

The ^{1}H NMR spectrum (Figure 32) of the indolizine-2-carboxamide **101** reveals multiplets at 1.40 and 1.56 ppm corresponding to the 5- and 4-methylene protons, respectively, the signals at 1.76 and 1.88 ppm to the separated 6-methylene protons (6-Ha and 6-Hb), the singlet at 1.99 ppm to the13-methyl protons, the two multiplets at 3.36 and 3.50 ppm to the separated 3-methylene protons (3-Ha and 3-Hb), the singlet at 3.70 ppm to the methoxy protons, the doublet at 4.02 ppm to the 10-methylene protons; the multiplet at 4.47 ppm to the 7-methine proton; the signals at 7.10, 7.76 and 7.89 ppm are due to the three NH protons and the rest of the signals are due to the indolizine protons . The DEPT 135 spectrum (Figure 33) confirms the presence of five methylene carbons.

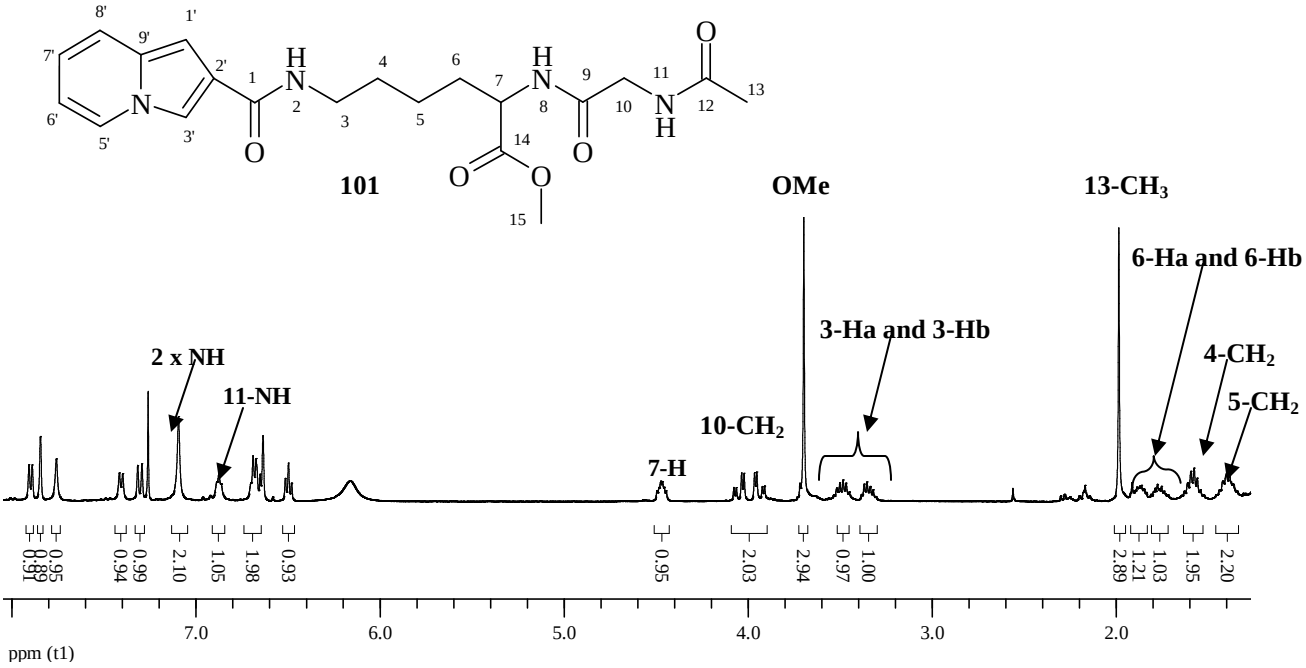

Figure 32. 400MHz ^{1}H NMR spectrum of compound **101** in $CDCl_3$.

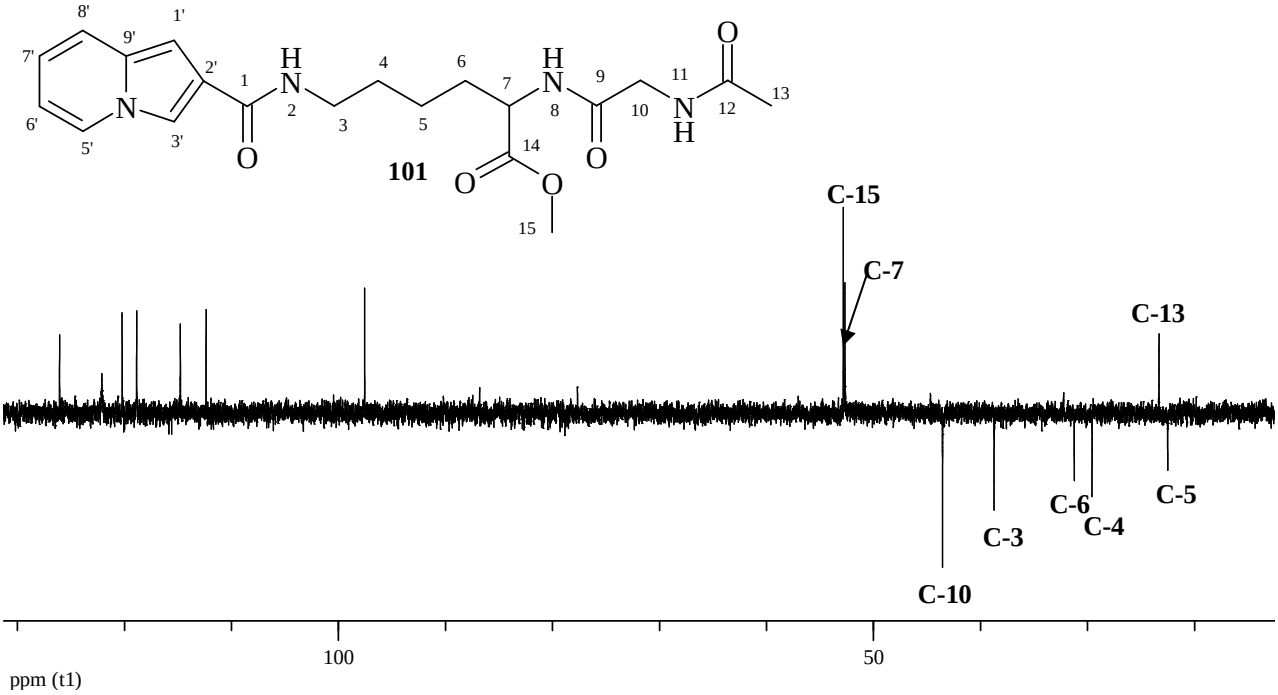

Figure 33. DEPT 135 NMR spectrum of compound **101** in $CDCl_3$.

2.3.7. Attempted synthesis of other indolizine-2-carboxamides

Indolizine-2-carboxylic acid **87a** was also treated with piperazine **102**, 1,3-diamino-2-hydroxypropane **104** and ethylenediamine **106** following the procedure used for the carboxamides **91a-c** but after being stirred overnight, the TLC plate showed that no products had formed from the mixtures. The three mixtures were allowed to stir further for five days at room temperature but ^{1}H NMR analysis indicated that no reactions had occurred. This problem might be solved by converting the carboxylic acids into the corresponding and more reactive acid chlorides, following the procedure described by Ankalgi and co-workers. [57]

2.4. Synthesis and characterization of aza-Michael adducts

The aza-Michael reaction is a carbon-nitrogen bond forming reaction between α,β-unsaturated carbonyl compounds and nitrogen nucleophiles.[147] The reaction with α,β-unsaturated esters usually takes place under basic conditions or in the presence of an acidic catalyst to afford β-amino esters.[148] In the present study, the procedure described by Perlmutter and Tabone in 1988 was used to synthesize the aza-Michael products **106a-f**.[149] The Baylis-Hillman adduct **61g** was reacted with various amino acid esters (*S*-benzylcysteamine hydrochloride **90**, glycine ethyl and methyl ester hydrochlorides **92** and **96**, L-serine methyl ester hydrochloride **94**, L-proline methyl ester hydrochloride **98** and benzylamine **108**) in methanol and triethylamine (Et_3N) at 0 ºC for 4 days (Scheme 28). ^{1}H NMR spectroscopic analysis indicated the formation of diastereomeric mixtures of the aza-Michael products **109a-f**. The diastereoselectivity was poor ranging from 20 to 40% for the products **109a-e** but much better for **109f** (Table 3). Purification of the crude diastereomeric mixtures by preparative layer chromatography permitted isolation and characterization of the diastereomeric components in each case. In the reactions with the achiral amines, *S*-benzylcysteamine **90**, benzylamine **105** and glycine ester hydrochlorides **92** and **96**, the diastereomeric products, in each case, are presumed to comprise a pair of racemic components. In reactions with the chiral L-serine and L-proline ester hydrochlorides **94** and **98**, however, all four of the possible products, in each case, would be expected to be diastereomeric.

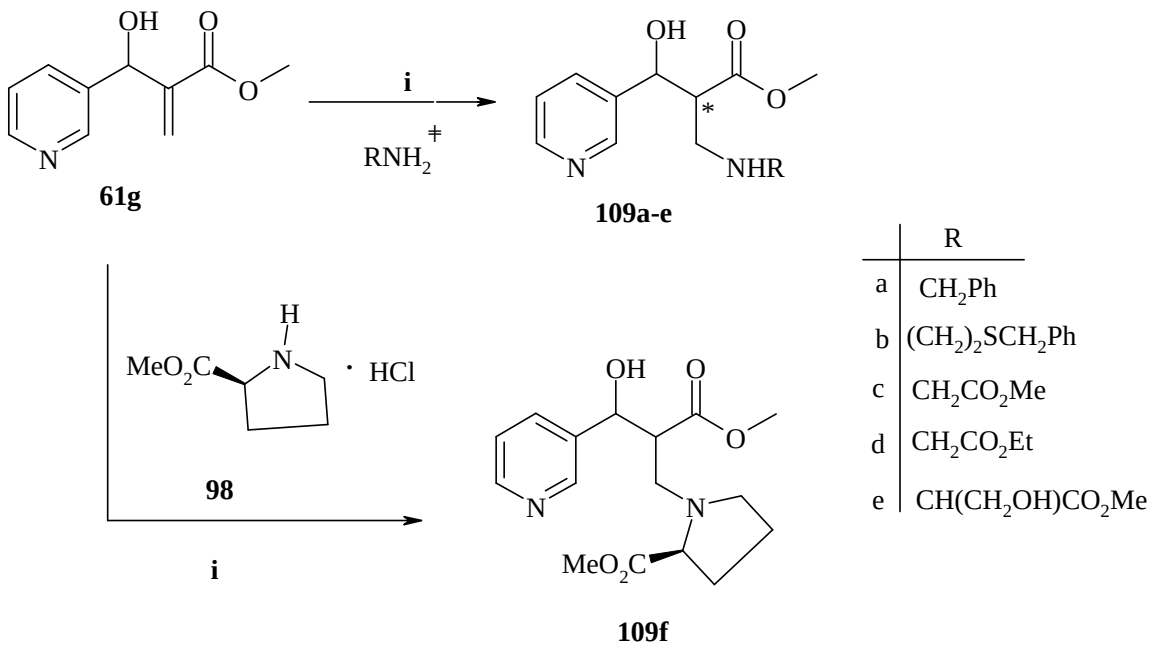

Scheme 28

Reaction conditions: (i) MeOH, 0°C, 4 d. (‡ Hydrochloride salts neutralized with Et_3N. * New stereogenic centre.)

Table 3. Reaction yields, diastereomeric ratios and % d.e. of the aza-Michael products **109a-f**.

Compound	R	Diastereomeric ratio [a]	% d.e. [b]	Total yield (%) [c]
109a	-CH_2Ph	1:1.5	20	69
109b	-$(CH_2)_2SCH_2Ph$	1:2	33	41
109c	-CH_2CO_2Me	1:2.6	44	75
109d	-CH_2CO_2Et	1:1.6	23	96
109e	-$CH(CH_2OH)CO_2Me$	1:1.3	13	31
109f		1:7	75	76

[a] Determined by 400 MHz ^1H NMR spectroscopy. [b] % Diastereomeric excess. [c] Yield before purification. [d] R_2N.

2.4.1. Synthesis of benzylamine aza-Michael products 109a

Figure 34 illustrates the doubling of signals in ^{1}H NMR spectrum of the crude aza-Michael product **109a**, indicating that the amine product was a diastereomeric mixture. The diastereomeric ratio was calculated from the intensities of the respective 3-methine signals (Figure 34). Preparative layer chromatography afforded the diastereomers **109a$_1$** and **109a$_2$** in 33 and 14% yield, respectively.

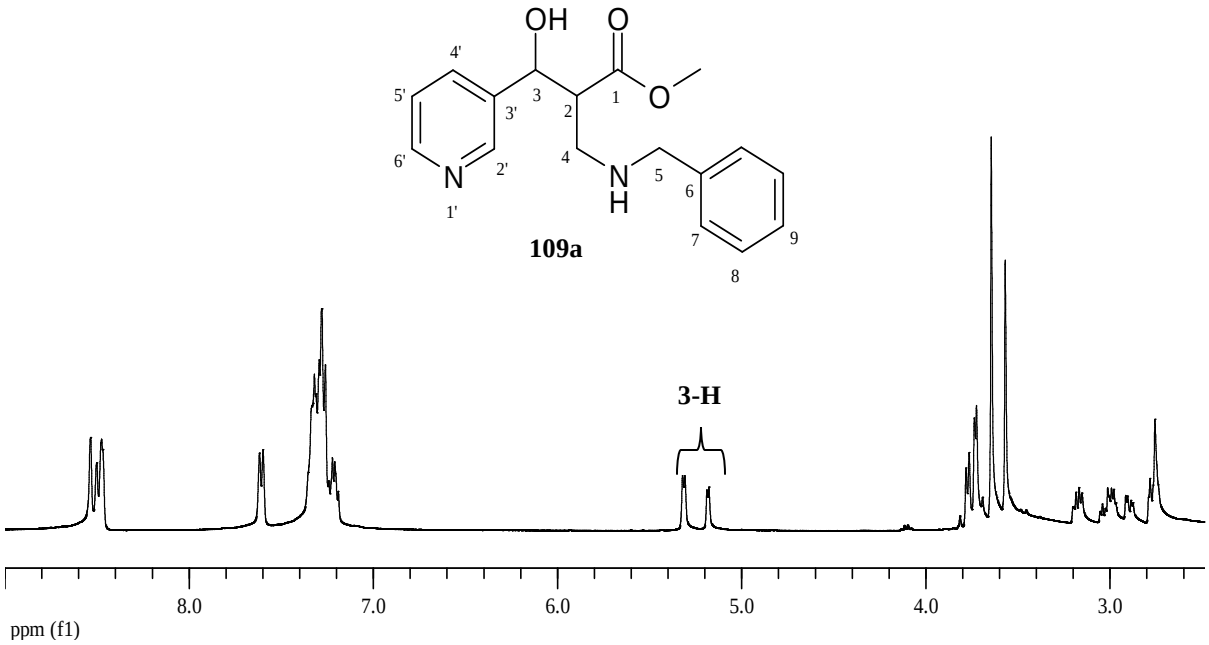

Figure 34. 400 MHz ^{1}H NMR spectrum of the crude diastereomeric aza-Michael products **109a** in $CDCl_3$.

The ^{1}H NMR spectrum (Figure 35) of diastereomer **109a$_1$** reveals well separated signals for each of the diastereotopic 4-methylene protons, with the 4-Ha signal overlapping the 2-methine proton signal at 2.77 ppm; the 4-Hb proton resonates at 3.18 ppm. The singlet at 3.65 ppm is due to the methoxy protons, the doublets at 3.71 and 5.32 ppm to the 5-methylene and 3-methine protons, respectively, and the signals in the region 7.21-8.59 ppm to the phenyl, hydroxide and pyridyl protons. The ^{13}C NMR spectrum (Figure 36) shows the expected 15 signals, with the 4-methylene and 2-methine carbons resonating at 47.5 and 50.9 ppm, respectively, the methoxy carbon at 52.1 ppm, the 5-methylene carbon at 53.9 ppm, the 3-methine carbon at 74.4 ppm and the carbonyl carbon at 172.5 ppm. The DEPT 135 spectrum (Figure 37) confirms the presence of two methylene

carbons. The COSY spectrum (Figure 38) reveals vicinal coupling between the 2- and 3-methine protons (**A**) and between the 2-methine and one of the 4-methylene protons (4-Hb) (**B**). The HSQC spectrum (Figure 39) shows correlation between the 3-methine proton and the carbon (C-3) resonating at 74.4 ppm; the 4-Ha and 4-Hb methylene protons correlate to the carbon resonating at 47.5 ppm and the 5-methylene protons to the carbon resonating at 53.9 ppm. In the HMBC spectrum (Figure 40), the cross-peaks **A** and **B** (and **B'**) reveal a three-bond ($^3J_{C,H}$) connectivity between the 3-methine proton and the carbonyl carbon, and between both of the 4-methylene protons and the carbonyl carbon. The diastereomers **109a$_1$** and **109a$_2$** exhibit significant differences in their NMR spectra, as is immediately evidenced from a comparison of their ^{1}H NMR spectra (Figure 41).

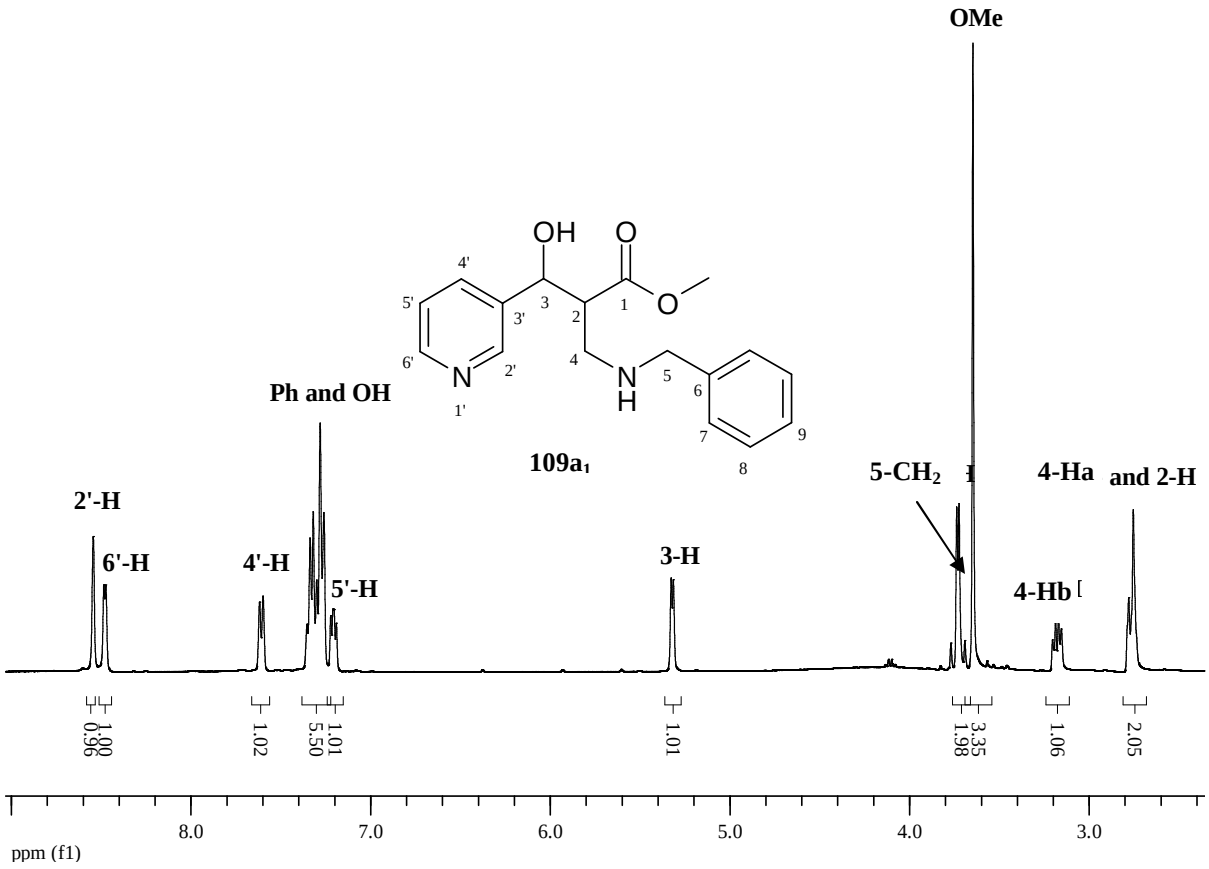

Figure 35. 400 MHz ^{1}H NMR spectrum of diastereomer **109a$_1$** in $CDCl_3$.

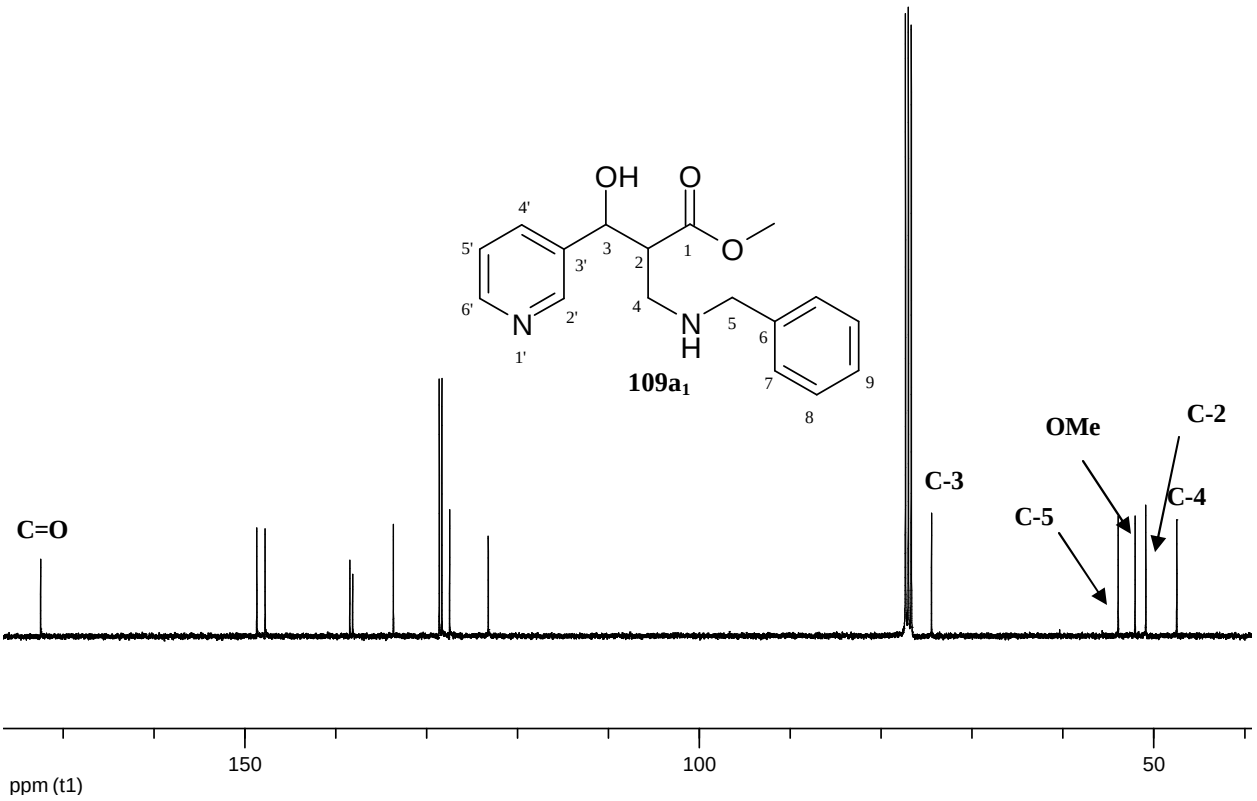

Figure 36. 100 MHz ^{13}C NMR spectrum of diastereomer **109a$_1$** in $CDCl_3$.

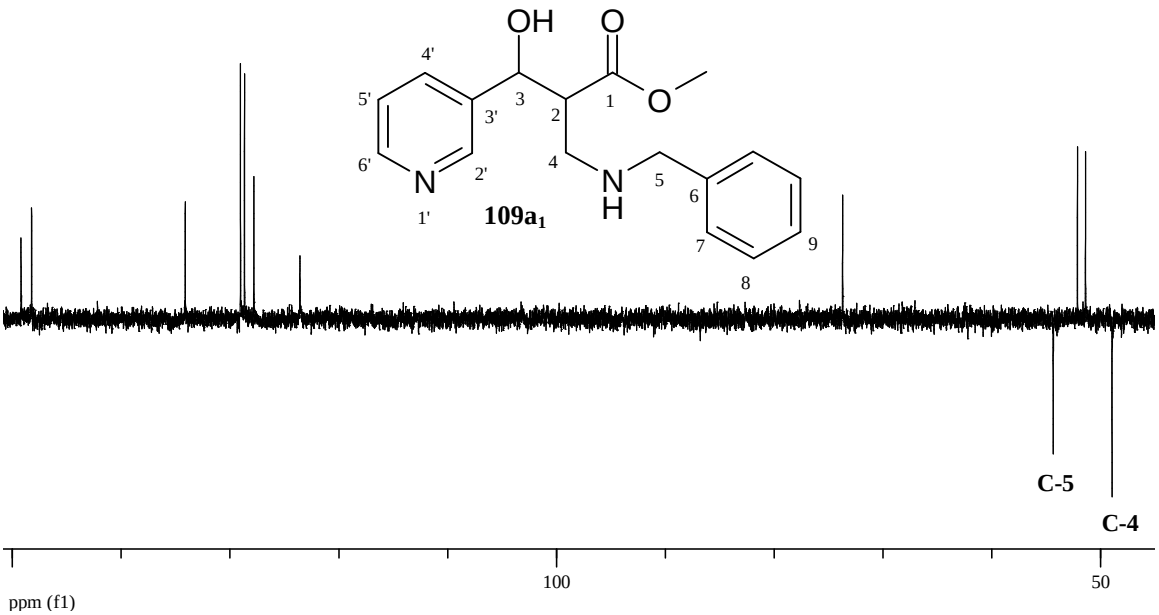

Figure 37. DEPT 135 spectrum of diastereomer **109a$_1$** in $CDCl_3$.

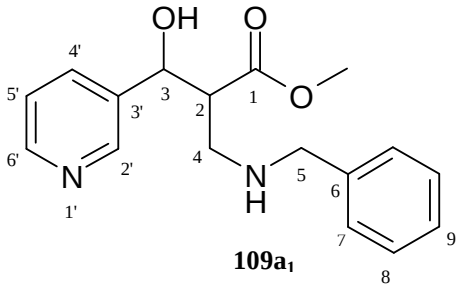

109a$_1$

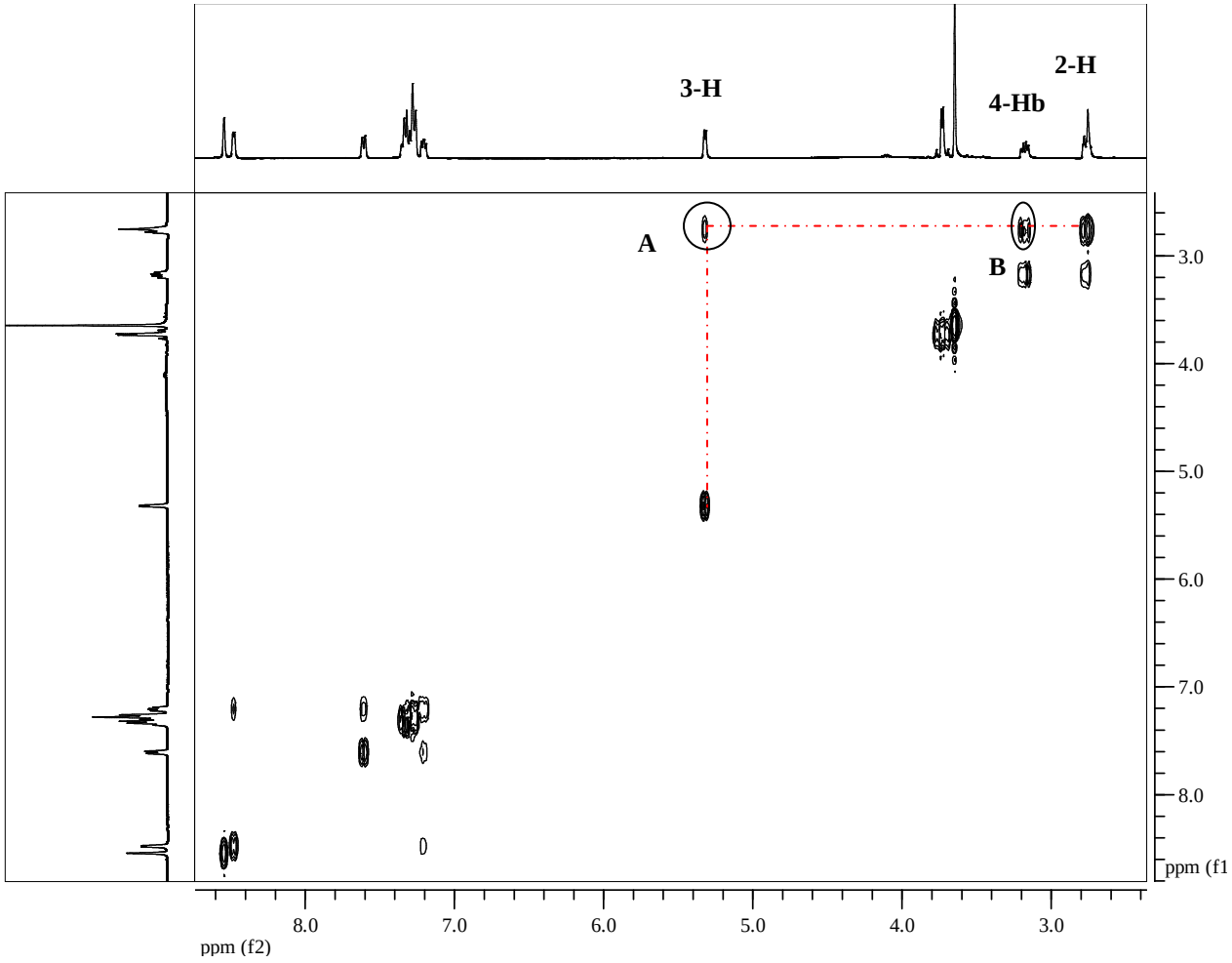

Figure 38. 400 MHz COSY spectrum of diastereomer **109a$_1$** in $CDCl_3$.

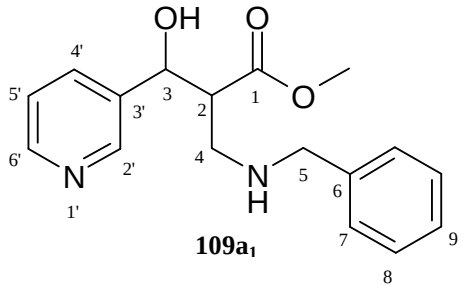

109a$_1$

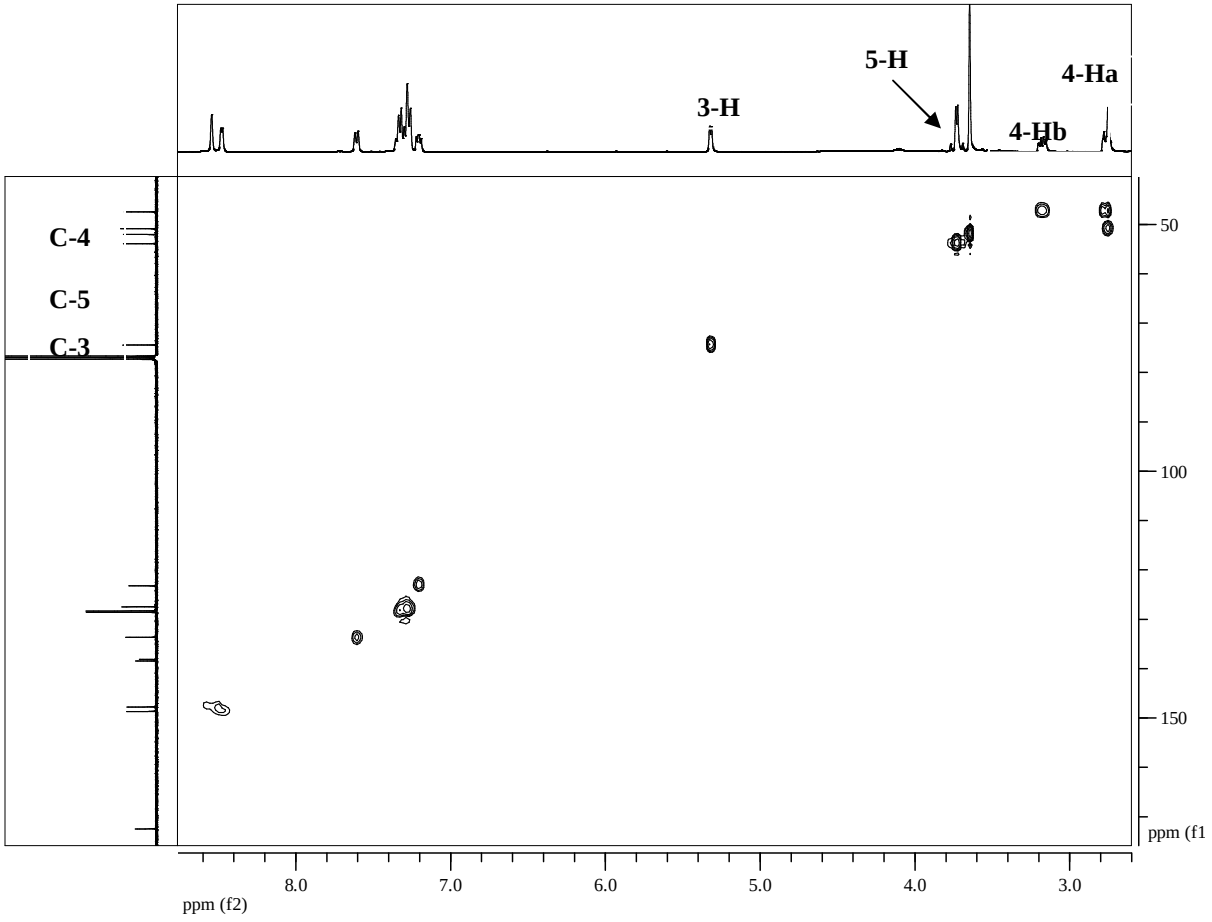

Figure 39. HSQC spectrum of diastereomer **109a$_1$** in $CDCl_3$.

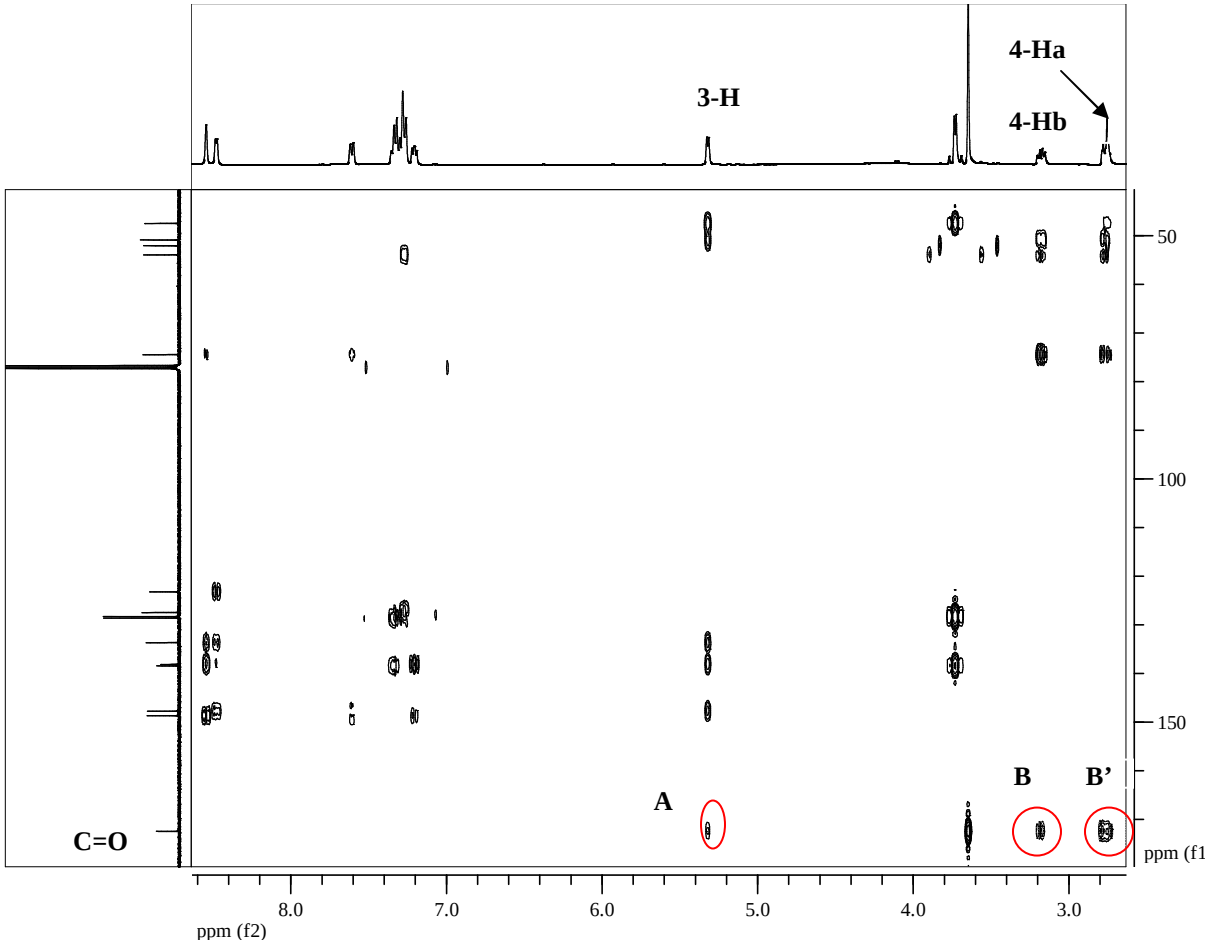

Figure 40. HMBC spectrum of diastereomer **109a$_1$** in $CDCl_3$.

The ^{1}H NMR spectrum (Figure 41) of diastereomer **109a$_2$** reveals that the 2- and 4a-methine signals do not coalesce as they do in the spectrum of diastereomer **109a$_1$**, whereas the opposite effect is observed for the 2'- and 6'-methine proton signals.

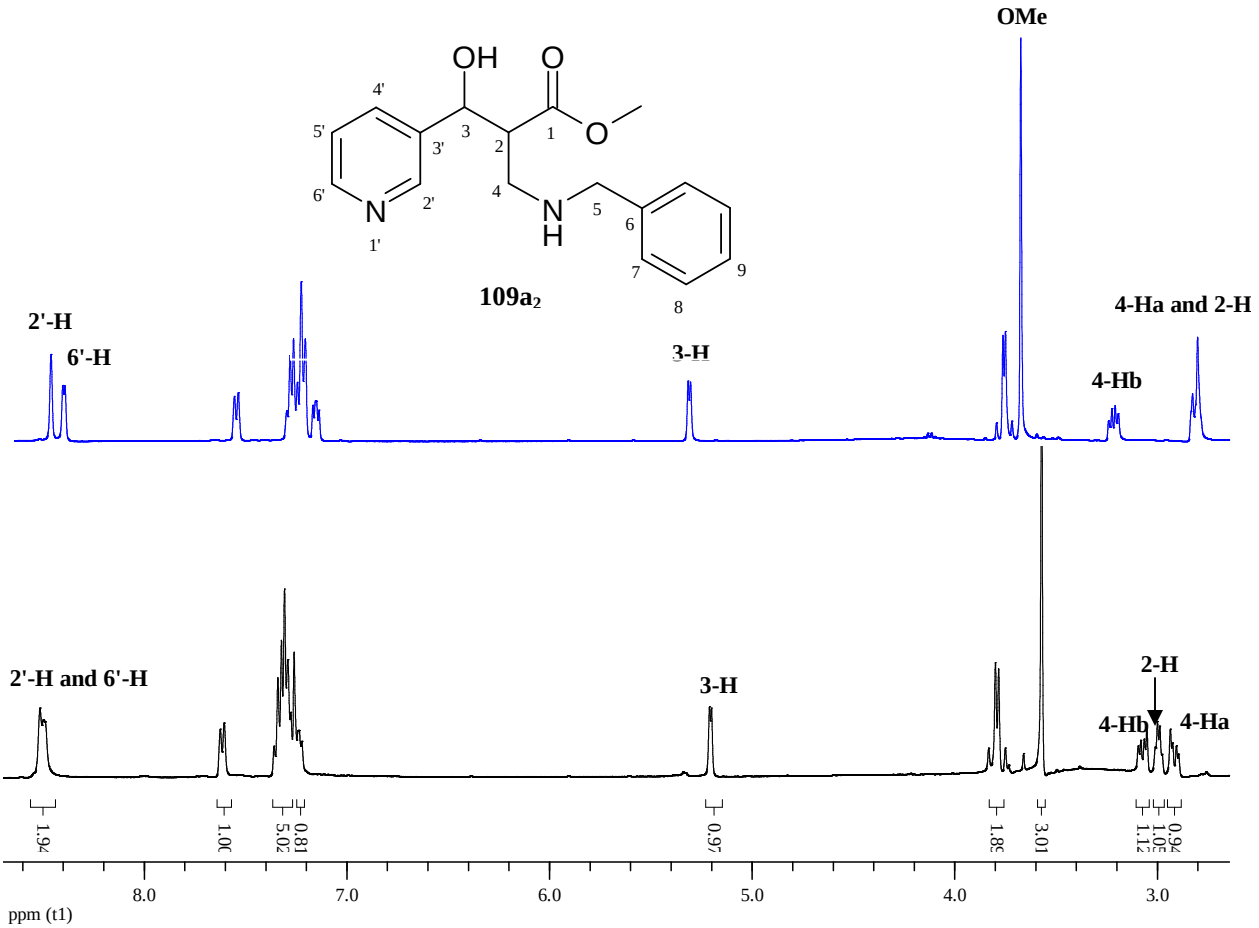

Figure 41. 400 MHz ^{1}H NMR spectrum of diastereomer **109a$_2$** in $CDCl_3$, with the spectrum of diastereomer **109a$_1$** superimposed in blue.

2.4.2. Synthesis of the *S*-benzylcysteamine aza-Michael products 109b

Figure 42 illustrates the ^{1}H NMR spectra of the crude mixture obtained from the reaction with *S*-benzylcysteamine hydrochloride **90** (Scheme 28) and of the separated diastereomers **109b$_1$** and **109b$_2$**. In the ^{1}H NMR spectrum (Figure 42c) of the major diastereomer **109b$_2$**, signals in the region 2.60-3.02 ppm are clearly resolved while in the spectrum of diastereomer **109b$_1$** (Figure 42b) they overlap. In the former spectrum (Figure 42c), the triplets at 2.55 and 2.71 ppm correspond to the 6- and 5-methylene protons, the multiplets at 2.83, 2.95 and 2.98 ppm to the diastereotopic methylene proton, 4-Ha, the 2-methine proton and the second methylene proton, 4-Hb, respectively. The

singlets at 3.60 and 3.71 ppm are assigned to the methoxy group and the 7-methylene protons, respectively, the doublet at 5.32 ppm to the 3-methine proton and the signals in the region 7.21-8.59 ppm to the phenyl and pyridyl protons.

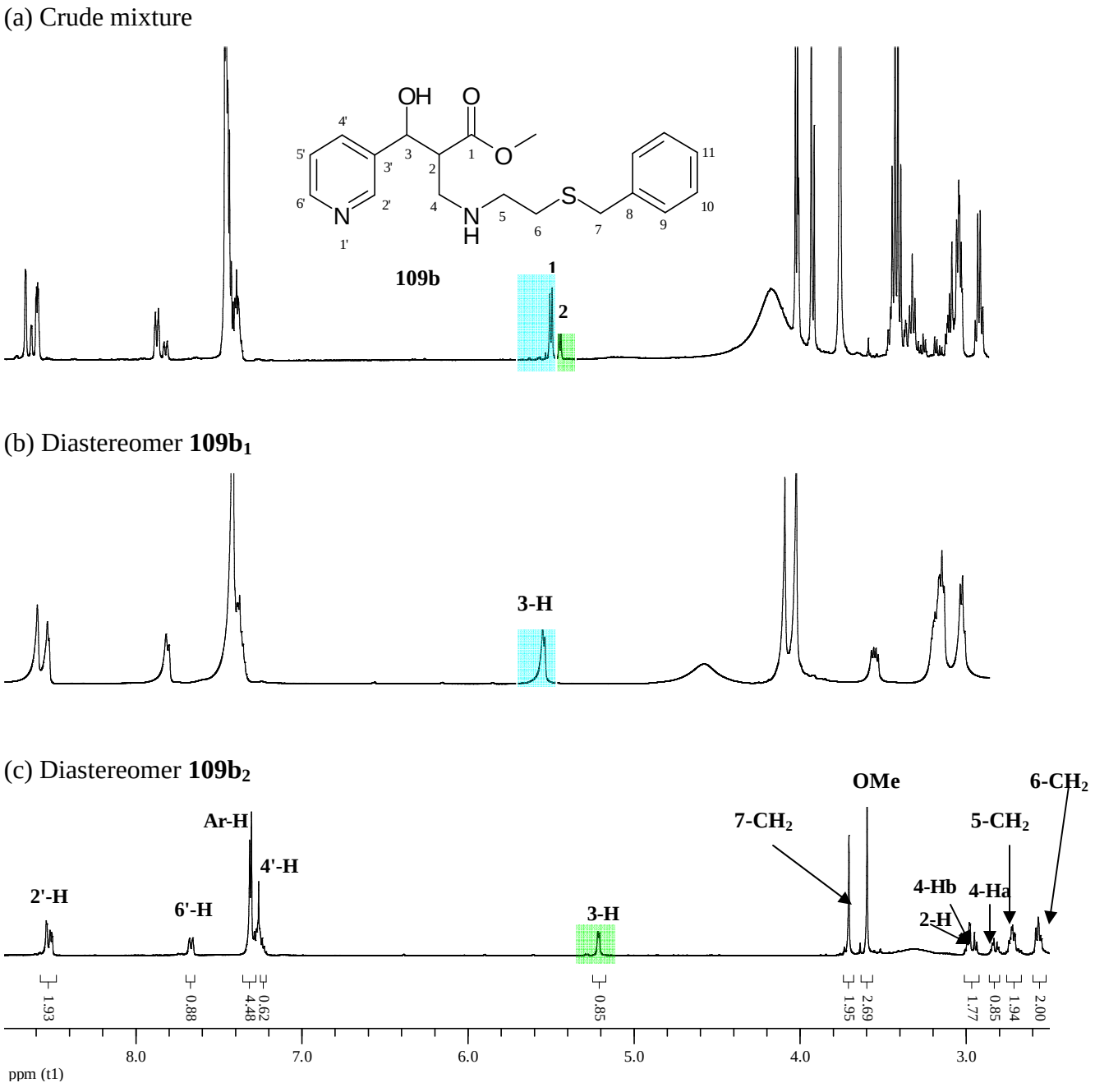

Figure 42. Comparison of the 400 MHz ^{1}H NMR spectra of the crude mixture (a) and the separated diastereomeric components **109b$_1$** (b) and **109b$_2$** (c) in $CDCl_3$.

Signal assignments are supported by the DEPT 135 and HSQC data. Thus, for the major diastereomer **109b$_2$**, the DEPT spectrum (Figure 43) confirms the presence of four methylene carbons, as required, while the HSQC spectrum (Figure 44) was used to confirm the assignments of carbon signals, with the 4-Ha and 4-Hb, and 5-methylene protons correlating to the carbon signals at 48.5 and 48.1 ppm, respectively.

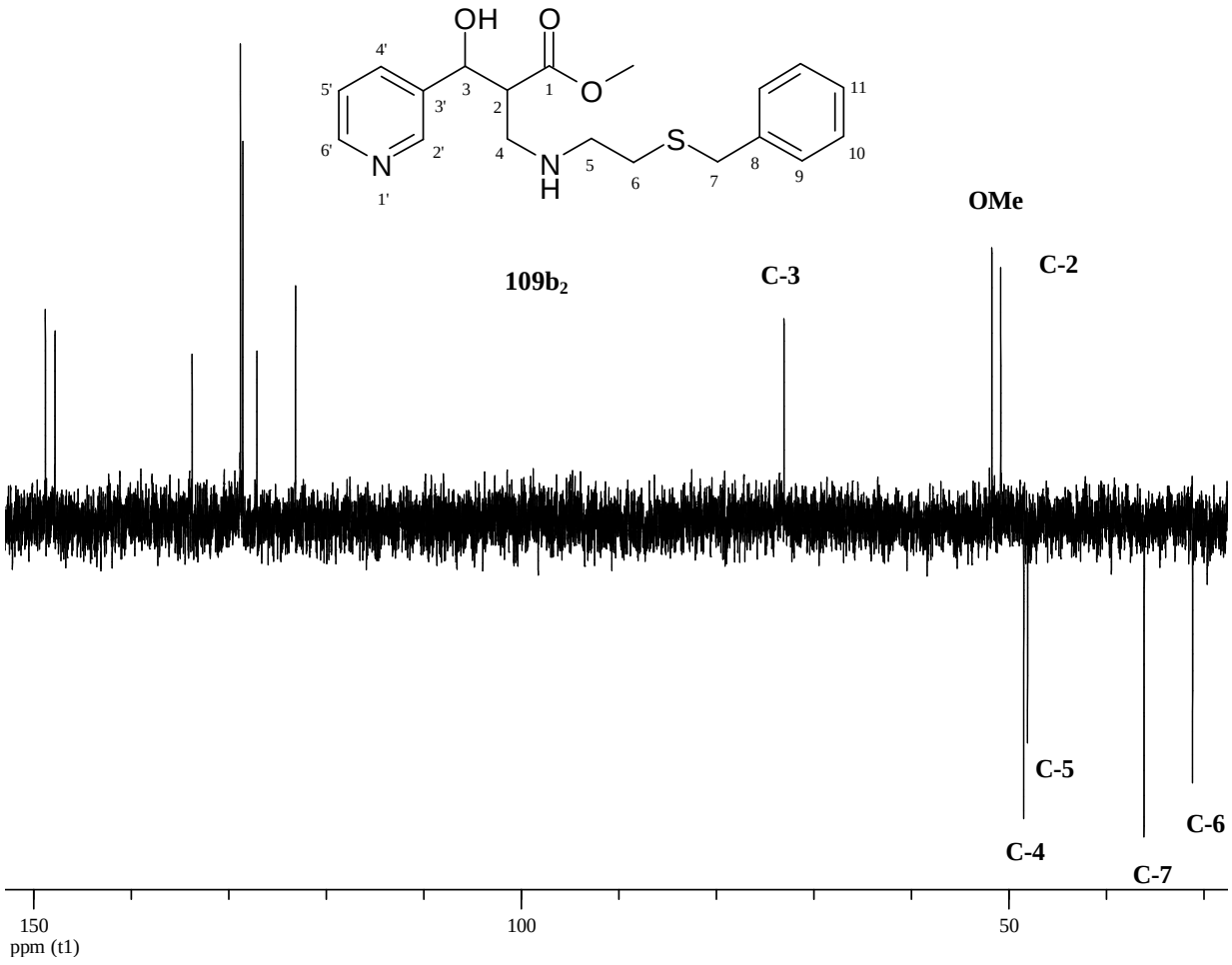

Figure 43. DEPT 135 spectrum of diastereomer **109b$_2$** in $CDCl_3$.

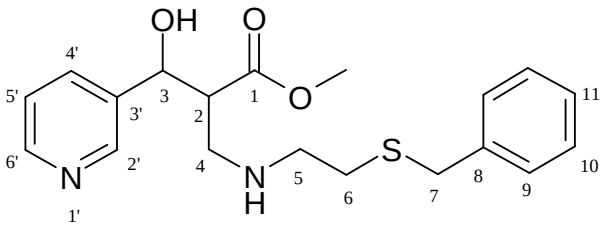

109b$_2$

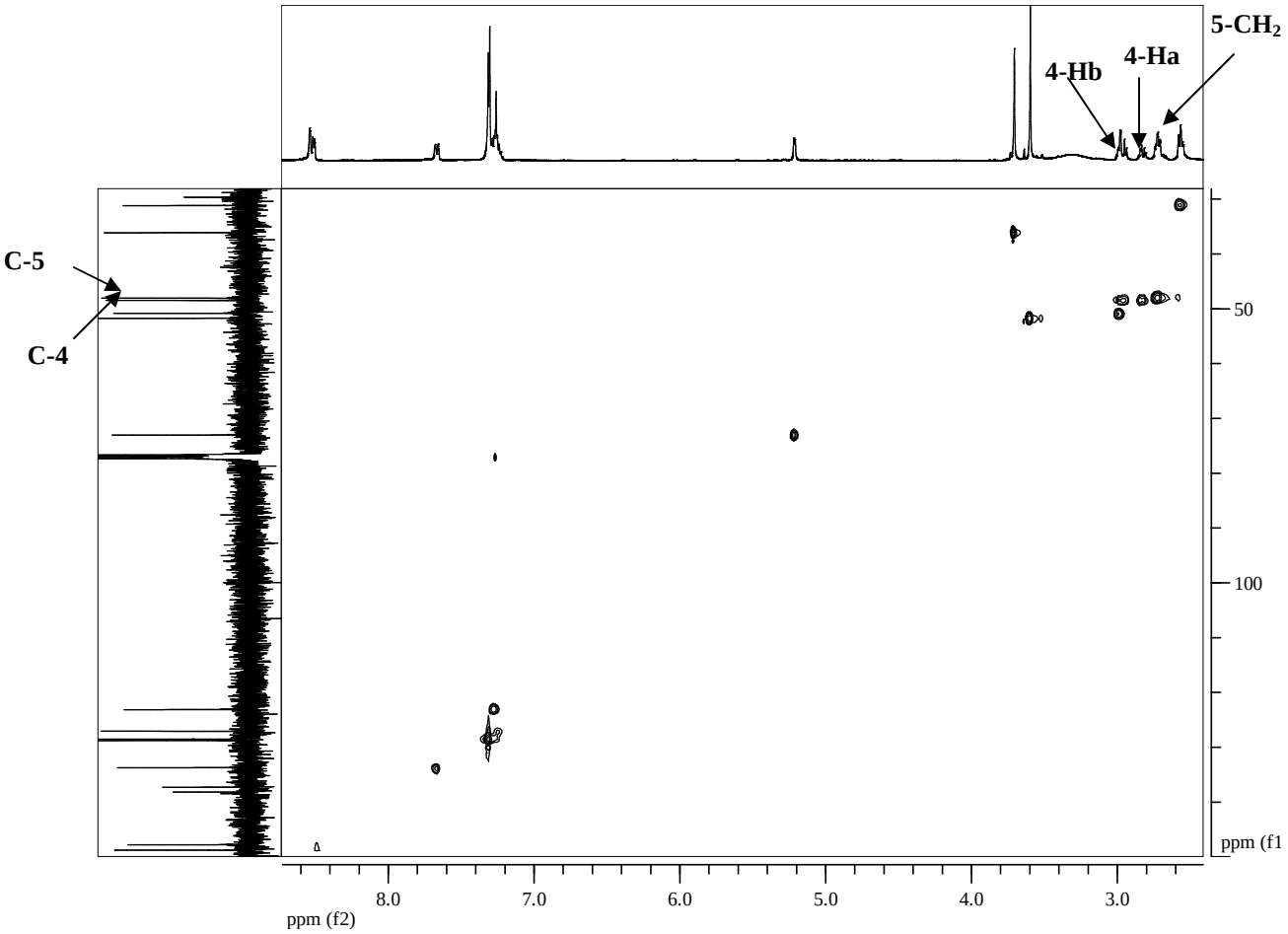

Figure 44. HSQC spectrum of diastereomer **109b$_2$** in $CDCl_3$.

2.4.3. Synthesis of the glycine methyl ester aza-Michael products 109c

Figure 45 illustrates the ^{1}H NMR spectra of the crude mixture obtained from the reaction with glycine methyl ester hydrochloride **96** (Scheme 28) and of the separated diastereomers **109c$_1$** and **109c$_2$**, the latter spectrum (Figure 45c) being that of the major product.

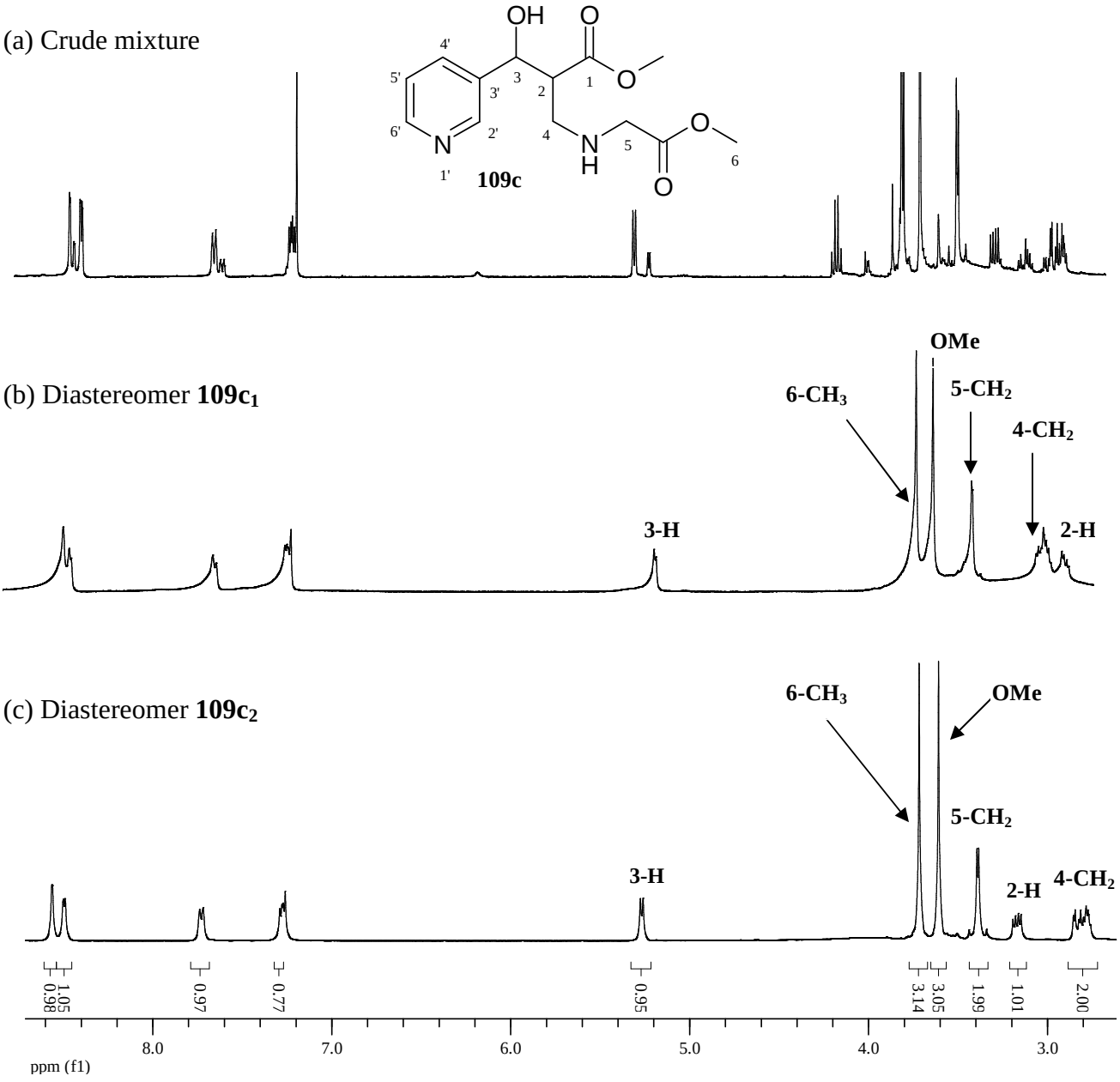

Figure 45. Comparison of the 400 MHz ^{1}H NMR spectra of the crude mixture (a) and the separated diastereomeric components **109c$_1$** (b) and **109c$_2$** (c) in $CDCl_3$.

A significant difference between the ^{1}H NMR spectra of diastereomers **109c$_1$** and **109c$_2$** is that, in the spectrum (Figure 45b) of diastereomer **109c$_1$**, the 2-methine proton resonates at high field than in the spectrum of diastereomer **109c$_2$** (Figure 45c) where it appears downfield compared to the 4-methylene protons. In Figure 45c, the multiplet at 2.81 ppm corresponds to the diastereotopic 4-methylene protons, the multiplet at 3.17 ppm and the doublet at 3.39 ppm to the 2-methine and 5-methylene protons, respectively. The singlets at 3.61 and 3.72 ppm are due to the methoxy group and the 6-methyl protons, the doublet at 5.27 ppm to the 3-methine proton and the signals in the region 7.21-8.59 ppm to the pyridyl protons.

2.4.4 Synthesis of the glycine ethyl ester aza-Michael product 109d

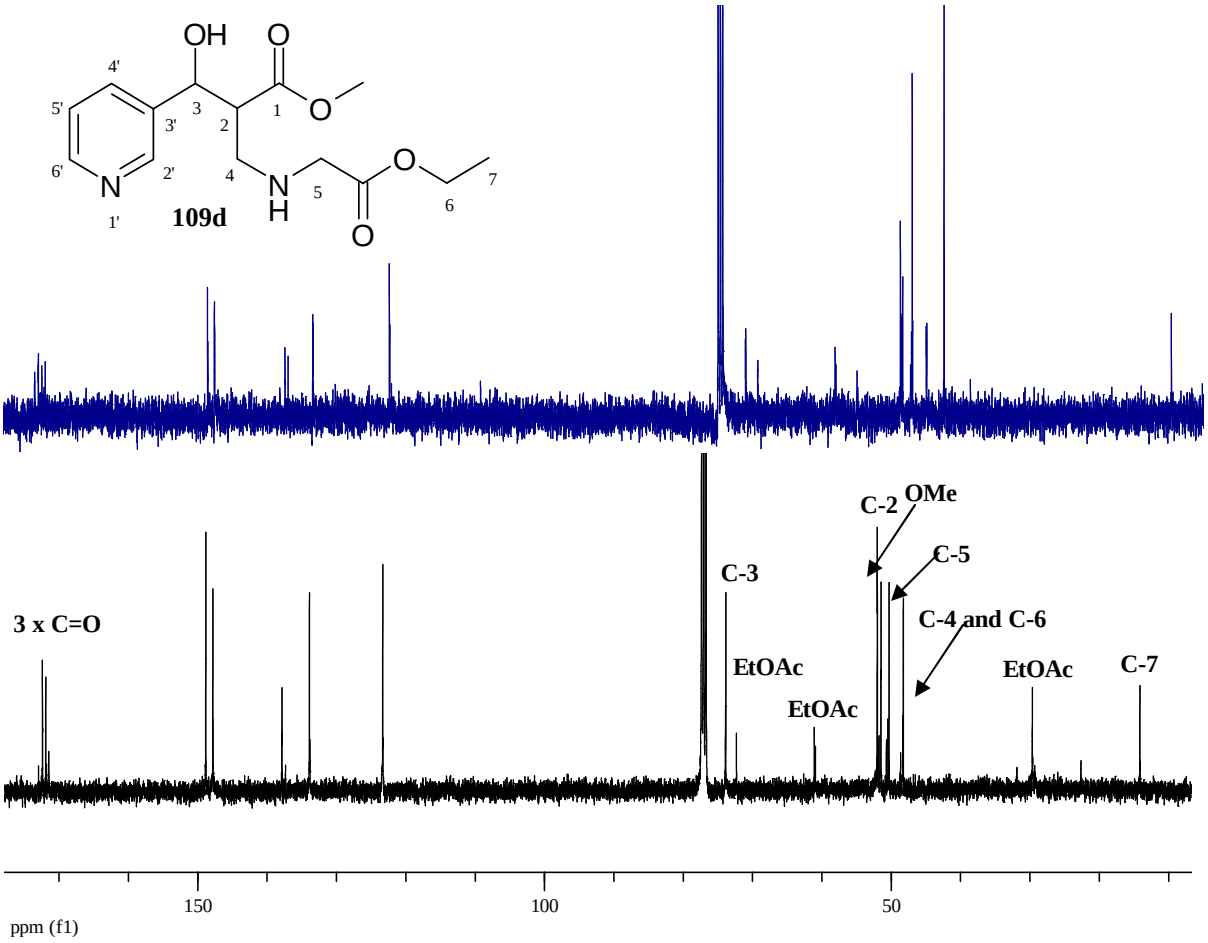

Figure 46. 100 MHz ^{13}C NMR spectra of the crude (blue) and the purified diastereomeric component **109d$_1$** (black) in $CDCl_3$.

Figure 46 illustrates the ^{13}C NMR spectra of the crude mixture (blue) obtained from the reaction with glycine ethyl ester hydrochloride **92** (Scheme 28) and of the recovered diastereomer **109d** (black) after purification. In the ^{13}C NMR spectrum (blue) of the crude mixture, many of the signals are doubled- an indication of a diastereomeric mixture, purification of which gave only one product. The ^{13}C NMR spectrum (black) of the purified product **109d** shows the expected 14 signals, with the 7-methyl carbon resonating at 14.1 ppm, the 4-, 6- and 5-methylene carbons at 48.2, 50.3 and 51.5 ppm, respectively, the methoxy carbon at 52.0 ppm, the 2- and 3-methine carbons at 52.1 and 73.8 ppm, respectively, and the two carbonyl carbons at 171.9 and 172.4 ppm.

2.4.5. Synthesis of the L-serine methyl ester aza-Michael product 109e

L-serine methyl ester hydrochloride **94** was also reacted with the Baylis-Hillman adduct **61g** to afford a diastereomeric mixture of the amino derivatives **109e** (Scheme 28). Figure 47 illustrates the ^{1}H NMR spectrum of the crude mixture still showing the characteristic Baylis-Hillman adduct signals (an indication of incomplete reaction) and the 3-methine protons of the newly-formed diastereomeric products in the region 5.16-5.29 ppm, labelled in green.

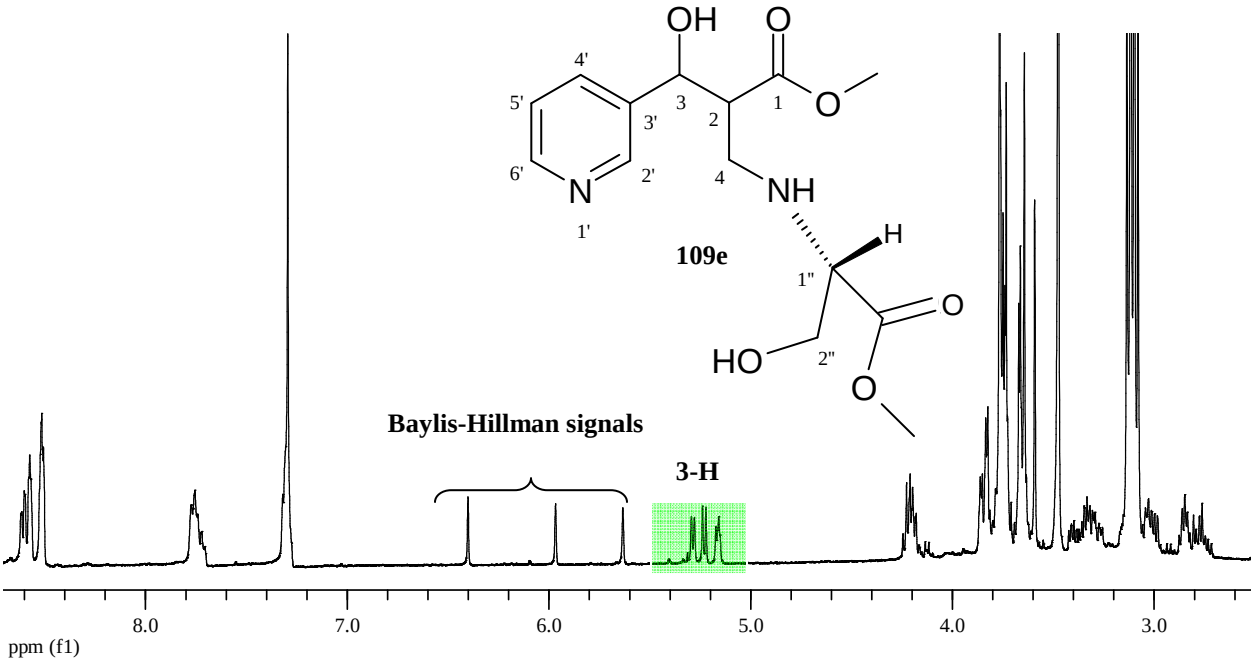

Figure 47. 400 MHz ^{1}H NMR spectrum of the crude mixture of **109e** in $CDCl_3$.

Purification of the crude mixture by preparative layer and high performance liquid chromatography (HPLC), permitted removal of the Baylis-Hillman adduct **61g** but failed to separate the diastereomeric products. The ^{1}H NMR spectrum (Figure 48) of the mixture exhibits the doubling of the 3-methine signal, while the Baylis-Hillman adduct signals observed in Figure 47 are clearly absent. Further purification is still needed to obtain clean products but was precluded by time constraints. The signals can, nevertheless, be assigned as follows; the multiplets at 2.72, 2.81, 2.85 and 3.32 ppm are due to the diastereotopic 4-methylene protons (4-Ha and 4-Hb), while the 2''-methylene proton signal overlaps with the amino and the 2-methine proton signals, respectively. The singlet at 3.59 ppm corresponds to the hydroxyl group, the signals at 3.66, 3.72 and 5.12 ppm to the methoxy groups and the 3-methine protons, respectively; the remaining signals in the region 7.30-8.55 ppm are due to the pyridyl protons.

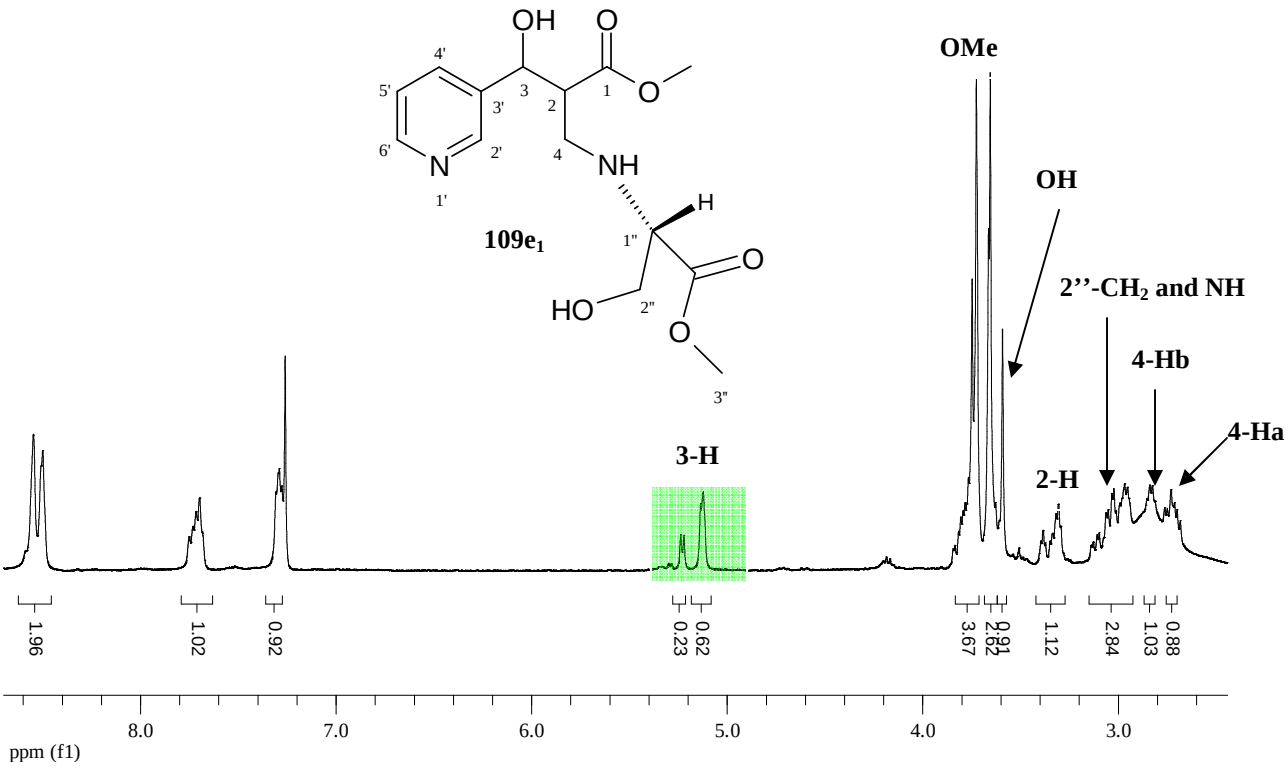

Figure 48. 400 MHz ^{1}H NMR spectrum of the chromatographed mixture of diastereomers **109e** in $CDCl_3$.

2.4.6. Synthesis of L-proline methyl ester aza-Michael products 109f

Figures 49 and 50 illustrate the assignment of the ^{1}H NMR signals for the separated aza-Michael products **109f$_1$ and 109f$_2$**, obtained from the reaction with L-proline methyl ester hydrochloride **98** (Scheme 28).

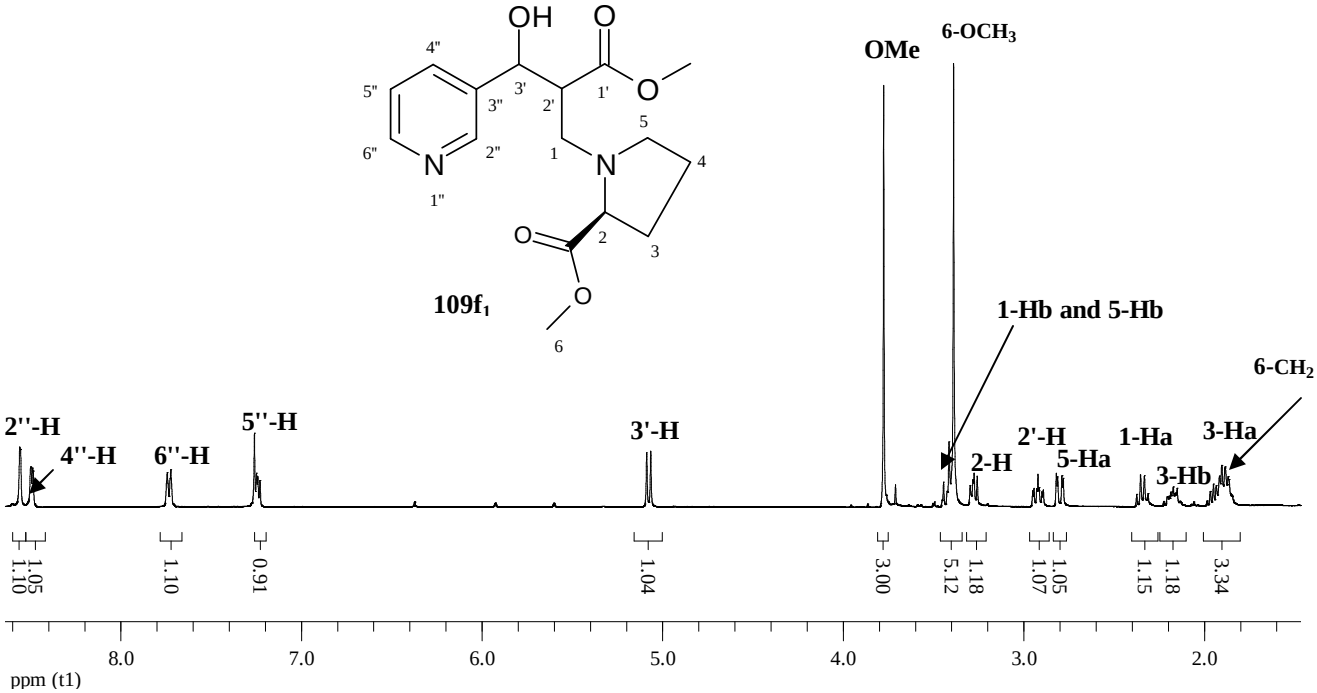

Figure 49. 400 MHz ^{1}H NMR spectrum of diastereomer **109f$_1$** in $CDCl_3$.

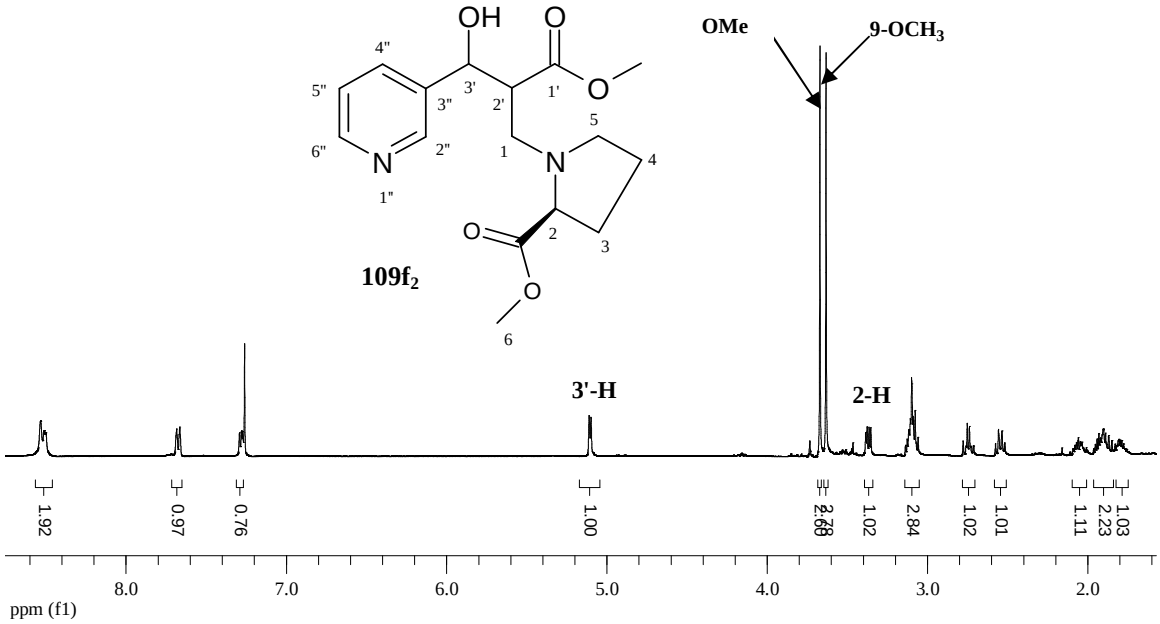

Figure 50. 400 MHz ^{1}H NMR spectrum of diastereomer **109f$_2$** in $CDCl_3$.

The spectrum of the diastereomer **109f$_1$** (Figure 49) reveals greater separation and resolution of almost all the signals, compared to the spectrum of diastereomer **109f$_2$**. In the spectrum of diastereomer **109f$_1$** the multiplets at 1.87, 2.16, 2.34, 2.81, 2.92 and 3.28 ppm are attributed, respectively, to the 4-, 3-, 1- and 5-methylene protons and to the 2'- and 2-methine protons, the singlets at 3.31 and 3.78 ppm to the methoxy groups, the doublet at 5.32 ppm to the 3'-methine proton and the signals in the region 7.21-8.59 ppm to the pyridyl protons. The ^{13}C NMR spectrum of diastereomer **109f$_1$** (Figure 51) shows the expected 16 carbon signals, with the 4- and 3-methylene carbons resonating at 23.7 and 29.5 ppm, respectively, the methoxy groups at 52.1 and 52.7 ppm, the 2-, 2'- and 3'-methine carbons at 57.8, 66.6 and 75.9 ppm, respectively, and the two carbonyl carbons at 171.4 and 173.6 ppm. The DEPT spectrum (Figure 52) confirms the presence of the four methylene groups.

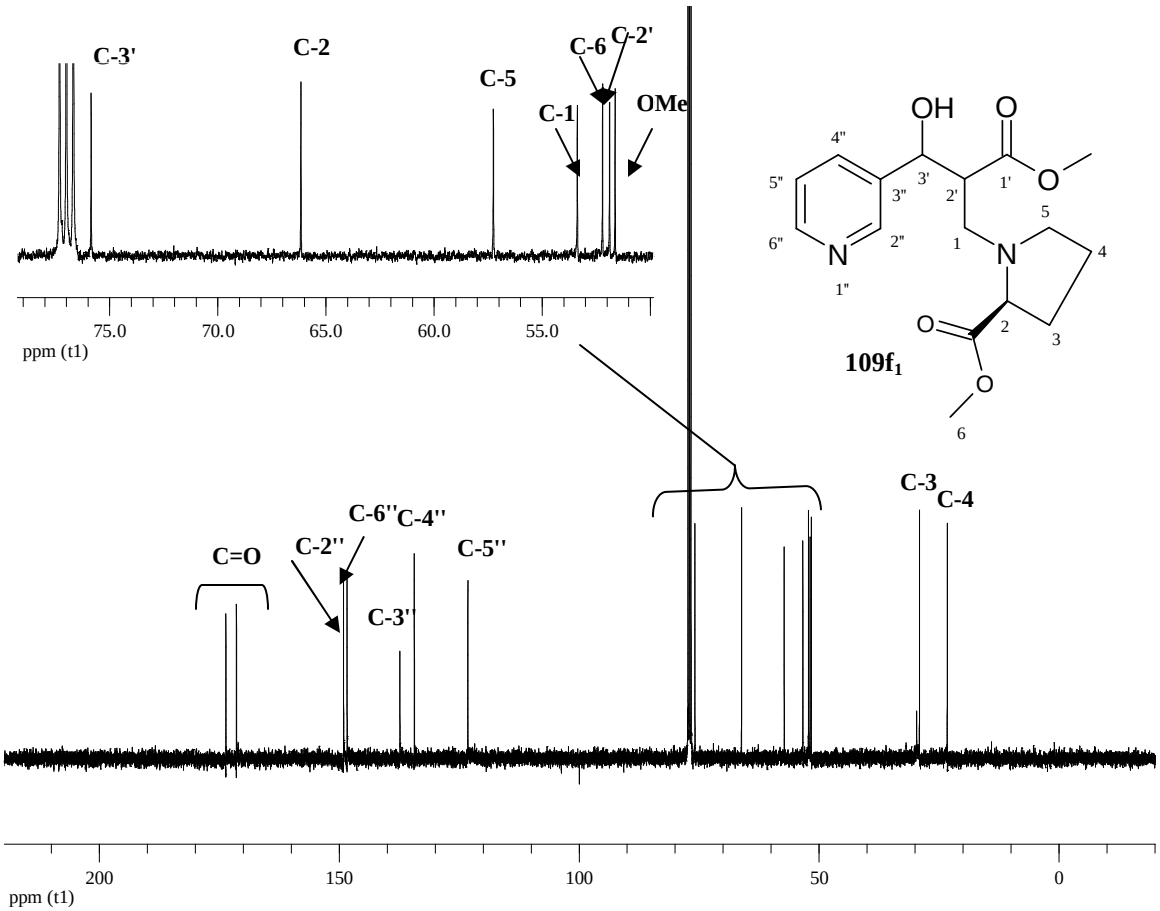

Figure 51. 100 MHz ^{13}C NMR spectrum of diastereomer **109f$_1$** in $CDCl_3$.

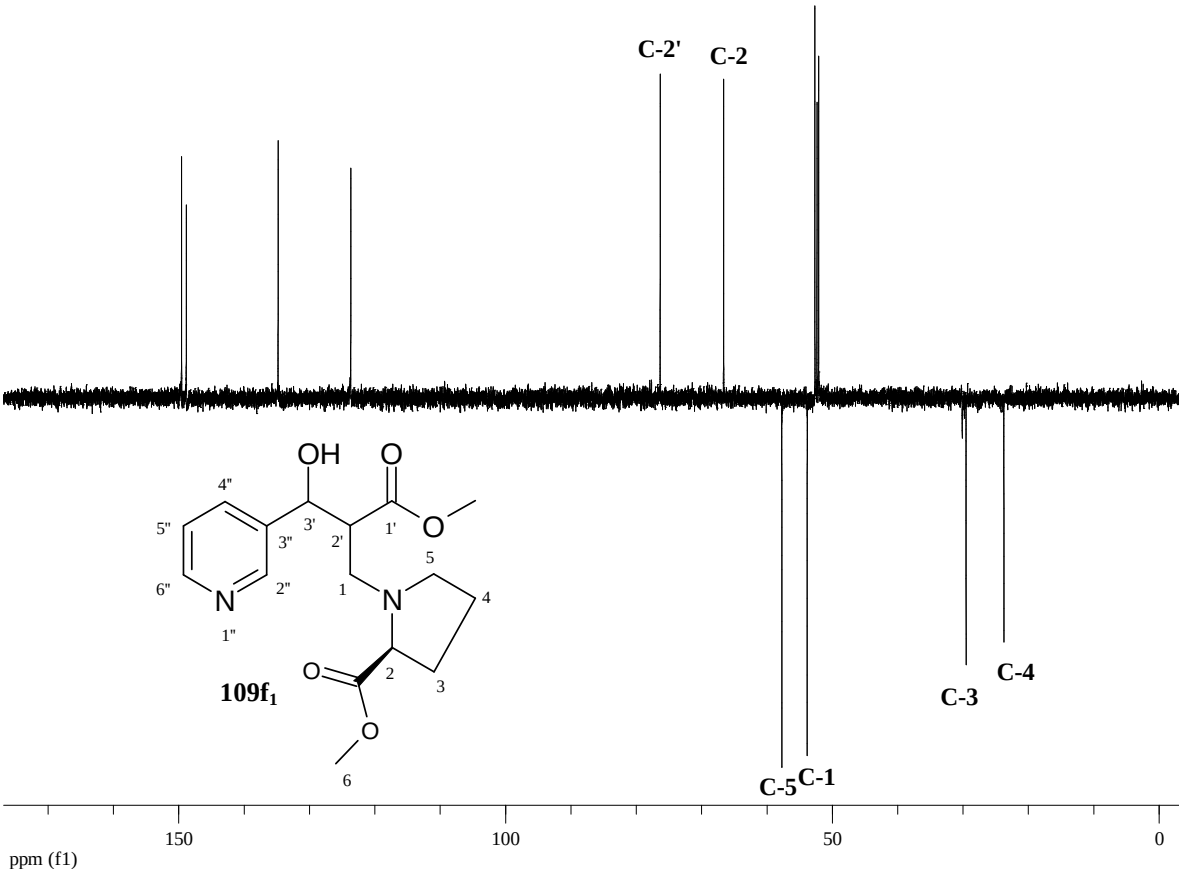

Figure 52. DEPT 135 spectrum of diastereomer **109f$_1$** in $CDCl_3$.

2.4.7. Assignment of the relative stereochemistry of the aza-Michael adducts 109a-f

Gomez-Paloma *et al.*, [150] wrote that "the most crucial part of structural elucidation of organic molecules in organic chemistry is the analysis of their stereochemical features". Stereochemistry plays a significant role in the reactivity and biological activity of organic molecules, and various techniques for assigning stereochemistry have been developed, especially in the last five decades. Among these techniques, nuclear magnetic resonance-[151-153] and computer modelling-based [154-158] methods have been particularly useful in assigning the relative stereochemistry of simple and even complex organic structures. In the present study, both of these techniques were employed to assign the relative stereochemistry at the new stereogenic centres in the aza-Michael products **109a** (Scheme 29), as a model study for the other aza-Michael products **109b-f**. For the sake of

argument, the C-3 stereogenic centre was arbitrarily assigned (*S*). The Baylis-Hillman precursor **61g** is presumed to be racemic and the asymmetric induction effected in the aza-Michael reaction with benzylamine **105**, *S*-benzylcysteamine hydrochloride **90**, the hydrochloride salts of glycine ethyl and methyl esters **92** and **96**, at least, will be mirrored by both enantiomers [*i.e*. the (3*S*) enantiomer of the precursor **61g** will afford the (2*R*, 3*S*) and (2*S*, 3*S*) aza-Michael adducts **109** in the same diastereomeric ratios as the (3*R*) must afford the (2*S*, 3*R*) and (2*R*, 3*R*) products]. The chiral amino nucleophiles, used in the preparation of the aza-Michael products **109e** and **f**, however, may well influence the stereochemical outcome in these two cases.

2.4.7.1. NMR-Based methods

Vicinal proton-proton coupling ($^3J_{H,H}$) constants between protons on adjacent stereogenic centers can give an indication of the spatial orientation of such protons relative to each other. Dihedral angles can be calculated from the vicinal coupling constants using the Karplus curve [158-160]or Karplus equation [158] and the usual "rule" employed is $J_{trans}>J_{cis}$.[152] However, this "rule" fails when the structures have three or more stereogenic centres or when hydrogen-bonding "involves" the stereogenic centre.[152, 161] The vicinal coupling constants between 2- and 3-methine protons were measured for diastereomers **109a$_1$** and **109a$_2$** and found to be 4.84 and 3.93 Hz, respectively, suggesting that diastereomer **109a$_1$** is *trans* (*i.e* 2*R*, 3*S*) and **109a$_2$** is *cis* (2*S*, 3*S*). However, the vicinal coupling constants are not very different, and intramolecular hydrogen-bonding may give rise to a "pseudo-cyclic" structure **109a'** (Scheme 29). Such a 6-membered hydrogen-bonded chelate may well be expected in this case, and this is reinforced by the data obtained from the ^{1}H NMR and IR spectra of these compounds (**109a$_1$** and **109a$_2$**), where the IR spectra were measured in CCl_4 at different concentrations, suggesting that these compounds indeed adopt the hydrogen-bonded conformations.

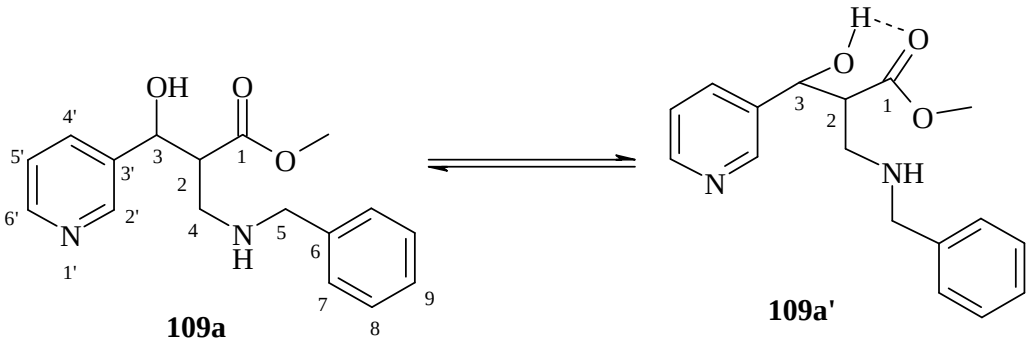

Scheme 29

In order to explore the structures more carefully, 1- and 2-D nuclear Overhauser effect (NOESY) experiments were conducted.[162-163] The NOESY experiment reveals direct, through-space interactions between nuclei and is independent of the through-bond couplings.[162, 164-165] The 2-D phase-sensitive NOESY spectrum of diastereomer **109a$_1$** (Figure 53) reveals cross-peaks showing the following through-space correlations:- (**A**) between the 2- and 3-methine protons, suggesting that the protons may be on the same side of the hydrogen-bonded, dominant conformation of the molecule (*i.e. syn*); (**B**) between 3-H and the 4-Hb methylene protons; (**C**) weak NOE interaction between the 3-methine and the methoxy protons; and (**D**) and (**E**) between the 3-methine and the 4'- and 2'-methine protons of the pyridine ring. The 2-D NOESY spectrum of diastereomer **109a$_2$** (Figure 54) does not show any correlation between the 2- and 3-methine protons of diastereomer **109a$_2$** or between the 3-methine and methoxy protons, but cross-peaks (**B**), (**D**) and (**E**) are observed, suggesting that the 2- and 3-methine protons may be on the opposite sides of the molecule (*i.e. anti*).

In order to verify these results, 1-D selective excitation NOESY experiments were performed on the same molecules by applying a selective 180° Gaussian pulse on the 3-methine proton in each case. This magnetization is only transferred to protons that are correlated to the excited nucleus and does not show those that are not correlated. The results illustrated in Figure 55 confirm the 2-D NOESY data for diastereomer **109a$_1$** since the excitation of 3-H results in clear NOE difference signals for 2-H, 4-Ha and Hb, 2'-H and 4'-H. Figure 56 illustrates the corresponding results for the diastereomer **109a$_2$**

showing NOE difference signals for 4-Hb, 2'-H and 4'-H, thus also supporting the 2-D NOESY data.

The intensities of the signals in the 1-D NOE difference spectra can be plotted against mixing times to obtain NOE build-up curves which should follow a linear, or close to linear relationship.[164] The data obtained from the 1-D NOE difference experiments for diastereomer **109a$_1$** are shown in Table 4 and exhibit the expected linear relationship between 100 and 700 ms; beyond this range abnormalities become evident with the intensities 2'-, 4-Hb, 2-methine and methoxy proton signals beginning to decrease. This pattern beyond 700 ms may be due to the nuclei losing the magnetization obtained from the excitation of the 3-methine proton to the surrounding medium. Figure 57 shows the 1-D NOE build-up curves and R^2 values obtained for the region that obeys the linear relationship, *i.e.* 100 to 700 ms. The build-up curves also confirm the results observed from the 2-D NOESY data of diastereomer **109a$_1$**, thus we can be confident that the 2- and 3-methine protons in the dominant conformation(s) of diastereomer **109a$_1$** are on the same side (*syn*). Similarly, the data (Table 5) from the 1-D NOE difference experiments for diastereomer **109a$_2$** show abnormalities beyond 500 ms, this may also be due to the nuclei losing magnetization to the surrounding medium or to the scalar couplings between the nuclei.[152] Thus, the region plotted in the graph (Figure 58) is the one that appears to obeys the expected linear relationship (*i.e.* from 100 to 500 ms). Again the results support those observed from the 2-D NOESY data of diastereomer **109a$_2$**.

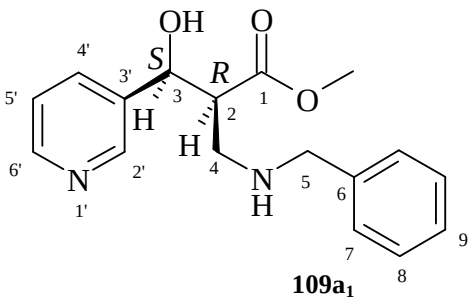

109a$_1$

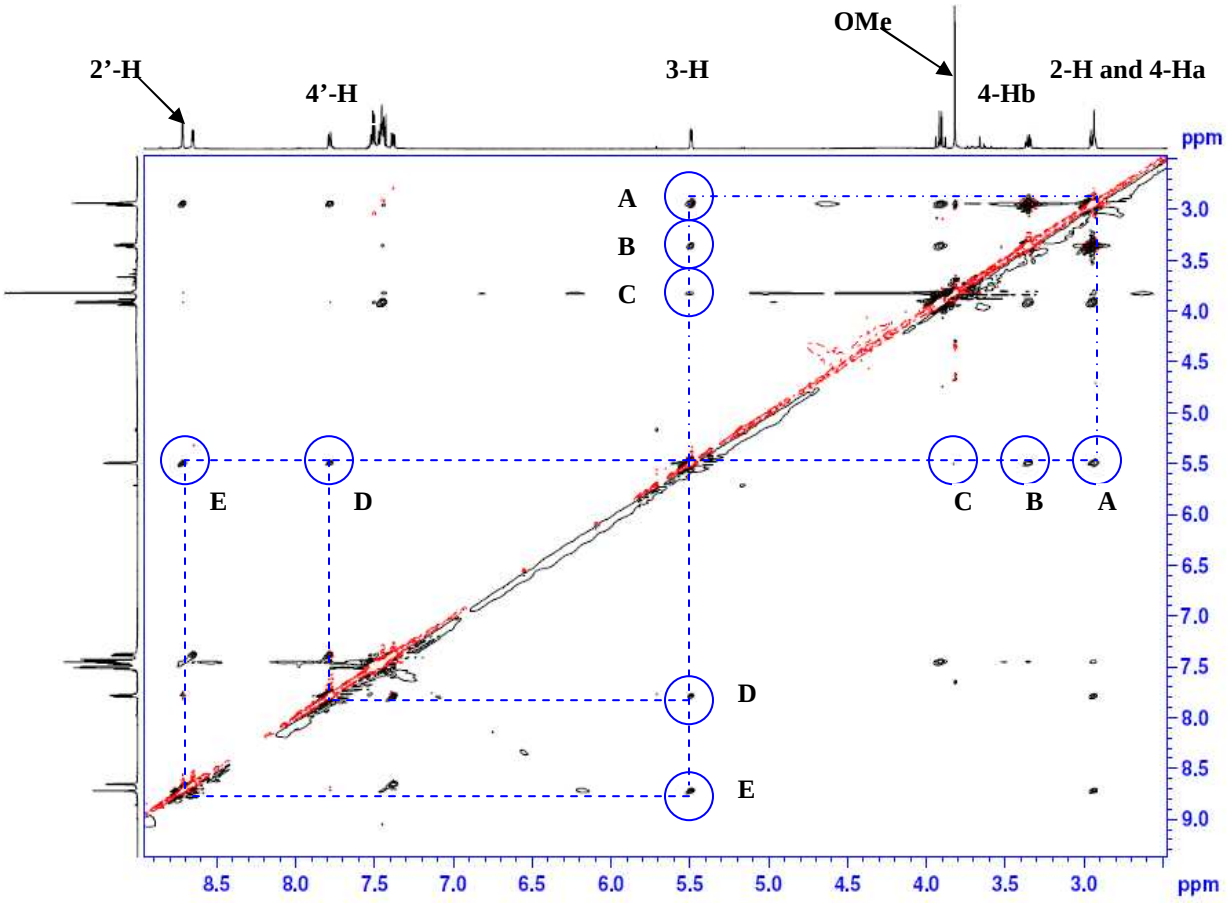

Figure 53. 600 MHz 2-D NOESY spectrum of diastereomer **109a$_1$** in $CDCl_3$, and the structure showing the proposed relative configurations (2*R*, 3*S*) at C-2 and C-3.

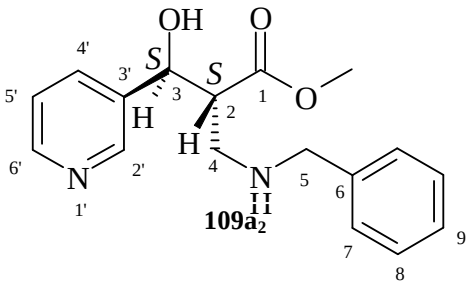

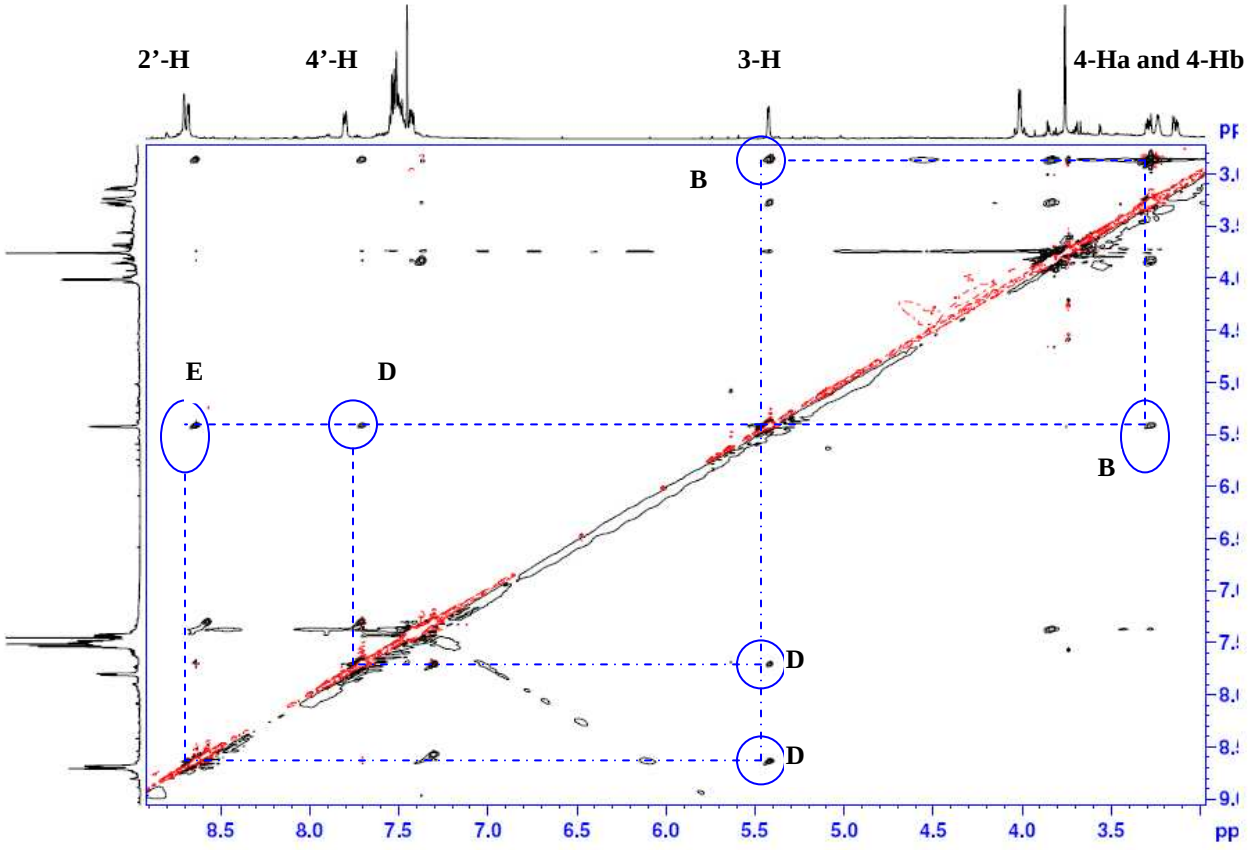

Figure 54. 600 MHz 2-D NOESY spectrum of diastereomer **109a$_2$** in $CDCl_3$, and structure showing the proposed relative configurations at C-2 and C-3 (2*S*, 3*S*).

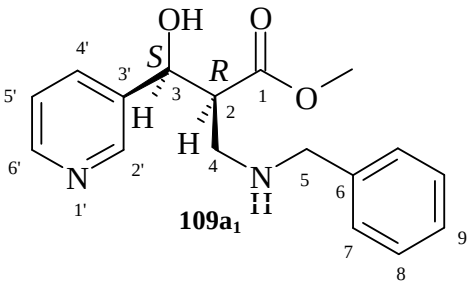

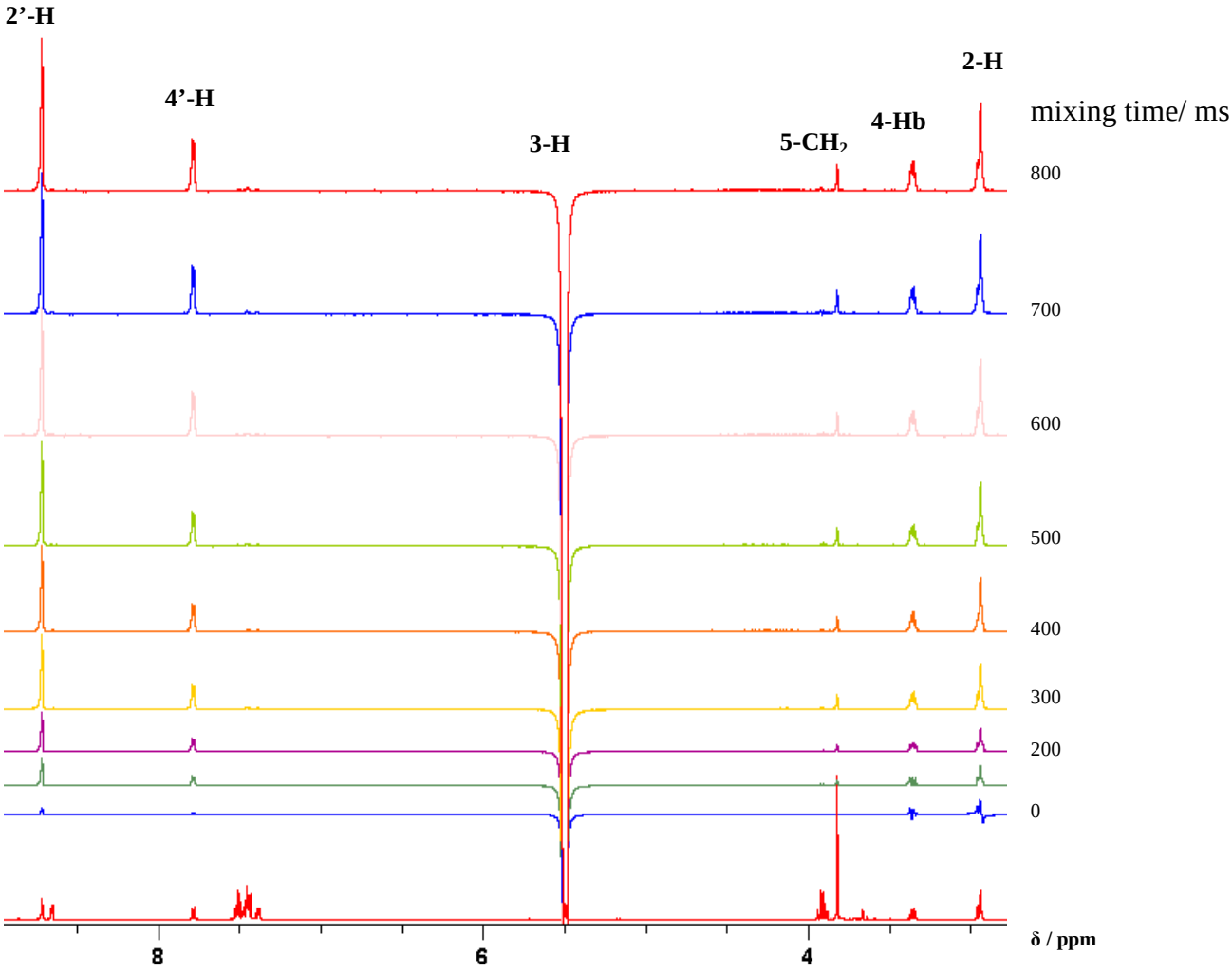

Figure 55. 600 MHz 1-D NOE difference spectra for diastereomer **109a$_1$** recorded over different mixing times, following selective excitation of the 3-H nucleus.

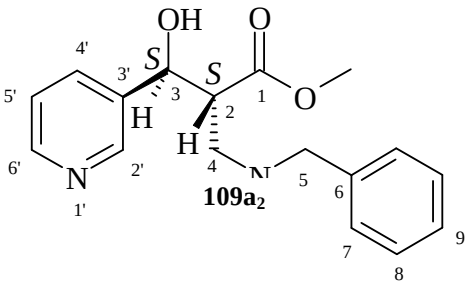

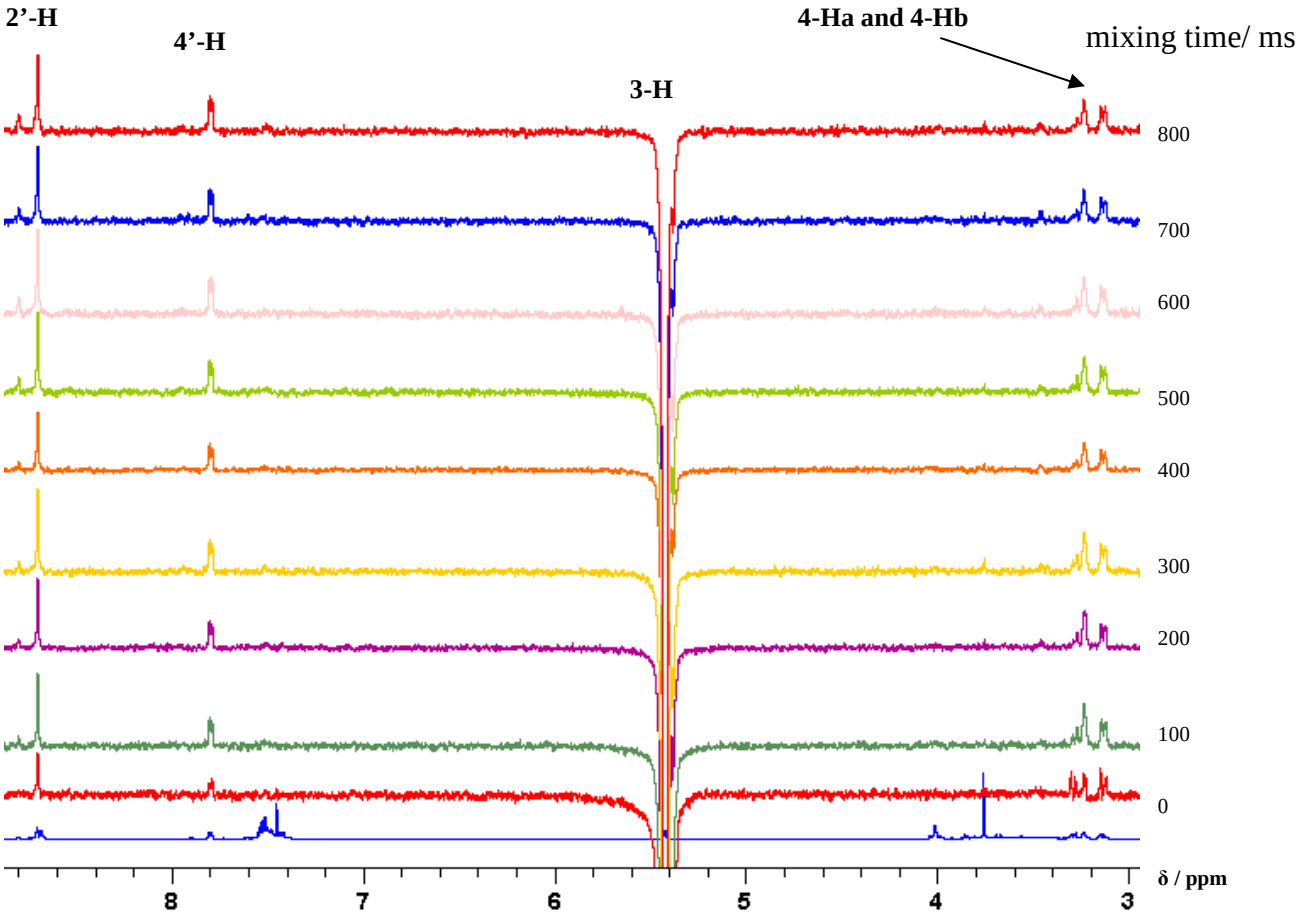

Figure 56. 600 MHz 1-D NOE difference spectra for diastereomer **109a$_2$** recorded over different mixing times, following selective excitation of the 3-H nucleus.

Table 4. Signal intensity values obtained from the 1-D NOE difference experiments for diastereomer **109a$_1$**.

		2'-H	4'-H	OMe	4-Hb	2-H
Exp no	**time(ms)**	**8.77-8.67[a]**	**7.83-7.73[a]**	**3.85-3.79[a]**	**3.41-3.30[a]**	**3.02-2.81[a]**
102	100	1.4237	0.8652	0.2586	1.3520	1.4359
103	200	2.8741	1.6409	0.3498	1.2603	3.4091
104	300	4.0471	2.2931	0.5214	2.1623	4.2319
105	400	5.1111	2.9519	0.6754	2.6882	5.2161
106	500	6.0475	3.4435	0.7455	3.1319	6.0612
107	600	6.8809	3.9811	0.8535	3.3666	6.8530
108	700	7.6126	4.3677	0.9174	3.5182	7.2853
109	800	8.2165	4.8435	1.0101	3.6796	7.7402
110	900	8.8555	5.1208	1.0998	3.7975	8.2272
111	1000	8.9216	5.1417	1.068	3.7736	8.1376

[a] Integration range (δ/ppm)

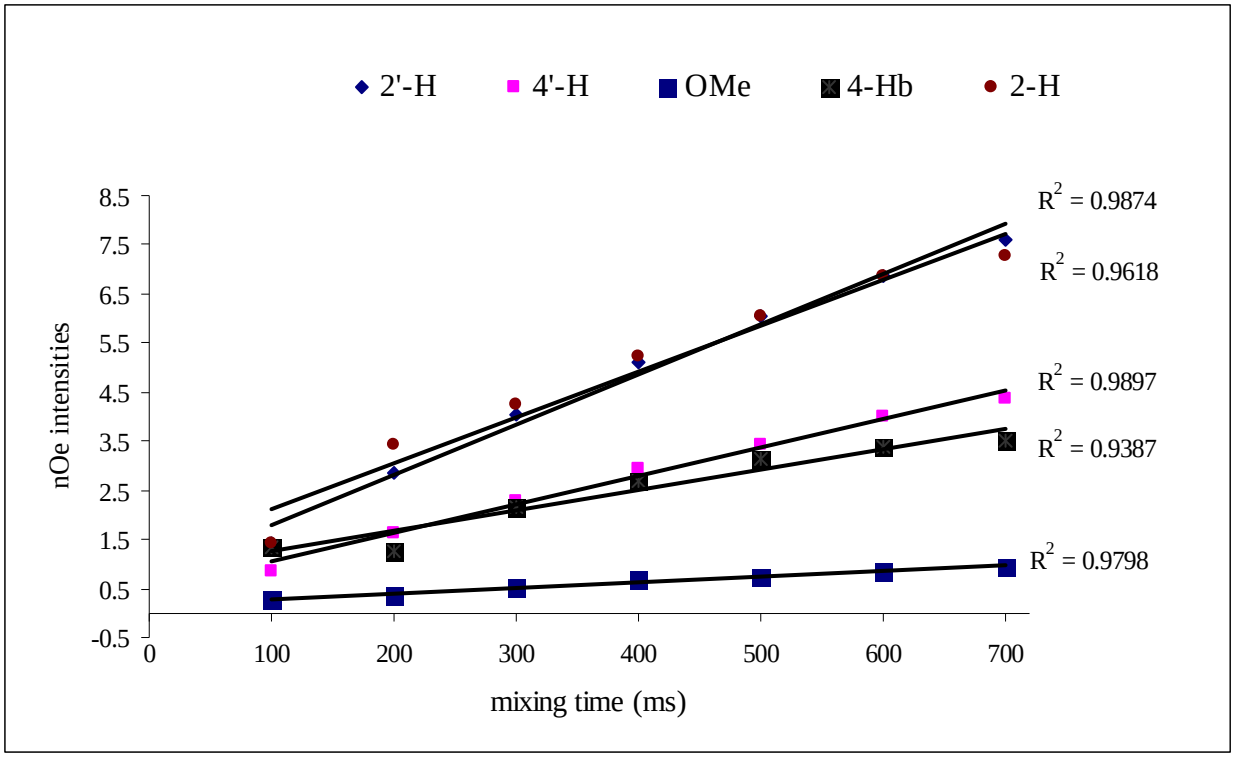

Figure 57. 1-D NOE build-up curves measured for five different nuclei (2'-H, 4'-H, OMe, 4-Hb and 2-H) when 3-H was selectively excited in diastereomer **109a$_1$**.

Table 5. Signal intensity values obtained from the 1-D NOE difference experiments for diastereomer **109a$_2$**.

		2'-H	4'-H	4-Hb	4-Ha
Exp no	**time(ms)**	**8.79-8.63[a]**	**7.87-7.73[a]**	**3.33-3.21[a]**	**3.174-3.09[a]**
102	100	1.1504	0.4686	1.4056	0.9021
103	200	2.0875	1.1580	2.5077	1.7414
104	300	2.1081	1.5111	3.3865	1.9265
105	400	2.6661	1.5487	3.5890	2.1380
106	500	3.0298	1.6419	3.3016	2.3676
107	600	2.7485	1.8013	3.3567	2.1559
108	700	3.0009	1.9958	3.1440	2.1289
109	800	3.0638	2.0905	2.7955	1.9271
110	900	2.5710	1.8693	3.4746	1.7751
111	1000	2.7225	2.0101	2.5145	1.8617

[a] Integration range (δ/ppm)

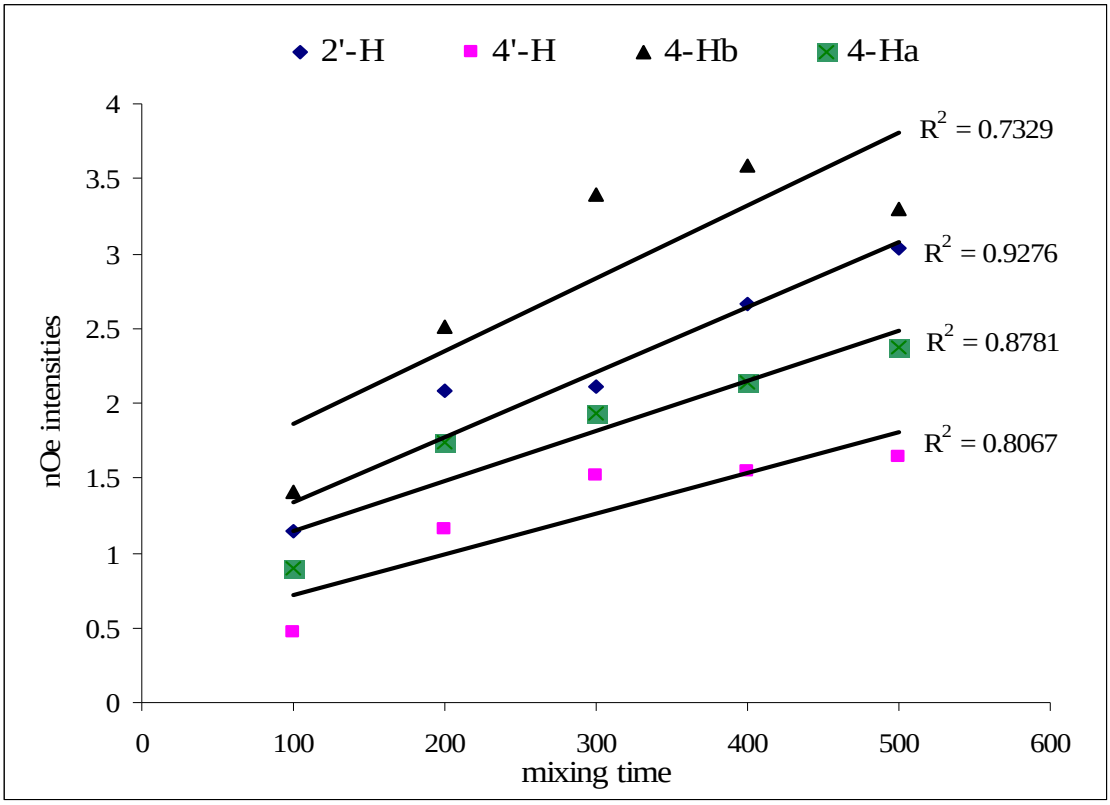

Figure 58. 1-D NOE build-up curves measured for five different nuclei (2'-H, 4'-H, 4-Ha and 4-Hb) when 3-H was selectively excited in diastereomer **109a$_2$**.

2.4.7.2. Computer modelling-Based methods

The goal of using computer modelling techniques was to establish the most stable conformers of the aza-Michael products **109a-f**. In order to achieve this, geometrical-optimization of selected structures was conducted, including an exploration of their conformational space in order to locate the global minima. The modelled structures of the four diastereomers of compound **109a** were minimized using the Universal Force Field, [166] followed by molecular dynamics simulation using the Cerius^2 software package.[167] Dynamics simulations were performed by applying one million steps using the quench dynamics method with a thousand steps between quenches. The trajectory data files obtained from the simulations were analyzed and the ten lowest energy conformers of each of the four theoretical diastereomers of compound **109a** were saved, and the lowest energy conformer was assumed to be the global minimum in each case. Table 6 shows the number of the conformer in each Boltzmann population, the stereochemistry, energy, dihedral angle (and the corresponding vicinal coupling constant) and the distance between H_A and H_B obtained for each conformer, where **109a(I)** and **109a(I')**, and **109a(II)** and **109a(II')** are enantiomeric pairs of diastereomers **109a.** Enantiomers are mirror-images of each other and are expected to have identical physical properties, except for their ability to rotate plane-polarized light by equal amounts in opposite directions.[168] In theory, enantiomers are expected to have the same energy in molecular dynamics simulations (a random search method) but the energies obtained here for the enantiomeric systems were clearly different, although the differences are small (< 1 kcal.mol^{-1}). This is attributed to the large number of torsions in the stereoisomers of **109a**, for which an even more systematic search of conformational space may be necessary. Nevertheless, the (2*S*, 3*S* and 2*R*, 3*R*) enantiomers appear to be more stable than the (2*R*, 3*S* and 2*S*, 3*R*) enantiomers, as evidenced by their lower energy values. The geometries of the four conformers were then optimized at the B3LYP level,[169] with a 6-31G(d) basis set,[169] using the Gaussian 03 package, [170] and Figure 59 shows the orientation of H_A, the 3-methine proton, relative to H_B, the 2-methine proton (Figure 59) in each case.

The percentage diastereomeric excess obtained for the aza-Michael products **109a-f** (Table 3, page 60), with the second fractions (**109a$_2$-f$_2$**) being more favoured in each

case, can be explained by an analysis of the NMR and computer modelling results. From Table 6, the dihedral angles obtained for the lower energy 2*R*, 3*R*/2*S*, 3*S* enantiomers [**109a(I)** and **109a(I')**] are closer to 90° than the higher energy enantiomers 2*R*, 3*S*/2*S*, 3*R*, [**109a(II)** and **109a(II')**], and hence should have smaller coupling constants. In a typical Karplus curve, a dihedral angle of *ca* 90° corresponds to negligible vicinal coupling constant.[158-160] These theoretical results are consistent with the experimental NMR data, where the favoured diastereomer (**109a$_2$**) has a smaller coupling constant than diastereomer **109a$_1$**. Measurements of the distances between the 2- and 3-methine protons in the modelled structures (Table 6, Figure 59) reveal that the larger separation (> 3Å) of these protons in the geometry-optimized conformers of the 2*R*, 3*R*/2*S*, 3*S* enantiomers is consistent with the absence of an NOE interactions for **109a$_2$**. The corresponding distances between the vicinal protons (1.6 ± 0.3 Å) in the modelled conformers of the 2*R*, 3*S*/2*S*, 3*R* enantiomers, however, is consistent with the relatively strong NOE interactions observed for **109a$_1$**.

Assuming similar stereochemical preferences for all of the other aza-Michael products **109b-f**, we suggest that the less favoured, first set of diastereomers **109a$_1$-f$_1$** exhibit 2*R*, 3*S*/2*S*, 3*R* configurations, while the more favoured second set (**109a$_2$-f$_2$**) exhibit 2*R*, 3*R*/2*S*, 3*S* stereochemistry. A detailed mechanistic study would be needed to determine whether the observed diastereoselectivity is due to kinetic or thermodynamic factors.

Table 6. Results from the molecular dynamics simulations using the quench dynamics for the stereomeric possibilities of **109a**.

Conformer number	**conformer name**	**Stereochemistry**	**Energy (kcal.mol^{-1})**	**Dihedral angle/(°)**	**$^3J_{H-H}$ (Hz)**	**Distance (H_A-H_B)/Å**
887	**109a(I)**	2*R*, 3*R*	54.63	107.7	1.27	3.082
587	**109a(I')**	2*S*, 3*S*	53.8	109.8	1.39	3.074
139	**109a(II)**	2R, 3S	57.08	50.5	4.61	1.867
751	**109a(II')**	2*S*, 3*R*	56.8	57.6	3.76	1.357

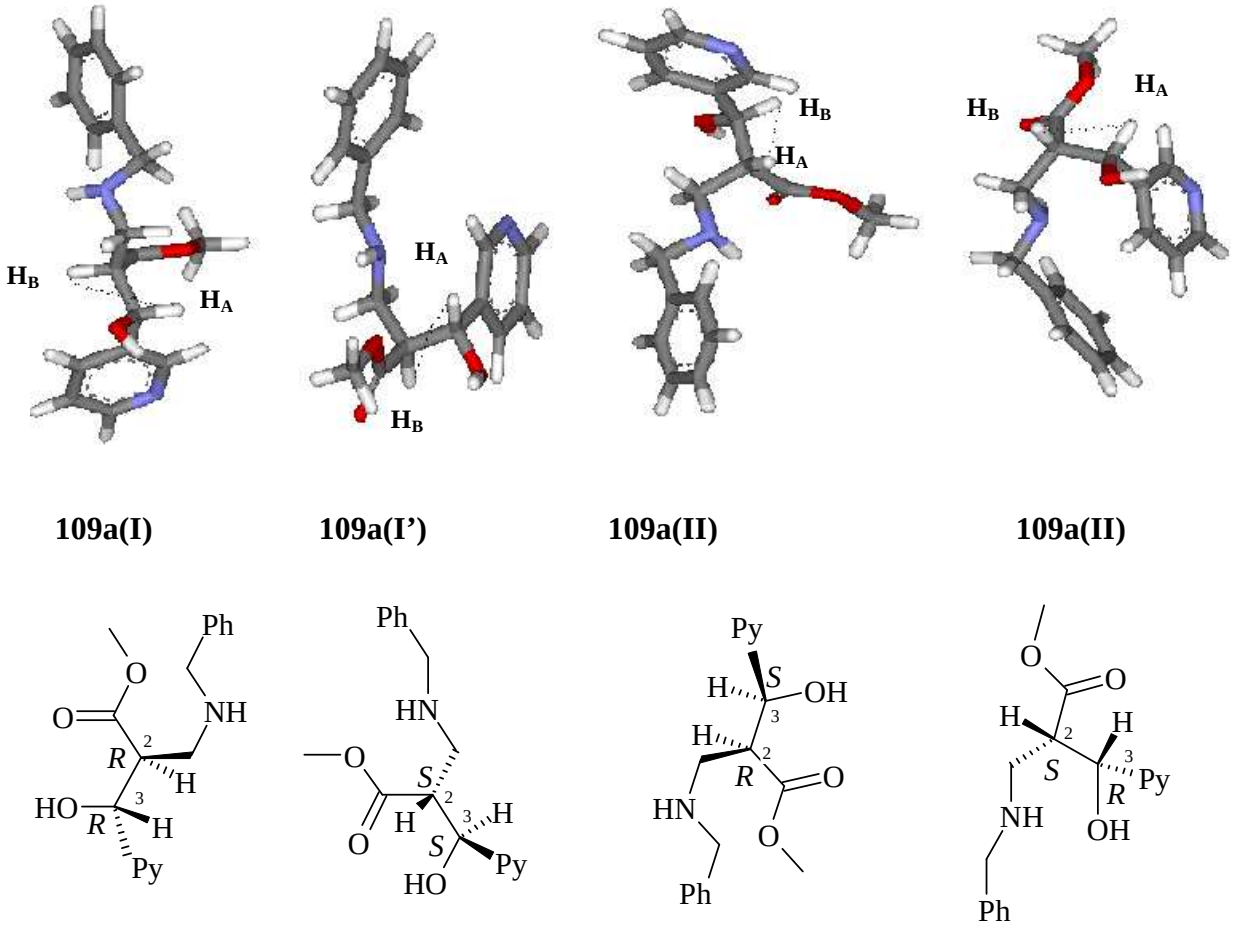

Figure 59. Gaussian B3LYP/6-31G(d) optimized structures of the stereoisomers of **109a**.

2.5. *In silico* receptor-site docking and protein NMR studies of selected compounds

2.5.1. Docking experiments using Autodock 4.0

The aza-Michael products **109a-f** had all been subjected to energy minimization and optimization as described in section 2.4.7.2 (Figure 60), and were selected for molecular docking, choosing only the theoretical structures exhibiting the *trans* conformations on the C-2 and C-3 carbons as ligands. The HIV-1 protease enzyme structure (1HXW, an x-ray diffraction structure complexed with Ritonavir®) was downloaded from the Brookhaven Protein Database (PDB) (Figure 61).[171] The inhibitor, Ritonavir®, was removed from the enzyme's active site using Accerlrys DS visualizer.[172] Protein-inhibitor docking calculations were carried out on AutoDock version 4.0 equipped with the AutoDock Tools (ADT) graphical user interface, [173-176] using the Lamarckian genetic algorithms search method.[177] Polar hydrogens were added to the protease enzyme and charges were assigned to the ligands prior to docking. AutoDock 4.0 default docking parameters were used with the exception of using a bigger grid box (number of grid points) with dimensions 60 x 60 x 60 (x, y and z) separated by 0.375 Å on Autogrid in order for the ligand to "explore" a large area of the active site of the protease enzyme. The number of docking runs was increased from the default 10 to 100 runs. Samudrala *et al*., [178-180] described an efficient method of improving correlation between the experimental and calculated binding energies by applying dynamics simulation on the receptor enzyme. This procedure was followed and the protease enzyme was subjected to energy minimization and dynamics simulation for a very short time and, thereafter, ligands were docked into the active site of the enzyme and three best energy terms were obtained (intermolecular, internal energy of the ligand and torsion free-energy) for the ligands **109a-f** (Table 7). The final docked energy was calculated from the sum of the intermolecular and internal energies and the ligands in Table 7 are ranked according to their final docked energy. [180]

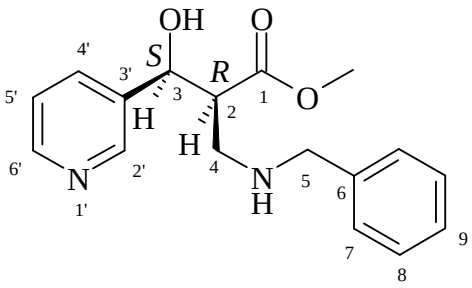

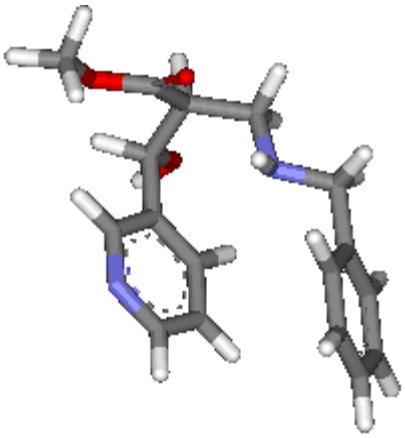

Compound **109a**

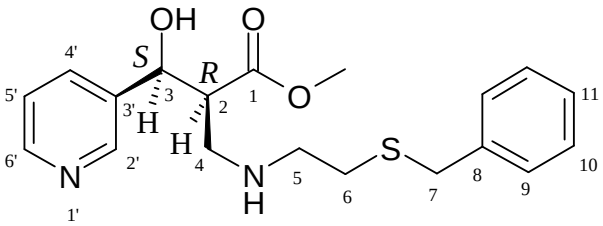

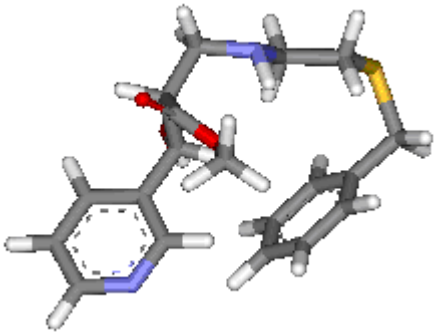

Compound **109b**

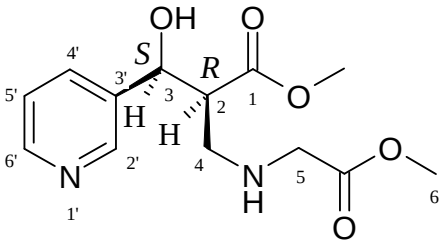

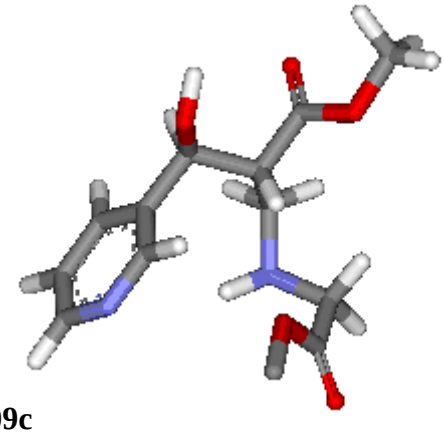

Compound **109c**

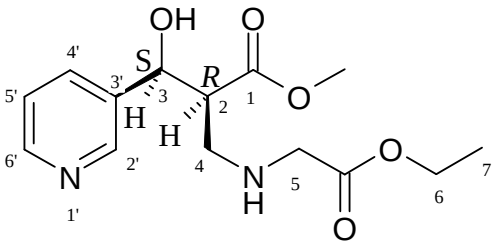

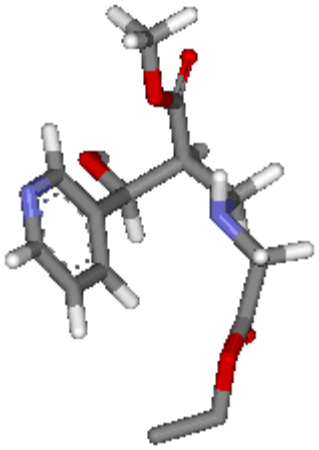

Compound **109d**

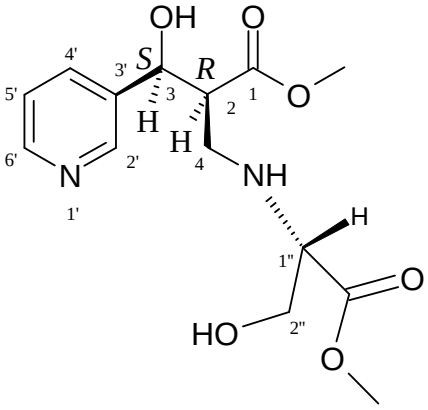

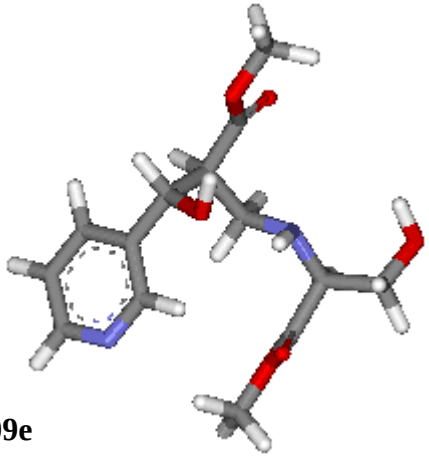

Compound **109e**

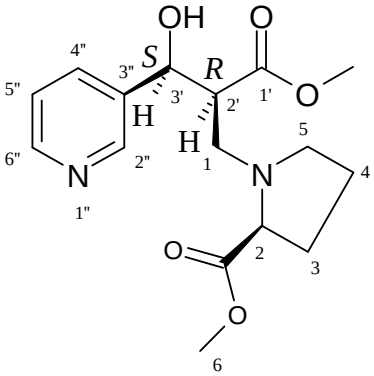

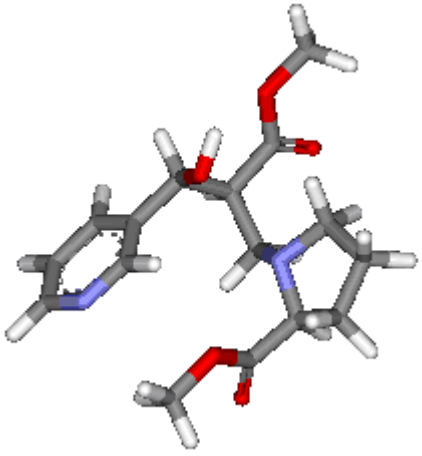

Compound **109f**

Figure 60. Gaussian B3LYP/6-31G(d) optimized structures

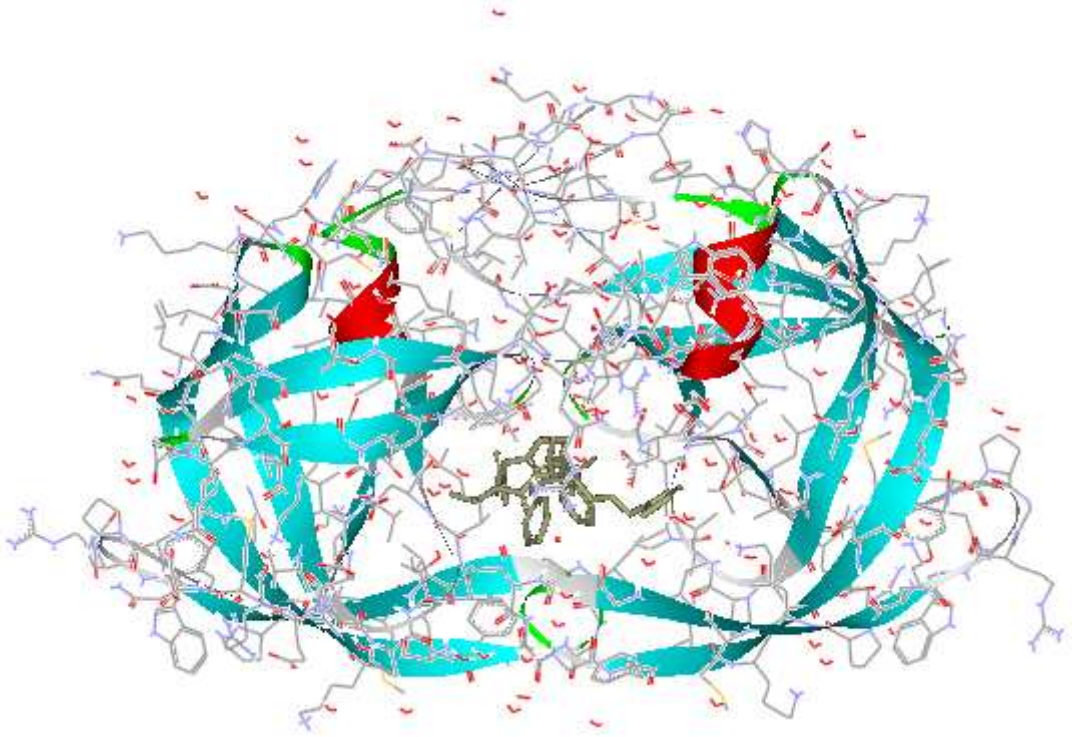

Figure 61. 1HXW X-ray diffraction structure of the HIV-1 protease enzyme complexed with ritonavir.

Table 7. Energy results of the aza-Michael products **109a-f** obtained from Autodock 4.0 and ranked according to their final docked energies.

Compound	Intermolecular energy ($kcal.mol^{-1}$)	Internal energy of ligands ($kcal.mol^{-1}$)	Torsion free-energy ($kcal.mol^{-1}$)	Final docked energy ($kcal.mol^{-1}$)
Ritonavir	-12.97	-2.23	4.94	-15.2
109b	-9.42	-4.4	3.29	-13.82
109a	-9.94	-0.58	2.47	-10.69
109e	-8.73	-1.96	3.29	-10.52
109d	-8.31	-2.13	3.02	-10.44
109f	-8.75	-0.74	2.47	-9.49
109c	-8.63	-0.76	2.74	-9.39

Each docking experiment was derived from 100 different runs that were set to terminate after a maximum of 1,5 million energy evaluations or 27 thousand generations, yielding 100 docked conformations. Upon examination of the docking features between the ligands and the HIV-1 protease, hydrogen-bonding interactions were observed. Figure 63 and 64 reveal favorable hydrogen-bonding interactions formed between compound **109b** and some residues in the receptor cavity of the HIV-1 protease: (i) the basic nitrogen atom of the pyridyl group and the oxygen atom of the carbonyl ester group with the catalytic water molecule; (ii) the oxygen atom of the hydroxyl group at position 3 with Ala 28 residue found in the S2 subsite; (iii) the hydrogen atom of the hydroxyl group at position 3 with the catalytic Asp 25' residue found in the S1' subsite; and (iv) the NH group with the catalytic Asp 25 residue found in the S1 subsite. Similarly, Figure 65 and 66 show favorable hydrogen-bonding interactions of compound **109a** and the receptor site: (i) the NH group with the catalytic water molecule; (ii) the oxygen atom of the carbonyl ester group with the catalytic Asp 29 and Asp 30 residues found in the S3' and S2' subsites, respectively; (iii) the oxygen atom of the hydroxyl group at position 3 with Gly 48 residue found in the hydrophobic pocket of the cavity; and the basic nitrogen atom of the pyridyl group form a bond with the catalytic water molecule. Compound **109e** (Figure 67 and 68) forms hydrogen-bonding interactions as follows: (i) the oxygen atom of the carbonyl ester group at position 1 forms hydrogen-bonds with Ile 50 and Gly 49 residues found in the S4' subsite and in the hydrophobic pocket of the cavity, respectively; (ii) the hydrogen atom of the hydroxyl group at position 2'' forms a hydrogen-bond with the catalytic Asp 25 residue; and (iii) the basic nitrogen atom of the pyridyl group forms hydrogen-bonds with the Asp 29 residue and the catalytic water molecule.

Also, compounds **109d**, **c** and **f** showed favorable hydrogen-bonding interactions with the receptor cavity of the HIV-1 protease but these were not as significant as compounds **109a**, **b** and **e**, and the more functional groups the ligand has the better the interactions. The docking results suggest that the ligands **109a-f** exhibit the potential to act as HIV-1 protease inhibitors.

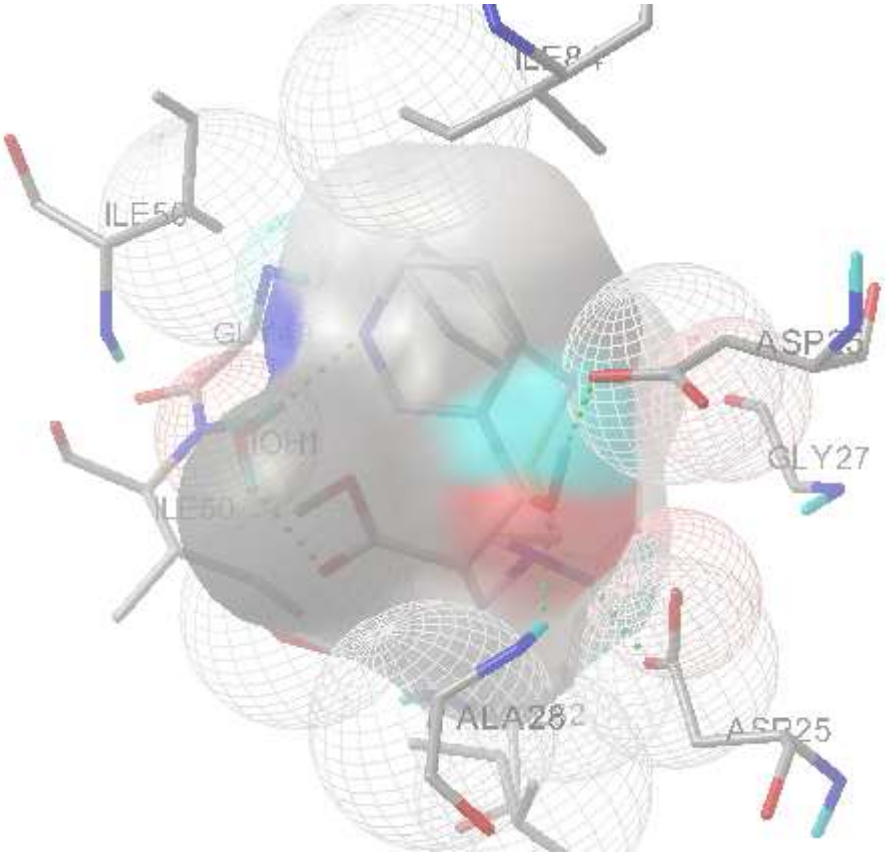

Figure 63. Compound **109b** docked in the receptor cavity of the HIV-1 Protease. Hydrogen-bonding interactions are indicated by the green dotted lines.

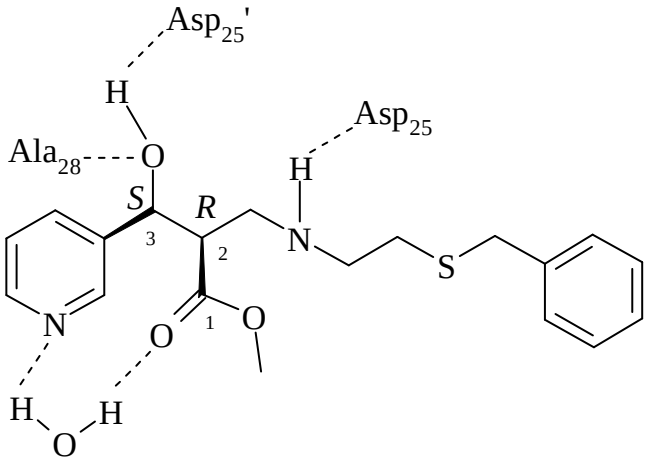

Figure 64. Schematic representation of hydrogen-bonding interactions between aza-Michael product **109b** and the residues in the receptor cavity of the HIV-1 protease as determined by Autodock 4.0.

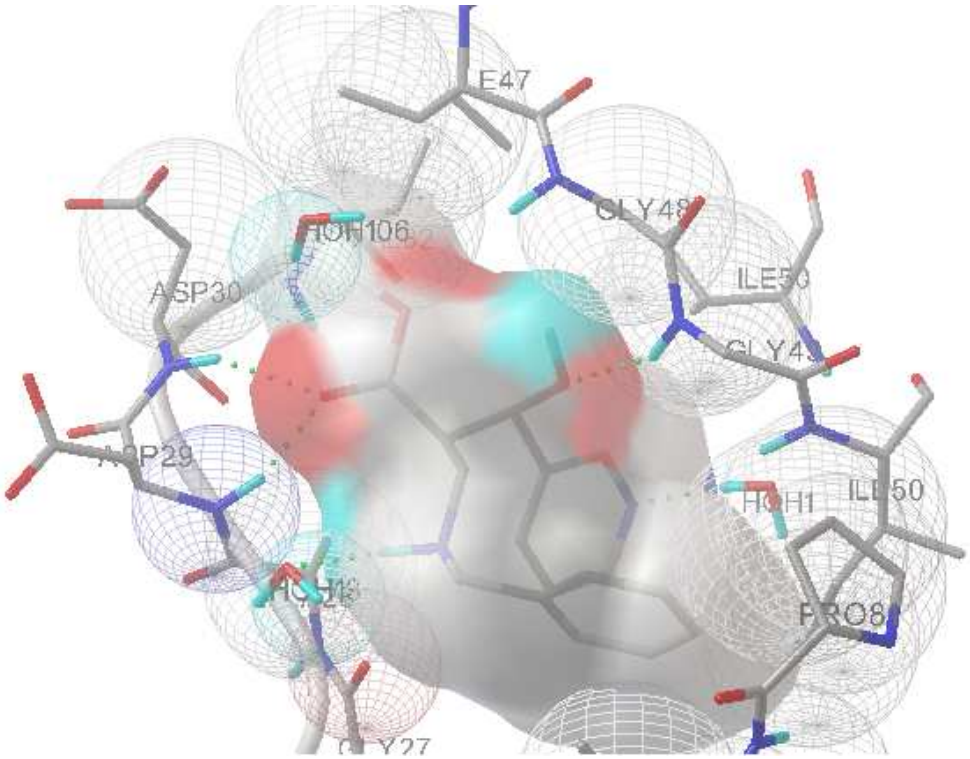

Figure 65. Compound **109a** docked in the receptor cavity of the HIV-1 Protease. Hydrogen-bonding interactions are indicated by the green dotted lines.

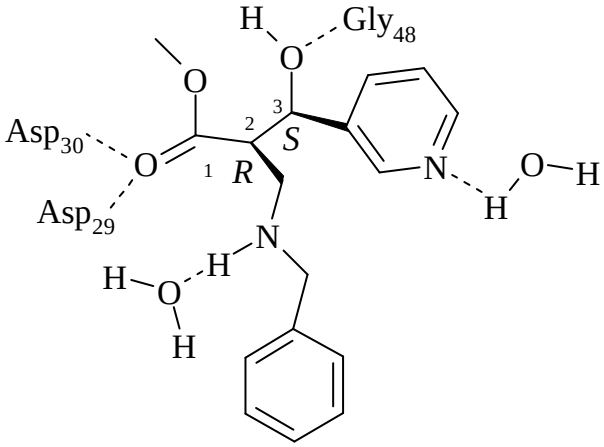

Figure 66. Schematic representation of hydrogen-bonding interactions between compound **109a** and the residues in the receptor cavity of the HIV-1 protease as determined by Autodock 4.0.

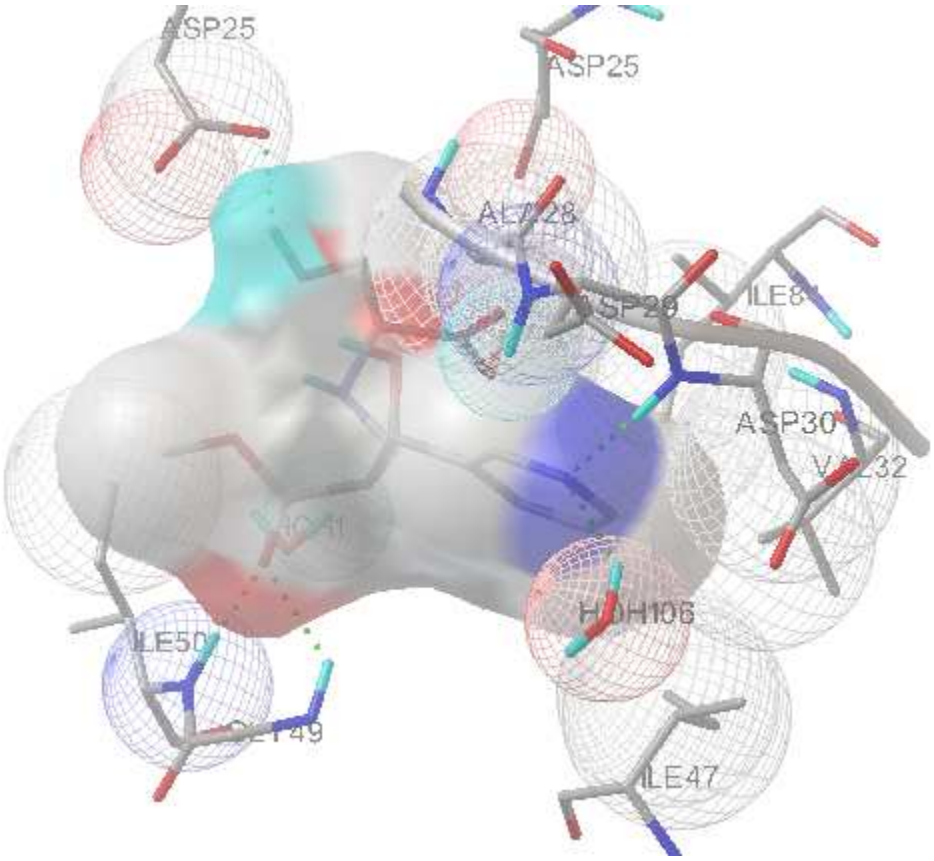

Figure 67. Compound **109e** docked in the receptor cavity of the HIV-1 Protease. Hydrogen-bonding interactions are indicated by the green dotted lines.

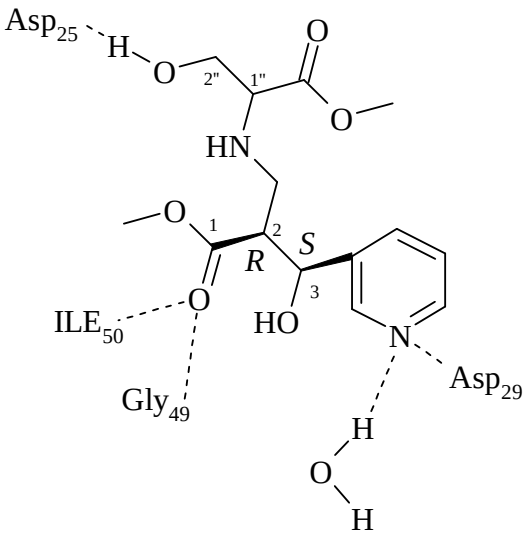

Figure 68. Schematic representation of hydrogen-bonding interactions between compound **109e** and the residues in the receptor cavity of the HIV-1 protease as determined by Autodock 4.0.

2.5.2. Saturation Transfer Difference (STD) NMR studies

The Saturation Transfer Difference (STD) experiment is a double resonance NOE experiment used to detect and characterize protein-ligand interactions.[181-182] In this experiment, the magnetization or saturation transfer is from the irradiated protons of the receptor protein to the protons of the bound ligand. The rate of saturation transfer depends on the protein's mobility, protein-ligand complex life-time and the geometry of both the protein and the ligand.[183] The STD technique is highly sensitive, requires only minute quantities of the samples and can be conducted on each ligand separately or on a mixture of ligands to identify "hit" compounds.[182-183] Figure 69 indicates the pulse sequence for the 1-D STD NMR spectrum in an H_2O-D_2O mixture; (**A**) shows the 90° pulse applied (blue) and the water-gate step including the 180° pulse used to re-phase the signals (green), (**B**) shows the envelop peak (orange) of the successive (5x) Gaussian pulses applied and (**C**) indicates the gradient of the water-gate step. In the present study, the solution of the protein-ligand mixture was selectively irradiated at 0.5 ppm for the on-resonance and at 20 ppm for the off-resonance irradiation.

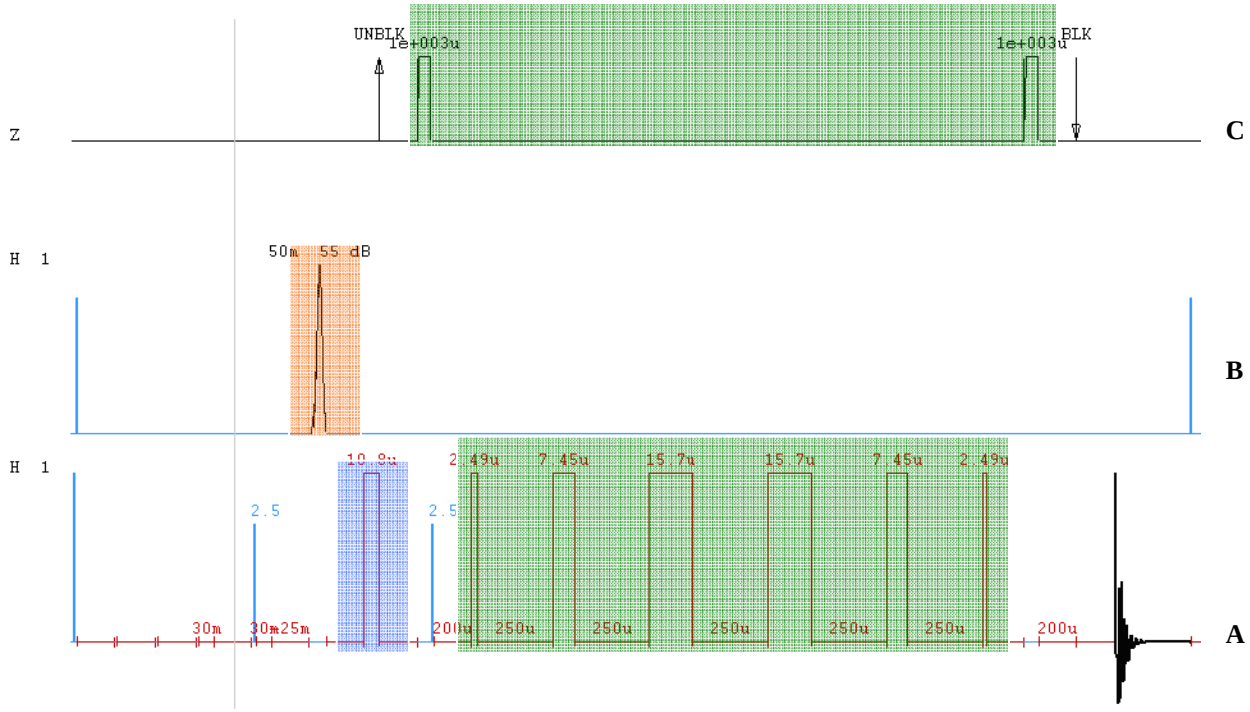

Figure 69. Pulse sequences for the 1D STD NMR spectra recorded in a mixture of H_2O and D_2O.

During on-resonance irradiation, only the magnetization of the protein protons are affected-not those of the ligands or the solvent mixture. On the other hand, during off-resonance irradiation, the sample is irradiated at a frequency far from the resonance frequencies of the protein, ligands (Figure 70) and solvent mixture. The STD difference spectrum represents the difference between the spectra produced by the two resonances. [181-186] Figure 71 illustrates the 1-D STD difference spectrum (for a 40:1 solution of the ligand-mixture and HIV-1 protease subtype C in H_2O-D_2O) and the reference spectrum. The new signals in the STD difference spectrum (blue) at *ca*. 5.2 ppm are due to the 3-methine protons of the ligands (aza-Michael adducts **109a$_1$-f$_1$**), while the other signals for the ligands cannot be accurately identified because of the overlap with those of the protein and the buffer solution. Figure 72 shows an expanded portion of the STD spectrum superimposed on the spectra of selected individual ligands (*i.e*. those that appear to bind to the enzyme). Inspection of the STD spectrum with the spectra of these ligands (Figure 72), it seems that the aza-Michael products **109c**, **109e** and **109f** bind to the HIV-1 protease subtype C enzyme, while aza-Michael products **109a**, **109b** and **109d** (not shown in the Figure 72) did not reveal any signals in the STD spectrum. This lack of visible signals for aza-Michael adducts **109a**, **b** and **d** in the STD spectrum, however, does not necessary mean that they do not bind with the enzyme; they may be binding so strongly that they do not dissociate from the enzyme to be detected in the STD NMR experiment. Of cause, the opposite may also be true, *i.e.* these products may not be binding at all with the enzyme

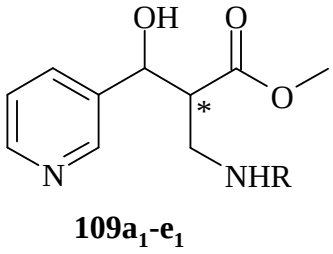

109a$_1$-e$_1$

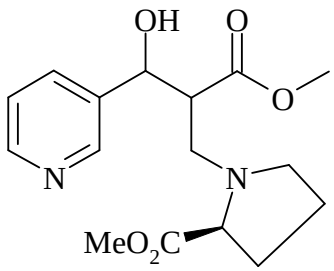

109f$_1$

	R
a	CH_2Ph
b	$(CH_2)_2SCH_2Ph$
c	CH_2CO_2Me
d	CH_2CO_2Et
e	$CH(CH_2OH)CO_2Me$

Figure 70. Aza-Michael products **109a$_1$-f$_1$**.

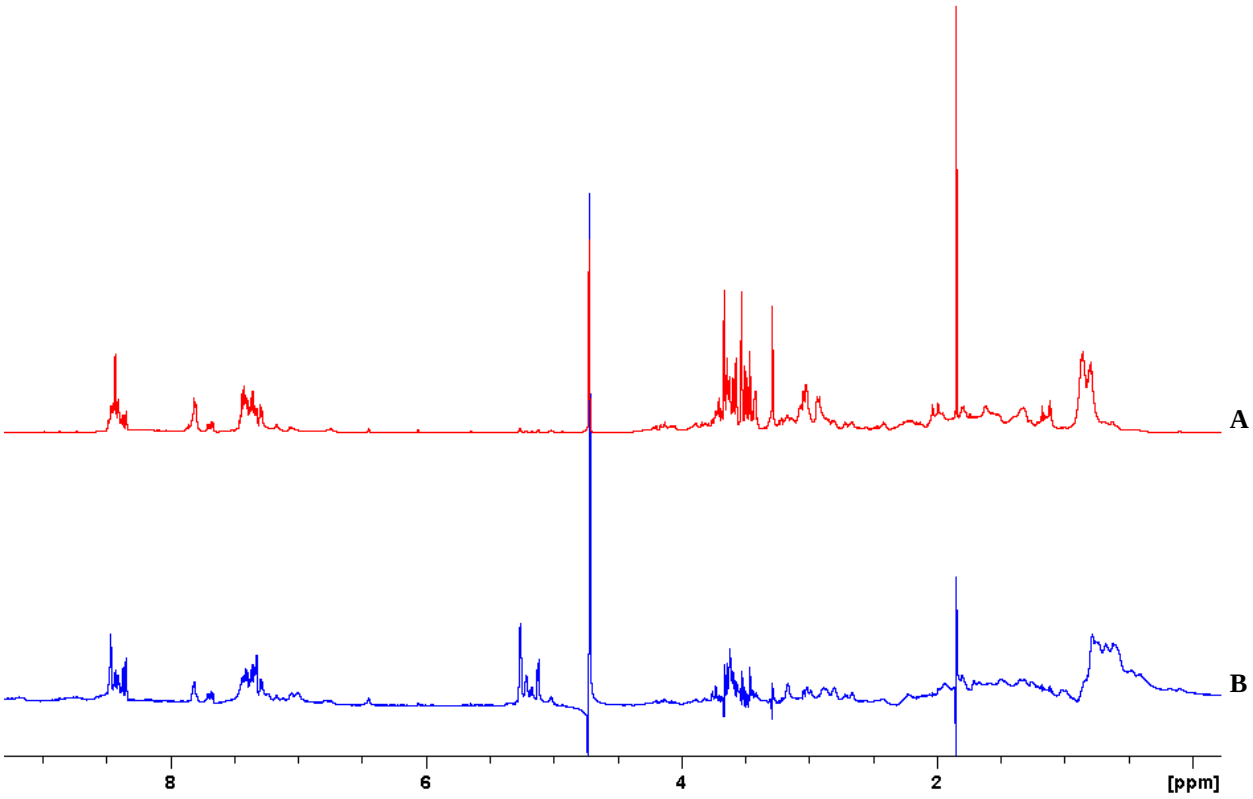

Figure 71. (A) Reference spectrum of 0.38 mM HIV-1 protease sub-type C and (B) STD NMR spectrum of spectra of 0.38 mM HIV-1 protease sub-type C and aza-Michael products **109a-f** in H_2O-D_2O.

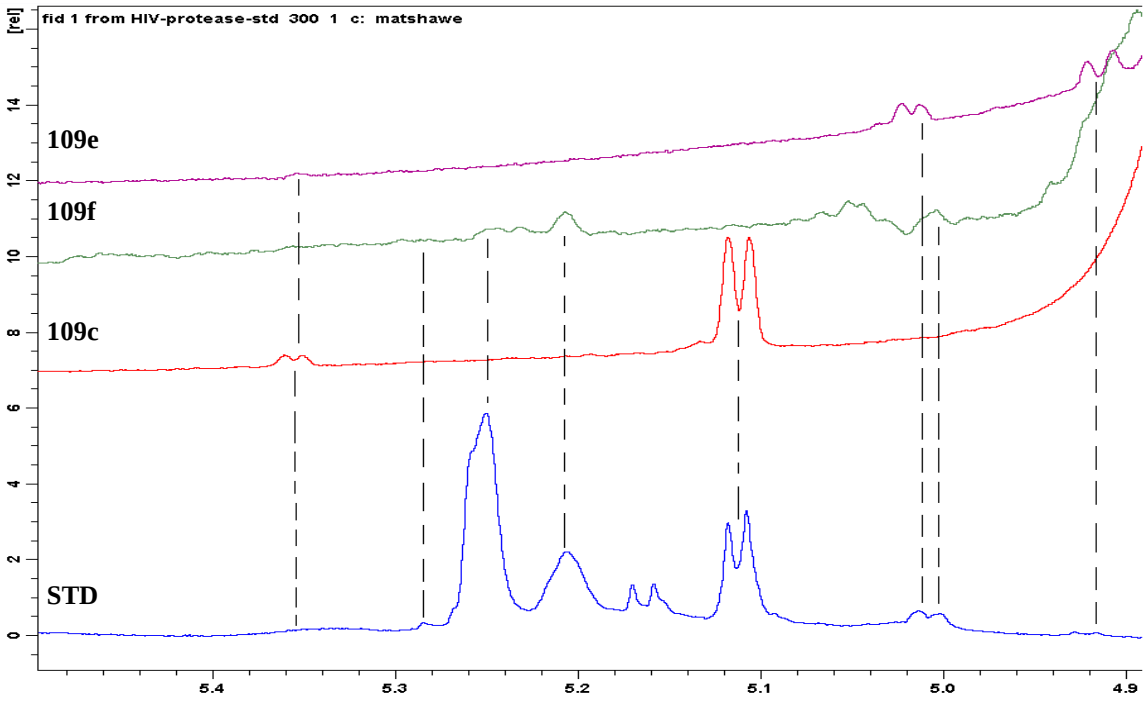

Figure 72. Cross-section spectra of the region *ca*. 3.8-5.8 ppm.

2.6. Conclusions

In this study, "pseudo-peptide"-based truncated Ritonavir® analogues have been prepared as potential HIV-1 protease inhibitors. Compounds bearing an indolizine heterocyclic moiety have been successfully synthesized from the Baylis-Hillman adducts of pyridine-2- and quinoline-2-carbaldehydes with methyl acrylate in yields ranging from 79 to 100%. Acetylation and cyclisation have given rise to indolizine-2-carboxylate esters **63a-c**, base-catalyzed hydrolysis of which has afforded the corresponding indolizine-2-carboxylic acids **87a-c**. The acids have been successfully coupled with various amino compounds using the peptide coupling agent, 1,1'-carbonyldiimidazole (CDI) to afford a series of novel indolizine-2-carboxamides **89-101** in quantitative yields.

Attention has also been given to aza-Michael reactions of the pyridine-3-carbaldehyde-derived methyl acrylate Baylis-Hillman adduct **61g** using various amino compounds under basic conditions to afford a series of novel diastereomeric aza-Michael adducts **109a-f** in yields ranging from 41 to 96%. Assignment of the relative stereochemistry of the aza-Michael adducts has been established using 1- and 2-D NOESY experiments and molecular modeling techniques. The novel indolizine-2-carboxamides **89-101** and diastereomeric aza-Michael adducts **109a-f** were all fully characterized by spectroscopy (IR, 1- and 2-dimensional NMR) and elemental (HRMS) analysis.

Computer modelling of potential HIV-1 protease inhibitors have been undertaken using the ACCELRYS Cerius^2 platform, and interactive *in silico* docking into the active site of the HIV-1 protease enzyme, using the AUTODOCK 4.0 docking software, have revealed likely hydrogen-bonding interactions between the enzyme and the ligands. A protein (STD) NMR experiment has been undertaken to explore binding of selected aza-Michael adducts **109a-f** which the HIV-1 protease subtype C enzyme, providing experimental evidence that some of the ligands do in fact, bind to the enzyme.

It is clear that various objectives of this study have been largely achieved and future research in this area is expected to include the following.

(i) Growing crystals of the aza-Michael products, protected as hydrochloride salts, to confirm their stereochemistry by X-ray analysis.

(ii) Conducting molecular modelling and STD-NMR experiments on the indolizine-2-carboxamides **89-101**.

(iii) Conducting STD-NMR experiments on all of the potential inhibitors prepared in this study in order to identify the products that exhibit binding to the enzyme.

(iv) Performing enzyme-inhibition assays on the aza-Michael products and indolizine-2-carboxamides that exhibit binding in the STD experiments to obtain inhibition constants, and thus guide the design of new inhibitors.

3. EXPERIMENTAL

3.1. General details

The reagents used in this project were supplied by Aldrich® and were used without further purification. Thin layer chromatography (TLC) was carried out using Merck silica gel 60 PF_{254} plates and were viewed under ultraviolet (UV) light or visualized using iodine vapor, while flash column chromatography was carried out using MN Kieselgel 60 (particle size 0.063 – 0.200 mm) and HPLC was done on Partisil 10 Magnum 6 normal phase column using a Spectra-Physics P100 isocratic pump and a Waters K1410 differential refractometry detector..

Low-resolution mass spectra were obtained on a Finnegan Mat GCQ spectrometer. High resolution mass spectra were recorded on Micromass 70-70E (University of Potchefstroom) and Waters API-Q-TOF Ultima spectrometers (University of Stellenbosch). NMR spectra were recorded on Bruker 400 MHz AVANCE and Bruker Biospin 600 MHz spectrometers and were referenced using solvent signals (δ_H: 7.26 ppm for $CDCl_3$, 2.50 ppm for DMSO-d_6; δ_C: 77.0 ppm for $CDCl_3$, 39.4 ppm for DMSO-d_6). IR spectra were recorded on a Perkin-Elmer FT-IR Spectrum 2000 spectrometer using KBr discs, nujol mulls or thin films. Melting points were determined using a Reichert hot-stage apparatus and are uncorrected.

Solvents were purified according to the methods described by Perrin and Armarego [187]; hence hexane, was distilled before use, methanol was distilled from magnesium methoxide (generated from Mg turnings with I_2 catalyst), DMF was distilled under reduced pressure after standing over anhydrous $MgSO_4$ for 48 hours and pyridine was distilled over CaH_2 and stored over 5A molecular sieves before use.

Signal assignment for some structures was achieved with the aid of NMR prediction software [NMR predict [188] and MestRecNova [189]]

3.2. Synthesis of the Baylis-Hillman derivatives

Methyl 2-[hydroxy(pyridin-2-yl)methyl]acrylate **61a**

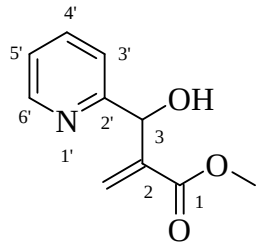

A solution of pyridine-2-carbaldehyde (2.95 g, 28.0 mmol), methyl acrylate (2.50 g, 29.0 mmol) and DABCO (0.150 g, 1.34 mmol) in $CHCl_3$ (2 ml) was stirred in a stoppered round-bottomed flask at room temperature for 3 days. The solvent was then removed *in vacuo* and the crude product purified by flash chromatography (on silica gel; elution with EtOAc) to give methyl 2-[hydroxy(pyridin-2-yl)methyl]acrylate **61a** as a brown oil (4.52 g, 93%); ν_{max} (thin film)/cm^{-1} 3423 (OH) and 1708 C=O); δ_H (400 MHz; $CDCl_3$) 3.73 (3H, s, OCH_3), 4.82 (1H, br s, OH), 5.62 and 5.95 (2H, 2 x s, CH_2), 6.35 (1H, s, C*H*OH), 7.22 (1H, dd, *J* 5.0 and 4.5 Hz, 4'-H), 7.42 (1H, d, *J* 8.0 Hz, 6'-H), 7.69 (1H, m, 5'-H) and 8.54 (1H, d, *J* 4.8 Hz, 3'-H); δ_C (100 MHz; $CDCl_3$) 31.1 (OCH_3), 60.9 (CH_2), 76.7 (C-3), 126.8 (C-3'), 127.9 (C-5'), 128.9 (C-2), 130.5 (C-4') , 132.7 (C-6'), 144.2 (C-2') and 207.3 (C=O); *m*/*z* 194 (**M**+1, 100%).

Methyl 2-[hydroxy(6-methylpyridin-2-yl)methyl]acrylate **61b**

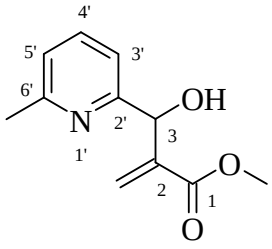

The procedure described for the synthesis of methyl 2-[hydroxy(pyridin-2-yl)methyl]acrylate **61a** was followed, using 6-methylpyridine-2-carbaldehyde (2.96 g, 24.2 mmol), methyl acrylate (2.53 g, 29.4 mmol) and DABCO (0.153 g, 1.34 mmol) in $CHCl_3$ (2 ml). The precipitated solid was filtered off, yielding methyl 2-[hydroxy(6-methylpyridin-2-yl)methyl]acrylate **61b** as a tan-coloured powder (4.87 g, 87%), m.p. 86-

87 °C (lit.[66] 84-85 °C); ν_{max} (KBr)/cm^{-1} 3476 (OH) and 1698 (C=O); δ_H (400 MHz; $CDCl_3$) 2.50 (3H, s, CH_3), 3.70 (3H, s, OCH_3), 5.25 (1H, br s, OH), 5.58 and 5.92 (2H, 2 x s, CH_2), 6.30 (1H, s, C*H*OH), 7.02 (1H, d, *J* 7.6 Hz, 5'-H), 7.14 (1H, d, *J* 8.0 Hz, 3'-H) and 7.53 (1H, t, *J* 7.8 Hz, 4'-H); δ_C (100 MHz; $CDCl_3$) 24.4 (CH_3), 52.0 (OCH_3), 71.5 (C-3), 118.2 (C-3'), 122.3 (C-5'), 126.8 (CH_2), 137.3 (C-4'), 142.3 (C-2), 157.3 (C-6'), and 158.6 (C-2') and 166.8 (C=O); *m*/*z* 208 (**M**+1, 100%).

***Methyl 2-[hydroxy(quinolin-2-yl)methyl]acrylate* 61c**

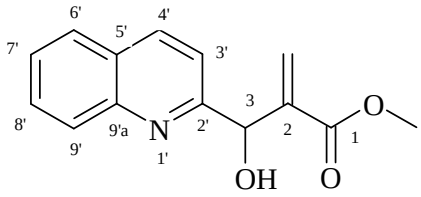

The procedure described for the synthesis of methyl 2-[hydroxy(pyridin-2-yl)methyl]acrylate **61a** was followed, using quinoline-2-carbaldehyde (2.20 g, 14.0 mmol), methyl acrylate (1.26 g, 14.6 mmol) and 3-hydroxyquinuclidine (0.086 g, 0.68 mmol) in $CHCl_3$ (2 ml). After 4 days the solvent was removed *in vacuo* and the crude product purified by flash chromatography [on silica gel; elution with hexane-EtOAc (5:5)] to afford methyl 2-[hydroxy(quinolin-2-yl)methyl]acrylate **61c** as a yellow oil (3.29 g, 96%); ν_{max} (thin film)/cm^{-1} 3260 (OH) and 1735 (C=O); δ_H (400 MHz; $CDCl_3$) 3.67 (3H, s, OCH_3), 5.68 (1H, br s, OH), 5.87 and 5.97 (2H, 2 x s, CH_2), 6.36 (1H, s, C*H*OH), 7.42 (1H, d, *J* 8.4 Hz, 3'-H), 7.46 (1H, d, *J* 7.6 Hz, 4'-H), 7.66 (1H, t, *J* 7.6 Hz, 6'-H), 7.82 (1H, d, *J* 8.0 Hz, 9'-H) and 8.04 (2H, m, 7'-H and 8'-H); δ_C (100 MHz; $CDCl_3$) 51.6 (OCH_3), 71.7 (C-3), 118.6 (C-3'), 126.3 (C-4'), 127.1 (CH_2), 127.3 (C-2'), 128.5 (C-2), 128.6 (C-6'), 129.5 (C-8'), 136.8 (C-7'), 141.5 (C-9'), 146.1 (C-5'), 159.3 (C-9'a) and 166.3 (C=O); *m*/*z* 244 (**M**+1, 100%).

Methyl 2-[hydroxy(pyridin-3-yl)methyl]acrylate **61g**

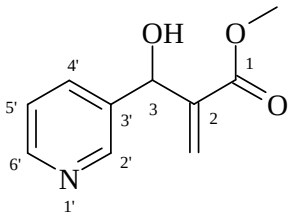

The procedure described for the synthesis of methyl 2-[hydroxy(pyridin-2-yl)methyl]acrylate **61a** was followed, using pyridine-3-carbaldehyde (2.96 g, 24.2 mmol), methyl acrylate (2.53 g, 29.4 mmol) and DABCO (0.153 g, 1.34 mmol) in $CHCl_3$ (2 ml). The precipitated solid was filtered off, yielding methyl 2-[hydroxy(pyridin-3-yl)methyl]acrylate **61g** as a pale yellow powder (5.53 g, 100%), m.p. 102-104 °C (lit.[66] 99-101 °C); ν_{max} (KBr)/cm^{-1} 3390 (OH) and 1701 (C=O); δ_H (400 MHz; $CDCl_3$) 3.67 (3H, s, OCH_3), 4.95 (1H, br s, OH), 5.58 and 5.60 (2H, 2 x s, CH_2), 6.36 (1H, s, C*H*OH), 7.24 (1H, m, 2'-H), 7.71 (1H, d, *J* 8.0 Hz, 4'-H), 8.38 (1H, dd, *J* 1.2 and 1.0 Hz, 5'-H) and 8.57 (1H, d, *J* 1.6 Hz, 6'-H); δ_C (100 MHz; $CDCl_3$) 51.9 (OCH_3), 70.4 (C-3), 123.4 (C-2'), 126.0 (CH_2), 134.6 (C-4'), 137.6 (C-5'), 141.7 (C-6'), 148.2 (C-2), 148.4 (C-3') and 166.2 (C=O); *m*/*z* 193 ($\mathbf{M}^+$, 100%).

Methyl 2-[hydroxy(pyridin-4-yl)methyl]acrylate **61h**

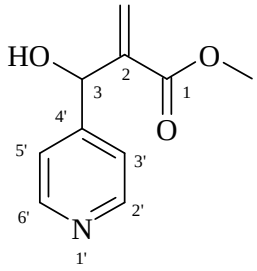

The procedure described for the synthesis of methyl 2-[hydroxy(pyridin-2-yl)methyl]acrylate **61a** was followed, using pyridine-4-carbaldehyde (2.96 g, 24.2 mmol), methyl acrylate (2.53 g, 29.4 mmol) and DABCO (0.153 g, 1.34 mmol) in $CHCl_3$ (2 ml). The precipitated solid was filtered off, yielding methyl 2-[hydroxy(pyridin-4-yl)methyl]acrylate **61h** as a bright yellow powder (4.43 g, 79%), m.p. 144-148 °C (lit.[66] 152-156 °C), ν_{max} (KBr)/cm^{-1} 3400 (OH) and 1676 (C=O); δ_H (400 MHz; $CDCl_3$) 2.78

(1H, s, OH), 3.73 (3H, s, OCH_3), 5.52 and 5.90 (2H, 2 x s, CH_2), 6.37 (1H, s, C*H*OH), 7.32 (2H, 2 x d, *J* 6.0 and 5.9 Hz, 3'-H and 5'-H) and 8.53 (2H, 2 x d, *J* 1.6 and 1.3 Hz, 2'-H and 6'-H); δ_C (100 MHz; $CDCl_3$) 52.1 (OCH_3), 72.0 (C-3), 121.4 (C-2' and C-6'), 127.0 (CH_2), 141.1 (C-3' and C-5'), 149.7 (C-2) ,150.8 (C-4') and 166.3 (C=O); *m*/*z* 193 ($\mathbf{M}^+$, 100%).

***Methyl 2-[acetoxy(pyridin-2-yl)methyl]acrylate* 62a and *Methyl indolizine-2-carboxylate* 63a**

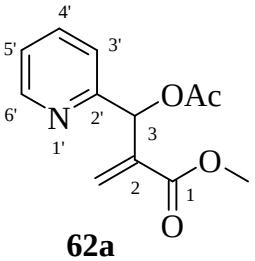

62a

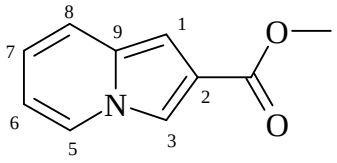

63a

Methyl 2-[hydroxy(pyridin-2-yl)methyl]acrylate **61a** (1.0 g, 5.2 mmol) was heated in acetic anhydride (Ac_2O) (5 ml) at 100 °C for 30 minutes. The resulting mixture was allowed to cool, then poured into aqueous $NaHCO_3$-ice and stirred for another 30 minutes. The mixture was extracted with Et_2O (2 x 100 ml) and the organic solution was washed successively with aqueous $NaHCO_3$ (100 ml) and saturated brine (100 ml). The resulting solution was dried ($MgSO_4$), and the Et_2O removed *in vacuo*. The crude product was purified by flash chromatography [on silica gel; elution with hexane-EtOAc (4:6)] to afford two fractions.

Fraction (i): methyl 2-[acetoxy(pyridin-2-yl)methyl]acrylate **62a** as an olive-green oil (0.60 g, 49%); ν_{max} (thin film)/cm^{-1} 1699 (CH_3C=O) and 1710 (CH_3OC=O); δ_H (400 MHz; $CDCl_3$) 2.13 (3H, s, OAc), 3.68 (3H, s, OCH_3), 5.94 (1H, s, C*H*OAc), 6.71 and 7.17 (2H, 2 x s, CH_2), 7.21 (1H, m, 6'-H), 7.43 (1H, d, *J* 8.0 Hz, 3'-H), 7.67 (1H, dt, *J* 3.7, 3.5 and 3.6 Hz, 5'-H), 8.56 (1H, t, *J* 2.4 Hz, 4'-H); δ_C (100 MHz; $CDCl_3$) 20.6 (OAc), 51.5 (OCH_3), 73.5 (C-3), 122.3 (C-3'), 122.8 (C-5'), 127.2 (CH_2), 136.4 (C-4'), 137.7 (C-2), 149.0 (C-6'), 156.5 (C-2'), 165.0 and 169.1 (2 x C=O); *m*/*z* 175 ($\mathbf{M}^+$-$C_2H_4O_2$, 34) and 117 (100%).

Fraction (ii): methyl indolizine-2-carboxylate **63a** as green flakes (0.31 g, 33.7%), m.p. 98-100 °C (lit.[66] 97-99 ° C); ν_{max}(nujol)/cm^{-1} 1712 (C=O); δ_H (400 MHz; $CDCl_3$) 3.88

(3H, s, OCH_3), 6.54 (1H, t, *J* 6.6 Hz, 6-H), 6.69 (1H, m, 7-H), 6.82 (1H, s, 1-H), 7.36 (1H, d, *J* 9.2 Hz, 8-H), 7.79 (1H, s, 3-H) and 7.86 (1H, d, *J* 6.8 Hz, 5-H); δ_C (100 MHz; $CDCl_3$) 51.1 (OCH_3), 100.7 (C-1), 112.5 (C-6), 116.2 (C-3), 118.4 (C-8), 120.0 (C-7), 120.6 (C-5), 125.6 (C-2), 133.1 (C-9) and 165.8 (C=O); *m*/*z* 175 ($\mathbf{M}^+$, 100%).

Note: Methyl 2-[acetoxy(pyridin-2-yl)methyl]acrylate **62a** (1.1 g, 4.5 mmol) was heated at 120 °C for 1 hour. The resulting mixture was purified by flash chromatography [on silica gel; elution with hexane-EtOAc (7:3)] to afford methyl indolizine-2-carboxylate **63a** (0.61 g, 77%).

3.3. Synthesis of indolizine-2-carboxylates

Attempted synthesis of *Methyl indolizine-2-carboxylate* 63a

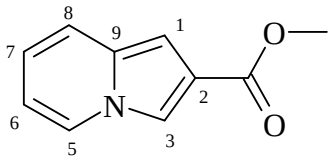

Methyl acrylate (0.977 g, 11.3 mmol) was reacted with pyridine-2-carbaldehyde (1.08 g, 10 mmol) and trimethylsilyl chloride (1.09 g, 10 mmol) in acetonitrile (2 ml) for 7 days. ^{1}H NMR spectroscopy indicated that no reaction occurred. The mixture was left to stand for a further 3 weeks, but ^{1}H NMR analysis again confirmed that no reaction had occurred.

***Methyl 2-[acetoxy(6-methylpyridin-2-yl)methyl]acrylate* 62b and *methyl 5-methylindolizine-2-carboxylate* 63b**

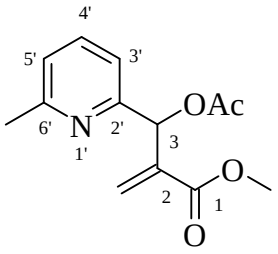

62b

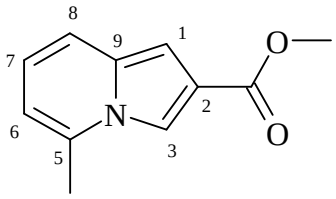

63b

Following the procedure used to synthesize methyl 2-[acetoxy(pyridin-2-yl)methyl]acrylate **62a**, methyl 2-[hydroxy(6-methylpyridin-2-yl)methyl]acrylate **61b**

(1.0 g, 5.2 mmol) was reacted to give a crude product which was purified by flash chromatography [on silica gel: elution with hexane-EtOAc (7:3)] to afford two fractions.

Fraction (i): Methyl 2-[acetoxy(6-methylpyridin-2-yl)methyl]acrylate **62b** as a yellow oil (0.84 g, 64%); ν_{max}(thin film)/cm^{-1} 1700 (CH_3C=O) and 1720 (CH_3OC=O); δ_H (400 MHz; $CDCl_3$) 2.14 (3H, s, CH_3), 2.51 (3H, s, OAc), 3.71 (3H, s, OCH_3), 5.80 (1H, s, C*H*OAc), 6.43 and 6.69 (2H, 2 x s, CH_2), 7.06 (1H, d, *J* 7.6 Hz, 3'-H), 7.19 (1H, d, *J* 8.0 Hz, 5'-H) and 7.57 (1H, t, *J* 7.6 Hz, 4'-H); δ_C (100 MHz; $CDCl_3$) 21.0 (CH_3), 24.4 (OAc), 51.8 (OCH_3), 74.0 (C-3), 119.0 (C-3'), 122.5 (C-5'), 127.6 (CH_2), 136.6 (C-4'), 138.4 (C-2), 156.2 (C-6'), 158.2 (C-2'), 165.5 and 169.2 (2 x C=O); *m*/*z* 190 (**M**$^+$-$C_2H_3O_2$, 54) and 83 (100%).

Fraction (ii): methyl 5-methylindolizine-2-carboxylate **63b** as a bright yellow oil (0.36 g, 37%); ν_{max}(thin film)/cm^{-1} 1710 (C=O); δ_H (400 MHz; $CDCl_3$) 2.50 (3H, s, CH_3), 3.90 (3H, s, OCH_3), 6.42 (1H, d, *J* 6.8 Hz, 8-H), 6.72 (1H, m, 7-H), 6.91 (1H, s, 1-H), 7.32 (1H, d, *J* 8.8 Hz, 6-H) and 7.72 (1H, s, 3-H); δ_C (100 MHz; $CDCl_3$) 18.5 (CH_3), 51.4 (OCH_3), 101.0 (C-1), 111.3 (C-6), 113.0 (C-3), 118.0 (C-8), 118.5 (C-7), 120.0 (C-2), 133.0 (C-9), 133.5 (C-5) and 165.7 (C=O); *m*/*z* 189 (**M**$^+$, 1) and 320 (100%).

Note: Methyl 2-[acetoxy(6-methylpyridin-2-yl)methyl]acrylate **62b** (1.54 g, 6.2 mmol) was reacted following the procedure used to synthesize methyl indolizine-2-carboxylate **9**. The resulting mixture was purified by flash chromatography [on silica gel; elution with hexane-EtOAc (7:3)] to afford methyl 5-methylindolizine-2-carboxylate **63b** (0.85 g, 73%).

***Methyl 2-[acetoxy(quinolin-2-yl)methyl]acrylate* 62c, *methyl pyrrolo[1,2-a]quinoline-2-carboxylate* 63c and *methyl 1-acetylpyrrolo[1,2-a]quinoline-2-carboxylate* 83**

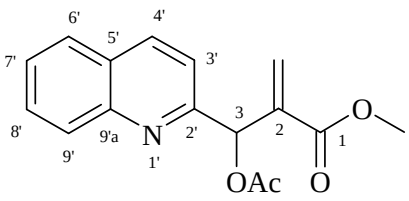

62c

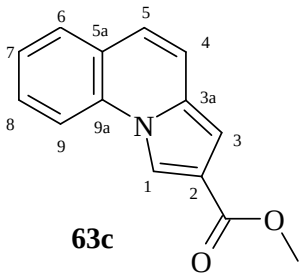

63c

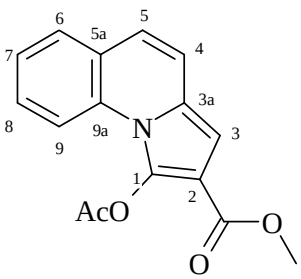

83

Following the procedure used to synthesize methyl 2-[acetoxy(pyridin-2-yl)methyl]acrylate **62a**, methyl 2-[hydroxy(quinolin-2-yl)methyl]acrylate **61c** (3.0 g, 12.3 mmol) was reacted to give a crude product (2.46g, 82%) which was purified by flash chromatography [on silica gel; elution with hexane-EtOAc (7:3)] to afford three fractions. **Fraction (i):** Methyl 2-[acetoxy(quinolin-2-yl)methyl]acrylate **62c** as a green oil (0.93 g, 32%); ν_{max} (thin film)/cm^{-1} 1705 (CH_3C=O) and 1730 (CH_3OC=O); δ_H (400 MHz; $CDCl_3$) 2.17 (3H, s, OAc), 3.68 (3H, s, OCH_3), 5.91 (1H, s, C*H*OAC), 6.49 and 6.90 (2H, 2 x s, CH_2), 7.49 (1H, d, *J* 7.2 Hz, 4'-H), 7.53 (1H, d, *J* 8.4 Hz, 6'-H), 7.68 (1H, t, *J* 7.0 Hz, 7'-H), 7.78 (1H, d, *J* 8.0 Hz, 9'-H), 8.06 (1H, d, *J* 8.4 Hz, 3'-H) and 8.14 (1H, d, *J* 8.4 Hz, 8'-H); δ_C (100 MHz; $CDCl_3$) 20.9 (OAc), 51.9 (OCH_3), 74.4 (C-3), 119.8 (C-3'), 125.6 (C-4'), 127.4 (C-6'), 127.8 (CH_2), 129.4 (C-9'), (C-7'),136.6 (C-8'), 138.0 (C-5'), 147.4 (C-2), 157.1 (C-2'), 165.4 and 169.5 (2 x C=O); *m*/*z* 285 (**M**$^+$, 10) and 226 (100%).

Fraction (ii): Methyl pyrrolo[1,2-*a*]quinoline-2-carboxylate **63c** as colourless crystals (0.862 g, 29.1%), m.p. 98-102 °C (lit.[66] 109-110 °C); ν_{max}(nujol)/cm^{-1} 1704 (C=O); δ_H (400 MHz; $CDCl_3$) 3.90 (3H, s, OCH_3), 6.87 (1H, s, 1-H), 6.99 (1H, t, *J* 4.8 Hz, 5-H), 7.23 (1H, m, 6-H), 7.35 (1H, m, 8-H), 7.50 (1H, t, *J* 7.0 Hz, 4-H), 7.59 (1H, t, *J* 3.6 Hz, 7-H), 7.86 (1H, t, *J* 4.0 Hz, 9-H) and 8.35 (1H, s, 3-H); δ_C (100 MHz; $CDCl_3$) 51.6 (OCH_3), 103.7 (C-3), 114.5 (C-9), 115.9 (C-1), 118.5 (C-2), 119.1 (C-4), 120.4 (C-5), 124.8 (C-5a), 127.7 (C-7), 128.3 (C-8), 128.9 (C-6), 131.4 (C-3a), 133.0 (C-9a) and 165.5 (C=O); *m*/*z* 225 (**M**$^+$, 100%).

Fraction (iii): *Methyl 1-acetylpyrrolo[1,2-*a*]quinoline-2-carboxylate* **83** as a brown powder (0.20 g, 5.8%), m.p. 168-172 °C, (Found **M**$^+$: 283.084513. $C_{16}H_{13}NO_4$ requires **M**, 283.084458); ν_{max}(nujol)/cm^{-1} 1701 (CH_3C=O) and 1757 (CH_3OC=O); δ_H (400 MHz; $CDCl_3$) 2.42 (3H, s, OAc), 3.88 (3H, s, OCH_3), 7.01 (1H, d, *J* 9.2 Hz, 6-H), 7.16 (1H, d, *J* 9.6 Hz, 5-H), 7.40 (1H, t, *J* 7.2 Hz, 7-H), 7.56 (1H, t, *J* 7.2 Hz, 8-H), 7.63 (1H, d, *J* 7.6 Hz, 4-H), 7.88 (1H, d, *J* 8.4 Hz, 9-H) and 8.26 (1H, s, 3-H); δ_C (100 MHz; $CDCl_3$) 21.0 (OAc), 51.8 (OCH_3), 111.0 (C-1) 113.8 (C-3), 114.3 (C-9), 115.7 (C-5), 120.4 (C-6), 122.7 (C-2), 124.7 (C-3a), 125.5 (C-7), 128.5 (C-8), 128.9 (C-4), 129.3 (C-5a), 132.6 (C-9a), 163.9 and 170.2 (2 x C=O); *m*/*z* 209 (**M**$^+$ -$C_3H_6O_2$, 100) and 283 (**M**$^+$, 55%).

Note: Methyl 2-[acetoxy(quinolin-2-yl)methyl]acrylate **62c** (0.93 g, 3.2mmol) was reacted following the same procedure used to synthesize methyl indolizine-2-carboxylate

63a. The resulting mixture was purified by flash chromatography [on silica gel; elution with hexane-EtOAc (7:3)] to afford methyl pyrrolo[1,2-*a*]pyridine-2-carboxylate **63c** (0.62 g, 70%).

3.3.1 One-pot synthesis of indolizine derivatives

2-Acetylindolizine **63d**

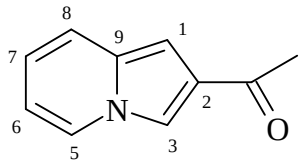

Methyl vinyl ketone (0.70 g, 10 mmol) was reacted with pyridine-2-carbaldehyde (1.07 g, 10 mmol) and trimethylsilyl chloride (1.09 g, 10 mmol) in acetonitrile (2 ml) for 4 days. The resulting mixture was poured into an aqueous solution of potassium carbonate and the mixture was extracted with diethyl ether. The combined organic extracts were dried over $MgSO_4$ and the solvent was removed *in vacuo* to afford 2-acetylindolizine **63d** as light green flakes (1.45 g, 91%), m.p. 120-124 ºC (lit.[69] 127 °C); ν_{max}(nujol)/cm^{-1} 1675 (C=O); δ_H (400 MHz; $CDCl_3$) 2.55 (3H, s, CH_3), 6.55 (1H, m, 7-H), 6.69 (1H, m, 6-H), 6.78 (1H, s, 1-H), 7.36 (1H, d, *J* 9.2 Hz, 5-H), 7.76 (1H, s, 3-H), 7.85 (1H, t, *J* 6.4 Hz, 8-H); δ_C (100 MHz; $CDCl_3$) 27.7 (CH_3), 99.5 (C-1), 112.6 (C-6), 115.2 (C-3), 118.4 (C-8), 120.5 (C-7), 125.5 (C-5), 128.4 (C-2), 133.1 (C-9) and 195.1 (C=O); *m*/*z* 159 (**M^+**, 100%).

2-Propanoylindolizine **63e**

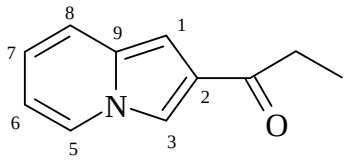

Ethyl vinyl ketone (0.84 g, 10 mmol) was reacted with pyridine-2-carbaldehyde (1.07 g, 10 mmol) following the procedure described for the synthesis of 2-acetylindolizine **63d** to give, after 6 days, a crude product (1.12 g), which was purified by flash chromatography (on silica gel; elution with EtOAc) to afford 2-propanoylindolizine **63e** as a brown oil (0.66 g, 38%); ν_{max}(nujol)/cm^{-1} 1705 (C=O); δ_H (400 MHz; $CDCl_3$) 1.41

(3H, t, *J* 5.2 Hz, CH_3), 4.21 (2H, m, CH_2CH_3), 6.50 (1H, m, 7-H), 6.62 (1H, m, 6-H), 6.78 (1H, s, 1-H), 7.36 (1H, d, *J* 6.0 Hz, 5-H), 7.76 (1H, s, 3-H), 7.89 (1H, t, *J* 6.4 Hz, 8-H); δ_C (100 MHz; $CDCl_3$) 15.7 (CH_3), 65.0 (CH_2CH_3), 105.3 (C-1), 112.6 (C-6), 115.2 (C-3), 118.4 (C-8), 120.5 (C-7), 125.5 (C-5), 128.4 (C-2), 133.1 (C-9) and 195.1 (C=O); *m*/*z* 189 ($\mathbf{M}^+$, 100%).

Indolizine-2-carbonitrile **63f**

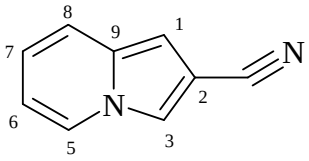

Acrylonitrile (0.599 g, 11 mmol) was reacted with pyridine-2-carbaldehyde (1.01 g, 9.4 mmol) following the procedure described for the synthesis 2-Acetylindolizine **63d** to afford, after 7 days, a crude product which was purified by flash chromatography [on silica gel; elution with hexane-EtOAc (2:8)] to obtain indolizine-2-carbontrile **63f** as colourless crystals (1.05 g, 65.7%), m.p. 56-60 ºC (lit.[66] 67.5-69 °C); ν_{max}(nujol)/cm^{-1} 2355 (CN); δ_H (400 MHz; $CDCl_3$) 6.60 (1H, t, *J* 6.4 Hz, 7-H), 6.67 (1H, s, 1-H), 6.79 (1H, m, 6-H), 7.37 (1H, d, *J* 8.8 Hz, 5-H), 7.66 (1H, s, 3-H), 7.85 (1H, t, *J* 6.4 Hz, 8-H); δ_C (100 MHz; $CDCl_3$) 97.3 (C-2), 102.5 (C-1), 113.0 (C-6), 116.4 (CN), 117.5 (C-3), 119.4 (C-7), 119.7 (C-8), 125.0 (C-2) and 132.6 (C-9); *m*/*z* 142 ($\mathbf{M}^+$, 100%).

3.3.1.1. Attempted one-pot synthesis of indolizine derivatives

2-(Benzylsulfonyl)indolizine **63g**

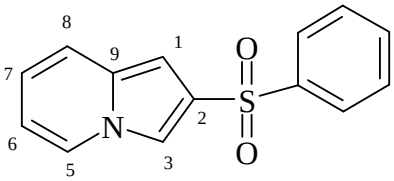

Phenyl vinyl sulfone (1.57 g, 9.35 mmol) was reacted with pyridine-2-carbaldehyde (1.03 g, 9.3 mmol) following the procedure described for the synthesis of 2-acetylindolizine **63d**. After 5 days, ^{1}H NMR spectroscopy indicated that no reaction occurred. The mixture was left to stand for a further 3 months, but ^{1}H NMR analysis again confirmed that no reaction had occurred.

Phenyl indolizine-2-sulfonate **63h**

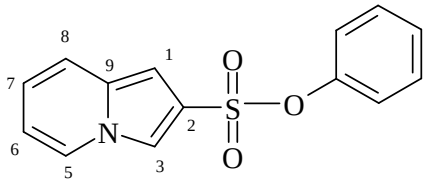

Phenyl vinyl sulfonate (0.902 g, 4.89 mmol) was reacted with pyridine-2-carbaldehyde (1.03 g, 9.3 mmol) following the procedure described for the synthesis of 2-acetylindolizine **63d**. After 7 days, ^{1}H NMR spectroscopy indicated that no reaction occurred. The mixture was left to stand for a further 3 months, but ^{1}H NMR analysis again confirmed that no reaction had occurred.

3.3.2. Hydrolysis of indolizine-2-carboxylates

Indolizine-2-carboxylic acid **87a**

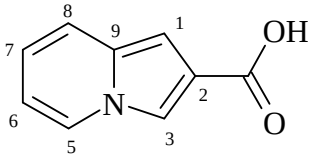

Methyl indolizine-2-carboxylate **63a** (1.42 g, 8.2 mmol) was added to a solution of KOH (2.84 g, 51 mmol) in EtOH (40 ml) and the resulting mixture was refluxed for 16 hours. Water was then added to solubilize the undissolved solid material and the pH adjusted to *ca*. pH=1 using dilute HCl. The mixture was then extracted with EtOAc (2 x 100ml), and the combined organic extracts were dried over $MgSO_4$. The solvent was removed *in vacuo* to afford indolizine-2-carboxylic acid **87a** as a pale yellow solid (0.76 g, 58%), m.p. 219-222 °C (lit.[66] 240-241 °C); ν_{max}(nujol)/cm^{-1} 3392 (OH) and 1680 (C=O); δ_H (400 MHz; DMSO-d_6) 6.47 (1H, m, 6-H), 6.63 (1H, d, *J* 6.8 Hz, 5-H), 6.65 (1H, d, *J* 7.2 Hz, 8-H), 7.30 (1H, d, *J* 8.8 Hz, 3-H), 7.82 (1H, s, 1-H) and 8.01 (1H, d, *J* 6.4 Hz, 7-H), δ_C (100 MHz; DMSO-d_6) 99.1 (C-1), 111.7 (C-6), 115.9 (C-3), 117.8 (C-8), 119.5 (C-7), 120.0 (C-5), 125.5 (C-2), 132.1 (C-9) and 166.0 (C=O); *m*/*z* 161 (**M**$^{+}$, 100%).

***5-Methylindolizine-2-carboxylic acid* 87b**

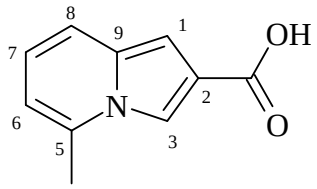

Methyl 5-methylindolizine-2-carboxylate **63b** (0.95 g, 5.0 mmol) was hydrolysed following the procedure described for the synthesis of indolizine-2-carboxylic acid **87a** to afford 5-methylindolizine-2-carboxylic acid **87b** as yellow crystals (0.50 g, 57%), m.p. 168-171 °C (lit.[66] 180-185 °C); ν_{max}(nujol)/cm^{-1} 3402 (OH) and 1664 (C=O); δ_H (400 MHz; DMSO-d_6) 2.13 (3H, s, CH_3), 6.39 (1H, d, *J* 6.4 Hz, 8-H), 6.66 (1H, m, 7-H), 6.76 (1H, d, *J* 0.8 Hz, 6-H), 7.26 (1H, d, *J* 9.2 Hz, 3-H) and 7.71 (1H, s, 1-H); δ_C (100 MHz; DMSO-d_6) 17.3 (CH_3), 99.8 (C-1), 110.0 C-6), 111.9 (C-3), 116.5 (C-8), 117.4 (C-7), 119.1 (C-2), 131.9 (C-9), 132.1 (C-5) and 165.5 (C=O); *m*/*z* 130 (**M**$^+$- CO_2H, 100) and 175 (**M**$^+$, 94%).

***Pyrrolo[1,2-*a*]quinoline-2-carboxylic acid* 87c**

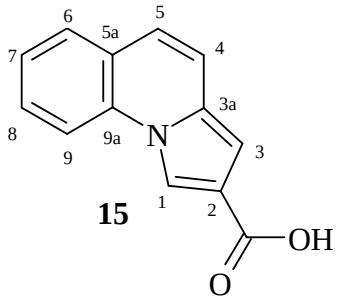

15

Methyl pyrrolo[1,2-*a*]quinoline-2-carboxylate **63c** (2.72 g, 12.1 mmol) was hydrolysed following the procedure described for the synthesis of indolizine-2-carboxylic acid **87a** to afford pyrrolo[1,2-*a*]quinoline-2-carboxylic acid **87c** as a cream coloured powder (1.65 g, 65%), m.p. 244-248 °C (lit.[66] 234-236 °C); ν_{max}(nujol)/cm^{-1} 3390 (OH) and 1675 (C=O); δ_H (400 MHz; DMSO-d_6) 6.07 (1H, s, 1-H), 6.30 (1H, d, *J* 9.2 Hz, 5-H), 6.55 (1H, d, *J* 9.2 Hz, 6-H), 6.62 (1H, t, *J* 7.6 Hz, 8-H), 6.78 (1H, t, *J* 7.6 Hz, 4-H), 6.91 (1H, d, *J* 7.6 Hz, 7-H), 7.40 (1H, d, *J* 8.0 Hz, 9-H) and 8.34 (1H, s, 3-H); δ_C (100 MHz;

DMSO-d_6) 103.4 (C-3), 114.5 (C-9), 116.1 (C-1), 118.6 (C-2), 119.5 (C-4), 119.7 (C-5), 123.4 (C-5a), 124.4 (C-7), 128.0 (C-8), 128.2 (C-6), 130.5 (C-3a), 132.3 (C-9a) and 165.6 (C=O); *m*/*z* 211 (**M**$^+$,100%).

3.4. Synthesis of imidazo[1,2-*a*]pyridine deivatives

***Ethyl brom pyruvate* 87d**

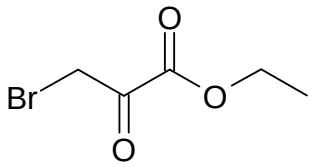

Bromine (24.2 g, 150 mmol) was added drop-wise to ethyl pyruvate (17.52 g, 0.15 mol) which had been heated to 70 °C. The resulting mixture was stirred for 30 minutes and then distilled under reduced pressure to give ethyl bromopyruvate **87d** as a yellow oil (21.7 g, 74.3%), b.p. 80-83 °C/2mmHg (lit.[66] 98-100 °C/10mmHg); ν_{max}(nujol)/cm^{-1} 1700 and 1690 (2 x C=O); δ_H (100 MHz; $CDCl_3$) 1.34 (3H, q, *J* 5.2 and 5.0 Hz, CH_3) and 4.33 (4H, m, 2 x CH_2); δ_C (400 MHz; $CDCl_3$) 14.2 (CH_2CH_3), 31.4 (CH_2CH_3) and 63.5 (CH_2Br).

***2-Amino-1-[(carbethoxycarbonyl)methyl]pyridinium bromide* 87e**

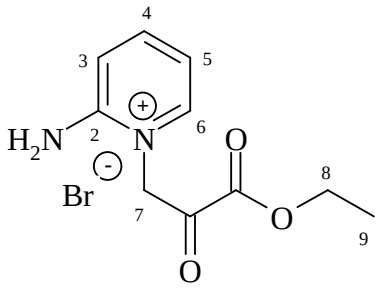

Ethyl bromopyruvate **87d** (11.7 g, 6 0 mmol) was added drop-wise to a stirred solution of 2-aminopyridine (5.62 g, 0.07 mol) in 1,2-dimethoxyethane (50 ml) while the temperature of the mixture was maintained below 50 °C throughout the addition. The resulting mixture was stirred for another 30 minutes and then filtered to give 2-amino-1-[(carbethoxycarbonyl)methyl]pyridinium bromide **87e** as a light brown powder (17 g,

94%), m.p. 128-132 ºC (lit.[66] 134-136 °C); ν_{max}(nujol)/cm^{-1} 1721 and 1649 (2 x C=O); δ_H (400 MHz; D_2O) 1.39 (3H, t, *J* 4.2 Hz, CH_2CH_3), 4.42 (2H, q, *J* 4.2 and 4.0 Hz, CH_3CH_2), 4.83 and 5.26 (2H, 2 x d, *J* 1.5 and 1.3 Hz, NCH_2), 7.23 (2H, m, 4-H and 5-H), 8.15 (1H, t, *J* 1.3 Hz, 3-H), 8.21 (1H, d, *J* 3.6 Hz, 6-H); δ_C (100 MHz; D_2O) 13.7 (C-9), 64.9 (C-8), 71.3 (C-7), 87.4 (C-3), 110.0 (C-5), 116.4 (C-4), 137.1 (C-6), 146.4 (C-2), 154.0 and 168.8 (2 x C=O).

***Ethyl imidazo[1,2-a]pyridine-2-carboxylate hydrobromide* 87f**

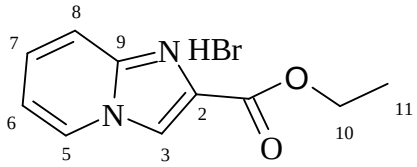

2-Amino-1-[(carbethoxycarbonyl)methyl]pyridinium bromide **87e** (15.1 g, 50 mmol) was refluxed in ethanol (400 ml) for 2 hours. Thereafter the volume of ethanol was reduced to 80 ml and ether (80 ml) was added. Filtration of the mixture gave ethyl imidazo[1,2-*a*] pyridine-2-carboxylate hydrobromide **87f** as a cream coloured powder (7.53 g, 53.1%), m.p. 158-162 °C (lit.[66] 174.5-175.5 °C); ν_{max}(nujol)/cm^{-1} 1710 (C=O); δ_H (400 MHz; D_2O) 1.47 (3H, t, *J* 4.8 Hz, CH_2CH_3), 4.56 (2H, q, *J* 4.8 and 5.2 Hz, CH_2CH_3), 7.56 (1H, t, *J* 4.0 Hz, 7-H), 7.94 (1H, d, *J* 8.2 Hz, 5-H), 8.08 (1H, t, *J* 5.2 Hz, 6-H), 8.69 (1H, s, 3-H) and 8.75 (1H, d, *J* 5.0 Hz, 8-H); δ_C (400 MHz; D_2O) 13.9 (C-11), 64.2 (C-10), 113.0 (C-8), 118.7 (C-5), 127.1 (C-7), 130.0 (C-6), 136.0 (C-3), 141.2 (C-2), 145.1 (C-9) and 160.0 (C=O); m/z 118 (**M**$^+$- $C_3H_6O_2Br$, 100) and 190 (**M**$^+$- HBr, 37%).

***Imidazo[1,2-a]pyridine-2-carboxylic acid* 87g**

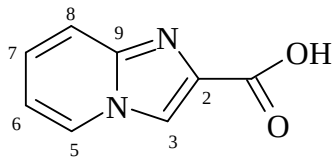

Ethyl imidazo[1,2-*a*]pyridine-2-carboxylate hydrobromide **87f** (10.5 g, 37.1mmol) was added to a solution of KOH (14.2 g, 0.251 mmol) in EtOH (350 ml). The resulting mixture was refluxed for 16 hrs. Thereafter water was added to solubilize the solidmaterial still present in the mixture, and the pH adjusted to *ca*. pH=6 with concentrated HCl (32%). Evaporation of the water yielded a solid product which was repeatedly washed with EtOH to afford imidazo[1,2-*a*]pyridine-2-carboxylic acid **87g** as a pale green powder (4.85 g, 81.8 %), m.p. 248-250 °C (lit.[66] 260-264 °C); ν_{max}(nujol)/cm^{-1} 3402 (OH) and 1705 (C=O); δ_H (400 MHz; DMSO) 7.53 (1H, t, *J* 4.8 Hz, 6-H), 7.90 (1H, d, *J* 6.4 Hz, 8-H), 8.00 (1H, m, 7-H) 8.94 (1H, d, *J* 6.0 Hz, 5-H) and 8.95 (1H, s, 3-H), δ_C (100 MHz; DMSO) 113.1 (C-6), 113.4 (C-3), 118.8 (C-8), 127.8 (C-7), 129.6 (C-5), 143.9 (C-2), 154 .0 (C-9) and 159.9 (C=O); *m*/*z* 118 (**M**$^+$ - CO_2, 100) and 162 (**M**$^+$, 88%).

3.5. SYNTHESIS OF CARBOXAMIDES

N-*[4-(Diethylamino)-1-methylbutyl]indolizine-2-carboxamide* 89

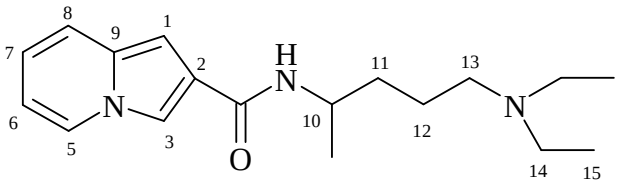

Indolizine-2-carboxylic acid **87a** (0.100 g, 0.63 mmol) was dissolved in dry DMF (3 ml) in a round-bottomed flask fitted with a reflux condenser and a drying tube. 1,1'-Carbonyldiimidazole (CDI) (0.160 g, 0.954 mmol) was added to the mixture. After heating at 40 °C for 5 minutes, the mixture was allowed to cool to room temperature and 1-methyl-5-(diethylamino)butylamine (0.245 g, 1.55 mmol) was added and the resulting mixture stirred overnight. The reaction was then quenched with water (1 ml) and the solvent removed under reduced pressure. 1M aqueous Na_2CO_3 (15 ml) was added to the residue and the mixture was extracted with EtOAc (2 x 24 ml) and then washed sequentially with water (24 ml) and brine (24 ml). The extract was dried over $MgSO_4$ and the solvent removed *in vacuo* to afford a yellow oil (0.241 g), which was purified by flash

chromatography [on silica; elution with CH_2Cl_2-ammonia(aqueous)-methanol (20:4:1)] to afford N-*[4-(diethylamino)-1-methylbutyl]indolizine-2-carboxamide* **89** as a yellow oil (0.132 g, 69.4%), (Found $\mathbf{M}^+$: 301.216652. $C_{18}H_{27}N_3O$ requires **M**, 301.215413); ν_{max}(KBr)/cm^{-1} 1609 (NHC=O); δ_H (400 MHz; $CDCl_3$) 1.00 (6H, t, *J* 7.2 Hz, 15- and 15'-CH_3), 1.25 (3H, d, *J* 7.6 Hz, 10-CH_3), 1.55 (4H, m, 11- and 12-CH_2), 2.44 (2H, t, *J* 3.2 Hz, 13-CH_2), 2.52 (4H, q, *J* 3.2 and 2.8 Hz, 14- and 14'-CH_2), 4.21 (1H, m, 10-H), 6.02 (1H, d, *J* 2.0 Hz, NH), 6.51 (1H, m, 6-H), 6.56 (1H, s, 1-H), 6.68 (1H, m, 8-H), 7.34 (1H, d, *J* 9.2 Hz, 5-H), 7.74 (1H, d, *J* 0.8 Hz, 3-H) and 7.86 (1H, q, *J* 1.0 Hz, 7-H); δ_C (100 MHz; $CDCl_3$) 11.5 (C-15), 21.1 (C-10a), 23.6 (C-11), 35.0 (C-12), 45.1 (C-10), 46.8 (C-14), 52.7 (C-13), 96.9 (C-1), 111.8 (C-6), 113.9 (C-3), 118.2 (C-2), 120.0 (C-8), 124.2 (C-5), 125.4 (C-9), 132.8 (C-7) and 164.1 (C=O); *m*/*z* 301 (**M**, 50) and 86 (**M** - $C_{13}H_{15}N_2O$, 100%) .

N-*[2-(Benzylthio)ethyl]indolizine-2-carboxamide* 91a

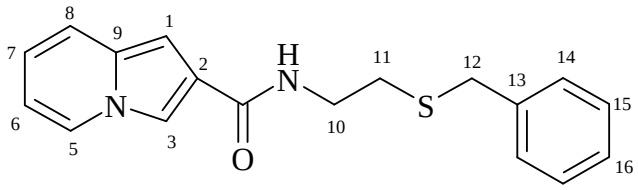

Indolizine-2-carboxylic acid **87a** (0.100 g, 0.63 mmol) in dry DMF (5 ml) and dry pyridine (3 ml) was reacted with *S*-benzylcysteamine hydrochloride (0.200 g, 0.960 mmol) following the procedure described for the preparation of *N*-[4-(diethylamino)-1-methylbutyl]indolizine-2-carboxamide **89** to afford a crude product, which was purified by preparative layer chromatography [on silica; elution with CH_2Cl_2-methanol (20:4)] to afford N-*[2-(benzylthio)ethyl]indolizine-2-carboxamide* **91a** as a yellow solid (0.12 g, 65%), m.p. 104-106 ºC, (Found $\mathbf{M}^+$: 310.113786. $C_{18}H_{18}N_2OS$ requires **M**, 310.113985); ν_{max}(KBr)/cm^{-1} 1652 (C=O); δ_H (400 MHz; $CDCl_3$) 2.69 (2H, t, *J* 6.4 Hz, 11-CH_2), 3.61 (2H, m, 10-CH_2), 3.76 (2H, s, 12-CH_2), 6.38 (1H, br s, NH), 6.52 (1H, m, 7-H), 6.57 (1H, s, 3-H), 6.69 (1H, q, *J* 0.8 and 1.0 Hz, 6-H), 7.24 (1H, d, *J* 1.2 Hz, 5-H), 7.33 (5H, m, 14-H, 15-H and 16-H), 7.74 (1H, d, *J* 1.2 Hz, 1-H) and 7.88 (1H, t, *J* 6.8 Hz, 8-H); δ_C (100 MHz; $CDCl_3$) 31.3 (C-11), 35.8 (C-12), 37.9 (C-10), 97.1 (C-1), 111.9 (C-6), 114.0 (C-

2), 118.3 (C-3), 120.0 (C-7), 123.5 (C-8), 125.4 (C-5), 127.1 (C-16), 128.6 (C-15), 128.8 (C-14), 132.9 (C-9), 138.1 (C-13) and 164.7 (C=O); *m*/*z* 310 (**M**, 53) and 144 (**M** - $C_9H_{12}NS$, 100%).

N-*[2-(Benzylthio)ethyl]-5-methylindolizine-2-carboxamide* 91b

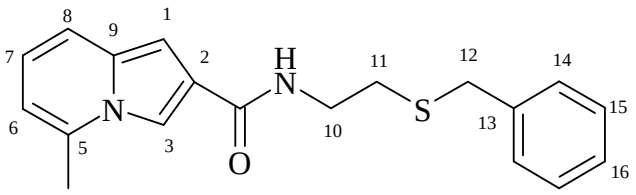

Following the procedure described for the synthesis of *N*-[2-(benzylthio)ethyl]indolizine-2-carboxamide **91a**, *S*-benzylcysteamine hydrochloride (0.200 g, 0.960 mmol) was reacted with 5-methyindolizine-2-carboxylic acid **87b** (0.100 g, 0.571 mmol) to afford N-*[2-(benzylthio)ethyl]-5-methylindolizine-2-carboxamide* **91b** as a green oil (0.147 g, 78.9%), (Found **M**+1: 325.1376. $C_{19}HN_{21}OS$ requires **MH**$^+$, 325.1376); ν_{max}(KBr)/cm^{-1} 1642 (C=O); δ_H (400 MHz; $CDCl_3$) 2.46 (3H, s, 5-CH_3), 2.69 (2H, t, *J* 6.8 Hz, 11-CH_2), 3.61 (2H, q, *J* 6.8 and 7.2 Hz, 10-CH_2), 3.74 (2H, s, 12-CH_2), 6.40 (1H, d, *J* 6.8 Hz, 6-H), 6.68 (3H, m, 1-H, 7-H and NH), 7.24 (1H, t, *J* 1.6 Hz, 8-H), 7.27 (5H, m, 14-H, 15-H and 16-H) and 7.70 (1H, s, 3-H); δ_C (100 MHz; $CDCl_3$) 18.5 (CH_3), 31.1 (C-11), 35.7 (C-10), 38.0 (C-12), 97.5 (C-1), 110.9 (C-3), 111.3 (C-6), 117.4 (C-8), 118.6 (C-7), 123.3 (C-13), 127.0 (C-16), 128.5 (C-14), 128.7 (C-15), 133.1 (C-9), 133.5 (C-5), 138.0 (C-2) and 165.0 (C=O); *m*/*z* 325 (**M**+1, 100%).

N-*[2-(Benzylthio)ethyl]pyrrolo[1,2-a]quinoline-2-carboxamide* 91c

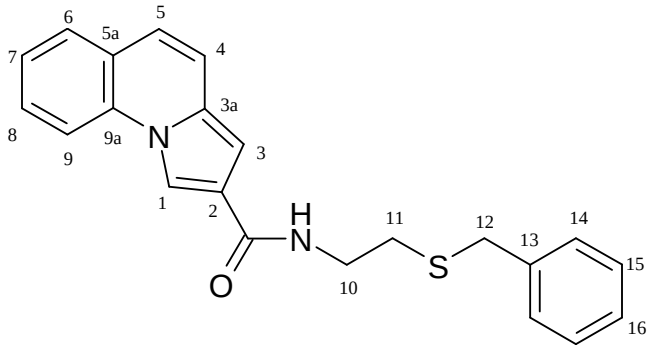

Following the procedure described for the synthesis of *N*-[2-(benzylthio)ethyl]indolizine-2-carboxamide **91a**, *S*-benzylcysteamine hydrochloride (0.200 g, 0.960 mmol) was reacted with pyrrolo[1,2-*a*]quinoline-2-carboxylic acid **87c** (0.100 g, 0.47 mmol) to afford N-*[2-(benzylthio)ethyl]pyrrolo[1,2-*a*]quinoline-2-carboxamide* **91c** as a yellow oil (0.162 g, 96.7%), (Found **M**+1: 361.1389. $C_{22}H_{21}N_2OS$ requires **MH**$^+$, 361.1375); ν_{max}(KBr)/cm^{-1} 1732 (C=O); δ_H (400 MHz; $CDCl_3$) 2.71 (2H, t, *J* 6.4 Hz, 11-CH_2), 3.63 (2H, m, 10-CH_2), 3.76 (2H, s, 12-CH_2), 6.68 (2H, m, 3-H and NH), 6.90 (1H, d, *J* 7.6 Hz, 5-H), 6.99 (1H, d, *J* 9.2 Hz, 6-H), 7.22 (1H, m, 7-H), 7.32 (5H, m, 14-H, 15-H and 16-H), 7.46 (1H, m, 8-H), 7.59 (1H, d, *J* 7.6 Hz, 9-H), 7.81 (1H, d, *J* 8.0 Hz, 4-H) and 8.34 (1H, s, 1-H); δ_C (100 MHz; $CDCl_3$) 31.2 (C-11), 35.8 (C-12), 38.1 (C-10), 100.5 (C-3), 114.0 (C-9), 114.3 (C-2), 118.7 (C-4), 120.3 (C-1), 122.6 (C-5), 123.9 (C-5a), 124.5 (C-7), 127.0 (C-8), 128.5 (C13, C-14, C-15 and C-16), 131.2 (C-6), 132.8 (C-3a), 138.0 (C-9a), 164.6 (C=O); *m*/*z* 361 (**M**+1, 100%).

N-*[(Carbethoxy)methyl]indolizine-2-carboxamide* 93a

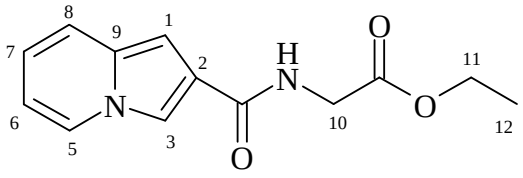

Following the procedure described for the synthesis of *N*-[2-(benzylthio)ethyl]indolizine-2-carboxamide **91a**, glycine ethyl ester hydrochloride (0.200 g, 1.40 mmol) was reacted with indolizine-2-carboxylic acid **87a** to afford N-*[(carbethoxy)methyl]indolizine-2-carboxamide* **93a** as a green oil (0.097 g, 66%), (Found **M**$^+$: 246.099889. $C_{13}H_{14}N_2O_3$ requires **M**, 246.100442); ν_{max}(KBr)/cm^{-1} 1637 (NHC=O) and 1705 (C=O); δ_H (400 MHz; $CDCl_3$) 1.31 (3H, t, *J* 7.2 Hz, 12-CH_3), 4.23 (2H, s, 10-CH_2), 4.27 (2H, q, *J* 7.2 and 7.6 Hz, 11-CH_2), 6.50 (1H, d, *J* 5.2 Hz, 7-H), 6.52 (1H, s, 3-H), 6.64 (1H, s, NH), 6.69 (1H, q, *J* 0.8 and 1.2 Hz, 6-H), 7.36 (1H, d, *J* 9.2 Hz, 5-H), 7.77 (1H, s, 1-H) and 7.88 (1H, d, *J* 6.8 Hz, 8-H); δ_C (100 MHz; $CDCl_3$) 14.2 (C-12), 41.5 (C-10), 61.6 (C-11), 97.3 (C-1), 112.0 (C-6), 114.1 (C-2), 118.3 (C-3), 120.0 (C-7), 122.9 (C-8), 125.4 (C-5), 132.9 (C-9), 164.7 and 170.3 (2 x C=O); *m*/*z* 246 (**M**, 48) and 144 (**M** - $C_4H_8NO_2$, 100%).

N-*Carbethoxymethyl-5-methylindolizine-2-carboxamide* 93b

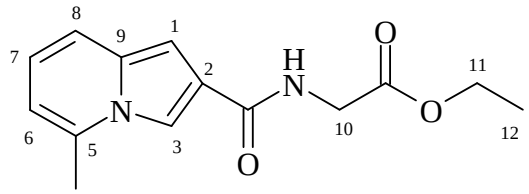

Following the procedure described for the synthesis of *N*-[2-(benzylthio)ethyl]indolizine-2-carboxamide **91a**, 5-methylindolizine-2-carboxylic acid **87b** (0.100 g, 0.571 mmol) and glycine ethyl ester hydochloride (0.200 g, 1.40 mmol) were reacted to afford N-*carbethoxymethyl-5-methylindolizine-2-carboxamide* **93b** as a yellow oil (0.059 g, 39.9%), (Found **M**+1: 261.1250. $C_{14}H_{17}N_2O_3$ requires **MH**$^+$, 261.1239); ν_{max}(KBr)/cm^{-1} 1647 (NHC=O) and 1693 (C=O); δ_H (400 MHz; $CDCl_3$) 1.29 (3H, t, *J* 7.2 Hz, 12-CH_3), 2.45 (3H, s, 5-CH_3), 4.21 (2H, s, 10-CH_2), 4.24 (2H, q, *J* 7.2 and 7.4 Hz, 11-CH_2), 6.38 (1H, d, *J* 6.8 Hz, 6-H), 6.67 (1H, t, *J* 2.4 Hz, 7-H), 6.70 (1H, s, 1-H), 6.80 (1H, br m, NH), 7.26 (1H, t, *J* 4.4 Hz, 8-H) and 7.68 (1H, s, 3-H); δ_C (100 MHz; $CDCl_3$) 14.1 (C-12), 18.5 (CH_3), 41.5 (C-10), 61.5 (C-11), 97.9 (C-1), 111.0 (C-6), 111.3 (C-3), 117.5 (C-8), 118.6 (C-7), 122.6 (C-2), 133.1 (C-5), 133.5 (C-9), 165.1 and 170.4 (2 x C=O); *m*/*z* 261 (**M**+1, 100%).

N-*(Carbethoxymethyl)pyrrolo[1,2-*a*]quinoline-2-carboxamide* 93c

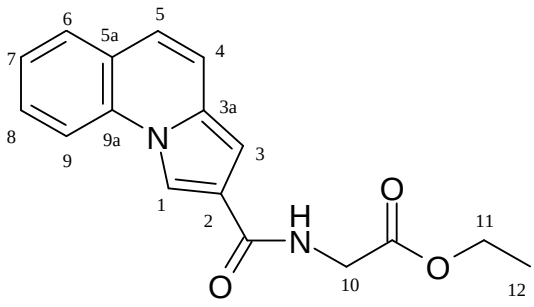

Following the procedure described for the synthesis of *N*-[2-(benzylthio)ethyl]indolizine-2-carboxamide **91a**, pyrrolo[1,2-*a*]quinoline-2-carboxylic acid **87c** (0.100 g, 0.47 mmol)

and glycine ethyl ester hydrochloride (0.200 g, 1.40 mmol) were reacted to afford N-*(carbethoxymethy)lpyrrolo[1,2*-a*]quinoline-carboxamide* **93c** as a brown oil (0.081 g, 58%), (Found **M**+1:, 297.1252. $C_{17}H_{17}N_2O_3$ requires **MH**$^+$, 297.1239); ν_{max}(KBr)/cm^{-1} 1649 (NHC=O) and 1732 (C=O); δ_H (400 MHz; $CDCl_3$) 1.25 (3H, t, *J* 5.2 Hz, 12-CH_3), 4.04 (2H, d, *J* 6.0 Hz, 10-CH_2), 4.20 (2H, q, *J* 5.2 and 4.4 Hz, 11-CH_2), 6.70 (1H, s, 1-H), 6.90 (1H, d, *J* 9.6 Hz, 5-H), 7.07 (1H, t, *J* 9.2 Hz, NH), 7.12 (1H, d, *J* 9.6 Hz, 6-H), 7.28 (1H, t, *J* 7.6 Hz, 7-H), 7.42 (1H, m, 8-H), 7.52 (1H, d, *J* 7.6 Hz, 9-H), 7.74 (1H, d, *J* 8.4 Hz, 4-H) and 8.30 (1H, s, 3-H); δ_C (100 MHz; $CDCl_3$) 14.1 (C-12), 41.4 (C-10), 61.5 (C-11), 100.8 (C-3), 114.1 (C-9), 114.2 (C-2), 118.6 (C-4), 120.2 (C-1), 121.8 (C-5), 123.8 (C-5a), 124.4 (C-7), 128.1 (C-8), 128.5 (C-6), 131.2 (C-3a), 132.8 (C-9a), 165.0 and 170.5 (2 x C=O); *m*/*z* 297 (**M**+1, 100%).

***Ethyl 3-hydroxy-2(S)-(indolizine-2-carboxamido)propanoate* 95a**

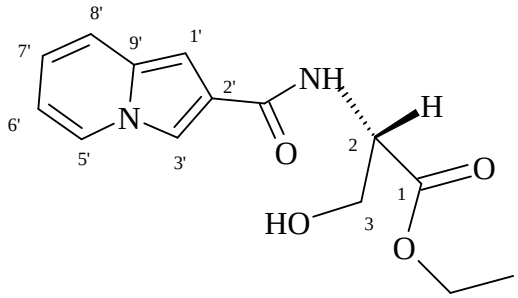

Following the procedure described for the synthesis of *N*-[2-(benzylthio)ethyl]indolizine-2-carboxamide **91a**, L-serine ethyl ester hydrochloride (0.200 g, 1.18 mmol) was reacted with indolizine-2-carboxylic acid **87a** to afford *ethyl 3-hydroxy-2-(indolizine-2-carboxamido)propanoate* **95a** as a yellow oil (0.080 g, 47%), (Found **M**$^+$: 276.109981. $C_{14}H_{16}N_2O_4$ requires **M**, 276.111007); ν_{max}(KBr)/cm^{-1} 1633 (NHC=O) and 1700 (C=O); δ_H (400 MHz; $CDCl_3$) 1.27 (4H, t, *J* 7.2 Hz, C*H*$_3$CH$_2$ and OH), 4.04 (2H, d, *J* 3.6 Hz, 3-C*H*$_2$), 4.24 (2H, q, *J* 8.2 and 7.2 Hz, CH$_3$C*H*$_2$), 4.83 (1H, m, 2-H), 6.45 (1H, m, 6'-H), 6.63 (2H, m, 7-H and 1'-H), 7.19 (1H, s, NH), 7.24 (1H, s, 5'-H), 7.72 (1H, s, 3'-H) and 7.88 (1H, q, *J* 0.5 and 0.9 Hz, 8'-H); δ_C (100 MHz; $CDCl_3$) 14.4 (*C*H$_3$CH$_2$), 55.4 (C-2), 62.2 (CH$_3$*C*H$_2$), 63.8 (C-3), 98.0 (C-1), 112.2 (C-6'), 114.5 (C-3'), 118.6 (C-7'), 120.2

(C-5'), 122.8 (C-2'), 125.7 (C-8), 133.1 (C-9'), 165.6 and 171.1 (2 x C=O); *m*/*z* 276 (**M**, 45) and 144 ($\mathbf{M}^+$ - $C_5H_{10}NO_3$, 100%).

***Ethyl (2S)-3-hydroxy-2-(5-methylindolizine-2-carboxamido)propanoate* 95b**

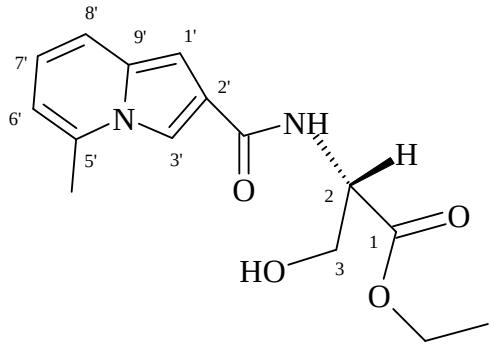

Following the procedure described for the synthesis of *N*-[2-(benzylthio)ethyl]indolizine-2-carboxamide **91a**, L-serine ethyl ester hydrochloride (0.200 g, 1.18 mmol) was reacted with 5-methyindolizine-2-carboxylic acid **87b** (0.100 g, 0.571 mmol) to afford *ethyl (2S)-3-hydroxy-2-(5-methylindolizine-2-carboxamido)propanoate* **95b** as a yellow oil (0.072 g, 44%), (Found **M**+1: 291.1374. $C_{15}H_{19}N_2O_4$ requires $\mathbf{MH}^+$, 291.1395); ν_{max}(KBr)/cm^{-1} 1649 (NHC=O) and 1732 (C=O); δ_H (400 MHz; $CDCl_3$) 1.27 (4H, t, *J* 7.2 Hz, CH_2CH_3 and OH), 2.39 (3H, s, 5-CH_3), 4.05 (2H, d, *J* 3.6 Hz, 3-CH_2), 4.24 (2H, q, *J* 3.6 and 3.2 Hz, CH_2CH_3), 4.85 (1H, t, *J* 3.6 Hz, 2-H), 6.34 (1H, d, *J* 6.8 Hz, 8'-H), 6.65 (1H, m, 7'-H), 6.71 (1H, d, *J* 1.2 Hz, NH), 7.21 (1H, d, *J* 8.8 Hz, 6'-H), 7.24 (1H, s, 3'-H) and 7.64 (1H, s, 1'-H); δ_C (100 MHz; $CDCl_3$) 14.0 (C-13), 18.4 (5-CH_3), 55.2 (C-2), 61.9 (CH_2CH_3), 63.5 (C-3), 98.2 (C-1'), 111.0 (C-6'), 111.3 (C-2'), 117.5 (C-3'), 118.6 (C-7'), 122.3 (C-8'), 133.1 (C-5'), 133.5 (C-9'), 165.5 and 170.8 (2 x C=O); *m*/*z* 291 (**M**+1, 100%).

***Ethyl (2S)-3-hydroxy-2-{pyrrolo[1,2-a]quinoline-2-carboxamido}propanoate* 95c**

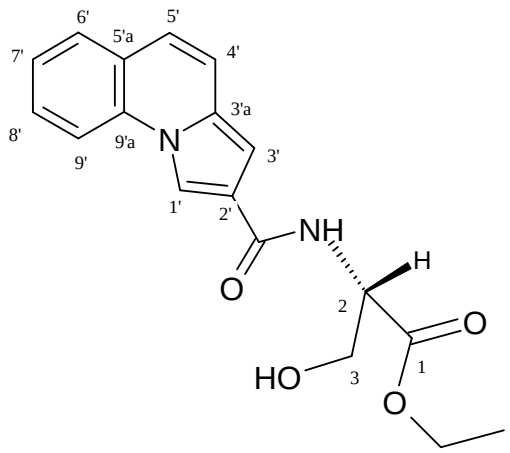

Following the procedure described for the synthesis of *N*-[2-(benzylthio)ethyl]indolizine-2-carboxamide **91a**, L-serine ethyl ester hydrochloride (0.200 g, 1.18 mmol) was reacted with pyrrolo[1,2-*a*]quinoline-2-carboxylic acid **87c** (0.100 g, 0.47 mmol) to afford *ethyl (2S)-3-hydroxy-2-{pyrrolo[1,2-a]quinoline-2-carboxamido}propanoate* **95c** as a brown oil (0.0524 g, 34.2%), (Found **M**+1: 327.1348. $C_{18}H_{19}N_2O_4$ requires **MH**$^+$, 327.1345); ν_{max}(KBr)/cm^{-1} 1638 (NHC=O) and 1732 (C=O); δ_H (400 MHz; $CDCl_3$) 1.31 (3H, t, *J* 7.2 Hz, CH_2CH_3), 3.08 (1H, br s, OH), 4.09 (2H, d, *J* 3.6 Hz, 3-CH_2), 4.27 (2H, q, *J* 7.2 and 7.0 Hz, CH_2CH_3), 4.87 (1H, m, 2-H), 6.71 (2H, s, 3'-H), 6.91 (1H, d, *J* 9.2 Hz, 6'-H), 7.12 (1H, d, *J* 9.2 Hz, 5'-H), 7.17 (1H, d, *J* 7.2 Hz, NH), 7.30 (1H, t, *J* 7.6 Hz, 8'-H), 7.44 (1H, t, J 7.6 Hz, 7'-H), 7.54 (1H, d, *J* 7.6 Hz, 4'-H), 7.78 (1H, d, *J* 8.0 Hz, 9'-H) and 8.30 (1H, s, 1'-H); δ_C (100 MHz; $CDCl_3$) 14.1 (CH_2CH_3), 55.2 (C-2), 62.0 (CH_2CH_3), 63.7 (C-3), 101.0 (C-3'), 114.2 (C-9'), 114.4 (C-2'), 118.7 (C-4'), 120.4 (C-1'), 121.8 (C-5'), 124.0 (C-5'a), 124.6 (C-7'), 128.2 (C-8'), 128.6 (C-6'), 131.3 (C-3'a), 132.8 (C-9'a), 165.1 and 170.8 (2 x C=O); *m*/*z* 327 (**M**+1, 100%).

N-*Carbomethoxymethyl-5-methylindolizine-2-carboxamide* 97b

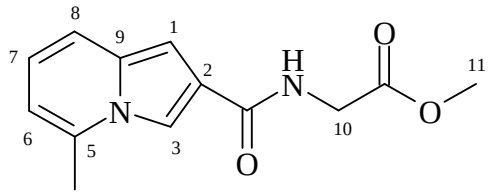

Following the procedure described for the synthesis of *N*-[2-(benzylthio)ethyl]indolizine-2-carboxamide **91a**, glycine methyl ester hydrochloride (0.200 g, 1.59 mmol) was reacted with 5-methyindolizine-2-carboxylic acid **87b** (0.100 g, 0.571 mmol) to afford N-*carbomethoxymethyl-5-methylindolizine-2-carboxamide* **97b** as a brown oil (0.115 g, 81.9%), (Found **M**+1: 247.1091. $C_{13}H_{15}N_2O_3$ requires **MH**$^+$, 247.1083); ν_{max}(KBr)/cm^{-1} 1649 (NHC=O) and 1730 (C=O); δ_H (400 MHz; $CDCl_3$) 2.46 (3H, s, 11-CH_3), 3.78 (3H, s, 5-CH_3), 4.25 (2H, d, *J* 5.2 Hz, 10-CH_2), 6.39 (1H, d, *J* 6.4 Hz, 6-H), 6.70 (1H, t, *J* 2.0 Hz, 7-H), 6.71 (1H, s, 3-H), 6.76 (1H, s, NH), 7.27 (1H, d, *J* 9.6 Hz, 8-H) and 7.69 (1H, s, 1-H); δ_C (100 MHz; $CDCl_3$) 18.5 (CH_3), 41.3 (C-10), 52.3 (C-11), 97.8 (C-1), 111.0 (C-6), 111.4 (C-2), 117.6 (C-3), 118.7 (C-7), 122.6 (C-8), 133.2 (C-5), 133.6 (C-9), 165.1 and 170.8 (2 x C=O); *m*/*z* 247 (**M**+1, 100%).

N-*(Carbomethoxymethyl)pyrrolo[1,2-*a*]quinoline-2-carboxamide* 97c

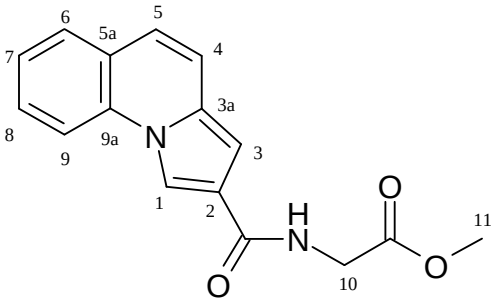

Following the procedure described for the synthesis of *N*-[2-(benzylthio)ethyl]indolizine-2-carboxamide **91a**, glycine methyl ester hydrochloride (0.200 g, 1.59 mmol) was reacted with pyrrolo[1,2-*a*]quinoline-2-carboxylic acid **87c** (0.100 g, 0.47 mmol) to afford N-

(carbomethoxymethy)lpyrrolo[1,2-a*]quinoline-2-carboxamide* **97c** as a brownish-yellow oil (0.094 g, 70%), (Found **M**+1: 283.1083. $C_{16}H_{15}N_2O_3$ requires **MH**$^+$, 283.1083); ν_{max}(KBr)/cm^{-1} 1659 (NHC=O) and 1733 (C=O); δ_H (400 MHz; $CDCl_3$) 3.80 (3H, s, 11-CH_3), 4.27 (2H, d, *J* 5.2 Hz, 10-CH_2), 6.71 (1H, s, 3-H), 6.75 (1H, s, NH), 6.90 (1H, d, *J* 7.6 Hz, 5-H), 7.20 (1H, d, *J* 9.6 Hz, 6-H), 7.33 (1H, t, *J* 7.6 Hz, 7-H), 7.48 (1H, m, 8-H), 7.58 (1H, d, *J* 7.6 Hz, 9-H), 7.82 (1H, d, *J* 8.4 Hz, 4-H) and 8.33 (1H, s, 1-H); δ_C (100 MHz; $CDCl_3$) 41.3 (C-10), 52.3 (C-11), 100.7 (C-3), 114.2 (C-9), 114.4 (C-2), 118.7 (C-4), 120.4 (C-1), 122.0 (C-5), 124.0 (C-5a), 124.6 (C-7), 128.2 (C-8), 128.7 (C-6), 131.3 (C-3a), 132.9 (C-9a), 164.7 and 170.9 (2 x C=O); *m*/*z* 283 (**M**+1, 100%).

***Methyl (2S)-1-[(5-methylindolizin-2-yl)carbonyl]pyrrolidine-2-carboxylate* 99**

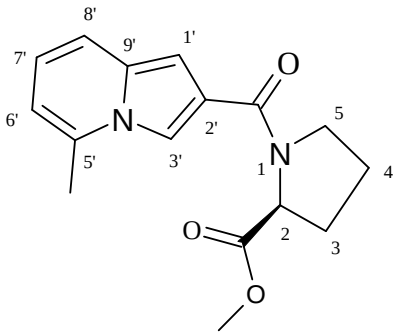

Following the procedure described for the synthesis of *N*-[2-(benzylthio)ethyl]indolizine-2-carboxamide **91a**, L-proline methyl ester hydrochloride (0.200 g, 1.20 mmol) was reacted with 5-methyindolizine-2-carboxylic acid **87b** (0.100 g, 0.571 mmol) to afford *methyl (2*S*)-1-[(5-methylindolizin-2-yl)carbonyl]pyrrolidine-2-carboxylate* **99** as a brown oil (0.080g, 50%), (Found **M**+1: 287.1383. $C_{16}H_{19}N_2O_3$ requires **MH**$^+$, 287.1396); ν_{max}(KBr)/cm^{-1} 1603 (NC=O) and 1736 (C=O); δ_H (400 MHz; $CDCl_3$) 2.00 (2H, m, 3-CH_2), 2.13 (1H, m, 4-CH_a), 2.30 (1H, m, 4-CH_b), 2.48 (3H, s, 5'-CH_3), 3.75 (3H, s, OCH_3), 3.96 (2H, m, 5-CH_2), 4.69 (1H, q, *J* 3.0 and 2.4 Hz, 2-H), 6.40 (1H, d, *J* 6.8 Hz, 8'-H), 6.68 (1H, m, 7'-H), 6.78 (1H, s, 3'-H), 7.29 (1H, d, *J* 9.2 Hz, 6'-H) and 7.68 (1H, s, 1'-H); δ_C (100 MHz; $CDCl_3$) 18.5 (5-CH_3), 25.4 (C-4), 28.9 (C-3), 49.1 (C-5), 52.1 (OCH_3), 59.8 (C-2), 99.7 (C-1'), 110.9 (C-6), 112.7 (C-2'), 117.5 (C-3'), 118.3 (C-7'), 122.8 (C-8'), 132.9 (C-9'), 165.2 and 173.0 (2 x C=O); *m*/*z* 287 (**M**+1, 100%).

***1-(Indolizin-2-yl)-7-carbomethoxy-1,9,12-trioxo-2,8,11-triazatridecane* 101**

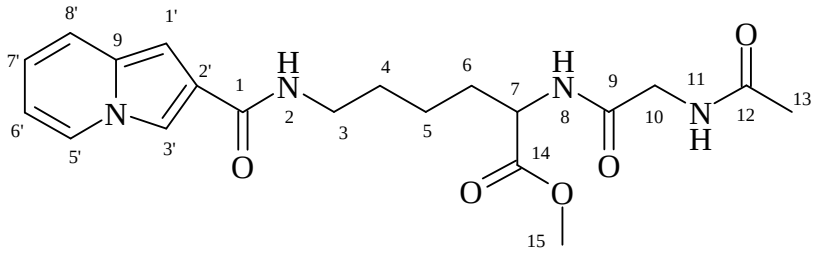

Indolizine-2-carboxylic acid **87a** (0.100 g, 0.63 mmol) in dry DMF (5 ml) was reacted with *N*-acetyl-glycine-lysine methyl ester acetate salt (0.150 g, 0.578 mmol) following the procedure described for the preparation of *N*-[4-(diethylamino)-1-methylbutyl]indolizine-2-carboxamide **89**. The crude product was purified using preparative layer chromatography [on silica; elution with CH_2Cl_2-methanol (20:4)] to afford *1-(indolizine-2-yl)-7-carbomethoxy-1,9,12-trioxo-2,8,11-triazadecane* **101** as a brown solid (0.150 g, 60.1%), m.p. 114-116 ºC, (Found $\mathbf{M}^+$: 402.1880. $C_{20}H_{26}N_4O_5$ requires **M**, 402.1903); ν_{max}(nujol)/cm^{-1} 1741 (C=O), 1664, 1638, 1630 (3 x NHC=O); δ_H (400 MHz; $CDCl_3$) 1.40 (2H, m, 5-CH_2), 1.56 (2H, m, 4-CH_2), 1.76 (1H, m, 6-CH_a), 1.88 (1H, m, 6-CH_b), 1.99 (3H, s, 13-H), 3.36 (1H, m, 3-CH_a), 3.50 (1H, m, 3-CH_b), 3.70 (3H, s, OMe), 4.02 (2H, ddd, *J* 5.6, 5.0 and 6.0 Hz, 10-H), 4.47 (1H, m, 7-H), 6.50 (1H, t, *J* 6.8 Hz, 6'-H), 6.67 (1H, m, 7'-H), 6.88 (1H, t, *J* 4.8 Hz, 8'-H), 7.10 (1H, s, 11-NH), 7.30 (1H, d, *J* 8.8 Hz, 5'-H), 7.40 (1H, d, *J* 7.2 Hz, 1'-H), 7.76 (1H, s, 2-NH), 7.85 (1H, s, 3'-H) and 7.89 (1H, d, *J* 6.8 Hz, 8-NH); δ_C (100 MHz; $CDCl_3$) 22.0 (C-5), 22.9 (C-13), 29.1 (C-4), 30.8 (C-6), 38.3 (C-3), 43.1 (C-10), 52.2 (C-7), 52.4 (C-15), 97.1 (C-1'), 111.9 (C-6'), 114.3 (C-2'), 118.4 (C-3'), 119.7 (C-7'), 123.3 (C-5'), 125.6 (C-8'), 132.9 (C-9'), 165.6 (1-C=O), 169.2 (9-C=O), 170.8 (CH_3OC=O) and 172.5 (12-C=O); *m*/*z* 402 ($\mathbf{M}^+$, 100%).

3.5.1. Attempted synthesis of indolizine-2-carboxamides

2-(Piperazin-1-ylcarbonyl)indolizine **103**

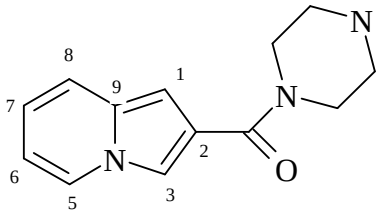

Piperazine (0.200 g, 2.32 mmol) was reacted indolizine-2-carboxylic acid (0.100 g, 0.63 mmol) following the procedure described for the preparation of *N*-[4-(diethylamino)-1-methylbutyl]indolizine-2-carboxamide **89** and ^{1}H NMR spectroscopy indicated that no reaction occurred. The mixture was left to stand for a further 5 days, but ^{1}H NMR analysis again confirmed that no reaction had occurred.

N-*(3-Amino-2-hydroxypropyl)indolizine-2-carboxamide* **105**

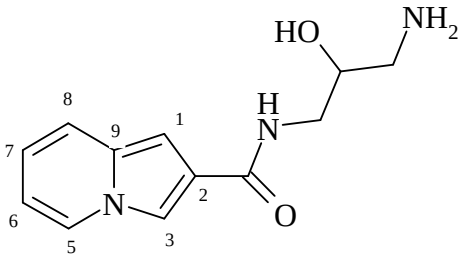

1,3-Diamine-2-hydroxypropane (0.200 g, 2.22 mmol) was reacted indolizine-2-carboxylic acid (0.100 g, 0.63 mmol) following the procedure described for the preparation of *N*-[4-(diethylamino)-1-methylbutyl]indolizine-2-carboxamide **89**. After 2 days the TLC plate showed no presence of the product and the ^{1}H NMR spectroscopy confirmed that no reaction had occurred.

N-*(2-aminoethyl)indolizine-2-carboxamide* 107

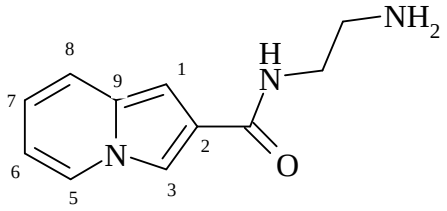

1,2-Diamine ethane (0.200 g, 3.33 mmol) was reacted indolizine-2-carboxylic acid (0.100 g, 0.63 mmol) following the procedure described for the preparation of *N*-[4-(diethylamino)-1-methylbutyl]indolizine-2-carboxamide **89** and ^{1}H NMR spectroscopy indicated that no reaction occurred. The mixture was left to stand for a further 3 days, but ^{1}H NMR analysis again confirmed that no reaction had occurred.

3.6. Synthesis of the aza-Michael products

***Methyl 2-[(benzylamino)methyl]-3-hydroxy-3-(pyridin-3-yl)propanoate* 109a**

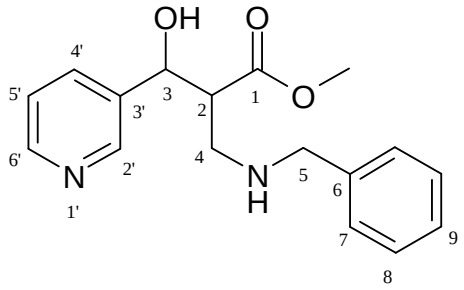

Methyl 2-[hydroxy(pyridin-3-yl)methyl]acrylate **61d** (0.200 g, 1.04 mmol) was dissolved in dry methanol (5 ml) and the resulting solution stirred in an ice-bath until the temperature reached 0 °C. Thereafter, benzylamine (0.25 g, 1.7 mmol) was added and the mixture was stirred at 0 °C for 46 hours. The solvent was removed *in vacuo* to afford *methyl 2-[(benzylamino)methyl]-3-hydroxy-3(-pyridin-3-yl)propanoate* **109a** (0.22 g, 69%) as a 1:1.5 mixture of diastereomers (*i.e.* 20% d.e.; as determined by the ^{1}H NMR analysis). The diastereomers (100 mg) were separated by preparative layer

chromatography [on silica; elution with CH_2Cl_2-hexane-EtOAC-MeOH (20:15:10:1)] to afford the two fractions.

Fraction 1. as a yellow oil (32.7mg, 33%), (Found **M**+1: 301.1565. $C_{17}H_{21}N_2O_3$ requires **MH**$^+$, 301.1552); ν_{max}(KBr)/cm^{-1} 3313-3380 (OH and NH) and 1730 (C=O); δ_H (400 MHz; $CDCl_3$) 2.77 (2H, m, 2-H and 4-CH*a*), 3.18 (1H, q, *J* 6.8 an 6.0 Hz, 4-CH*b*), 3.63 (1H, br m, NH), 3.65 (3H, s, OCH_3), 3.71 (2H, d, *J* 5.2 Hz, 5-CH_2), 5.32 (1H, d, *J* 4.8 Hz, 3-H), 7.21 (1H, m, 5'-H), 7.30 (6H, m, 7-H, 8-H, 9-H and OH), 7.62 (1H, d, *J* 8.0 Hz, 4'-H), 8.49 (1H, d, *J* 4.4 Hz, 6'-H) and 8.54 (1H, s, 2'-H); δ_C (100 MHz; $CDCl_3$) 47.5 (C-4), 50.9 (C-2), 52.1 (OMe), 53.9 (C-5), 74.4 (C-3), 123.2 (C-5'), 127.5 (C-9), 128.3 (C-8), 128.6 (C-7), 133.7 (C-4'), 138.1 (C-6), 138.5 (C-3'), 147.8 (C-6'), 148.7 (C-2') and 172.5 (C=O); *m*/*z* 301 (**M**+1, 100%).

Fraction 2. as a yellow oil (13.7mg, 14%), (Found **M**+1: 301.1539. $C_{17}H_{21}N_2O_3$ requires **MH**$^+$, 301.1552); ν_{max}(nujol)/cm^{-1} 3340-3390 (OH and NH) and 1712 (C=O); δ_H (400 MHz; $CDCl_3$) 2.91 (1H, q, *J* 4.4 and 4.0 Hz, 4-CH*a*), 3.00 (1H, q, *J* 4.4 and 4.0 Hz, 2-H), 3.08 (1H, q, *J* 5.0 and 4.6 Hz, 4-CH*b*), 3.37 (1H, br m, NH), 3.57 (3H, s, OCH_3), 3.90 (2H, d, *J* 6.4 Hz, 5-CH_2), 5.21 (1H, d, *J* 3.9 Hz, 3-H), 7.26 (1H, m, 5'-H), 7.31 (6H, m, 7-H, 8-H, 9-H and OH), 7.62 (1H, d, *J* 7.6 Hz, 4'-H), 8.49 (1H, d, *J* 2.8 Hz, 6'-H) and 8.51 (1H, s, 2'-H); δ_C (100 MHz; $CDCl_3$) 48.5 (C-4), 50.9 (OCH_3), 51.7 (C-5), 53.9 (C-2), 73.2 (C-3), 123.1 (C-5'), 127.3 (C-9), 128.2 (C-8), 128.6 (C-7), 133.6 (C-4'), 137.3 (C-6), 139.0 (C-3'), 147.8 (C-6'), 148.7 (C-2') and 172.7 (C=O); *m*/*z* 301 (**M**+1, 100%).

***Methyl 2-[(2-(benzylthio)ethylamino)methyl]-3-hydroxy-3-(pyridin-3-yl)propanoate* 109b**

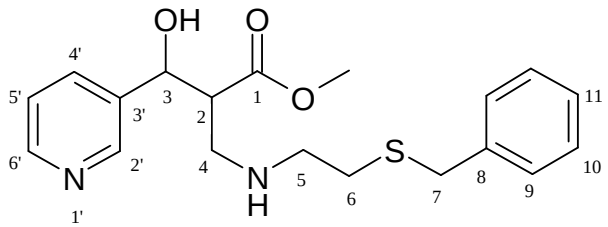

Following the procedure described for the synthesis of methyl 2-[(benzylamino)methyl]-3-hydroxy-3-(pyridin-3-yl)propanoate **109a**, *S*-benzylcysteamine hydrochloride (0.300 g,

1.50 mmol) and triethylamine (0.35 g, 3.5 mmol) were reacted with methyl 2-[hydroxy(pyridin-3-yl)methyl]acrylate **61d** (0.200 g, 1.04 mmol). The solvent was removed *in vacuo* and triethylamine hydrochloride salt was precipitated out on addition of EtOAc (5 ml). The salt was filtered off and the solvent removed from the filtrate *in vacuo* to afford *methyl 2-[(2-(benzylthio)ethylamino)methyl]-3-hydroxy-3-(pyridin-3-yl)propanoate* **109b** (0.15 g, 40.5%) as a 1:2 mixture of diastereomers (*i.e*. 33% d.e.; as determined by the ^{1}H NMR analysis).The diastereomers (0.100 g) were separated by preparative layer chromatography [on silica; elution with CH_2Cl_2-hexane-EtOAC-MeOH (20:15:10:1)] to afford two fractions.

Fraction (i). as a yellow oil (40.7mg, 41%), (Found **M**+1: 361.1557. $C_{19}H_{25}N_2O_3S$ requires **MH**$^+$, 301.1586); ν_{max}(nujol)/cm^{-1} 3296-3340 (OH and NH) and 1728 (OC=O); δ_H (400 MHz; $CDCl_3$) 2.55 (2H, t, *J* 6.0 Hz, 5-CH_2), 2.58 (2H, t, *J* 3.6 Hz, 6-CH_2), 2.70 (1H, s, NH), 2.74 (2H, m, 4-CH_2) 3.13 (1H, dd, *J* 6.0 and 5.9 Hz, 2-H), 3.63 (3H, s, OCH_3), 3.71 (2H, s, 7-CH_2), 3.94 (1H, br m, OH), 5.29 (1H, d, *J* 5.6 Hz, 3-H), 7.27 (1H, s, 2'-H), 7.29 (5H, Ar-H, 9-H, 10-H and 11-H), 7.73 (1H, d, *J* 7.6 Hz, 6'-H), 8.51 (1H, dd, *J* 1.2 and 1.0 Hz, 5'-H) and 8.58 (1H, d, *J* 2.0 Hz, 4'-H); δ_C (100 MHz; $CDCl_3$) 31.0 (C-6), 36.1 (C-7), 48.0 (C-4), 48.1 (C-5), 51.0 (OCH_3), 52.0 (C-2), 74.5 (C-3), 123.2 (C-5'), 127.1 (C-11), 128.5 (C-10), 128.8 (C-9), 133.8 (C-4'), 138.1 (C-3'), 138.1 (C-8), 147.8 (C-6'), 148.0 (C-2') and 172.3 (C=O); *m*/*z* 361 (**M**+1, 100%).

Fraction (ii). as a yellow oil (23.3mg, 23%), (Found **M**+1: 361.1576. $C_{19}H_{25}N_2O_3S$ requires **MH**$^+$, 361.1586); ν_{max}(nujol)/cm^{-1} 3306-3356 (OH and NH) and 1717 (C=O); δ_H (400 MHz; $CDCl_3$) 2.55 (2H, t, *J* 5.4 Hz, 6-CH_2), 2.72 (2H, td, *J* 2.7, 2.6 and 2.5 Hz, 5-CH_2), 2.82 (1H, dd, *J* 4.0 and 4.5 Hz, 2-H), 2.98 (2H, m, 4-CH_2), 3.32 (2H, br m, OH and NH), 3.60 (3H, s, OCH_3), 3.71 (2H, s, 7-CH_2), 5.21 (1H, d, *J* 4.0 Hz, 2-H), 7.23 (1H, d, *J* 0.8 Hz, 4'-H), 7.29 (5H, Ar-H, 9-H, 10-H and 11-H), 7.67 (1H, d, *J* 8.0 Hz, 6'-H), 8.51 (1H, t, *J* 3.6 Hz, 5'-H) and 8.56 (1H, d, *J* 1.6 Hz, 2'-H); δ_C (100 MHz; $CDCl_3$) 31.0 (C-6), 36.1 (C-7), 48.0 (C-4), 48.1 (C-5), 51.0 (OCH_3), 52.0 (C-2), 73.5 (C-3), 123.6 (C-5'), 127.5 (C-11), 129.0 (C-10), 129.2 (C-9), 134.2 (C-4'), 137.8 (C-3'), 138.7 (C-8), 148.3 (C-6'), 149.2 (C-2') and 173.1 (C=O); *m*/*z* 361 (**M**+1, 100%).

Methyl 2-[(carbomethoxymethylamino)methyl]-3-hydroxy--3-(pyridin-3-yl)propanoate **109c**

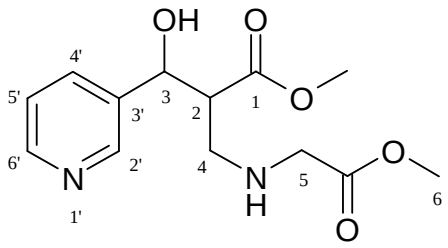

Following the procedure described for the synthesis of methyl 2-[(2-(benzylthio)ethylamino)methyl]-3-hydroxy-3-(pyridin-3-yl)propanoate **109b**, glycine methyl ester hydrochloride (0.21 g, 1.70 mmol) was reacted with methyl 2-[hydroxy(pyridin-3-yl)methyl]acrylate **61d** (0.200 g, 1.04 mmol) to *methyl 2-[(carbomethoxymethyamino)methyl]-3-hydroxy-3-(pyridin-3-yl)propanoate* **109c** (0.22 g, 74.8%) as a 1:2.6 mixture of diastereomers (*i.e*. 44% d.e.; as determined by the ^{1}H NMR analysis). The diastereomers (100 mg) were separated by preparative layer chromatography [on silica; elution with CH_2Cl_2-hexane-EtOAC-MeOH (20:15:10:1)] to afford two fractions.

Fraction (i). as a yellow oil (8.5mg, 9%), (Found **M**+1: 283.1295. $C_{13}H_{19}N_2O_5$ requires **MH**$^+$, 283.1294); ν_{max}(nujol)/cm^{-1} 3309-3323 (OH and NH), 1723 and 1741 (2 x C=O); δ_H (400 MHz; $CDCl_3$) 2.88 (2H, dd, *J* 4.8 and 5.0 Hz, 2-H and NH), 3.00 (2H, m, 4-CH_2), 3.40 (2H, d, *J* 2 Hz, 5-CH_2), 3.62 (4H, s, OCH_3 and OH), 3.72 (3H, s, 6-CH_3), 5.20 (1H, d, *J* 4.4 Hz, 3-H), 7.28 (1H, t, *J* 2.8 Hz, 5'-H), 7.70 (1H, d, *J* 8.0 Hz, 4'-H), 8.50 (1H, t, *J* 3.6 Hz, 6'-H) and 8.55 (1H, s, 2'-H); δ_C (100 MHz; $CDCl_3$) 48.7 (C-4), 50.5 (C-5), 51.3 (C-6), 51.6 (OCH_3), 72.3 (C-2), 72.4 (C-3), 123.3 (C-5'), 137.3 (C-4'), 147.7 (C-6'), 147.9 (C-3'), 148.9 (C-2'), 172.2 and 172.9 (2 x C=O); *m*/*z* 283 (**M**+1, 100%).

Fraction (ii). as a yellow oil (25.5mg, 26%), (Found **M**+1: 283.1295. $C_{13}H_{19}N_2O_5$ requires **MH**$^+$, 283.1294); ν_{max}(nujol)/cm^{-1} 3309-3323 (OH and NH), 1723 and 1741 (2 x C=O); δ_H (400 MHz; $CDCl_3$) 2.81 (2H, m, 4-CH_2), 3.17 (1H, dd, *J* 4.0 and 3.9 Hz, 2-H), 3.39 (2H, d, *J* 4.0 Hz, 5-CH_2), 3.40 (1H, s, NH), 3.61 (3H, s, OCH_3), 3.72 (3H, s, 6-CH_3), 3.92 (1H, br m, OH), 5.27 (1H, d, *J* 6.0 Hz, 3-H), 7.28 (1H, t, *J* 4.8 Hz, 5'-H), 7.73 (1H, d, *J* 7.6 Hz, 4'-H), 8.50 (1H, d, *J* 3.2 Hz, 6'-H) and 8.56 (1H, s, 2'-H); δ_C (100 MHz;

$CDCl_3$) 48.2 (C-4), 50.3 (C-5), 51.4 (C-6), 52.0 (OCH_3), 52. 0 (C-2), 73.8 (C-3), 123.3 (C-5'), 133.9 (C-4'), 137.8 (C-6'), 147.8 (C-3'), 148.8 (C-2'), 171.9 and 172.4 (2 x C=O); *m*/*z* 283 (**M**+1, 100%).

Attempted methods

Method 1. A mixture of methyl 2-[hydroxy(pyridin-3-yl)methyl]acrylate **61d** (0.123 g, 0.64 mmol), glycine methyl ester hydrochloride (0.187 g, 1.49 mmol) and proton sponge (0.684 g, 3.19 mmol) in THF (10ml) was stirred at room temperature for 5 days. ^{1}H NMR spectroscopy indicated the presence of substrate signals suggesting that the reaction had not occurred.

Method 2. A mixture of methyl 2-[hydroxy(pyridin-3-yl)methyl]acrylate **61d** (0.194 g, 1.00 mmol), glycine methyl ester hydrochloride (0.126 g, 1.00 mmol), NaOAc (0.038 g, 0.56 mmol) and TBAB (0.023 g, 0.072 mmol) in THF/$CHCl_3$ (10ml) was stirred at room temperature for 5 days. White flakes appeared and were analyzed by ^{1}H NMR spectroscopy which indicated only the presence of the starting material.

Method 3. A mixture of methyl 2-[hydroxy(pyridin-3-yl)methyl]acrylate **61d** (0.205 g, 1.06 mmol), glycine methyl ester hydrochloride (0.055 g, 0.043 mmol) and triethylamine (86 µL) in CH_2Cl_2 (10ml) was stirred vigorously at room temperature for 5 days. The mixture was then washed with saturated aqueous $NaHCO_3$ (3 ml), extracted with diethyl ether (2 x 5 ml) and dried over $MgSO_4$. The solvent was removed *in vacuo* but ^{1}H NMR analysis confirmed the presence of the starting material.

Attempted preparation of methyl-2-[chloro(pyridin-3-yl)methyl]acrylate. Acetyl chloride (0.5 ml) was added continuously to dry methanol (1 ml) with stirring in an ice-bath. Stirring was continued for 15 minutes. Methyl 2-[hydroxy(pyridin-3-yl)methyl]acrylate **61d** (0.193 g, 1.00 mmol) was then added and the mixture stirred overnight. The ^{1}H NMR spectroscopy of the mixture showed the characteristic Baylis-Hillman signals suggesting that the reaction had not occurred.

***Methyl 2-[(carbethoxymethylamino)methyl]-3-hydroxy-3-(pyridin-3-yl)propanoate* 109d**

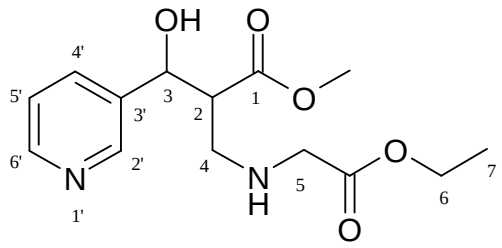

Following the procedure described for the synthesis of methyl 2-[(2-(benzylthio)ethylamino)methyl]-3-hydroxy-3-(pyridin-3-yl)propanoate **109b**, glycine ethyl ester hydrochloride (0.240 g, 1.72 mmol) was reacted with methyl 2-[hydroxy(pyridin-3-yl)methyl]acrylate **61d** (0.200 g, 1.04 mmol) to give *methyl 2-[(carbethoxymethylamino)methyl]-3-hydroxy-3-(pyridin-3-yl)propanoate* **109d** (0.295 g, 95.7%) as a 1:1.6 mixture of diastereomers (*i.e*. 23% d.e.; as determined by the ^{1}H NMR analysis). Preparative layer chromatography [on silica; elution with CH_2Cl_2-hexane-EtOAc-MeOH (20:15:10:1)] of the mixture (100 mg) afforded only one fraction as a yellow oil (16.9 mg, 17%), (Found **M**+1: 297.1454. $C_{14}H_{21}N_2O_5$ requires **MH**$^+$, 297.1450); ν_{max}(nujol)/cm^{-1} 3318-3326 (OH and NH), 1726 (CH_3OC=O) and 1739 (CH_2OC=O); δ_H (400 MHz; $CDCl_3$) 1.26 (3H, t, *J* 7.2 Hz, 7-CH_3), 2.80 (2H, m, 4-CH_2), 3.18 (1H, dd, *J* 5.2 and 5.0 Hz, 2-H), 3.55 (1H, s, OH), 3.39 (2H, q, *J* 7.2 and 6.6 Hz, 6-H_2), 3.61 (3H, s, OCH_3), 3.72 (2H, s, 5-CH_2), 4.17 (1H, m, NH), 5.28 (1H, d, *J* 5.6 Hz, 3-H), 7.28 (1H, q, *J* 1.0 and 1.2 Hz, 5'-H), 7.73 (1H, d, *J* 7.6 Hz, 4'-H), 8.50 (1H, d, *J* 3.6 Hz, 6'-H) and 8.57 (1H, s, 2'-H); δ_C (100 MHz; $CDCl_3$) 14.1 (C-7), 48.2 (C-4), 50.3 (C-6), 51.5 (C-5), 52.0 (OCH_3), 52. 1 (C-2), 73.8 (C-3), 123.3 (C-5'), 133.8 (C-4'), 138.8 (C-6'), 147.8 (C-3'), 148.8 (C-2'), 171.9 and 172.4 (2 x C=O); *m*/*z* 297 (**M**+1, 90) and 283 (**M**$^+$ - CH_2, 100%).

Methyl 2-[1(S)-carbomethoxy-2-hydroxyethylamino]methyl-3-hydroxy-3-(pyridin-3-yl)propanoate **109e**

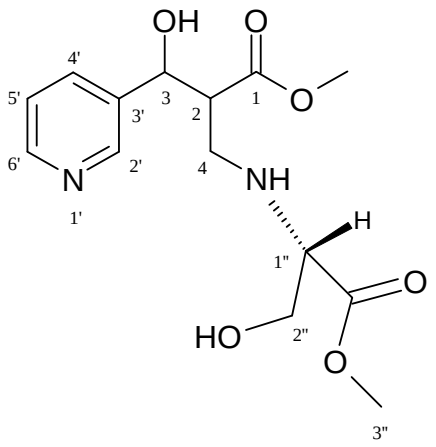

Following the procedure described for the synthesis of methyl 2-[(2-(benzylthio)ethylamino)methyl]-3-hydroxy-3-(pyridin-3-yl)propanoate **109b**, L-serine methyl ester hydrochloride (0.29 g, 1.70 mmol) was reacted with methyl 2-[hydroxy(pyridin-3-yl)methyl]acrylate **61d** (0.200 g, 1.04 mmol) to give *methyl 2-[1(S)-carbomethoxy-2-hydroxyethylamino]methyl-3-(pyridin-3-yl)propanoate* **109e** (99 mg, 31%) as a 1:1.3 mixture of diastereomers (*i.e*. 30% d.e.; as determined by the ^{1}H NMR analysis). Preparative layer chromatography [on silica; elution with CH_2Cl_2-hexane-EtOAC-MeOH (20:15:10:1)] of the mixture (0.099 g), followed by HPLC [on column, elution with (hexane-ETOAC (15:10)] afforded a mixture of the diastereomers **109e** as a yellow oil (13.7 mg, 14%), (Found **M**+1: 313.1407. $C_{14}H_{20}N_2O_6$ requires **MH**$^+$, 313.1400); ν_{max}(nujol)/cm^{-1} 3318-3333 (OH and NH), 1664 and 1730 (2 x C=O); δ_H (400 MHz; $CDCl_3$) 2.72 (1H, m, NHC*H-a*), 2.81 (1H, m, NHC*H-b*), 2.83 (3H, m, CH_2OH and N*H*), 3.32 (1H, m, NHC*H*), 3.59 (1H, s, OH), 3.66 (3H, s, 3''-CH_3), 3.72 (3H, m, OCH_3), 5.12 (1H, d, *J* 5.6 Hz, 3-H), 7.30 (1H, m, 5'-H), 7.72 (1H, d, *J* 6.8 Hz, 6'-H), 8.50 (1H, d, *J* 3.2 Hz, 4'-H) and 8.55 (1H, s, 2'-H); δ_C (100 MHz; $CDCl_3$) 47.9 (C-4), 52.5 (OCH_3), 52.8 (3''-CH_3), 52.9 (C-2), 63.1 (*C*H_2OH), 63.4 (NH*CH*), 72.2 (C-3), 123.9 (C-5'), 134.6 (C-4'), 137.7 (C-3'), 148.3 (C-6'), 149.4 (C-2'), 173.2 and 173.8 (2 x C=O); *m*/*z* 313 (**M**+1, 100%).

***Methyl 1-[2-carbomethoxy-3-hydroxy-3-(pyridin-3-yl)propyl]pyrrolidine-2(S)-carboxylate* 109f**

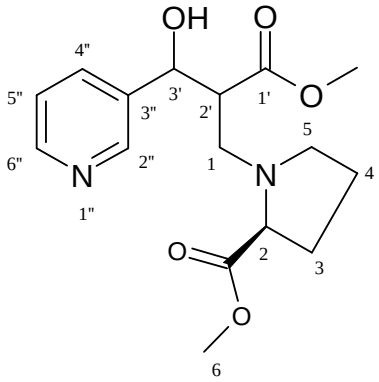

Following the procedure described to synthesis methyl 2-[(2-(benzylthio)ethylamino)methyl]-3-hydroxy-3-(pyridin-3-yl)propanoate **109b**, L-proline methyl ester hydrochloride (0.28 g, 1.70 mmol) was reacted with methyl 2-[hydroxy(pyridin-3-yl)methyl]acrylate **61d** (0.200 g, 1.04 mmol) to give *methyl 1-[2-carbomethoxyl-3-hydroxy-3-(pyridin-3-yl)propyl]pyrrolidine-2(S)-carboxylate* **109f** (0.25 g, 75.8%) as a 1:5 mixture of diastereomers (*i.e*. 50% d.e.; as determined by the ^{1}H NMR analysis), 75% de, 1:7). The diastereomers (0.100 g) were separated by preparative layer chromatography [on silica; elution with CH_2Cl_2-hexane-EtOAc-MeOH (20:15:10:1)] to afford two fractions.

Fraction (i). as a yellow oil (59.2 mg, 59.1%), (Found **M**+1: 323.1601. $C_{16}H_{23}N_2O_5$ requires **MH**$^+$, 323.1607); ν_{max} KBr/cm^{-1} 3305 (OH), 1647 and 1728 (2 x C=O); δ_H (400 MHz; $CDCl_3$) 1.85-1.99 (4H, m, 6-H, OH and 3-CH*a*), 2.18 (1H, m, 3-CH*b*), 2.35 (1H, q, *J* 2.5 and 2.0 Hz, 1-CH*a*), 2.80 (1H, dd, *J* 2.8 and 2.0 Hz, 5-CH*a*), 2.93 (1H, m, 2'-H), 3.29 (1H, q, *J* 1.0 and 1.4 Hz, 2-H), 3.39 (3H, s, 6-CH_3), 3.42 (2H, m, 1-CH*b* and 5-CH*b*), 3.78 (3H, s, OCH_3), 5.08 (1H, d, *J* 8.8 Hz, 3'-H), 7.24 (1H, t, *J* 2.8 Hz, 5''-H), 7.74 (1H, d, *J* 8.0 Hz, 6''-H), 8.49 (1H, t, *J* 3.6 Hz, 4''-H) and 8.56 (1H, s, 2''-H); δ_C (100 MHz; $CDCl_3$) 23.3 (C-4), 29.1 (C-3), 51.6 (OCH_3), 51.9 (C-2'), 52.2 (C-6), 53. 4 (C-1), 57.3 (C-5), 66.2 (C-2), 75.9 (C-3'), 123.2 (C-5''), 134.3 (C-4''), 137.3 (C-3''), 148.4 (C-6''), 149.1 (C-2''), 171.4 and 173.6 (2 x C=O); *m*/*z* 323 (**M**+1, 100%)

Fraction (ii). as a yellow oil (13.5 mg, 14%), (Found **M**+1: 323.1619. $C_{16}H_{23}N_2O_5$ requires $\mathbf{MH}^+$, 323.1607); ν_{max} KBr/cm^{-1} 3305 (OH), 1647 and 1728 (2 x C=O); δ_H (400 MHz; $CDCl_3$) 1.77-1.83 (2H, m, 4-CH*a* and OH), 1.93 (2H, m, 4-CH*b* and 3-CH*a*), 2.05 (1H, m, 3-CH*b*), 2.56 (1H, q, *J* 5.4 and 4.8 Hz, 1-CH*a*), 2.75 (1H, m, 1-CH*b*), 3.11 (3H, m, 2-H and 5-CH_2), 3.38 (1H, dd, *J* 4.0 and 3.8 Hz, 2'-H), 3.63 (3H, s, 6-H), 3.67 (3H, s, OCH_3), 5.10 (1H, d, *J* 4.8 Hz, 3'-H), 7.28 (1H, t, *J* 4.8 Hz, 5''-H), 7.67 (1H, d, *J* 7.6 Hz, 6''-H), 8.50 (1H, d, *J* 4.0 Hz, 4''-H) and 8.53 (1H, s, 2''-H); δ_C (100 MHz; $CDCl_3$) 23.5 (C-4), 29.2 (C-3), 51.0 (C-2'), 51.8 (OCH_3), 51.9 (C-6), 53. 4 (C-1 and C-5), 65.5 (C-2), 71.8 (C-3'), 123.3 (C-5''), 133.8 (C-4''), 137.6 (C-3''), 147.8 (C-6''), 148.9 (C-2''), 173.3 and 174.1 (2 x C=O); *m*/*z* 323 (**M**+1, 100%).

3.7. Saturation Transfer Difference (STD) Experiment

NMR spectra were recorded on a Bruker Biospin 600 MHz spectrometer. For the STD measurements, a 250 μL solution containing 0.38 mM HIV-1 protease sub-type C, with a 40-fold ligand (aza-Michael products) excess, sodium acetate (10 mM), sodium chloride (2 mM), Dithiothreitol (DTT) (2 mM) buffer at pH 5.0 and the mixture of D_2O:H_2O (1:9). The STD spectrum was obtained by using a pulse sequence with differences between the on- and off-resonance experiments created by phase cycling. Saturation of the protein NMR signals was performed using a series of five Gaussian-shaped pulses (50 ms, 2.5 milliseconds delay time between the pulses for a total saturation time of 2.5 seconds. The on-resonance frequency for saturation was set at 0.5 ppm, while the off-resonance irradiation was at 20 ppm, where no protein signals were present. The STD spectrum was processed on Bruker Topspin 2.1 software and the measurements of enhanced intensities were performed by direct comparison of the STD-NMR and reference spectra.

4. REFERENCES

1. Gao, F.; Bailes, E.; Robertson, D. L.; Chen, Y.; Rodenburg, C. M.; Michael, S. F.; Cummins, L. B.; Arthur, L. O.; Peeters, M.; Shaw, G. M.; Sharp, P. M.; Hahn, B. H., *Nature* **1999**, *397*-436.

2. Poiesz, B. J.; Ruscetti, F. W.; Gazdar, A. F.; Bunn, P. A.; Minna, J. D.; Gallo, R. C., *Proc. Natl. Acad. Sci. USA* **1980**, *77*, 7415-7419.

3. Kaleeba, J. A. R.; Berger, E. A., *Science* **2006**, *311*, 1921-1925.

4. Aversa, S. M. L.; Cattelan, A. M.; Salvagno, L.; Crivellari, G.; Banna, G.; Trevenzoli, M.; Chiarion-Sileni, V.; Monfardini, S., *Crit. Rev. Oncology/Hermatology* **2005**, *53*, 253-265.

5. Harper, M. E.; Marselle, L. M.; Gallo, R. C.; Wong-Staal, F., *Proc. Natl. Acad. Sci. USA* **1986**, *83*, 772-776.

6. Gallo, R. C., *Retrovirology* **2006**, *3*, 4690-4696.

7. Turner, B. G.; Summers, M. F., *J. Mol. Bio.* **1999**, *285*, 1-32.

8. Klotman, M. E.; Wong-Staal, F., *Human Immunodefiency Virus (HIV) Gene Structure and Gentic diversity;* The Retroviruses; Academic Press, Inc: 1991; pp 35-36.

9. Keele, B. F.; Van Heuverswyn, F.; Li, Y.; Bailes, E.; Takehisa, J.; Santiago, M. L.; Bibollet-Ruche, F.; Chen, Y.; Wain, L. V.; Liegeois, F.; Loul, S.; Ngole, E. M.; Bienvenue, Y.; Delaporte, E.; Brookfield, J. F. Y.; Sharp, P. M.; Shaw, G. M.; Peeters, M.; Hahn, B. H., *Science* **2006**, *313*, 523-526.

10. Sharp, P. M.; Bailes, E.; Chaudhuri, R. R.; Rodenburg, C. M.; Santiago, M. O.; Hahn, B. H., *Phil. Trans. R. Soc. Lond. B* **2001**, *356*, 867-876.

11. Pau, C.; Luo, W.; McDougal, S. J., *J. Immunol. Methods* **2007**, *318*, 59-64.

12. Kantor, R.; Katzenstein, D., *J. Clinic. Virol.* **2004**, *29*, 152-159.

13. Gilbert, P. B.; Novitsky, V.; Essex, M., *AIDS Res. Hum. Retroviruses* **2005**, *21*, 1016-1030.

14. Cilliers, T.; Moore, P.; Coetzer, M.; Morris, L., *AIDS Res. Hum. Retroviruses* **2005**, *21*, 776-783.

15. Patel, M.; Hoffman, N. G.; Swanstrom, R., *J. Virol.* **2008**, *82*, 903-916.

16. Perez, M. A. S.; Fernandes, P. A.; Ramos, M. J., *J. Mol. Graph. Model* **2007**, *26*, 634-642.

17. Walgate, R.; Degett, J., *New. Boitech.* **2008**, *25*, 29-33.

18. Pugach, P.; Ketas, T. J.; Michael, E.; Moore, J. P., *Virology* **2008**, *377*, 401-407.

19. Lusso, P., *J. EMBO.* **2006**, *25*, 447-456.

20. Scanlan, C. N.; Offer, J.; Zitzmann, N.; Dwek, R. A., *Nature* **2007**, *446*, 1038-1045.

21. Henderson, C., HIV-1 Viron Structure. *http://www.niaid.nih.gov/factsheets/howhiv.htm* (accessed July, 29, 2008).

22. Brik, A.; Wong, C., *Org. Biomol. Chem* **2003**, *1*, 5-14.

23. Beaulieu, P. L.; Proudfoot, J., *Ullmann. Encyclo. Ind. Chem* **2007**, 1-6.

24. Walker, B. D.; Burton, D. R., *Science* **2008**, *320*, 760-764.

25. Weiss, R. A., *IUBMB Life* **2002**, *53*, 201-205.

26. DeFranco, R., Immunity: The Immune Response in Infectious and Inflammatory Disease: Online Resources. *http://www.new-science-press.com/browse/immunity/illustrations/10/* (accessed July 29, 2008).

27. Pommier, Y.; Johnson, A. A.; Marchand, C., *Nature* **2005**, *4*, 237-249.

28. Nijhuis, M.; van Maarseveen, N. M.; Lastere, S.; Schiper, P.; Coakley, E.; Glass, B.; Rovenska, M.; de Jong, D.; Chappey, C.; Goedegebuure, I. W.; Heilek-Snyder, G.; Dulude, D.; Cammack, N.; Brakier-Gingras, L.; Konvalika, J.; Parkin, N.; Krausslic, H.; Brun-Vezinet, F.; Boucher, C. A., *Medicine* **2007**, *4*, 0152-0163.

29. Ghosh, A. K.; Dawson, Z. L.; Mitsuya, H., *Bioorg. Med. Chem.* **2007**, *15*, 7576-7580.

30. Wynn, G. H.; Zapor, M. J.; Smith, B. H.; Wortmann, G.; Oesterheld, J. R.; Armstrong, S. C.; Cozza, K. L., *Psychosomatics* **2004**, *45*, 262-270.

31. Aruksankunwong, O.; Hannongbua, S.; Wolschann, P., *J. Mol. Struct.* **2006**, *790*, 174-182.

32. Camarasa, M.; Velázquez, S.; San-Félix, A.; Pérez-Pérez, M.; Gago, F., *Antiviral Res.* **2006**, *71*, 260-267.

33. Prasana, M. D.; Vondrasek, J.; Wlodawer, A.; Bhat, T. N., *Proteins* **2005**, *60*, 1-4.

34. Prasana, M. D.; Vondrasek, J.; Wlodawer, A.; Bhat, T. N., *Proteins* **2006**, *63*, 907-917.

35. Vondrasek, J., HIV Protease. *http://xpdb.nist.gov/hiv2_d/hivsdb.html* (accessed 6 August, 2008).

36. Schechter, I.; Berger, A., *Biochem. Biophys. Res. Commun.* **1967**, *27*, 157-162.

37. Vacca, J. P.; Condra, J. H., *Therap. Foc. Rev.* **1997**, *2*, 261-272.

38. Drugs Used in the treatment of HIV infection. *http://www.fda.gov/oashi/aids/virals.html* (accessed 6 August, 2008).

39. Maeda, K.; Mitsuya, H., *Tuberculosis* **2007**, *87*, S31-S34.

40. Bartlet, J. A.; Muro, E. P., *J. Int. Ass. Physicians AIDS Care* **2007**, *6*, 15-33.

41. Pinheiro, E. S.; Antunes, O. A. C.; Fortunak, J. M. D., *Antiviral Res.* **2008**, *79*, 143-165.

42. Shigemitsu, Y.; Komiya, K.; Mizuyama, N.; Tominaga, Y., *THEOCHEM* **2008**, *855*, 92-101.

43. Lee, Y. S.; Lee, J. Y.; Kim, D. W.; Park, H., *Tetrahedron* **1999**, *55*, 4631-4636.

44. Uchida, T.; Matsumoto, K., *Synthesis: Reviews* **1976**, 209-236.

45. Bora, U.; Saikia, A.; Boruh, R. C., *Org. Lett.* **2002**, *5*, 435-438.

46. Troll, T.; Beckel, H.; Lentner-Böhm, C., *Tetrahedron* **1997**, *53*, 81-90.

47. Przewloka, T.; Chen, S.; Xia, Z.; Li, H.; Zhang, S.; Chimmanamada, D.; Kostik, E.; James, D.; Koya, K.; Sun, L., *Tetrahedron Lett.* **2007**, *48*, 5739-5742.

48. Weide, T.; Arve, L.; Prinz, H.; Waldmann, H.; Kessler, H., *Bioorg. Med. Chem.* **2006**, *16*, 59-63.

49. Kaloko Jr, J.; Hayford, A., *Org. Lett.* **2005**, *7*, 4305-4308.

50. Fang, X.; Wu, Y.; Deng, J.; Wang, S., *Tetrahedron* **2004**, *60*, 5487-5493.

51. Millet, R.; Domarkas, J.; Rigo, B.; Goossens, L.; Goossens, J.; Houssin, R.; Hénichart, J., *Bioorg. Med. Chem.* **2002**, *10*, 2905-2912.

52. Teklu, S.; Gundersen, L.; Rise, F.; Tilset, M., *Tetrahedron* **2005**, *61*, 4643-4656.

53. Gundersen, L.; Malterud, K. E.; Negussie, A. H.; Rise, F.; Teklu, S.; Østby, O. B., *Bioorg. Med. Chem.* **2003**, *11*, 5409-5415.

54. Katrizky, A. R.; Qiu, g.; Yang, B.; He, H., *J. Org. Chem.* **1999**, *64*, 7618-7621.

55. Cingolani, G. M.; Claudi, F.; Massi, M.; Venturi, F., *Eur. J. Med. Chem.* **1989**, *25*, 709-712.

56. Antonini, I.; Claudi, F.; Gulini, U.; Micossi, L.; Venturi, F., *J. Pharm. Sci.* **1979**, *68*, 321-324.

57. Ankalgi, A.; Das, A. K.; Baidya, M., *Orient. J. Chem.* **2006**, *22*, 83-88.

58. Gundersen, L.; Charnock, C.; Negussie, A. H.; Rise, F.; Teklu, S., *Eur. J. Pharm. Sci.* **2007**, *30*, 26-35.

59. Kuznetsov, A. G.; Bush, A. A.; Rybakov, V. B.; Babaev, E., *Molecules* **2005**, *10*, 1074-1083.

60. Kostik, E. I.; Abiko, A.; Oku, A., *J. Org. Chem.* **2001**, *66*, 2618-2623.

61. Wang, B.; Zhang, X.; Li, j.; Jiang, X.; Hu, Y.; Hu, H., *J. Chem. Soc. Perkin Trans. 1* **1999**, 1571-1575.

62. Matsumoto, K.; Uchida, T.; Ikemi, Y.; Tanaka, T.; Asahi, M.; Kato, T.; Konishi, H., *Bull. Chem. Soc. Jpn.* **1987**, *60*, 3645-3653.

63. Matsumoto, K.; Katsura, H.; Uchida, T.; Aoyama, K.; Machiguchi, T., *J. Chem. Soc. Perkin Trans. 1* **1996**, 2599-2602.

64. Mmutlane, E. M.; Harris, J. M.; Padwa, A., *J. Org. Chem.* **2005**, *70*, 8055-8063.

65. Kaye, P. T., *S. Afr. J. Sci.* **2004**, *100*, 545-548.

66. Bode, M. L., PhD Thesis, Rhodes University, 1994.

67. Bode, M. L.; Kaye, P. T., *J. Chem. Soc. Perkin Trans. 1* **1990**, *1*, 2612-2613.

68. Bode, M. L.; Kaye, P. T.; George, R., *J. Chem. Soc. Perkin Trans. 1* **1994**, *1*, 3023-3027.

69. Basavaiah, D.; Rao, A. J., *Chem. Commun.* **2003**, 604-605.

70. Bode, M. L.; Kaye, P. T., *J. Chem. Soc. Perkin Trans. 1* **1993**, *1*, 1809-1815.

71. Krohnke, F.; Zecher, W., *Chem. Ber* **1962**, *95*, 1128-1139.

72. Tamura, Y.; Tsujimoto, N.; Sumida, Y.; Ikeda, M., *Tetrahedron* **1972**, *28*, 21-27.

73. Sasaki, T.; Kanematsu, K.; Kakehi, A.; Ito, G., *Tetrahedron* **1972**, *28*, 4947-4958.

74. Morita, K.; Suzuku, Z.; Hirose, H., *Short Commun.* **1968**, 2815-2815.

75. Baylis, A. B.; Hillman, M E. D., 3743669, 1973.

76. Drewes, S. E.; Roos, Gregory H. P., *Tetrahedron* **1988**, *44*, 4653-4670.

77. Basavaiah, D.; Muthukumaran, K., *Tetrahedron* **1998**, *54*, 4943-4948.

78. Li, G.; Wei, H.; Willis, S., *Tetrahedron Lett.* **1998**, *39*, 4607-4610.

79. Basavaiah, D.; Rao, K. V.; Reddy, R. J., *Chem. Soc. Rev.* **2007**, *36*, 1581-1588.

80. Pachamuthu, K.; Vankar, Y. D., *Tetrahedron Lett.* **1998**, *39*, 5439-5442.

81. Basavaiah, D.; Hyma, S. R.; Padmaja, K.; Krishnamacharyulu, M., *Tetrahedron* **1999**, *55*, 6971-6976.

82. Krishna, P. R.; Kannan, V.; Ilangovan, A.; Sharma, G. V. M., *Tetrahedron: Asymmetry* **2001**, *12*, 829-837.

83. Brown, J. M.; Cutting, I., *Chem. Commun.* **1985**, *44*, 577-579.

84. Brzezinski, L. J.; Rafel, S.; Leahy, J. W., *J. Am. Chem. Soc.* **1997**, *119*, 4317-4318.

85. Brzezinski, L. J.; Rafel, S.; Leahy, J. W., *Tetrahedron* **1997**, *53*, 16423-16434.

86. Iwabuchi, Y.; Nakatani, M.; Yokoyama, N.; Hatakeyama, S., *J. Am. Chem. Soc.* **1999**, *121*, 10219-10220.

87. Krishna, P. R.; Sharma, G. V. M., *Org. Chem.* **2006**, *3*, 137-153.

88. Shi, M.; Jiang, J., *Tetrahedron: Asymmetry* **2002**, *13*, 1941-1947.

89. Dalaigh, C. O.; Connon, S. J., *J. Org. Chem.* **2007**, *72*, 7066-7069.

90. Roth, F.; Gygax, P.; Fráter, G., *Tetrahedron Lett.* **1992**, *33*, 1045-1048.

91. Black, G. P.; Dinon, F.; Fratucello, S.; Murphy, P. J.; Nielsen, M.; Williams, H. L.; Walshe, Nigel D. A., *Tetrahedron Lett.* **1993**, *38*, 8561-8564.

92. Krishna, P. R.; Kannan, V.; Sharma, G. V. M., *J. Org. Chem.* **2004**, *69*, 6467-6469.

93. Yeo, J. A.; Yang, X.; Kim, H. J.; Koo, S., *Chem. Commun* **2004**, *10*, 236-237.

94. Luo, S.; Zhang, B.; He, J.; Janzuk, A.; Wang, P. G.; Cheng, J., *Tetrahedron Lett.* **2002**, *43*, 7369-7371.

95. Lawrence, N. J.; Crump, P. J.; McGown, A. T.; Hadfield, J. A., *Tetrahedron Lett.* **2001**, *42*, 3939-3941.

96. Iwamura, T.; Fujita, M.; Kawakita, T.; Kinoshita, S.; Watanabe, S.; Kataoka, T., *Tetrahedron* **2001**, *57*, 8455-8462.

97. Yamada, Yoichi M. A.; Ikegami, S., *Tetrahedron Lett.* **2000**, *41*, 2165-2169.

98. Krishna, P. R.; Manjuvani, A.; Kannan, V.; Sharma, G. V. M., *Tetrahedron Lett.* **2003**, *45*, 1183-1185.

99. Aggarwal, V. K.; Dean, D. K.; Mereu, A.; Williams, R., *J. Org. Chem.* **2001**, *67*, 510-514.

100. Maher, D. J.; Connon, S. J., *Tetrahedron Lett.* **2004**, *45*, 1301-1305.

101. Lee, K. Y.; Gowrisankar, S.; Kim, J. N., *Tetrahedron Lett.* **2004**, *45*, 5485-5488.

102. Luo, S.; Wang, P. G.; Cheng, J., *J. Org. Chem.* **2003**, *69*, 555-558.

103. Kabalka, G. W.; Venkataiah, B.; Dong, G., *Tetrahedron Lett.* **2003**, *44*, 4673-4675.

104. Aggarwal, V. K.; Emme, I.; Fulford, S. Y., *J. Org. Chem.* **2003**, *68*, 692-693

105. Li, G.; Wei, H.; Gao, J. J.; Caputo, T. D., *Tetrahedron Lett.* **2000**, *41*, 1-5.

106. de Souza, R. M. A.; Vasconcellos, M. L. A. A., *Catalysis Commun.* **2004**, *5*, 21-24.

107. Mason, P. H.; Emslie, N. D., *Tetrahedron* **1994**, *50*, 12001-12008.

108. Yadav, J. S.; Subba Reddy, B. V.; Singh, A. P.; Basak, A. K., *Tetrahedron Lett.* **2007**, *48*, 4169.

109. Basavaiah, D.; Sreenivasulu, B.; Rao, A. J., *J. Org. Chem.* **2003**, *68*, 5983-5991.

110. Park, D. Y.; Lee, M. J.; Kim, T. H.; Kim, J. N., *Tetrahedron Lett.* **2005**, *46*, 8799-8803.

111. Aggarwal, V. K.; Patin, A.; Tisserand, S., *Org. Lett.* **2005**, *7*, 2555-2557.

112. Lee, H. J.; Seong, M. R.; Kim, J. N., *Tetrahedron Lett.* **1998**, *39*, 6223-6226.

113. Porzelle, A.; Williams, C. M., *Synthesis* **2006**, *2006*, 3025-3030.

114. Gowrisankar, S.; Lee, K. Y.; Kim, J. N., *Tetrahedron* **2006**, *62*, 4052-4058.

115. Vasbinder, M. M.; Imbriglio, J. E.; Miller, S. J., *Tetrahedron* **2006**, *62*, 11450-11459.

116. Yadav, L. D. S.; Srivastava, V. P.; Patel, R., *Tetrahedron Lett.* **2008**, *49*, 5652-5654.

117. Mamaghani, M.; Badrian, A., *Tetrahedron Lett.* **2004**, *45*, 1547-1550.

118. Guo, W.; Wu, W.; Fan, N.; Wu, Z.; Xia, C., *Synthetic Commun.* **2005**, *35*, 1239-1251.

119. Basavaiah, D.; Srivardhana R, J., *Tetrahedron Lett.* **2004**, *45*, 1621-1625.

120. Franck, X.; Figadère, B., *Tetrahedron Lett.* **2002**, *43*, 1449-1451.

121. Drewes, S. E.; Emslie, N. D., *J. Chem. Soc. Perkin Trans. 1* **1982**, 2079-2083.

122. Ameer, F.; Drewes, S. E.; Emslie, N. D.; Kaye, P. T.; Leigh Mann, R., *J. Chem. Soc. Perkin Trans. 1* **1983**, 2293-2295.

123. Ameer, F.; Drewes, S. E.; Houston-McMillan, M. S.; Kaye, P. T., *J. Chem. Soc. Perkin Trans. 1* **1985**, 1143-1145.

124. Ameer, F.; Drewes, S. E.; Hoole, R.; Kaye, P. T.; Pitchford, A. T., *J. Chem. Soc. Perkin Trans. 1* **1985**, 2713-2717.

125. Hoffman, H. M. R.; Rabe, J., *Angewandte Chemie* **1983**, *95*, 795-796.

126. Basavaiah, D.; Pandiaraju, S.; Sarma, P. K. S., *Tetrahedron Lett.* **1994**, *35*, 4227-4230.

127. Das, B.; Banerjee, J.; Chowdhurry, N.; Majhi, A., *Chem. Pharm. Bull.* **2006**, *54*, 1725-1727.

128. Davidson, D. N.; Kaye, P. T., *J. Chem. Soc. Perkin Trans. 2* **1991**, 927-930.

129. Kaye, P. T.; Nocanda, X. W., *J. Chem. Soc. Perkin Trans. 1* **2000**, 1331-1332.

130. Kaye, P. T.; Musa, M. A.; Nocanda, X. W.; Robinson, R. S., *Org. Biomol. Chem.* **2003**, *1*, 1133-1138.

131. Kaye, P. T.; Nocanda, X. W., *J. Chem. Soc. Perkin Trans 1* **2002**, *1*, 1318-1323.

132. Kaye, P. T.; Musa, M. A., *Synthesis* **2002**, 2701-2706.

133. Kaye, P. T.; Musa, M. A.; Nocanda, X. W., *Synthesis* **2003**, 531-534.

134. Narender, P.; Srinivas, U.; Ravinder, M.; Ananda Rao, B.; Ramesh, C. H.; Harakishore, K.; Gangadasu, B.; Murthy, U. S. N.; Jayathirtha Rao, V., *Bioorg. Med. Chem.* **2006**, *14*, 4600-4609.

135. Familoni, O. B.; Kaye, P. T.; Klaas, P. J., *Chem. Commun.* **1998**, 2563-2564.

136. Kim, J. N.; Lee, H. J.; Lee, K. Y.; Kim, H. S., *Tetrahedron Lett.* **2001**, *42*, 3737-3740.

137. Basavaiah, D.; Reddy, R. M.; Kumaragurubaran, N.; Sharada, D. S., *Tetrahedron* **2002**, *58*, 3693-3697.

138. Kim, J. N.; Chung, Y. M.; Kim, Y. J., *Tetrahedron Lett.* **2002**, *43*, 6209-6211.

139. Lee, C. G.; Lee, K. Y.; Gowrisankar, S.; Kim, J. N., *Tetrahedron Lett.* **2004**, *45*, 7409-7413.

140. Yi, H.; Park, H. W.; Song, Y. S.; Lee, K., *Synthesis* **2006**, 1953-1960.

141. Familoni, O. B.; Klass, P. J.; Lobb, K. A.; Pakade, V. E.; Kaye, P. T., *Org. Biomol. Chem.* **2006**, *4*, 3960-3965.

142. Kaye, P. T.; Nocanda, X. W., *Synthesis* **2001**, 2389-2392.

143. Basavaiah, D.; Rao, A. J., *Tetrahedron Lett.* **2003**, *44*, 4365-4368.

144. Davidson, D. N.; Kaye, P. T., *J. Chem. Soc. Perkin Trans. 2* **1991**, *2*, 927-930.

145. Kaye, P. T.; Musa, M. A.; Nchinda, A. T.; Nocanda, X. W., *Synthetic Commun.* **2004**, *34*, 2575-2589.

146. Chan, B. K.; Ciufolini, M. A., *J. Org. Chem.* **2007**, *72*, 8489-8495.

147. Kobayashi, S.; Kakumoto, K.; Sugiura, M., *Org. Lett.* **2002**, *4*, 1319-1322.

148. Duan, Z.; Xuan, X.; Li, T.; Yang, C.; Wu, Y., *Tetrahedron Lett.* **2006**, *47*, 5433-5436.

149. Perlmutter, P.; Tabone, M., *Tetrahedron Lett.* **1988**, *29*, 949-952.

150. Cimino, P.; Bifulco, G.; Evidente, A.; Abouzeid, M.; Riccio, R.; Gomez-Paloma, L., *Org. Lett.* **2002**, *4*, 2779-2782.

151. Menche, D., *Nat. Prod. Rep.* **2008**, *25*, 905-918.

152. Roush, W. R.; Bannister, T. D.; Wendt, M. D.; van Nieuwenhze, M. S.; Gustin, D. J.; Dilley, G. J.; Lane, G. C.; Scheidt, K. A.; Smith, W. J., *J. Org. Chem.* **2002**, *67*, 4284-4289.

153. Wu, M.; Okino, T.; Nogle, L. M.; Marquez, B. L.; Williamson, T. R.; Sitachitta, N.; Berman, F. W.; Murray, T. F.; McGough, K.; Jacobs, R.; Colsen, K.; Asano, T.; Yakokawa, F.; Shiori, T.; Gerwick, W. H., *J. Am. Chem. Soc.* **2000**, *122*, 12041-12042.

154. Fontana, C.; Incerti, M.; Moyna, G.; Manta, E., *Mag. Reson. Chem.* **2008**, *48*, 36-41.

155. Tamp, S.; Danilas, K.; Kreen, M.; Vares, L.; Kiirend, E.; Vija, S.; Pehk, T.; Parve, O.; Metsala, A., *THEOCHEM* **2008**, *851*, 84-91.

156. Karali, A.; Dais, P.; Mikros, E.; Heatley, F., *Macromelocules* **2001**, *34*, 5547-5554.

157. Victory, S. F.; Vander Velde, D. G.; Jalluri, R. K.; Grunewald, G. L.; Georg, G. I., *Bioorg. Med. Chem. Lett.* **1996**, *6*, 893-898.

158. Karplus, M., *J. Am. Chem. Soc.* **1969**, *91*, 1-10.

159. Alkorta, I.; Elguero, J., *Theor. Chem. Acc.* **2004**, *111*, 31-35.

160. Schmidt, J. M., *J. Biomol. NMR* **2007**, *37*, 287-301.

161. Daub, W. G.; Edwards, J. P.; Okada, C. R.; Allen, J. W.; Maxey, C. T.; Wells, M. S.; Goldstein, A. S.; Dibley, M. J.; Wang, C. J.; Ostercamp, D. P.; Chung, S.; Cunningham, P. S.; Beliner, M. A., *J. Org. Chem.* **1997**, *62*, 1976-1985.

162. Stott, K.; Keeler, J.; Van, Q.; Shaka, J., *J. Mag. Reson.* **1997**, *125*, 307-324.

163. Forgo, P.; Kover, K. E.; Hohmann, J., *Monatshefte fur Chemie* **2002**, *133*, 1249-1261.

164. Capriati, V.; Degennaro, L.; Florio, S.; Luisi, R.; Cuocci, C., *Tetrahedron Lett.* **2007**, *48*, 8655-8658.

165. Smurnyy, Y. D.; Elyashberg, M. E.; Blinov, K. A.; Lefebvre, B. A.; Martin, G. E.; Williams, A. J., *Tetrahedron* **2005**, *61*, 9980-9989.

166. Rappe, A.; Contonguay, L., *J. Am. Chem. Soc.* **1992**, *114*, 5832-5842.

167. Cerius^2, V.4.0, BIOSYMM/Molecular Simulations Inc.

168. McMurry, J., *Organic chemistry*, 6th edition, Thomson Brooks/Cole Publishers, 2004, 275-305.

169. Ramos, J. M.; Versiane, O.; Felcman, J.; Téllez S., C. A. *Spectrochimica Acta Part A: Mol. Biomol. Spectroscopy* **2009**, *72*, 182-189.

170. Frisch, M.J. *et al*., Gaussian 0.3, Revision B.5.0, Gaussian, Inc, Wallingford, CT, 2004.

171. Park, C. H.; Nienaber, V.; Kong, X. P. HIV-1 protease dimer complexed with A-84538. (HIV-1 protease x-ray crystallography structure, code entry: 1HWX *www.pdb.org*.)

172. Material Studio^{TM}, V.2.2, Accelrys Inc.

173. Goodsell, D.; Morris, G.; Olson, A., *J. Mol. Recognit.* **1996**, *9*, 1-5. (http://autodock.scripps.edu/downloads, Accessed 12 October 2008)

174. Akaho, E.; Morris, G.; Goodsell, D.; Wong, D.; Olson, A., *J. Chem. Software* **2001**, *7*, 101-114.

175. Chang, M. W.; Lindstrom, W.; Olson, A.; Belew, R. K., *J. Chem. Inf. Model* **2007**, *47*, 1258-1262.

176. Morris, G.; Goodsell, D.; Halliday, R.; Huey, R.; Hart, W.; Belew, R.; Olson, A., *J. Comput. Chem.* **1998**, *19*, 1639-1662.

177. Wiley, A. E.; MacDonald, M.; Lambropoulos, A.; Harriman, J. D.; Deslongchamps, G., *Can. J. Chem.* **2006**, *84*, 384-391.

178. Jenwitheesuk, E.; Samudrala, R., *Bioinformatics* **2007**, *23*, 2797-2799.

179. Jenwitheesuk, E.; Samudrala, R., *AIDS* **2005**, *19*, 529-533.

180. Jenwitheesuk, E.; Samudrala, R., *BMC Structural Biology* **2003**, *3*, 1-9.

181. Streif, J. H.; Juranic, N. O.; Macura, S., I.; Warner, D. O.; Jones, K. A.; Perkins, W. J., *Mol. Pharmacol.* **2004**, *66*, 929-935.

182. Johnson, M. A.; Pinto, B. M., *Bioorg. Med. Chem.* **2004**, *12*, 295-300.

183. Feher, K.; Groves, P.; Batta, G.; Jimenez-Barbero, J.; Muhle-Goll, C.; Kover, K., *J. Am. Chem. Soc.* **2008**, *xxxx*, xxxx.

184. Mayer, M.; James, T. L., *J. Am. Chem. Soc.* **2002**, *124*, 13376-13377.

185. Neffe, A. T.; Bilang, M.; Meyer, B., *Org. Biomol. Chem.* **2006**, *4*, 3259-3267.

186. Mayer, M.; Meyer, B., *J. Am. Chem. Soc.* **2001**, *123*, 6108-6117.

187. Perrin, D. D.; Armarego, W.L.F., *Purification of Laboratory Chemicals*, Pergamon Press, Oxford, 3rd editionn., 1988.

188. http://www.acdlabs.com/product/spec_lab/product_nmr. (Accessed 2006)

189. http://www.sciencesoftware.com/product.php (Accessed 2007)